

## **INFORMATION TO USERS**

This manuscript has been reproduced from the microfilm master. UMI films the text directly from the original or copy submitted. Thus, some thesis and dissertation copies are in typewriter face, while others may be from any type of computer printer.

**The quality of this reproduction is dependent upon the quality of the copy submitted.** Broken or indistinct print, colored or poor quality illustrations and photographs, print bleedthrough, substandard margins, and improper alignment can adversely affect reproduction.

In the unlikely event that the author did not send UMI a complete manuscript and there are missing pages, these will be noted. Also, if unauthorized copyright material had to be removed, a note will indicate the deletion.

Oversize materials (e.g., maps, drawings, charts) are reproduced by sectioning the original, beginning at the upper left-hand corner and continuing from left to right in equal sections with small overlaps.

Photographs included in the original manuscript have been reproduced xerographically in this copy. Higher quality 6" x 9" black and white photographic prints are available for any photographs or illustrations appearing in this copy for an additional charge. Contact UMI directly to order.

Bell & Howell Information and Learning  
300 North Zeeb Road, Ann Arbor, MI 48106-1346 USA  
800-521-0600

**UMI<sup>®</sup>**



**University of Alberta**

**Plant Dewatering and Strengthening of Mine Waste Tailings**

by

**Marvin Jose Silva**



A thesis submitted to the Faculty of Graduate Studies and Research in partial fulfillment of the requirements for the degree of **Doctor of Philosophy**

in

**Geoenvironmental Engineering**

**Department of Civil and Environmental Engineering**

Edmonton, Alberta

Fall, 1999



National Library  
of Canada

Acquisitions and  
Bibliographic Services

395 Wellington Street  
Ottawa ON K1A 0N4  
Canada

Bibliothèque nationale  
du Canada

Acquisitions et  
services bibliographiques

395, rue Wellington  
Ottawa ON K1A 0N4  
Canada

*Your file* *Votre référence*

*Our file* *Notre référence*

The author has granted a non-exclusive licence allowing the National Library of Canada to reproduce, loan, distribute or sell copies of this thesis in microform, paper or electronic formats.

The author retains ownership of the copyright in this thesis. Neither the thesis nor substantial extracts from it may be printed or otherwise reproduced without the author's permission.

L'auteur a accordé une licence non exclusive permettant à la Bibliothèque nationale du Canada de reproduire, prêter, distribuer ou vendre des copies de cette thèse sous la forme de microfiche/film, de reproduction sur papier ou sur format électronique.

L'auteur conserve la propriété du droit d'auteur qui protège cette thèse. Ni la thèse ni des extraits substantiels de celle-ci ne doivent être imprimés ou autrement reproduits sans son autorisation.

0-612-46918-2

**Canada**



**University of Alberta**  
**Library Release Form**

**Name of the Author:** Marvin Jose Silva

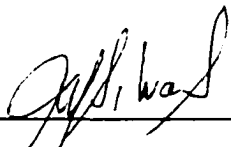
**Title of Thesis:** Plant dewatering and strengthening of mine waste tailings

**Degree:** Doctor of Philosophy

**Year this Degree Granted:** 1999

Permission is hereby granted to the University of Alberta Library to reproduce single copies of this thesis and to lend or sell such copies for private, scholarly or scientific research purposes only.

The author reserves all other publication and other rights in association with the copyright in the thesis, and except as hereinbefore provided, neither the thesis nor substantial portion thereof may be printed or otherwise reproduced in any material form whatever without the author's prior written permission.



---

9529 -180A Street  
Edmonton, Alberta  
Canada T6T 2Z4

July 20, 1999  
Date submitted to FGSR

University of Alberta

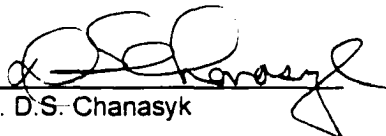
Faculty of Graduate Studies and Research

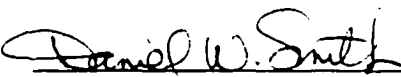
The undersigned certify that they have read, and recommend to the Faculty of Graduate Studies and Research for acceptance, a thesis entitled **Plant Dewatering and Strengthening of mine waste tailings** submitted by **Marvin Jose Silva** in partial fulfillment of the requirements for the degree of **Doctor of Philosophy in Geoenvironmental Engineering**.


  
\_\_\_\_\_  
Dr. D.C. Sego

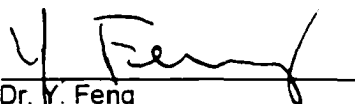
  
\_\_\_\_\_  
Dr. K.W. Biggar

  
\_\_\_\_\_  
Dr. M.A. Naeth

  
\_\_\_\_\_  
Dr. D.S. Chanasyk

  
\_\_\_\_\_  
Dr. D. Smith

  
\_\_\_\_\_  
Dr. G.W. Wilson

  
\_\_\_\_\_  
Dr. Y. Feng

13 July '99  
Date Approved

**to**

***my wife Isolda and my sons  
Marvin Jr., Ricardo and Joshua  
for all your support, love and understanding  
along the way***

**and to**

***mom and dad who continue taking care  
of me from heaven***

## **Abstract**

---

Large volumes of mine waste tailings are generated yearly in Canada and around the world by the mining industry. After ore extraction, a slurry waste consisting of residual ore, water, sand, silt and fine clay particles is hydraulically transported and stored within surface tailings ponds. The fast-settling sand particles segregate from the slurry upon deposition at the edge of the tailings ponds while the finer fraction accumulates in the center of the pond. One of the major environmental issues associated with the contents of tailings ponds are their instability and incapability of supporting the weight of animals or machines for a long period of time. Reclamation of these tailings to a desired dry landscape will not be possible until the surface of the deposit is capable of supporting at least human traffic.

The use of suitable plant species to dewater tailings has been identified as a mechanism, which can enhance the surface stability of these weak deposits. Plant species growing in high water content tailings have the ability to remove the water through evapotranspiration, ultimately increasing the matric suction in the deposit. This results in an increase in the shear strength and hence bearing capacity within the root zone. Furthermore, the plant root system provides fiber reinforcement, which also contributes to the increased bearing capacity of the rooted tailings.

A two-phase greenhouse experiment was first conducted to identify the most suitable species for dewatering and reclamation of composite tailings (CT) from Alberta oil sands operated by Syncrude Canada Ltd. and copper mine tailings (CMT) from the Kennecott site. Five species proved to be the best candidates for future field dewatering research in CT: Altai wildrye (*Elymus angustus*), creeping foxtail (*Alopecurus arundinaceus*), reed canarygrass (*Phalaris arundinacea*), red top (*Agrostis stolonifera*) and streambank wheatgrass (*Agropyron riparian*). Three species are recommended for further studies in CMT: Altai wildrye, creeping foxtail and smooth bromegrass (*Bromus inermis*).

A theoretical approach for predicting the contributions to bearing capacity of tailings by the strength enhancement mechanisms of plants was developed. The theoretical model was used to simulate the results of a second greenhouse experiment using the recommended five species in CT as the growth medium. The model slightly over-predicted the surface settlement, but a good match was found in the trend. Good agreement was found between the measured and predicted solids content and bearing capacity profiles. The model was then used to make a Class A prediction of the field performance of reed canarygrass in a field CT deposit using climatic data from the Syncrude site and the physical properties of a recent field CT deposit.

## **Acknowledgements**

---

I wish to thank Professor Dave C. Segó who exercised confidence in me to pursue this Ph.D. His interest in multidisciplinary research gave me the opportunity of being part of this exciting new area of research, which combines the traditional geotechnical engineering discipline with sciences like hydrology, soil physics and agricultural sciences.

I would like to express my sincere gratitude to Dr. K.W. Biggar, who provided valuable support and encouragement. The guidance, experiences and family matter conversations will never be forgotten.

I wish to thank Dr. M.A. Naeth, who provided guidance into the relevant aspects of the plants related to this research.

I wish to thank Dr. D.S. Chanasyk, who made me think profoundly in the difference between an engineer and a scientist. He provided guidance in putting a different focus into the writing of this thesis.

I wish to thank Gerry Cyre, Christine Hereygers and Steve Gamble for all their help in the laboratory. This research not only required technical assistance, but also a lot of heavy work. The energetic efforts of these geotechnical technologists were critical to the completion of this research and are really appreciated. I thank also Bruce Alexander for all his help and technical advice in the greenhouse room.

I gratefully acknowledge the financial support provided by the Natural Sciences and Engineering Research Council (NSERC), Luscar Ltd. and the University of Alberta. I am also grateful to the University of Alberta and the Department of Civil and Environmental Engineering for providing me with the opportunity to act as a teaching and research assistant during my time in graduate studies.

I would like to thank Syncrude Canada Ltd. and Kennecott Corporation for supplying and shipping the tailings material. Thanks also to Gord McKenna from Syncrude Canada Ltd. for supplying the climatic data from the mine site.

A special thanks to Renato Clementino, who became a friend in this adventure. I never understood why he speaks Spanish in a wrong way. However, he always tells me that it is my Portuguese that needs improvement.

The committal of time required for the completion of this doctorate was made in part at the expense of my sons Marvin Jr., Ricardo and Joshua. I hope that one day they will understand that their dad was just fulfilling an old dream.

The financial and spiritual support of my dear wife Isolda was essential to the completion of this thesis. Isolda worked extra hours to satisfy our family needs in the past four years. I could not have done it without her. Now she deserves a long free time.

- -

## **Table of contents**

---

### **Chapter 1** ***Introduction***

---

<b>1.1 INTRODUCTION</b>	<b>1</b>
<b>1.2 RESEARCH OBJECTIVES</b>	<b>4</b>
<b>1.3 ORGANIZATION OF THESIS</b>	<b>4</b>
<b>1.4 REFERENCES</b>	<b>6</b>

### **Chapter 2** ***Plant selection for dewatering and reclamation of tailings***

---

<b>2.1 INTRODUCTION</b>	<b>8</b>
<b>2.2 BACKGROUND</b>	<b>9</b>
2.2.1 Plant dewatering	9
2.2.2 Plant species selection	12
2.2.3 Fertilization of tailings	13
<b>2.3 MATERIALS AND METHODS</b>	<b>14</b>
2.3.1 Plant material	14
2.3.2 Tailings material, release and process water	15
2.3.3 Amount of fertilizer	16
2.3.4 Methods	16
2.3.4.1 Phase 1	16
2.3.4.2 Phase 2	17
<b>2.4 RESULTS</b>	<b>17</b>
2.4.1 Phase 1	17
2.4.1.1 Composite Tailings (CT)	17
2.4.1.2 Copper Mine Tailings (CMT)	18
2.4.2 Phase 2	19
2.4.2.1 Composite Tailings (CT)	19
2.4.2.2 Copper Mine Tailings (CMT)	20
<b>2.5 DISCUSSION</b>	<b>21</b>
2.5.1 Phase 1	21
2.5.2 Phase 2	21
2.5.3 Evaluation of plant performance	22
<b>2.6 CONCLUSIONS</b>	<b>23</b>
<b>2.7 REFERENCES</b>	<b>23</b>



## **Chapter 3**

### ***Model for the prediction of bearing capacity on vegetated tailings***

---

<b>3.1 INTRODUCTION</b>	<b>38</b>
<b>3.2 BACKGROUND</b>	<b>39</b>
<b>3.3 MODEL DEVELOPMENT</b>	<b>42</b>
3.3.1 Continuity of liquid phase	42
3.3.2 Continuity of solids phase	42
3.3.3 Darcy's law	42
3.3.4 Material coordinate system	44
3.3.5 Saturated condition	45
3.3.6 Unsaturated condition	47
3.3.7 Root water uptake, sink term	49
3.3.8 Root growth model	52
<b>3.4 NUMERICAL APPROACH</b>	<b>52</b>
<b>3.5 BOUNDARY CONDITIONS</b>	<b>54</b>
<b>3.6 HYDRAULIC CONDUCTIVITY</b>	<b>56</b>
<b>3.7 BEARING CAPACITY</b>	<b>57</b>
3.7.1 Calculation of $c_v$	58
3.7.2 Calculation of $c_R$	59
<b>3.8 MODEL BEHAVIOR</b>	<b>60</b>
<b>3.9 CONCLUSIONS</b>	<b>62</b>
<b>3.10 REFERENCES</b>	<b>62</b>

## **Chapter 4**

### ***Plant dewatering of tailings: experimental results and model predictions***

---

<b>4.1 INTRODUCTION</b>	<b>74</b>
<b>4.2 BACKGROUND</b>	<b>75</b>
<b>4.3 LABORATORY PROGRAM</b>	<b>76</b>
4.3.1 Materials and method	76
4.3.2 Measurements	78
<b>4.4 EXPERIMENTAL RESULTS</b>	<b>79</b>
<b>4.5 MODEL CALIBRATION/VALIDATION</b>	<b>80</b>
4.5.1 Model data input	81
4.5.2 Settlement predictions	85
4.5.3 Solids content profile predictions	85
4.5.4 Bearing capacity predictions	86
<b>4.6 PRACTICAL IMPLICATIONS</b>	<b>86</b>
<b>4.7 CONCLUSIONS</b>	<b>87</b>
<b>4.8 REFERENCES</b>	<b>88</b>

## **Chapter 5**

### ***Response of plants to oil sand tailings***

---

<b>5.1 INTRODUCTION</b>	<b>103</b>
<b>5.2 MATERIALS AND METHOD</b>	<b>105</b>
5.2.1 Composite tailings	105
5.2.2 Plant material and growth room conditions	106
5.2.3 Measurements	107
5.2.4 Statistical analysis	108
<b>5.3 EXPERIMENTAL RESULTS</b>	<b>108</b>
<b>5.4 DISCUSSION</b>	<b>111</b>
<b>5.5 CONCLUSIONS</b>	<b>112</b>
<b>5.6 REFERENCES</b>	<b>112</b>

## **Chapter 6**

### ***Prediction of bearing capacity of vegetated composite tailings***

---

<b>6.1 INTRODUCTION</b>	<b>120</b>
<b>6.2 SETTING</b>	<b>122</b>
<b>6.3 POTENTIAL EVAPOTRANSPIRATION</b>	<b>122</b>
<b>6.4 BOUNDARY AND INITIAL CONDITIONS</b>	<b>124</b>
<b>6.5 MODEL RESULTS</b>	<b>125</b>
6.5.1 Tailings deposit 5 m deep	125
6.5.2 Optimum CT deposit depth	127
<b>6.6 SENSITIVITY ANALYSIS</b>	<b>127</b>
<b>6.7 CONCLUSIONS</b>	<b>129</b>
<b>6.8 REFERENCES</b>	<b>130</b>

## **Chapter 7**

### ***Summary and conclusions***

---

<b>7.1 RESEARCH OBJECTIVES</b>	<b>140</b>
<b>7.2 CONCLUSIONS</b>	<b>141</b>
<b>7.3 SUGGESTED FUTURE RESEARCH</b>	<b>144</b>

## **Appendix A**

### ***Summary of results of the greenhouse experiment Phase 1 and Phase 2***

---

<b>A.1 INTRODUCTION</b>	<b>147</b>
<b>A.2 SEEDING</b>	<b>147</b>
<b>A.3 FERTILIZER CALCULATION</b>	<b>148</b>
A.3.1 Ratio	148
A.3.2 Analysis	148

**Appendix B*****TDR and neutron probe calibrations and measurements of solids contents***

---

B.1 INTRODUCTION	155
B.2 TDR AND NEUTRON PROBE CALIBRATION CURVES	156
B.3 SOLIDS CONTENT MEASUREMENTS	157
B.4 REFERENCES	157

**Appendix C*****Plate Load Test results***

---

C.1 INTRODUCTION	194
C.2 RESULTS	194

**Appendix D*****Plant measurements***

---

214

**Appendix E*****Surface settlement, model prediction, growth room ambient measurements and watering***

---

227

**Appendix F*****Climatic data and calculated  $ET_0$  for Fort McMurray for 1997 and 1998***

---

241

**Appendix G*****Input and output data and source code of the plant dewatering model***

---

254

G.1 INTRODUCTION
G.2 INPUT DATA SAMPLES
G.3 SAMPLE OF MODEL RESULTS
G.4 COMPUTER CODE OF THE PLANT DEWATERING MODEL

## List of Tables

---

Table 2.1	Plant species selected for testing	33
Table 2.2	Chemical analyses of CT and CMT samples	33
Table 2.3	Micronutrient status of CT and CMT	34
Table 2.4	Chemical composition of CT release water and CMT process water	34
Table 2.5	Chemical analyses of CT and CMT samples at beginning of phase 2	35
Table 2.6	Chemical analyses of five CT samples at end of phase 2	35
Table 2.7	Summary of plant behavior assessment for CT phase 2	36
Table 2.8	Chemical analyses of four CMT samples at end of phase 2	37
Table 2.9	Summary of plant behavior assessment for CMT phase 2	37
<hr/>		
Table 4.1	Fitting parameters of the S-shape curve that describes the LAI of plants	102
Table 4.2	Predicted and measured bearing capacity results	102
<hr/>		
Table 5.1	Chemical composition of CT	118
Table 5.2	Shoot and root dry weights	118
Table 5.3	Summary of plant behavior assessment	119
<hr/>		
Table 6.1	Comparison of climatic data for 1997 and 1998 to a long term average	138
Table 6.2	Tailings and plant parameters used in the model	139
<hr/>		
Table A.1	Summary of ET measured on CT in Phase 1 (ET is in grams)	150
Table A.2	Summary of ET measured on CMT in Phase 1 (ET is in grams)	152
Table A.3	Temporal variations of average ET on CT and CMT in Phase 1	153
Table A.4	Temporal variations of average ET on CT and CMT in Phase 2	154
<hr/>		
Table D.1	Summary of leaf areas and LAI	218
Table D.2	Fitting parameters of the S-shape curve, which describes LAI of plants	222
Table D.3	Dry shoot weights of plants	226
<hr/>		
Table E.1	Measurements of temperature, relative humidity and pan evaporation taken on the growth room (Day 26 corresponds to March 3, 1998)	239
Table E.2	Amount of water added to each lysimeter (Day 40 corresponds to March 17, 1998)	240

Table F.1	Climatic data and calculated potential evapotranspiration for May, 1997	242
Table F.2	Climatic data and calculated potential evapotranspiration for June, 1997	243
Table F.3	Climatic data and calculated potential evapotranspiration for July, 1997	244
Table F.4	Climatic data and calculated potential evapotranspiration for August, 1997	245
Table F.5	Climatic data and calculated potential evapotranspiration for September, 1997	246
Table F.6	Climatic data and calculated potential evapotranspiration for October, 1997	247
Table F.7	Climatic data and calculated potential evapotranspiration for May, 1998	248
Table F.8	Climatic data and calculated potential evapotranspiration for June, 98	249
Table F.9	Climatic data and calculated potential evapotranspiration for July, 1998	250
Table F.10	Climatic data and calculated potential evapotranspiration for August, 1998	251
Table F.11	Climatic data and calculated potential evapotranspiration for September, 1998	252
Table F.12	Climatic data and calculated potential evapotranspiration for October, 1998	253

---

Table G.1	Initial solids content input data	254
Table G.2	Rainfall, ET and root growth input data	255
Table G.3	Main data input	256
Table G.4	Model output data	257

## List of Figures

---

Figure 2.1	Evapotranspiration of CT phase 1 after 70 days (mean of 3 replicates)	27
Figure 2.2	Root depth into CT phase 1 (mean of 3 replicates)	27
Figure 2.3	Plant biomass on CT phase 1 (mean of 3 replicates)	28
Figure 2.4	Evapotranspiration of CMT phase 1 after 69 days (mean of 3 replicates)	28
Figure 2.5	Root depth into CMT phase 1 (mean of 3 replicates)	29
Figure 2.6	Plant biomass on CMT phase 1 (mean of 3 replicates)	29
Figure 2.7	Evapotranspiration of CT phase 2 after 56 days (mean of 3 replicates)	30
Figure 2.8	Root depth on CT phase 2 (mean of 3 replicates)	30
Figure 2.9	Plant biomass on CT phase 2 (mean of 3 replicates)	31
Figure 2.10	Evapotranspiration of CMT phase 2 after 56 days (mean of 3 replicates)	31
Figure 2.11	Root depth into CMT phase 2 (mean of 3 replicates)	32
Figure 2.12	Plant biomass on CMT phase 2 (mean of 3 replicates)	32
<hr/>		
Figure 3.1	Spatial and material coordinate systems	67
Figure 3.2	Tailings deposit	67
Figure 3.3	Root water uptake from a compartment	68
Figure 3.4	Linear water uptake distribution	68
Figure 3.5	Limited available water function	69
Figure 3.6	Finite difference scheme on the depth-time region	69
Figure 3.7	System of simultaneous linear equations	70
Figure 3.8	Scheme of the plant dewatering model	70
Figure 3.9	Comparison of excess pore water pressures	71
Figure 3.10	Tailings-water interface settlement	72
Figure 3.11	Isothermal infiltration	73
<hr/>		
Figure 4.1	Lysimeter layout	90
Figure 4.2	Bearing capacity tests	90
Figure 4.3	Mean measured solids content profiles at the end of the tests	91
Figure 4.4	Root biomass profile	91
Figure 4.5	Average bearing capacity test results	92
Figure 4.6	Leaf area index	93
Figure 4.7	Correlation of global cohesion	93
Figure 4.8	Tailings settlement (reed canary grass)	94
Figure 4.9	Tailings settlement (streambank wheatgrass)	94

Figure 4.10	Solids content profile (Altai wildrye)	95
Figure 4.11	Solids content profile (control)	96
Figure 4.12	Solids content profile (creeping foxtail)	97
Figure 4.13	Solids content profile (red top)	98
Figure 4.14	Solids content profile (reed canarygrass)	99
Figure 4.15	Solids content profile (streambank wheatgrass)	100
Figure 4.16	Bearing capacity results	101
<hr/>		
Figure 5.1	Lysimeter layout	114
Figure 5.2	Temporal variations in plant height	114
Figure 5.3	Temporal variations in Leaf area index (LAI)	115
Figure 5.4	Root biomass profile	115
Figure 5.5	Electrical conductivity profile at end of experiment	116
Figure 5.6	pH profile at end of experiment	116
Figure 5.7	Cumulative evapotranspiration	117
Figure 5.8	Mean measured solids content profiles at the end of the tests	117
<hr/>		
Figure 6.1	Conceptual model with boundary conditions	131
Figure 6.2	Solids content profile on a 5-m-initial deposit depth	132
Figure 6.3	Bearing capacity profile on a 5-m-initial deposit depth	132
Figure 6.4	Solids content profiles for different initial deposit depths at the end of 1997 (1 year of plant growth)	133
Figure 6.5	Bearing capacities profiles on different initial deposit depths at the end of 1997 (1 year of plant growth)	133
Figure 6.6	Solids content profiles for different initial deposit depths at the end of 1998 (2 years of plant growth)	134
Figure 6.7	Bearing capacities profiles on different initial deposit depths at the end of 1998 (2 years of plant growth)	134
Figure 6.8	Solids content profile variations caused by changes in the saturated hydraulic conductivity parameter C	135
Figure 6.9	Bearing capacity profile variations caused by changes in the saturated hydraulic conductivity parameter C	135
Figure 6.10	Solids content profile variations caused by changes in the unsaturated hydraulic conductivity parameter P	136
Figure 6.11	Bearing capacity profile variations caused by changes in the unsaturated hydraulic conductivity parameter P	136
Figure 6.12	Solids content profile variations caused by changes in the parameters d of the equation of the SWCC	137

---

Figure B.1	TDR calibration curve	158
Figure B.2	Neutron probe calibration curve	150
Figure B.3	Solids content profile of Altai wildrye measured on February 24, 1998	159
Figure B.4	Solids content profile of Altai wildrye measured on March 3, 1998	159
Figure B.5	Solids content profile of Altai wildrye measured on March 10, 1998	160
Figure B.6	Solids content profile of Altai wildrye measured on March 16, 1998	160
Figure B.7	Solids content profile of Altai wildrye measured on March 23, 1998	161
Figure B.8	Solids content profile of Altai wildrye measured on March 31, 1998	161
Figure B.9	Solids content profile of Altai wildrye measured on April 10, 1998	162
Figure B.10	Solids content profile of Altai wildrye measured on April 15, 1998	162
Figure B.11	Solids content profile of Altai wildrye measured on April 20, 1998	163
Figure B.12	Solids content profile of Altai wildrye measured on May 12, 1998	163
Figure B.13	Solids content profile of control measured on February 19, 1998	164
Figure B.14	Solids content profile of control measured on March 3, 1998	164
Figure B.15	Solids content profile of control measured on March 10, 1998	165
Figure B.16	Solids content profile of control measured on March 16, 1998	165
Figure B.17	Solids content profile of control measured on March 23, 1998	166
Figure B.18	Solids content profile of control measured on March 31, 1998	166
Figure B.19	Solids content profile of control measured on April 10, 1998	167
Figure B.20	Solids content profile of control measured on April 15, 1998	167
Figure B.21	Solids content profile of control measured on April 20, 1998	168
Figure B.22	Solids content profile of control measured on May 12, 1998	168
Figure B.23	Solids content profile of creeping foxtail measured on February 19, 1998	169
Figure B.24	Solids content profile of creeping foxtail measured on March 3, 1998	169
Figure B.25	Solids content profile of creeping foxtail measured on March 10, 1998	170
Figure B.26	Solids content profile of creeping foxtail measured on March 16, 1998	170
Figure B.27	Solids content profile of creeping foxtail measured on March 23, 1998	171
Figure B.28	Solids content profile of creeping foxtail measured on March 31, 1998	171
Figure B.29	Solids content profile of creeping foxtail measured on April 10, 1998	172
Figure B.30	Solids content profile of creeping foxtail measured on April 15, 1998	172
Figure B.31	Solids content profile of creeping foxtail measured on April 20, 1998	173
Figure B.32	Solids content profile of creeping foxtail measured on May 12, 1998	173
Figure B.33	Solids content profile of red top measured on February 19, 1998	174



Figure B.34	Solids content profile of red top measured on March 3, 1998	174
Figure B.35	Solids content profile of red top measured on March 10, 1998	175
Figure B.36	Solids content profile of red top measured on March 16, 1998	175
Figure B.37	Solids content profile of red top measured on March 23, 1998	176
Figure B.38	Solids content profile of red top measured on March 31, 1998	176
Figure B.39	Solids content profile of red top measured on April 10, 1998	177
Figure B.40	Solids content profile of red top measured on April 15, 1998	177
Figure B.41	Solids content profile of red top measured on April 20, 1998	178
Figure B.42	Solids content profile of red top measured on May 12, 1998	178
Figure B.43	Solids content profile of reed canarygrass measured on February 19, 1998	179
Figure B.44	Solids content profile of reed canarygrass measured on March 3, 1998	179
Figure B.45	Solids content profile of reed canarygrass measured on March 10, 1998	180
Figure B.46	Solids content profile of reed canarygrass measured on March 16, 1998	180
Figure B.47	Solids content profile of reed canarygrass measured on March 23, 1998	181
Figure B.48	Solids content profile of reed canarygrass measured on March 31, 1998	181
Figure B.49	Solids content profile of reed canarygrass measured on April 10, 1998	182
Figure B.50	Solids content profile of reed canarygrass measured on April 15, 1998	182
Figure B.51	Solids content profile of reed canarygrass measured on April 20, 1998	183
Figure B.52	Solids content profile of reed canarygrass measured on May 12, 1998	183
Figure B.53	Solids content profile of streambank wheatgrass measured on February 19, 1998	184
Figure B.54	Solids content profile of streambank wheatgrass measured on March 3, 1998	184
Figure B.55	Solids content profile of streambank wheatgrass measured on March 10, 1998	185
Figure B.56	Solids content profile of streambank wheatgrass measured on March 16, 1998	185
Figure B.57	Solids content profile of streambank wheatgrass measured on March 23, 1998	186
Figure B.58	Solids content profile of streambank wheatgrass measured on March 31, 1998	186
Figure B.59	Solids content profile of streambank wheatgrass measured on April 10, 1998	187
Figure B.60	Solids content profile of streambank wheatgrass measured on April 15, 1998	187
Figure B.61	Solids content profile of streambank wheatgrass measured on April 20, 1998	188
Figure B.62	Solids content profile of streambank wheatgrass measured on May 12, 1998	188
Figure B.63	Solids content profile of Altai wildrye 1 at end of experiment	189
Figure B.64	Solids content profile of Altai wildrye 2 at end of experiment	189
Figure B.65	Solids content profile of Altai wildrye 9 at end of experiment	189
Figure B.66	Solids content profile of creeping foxtail 5 at end of experiment	190
Figure B.67	Solids content profile of creeping foxtail 12 at end of experiment	190
Figure B.68	Solids content profile of creeping foxtail 18 at end of experiment	190
Figure B.69	Solids content profile of red top 3 at end of experiment	191

Figure B.70	Solids content profile of red top 11 at end of experiment	191
Figure B.71	Solids content profile of red top 16 at end of experiment	191
Figure B.72	Solids content profile of reed canarygrass 4 at end of experiment	192
Figure B.73	Solids content profile of reed canarygrass 13 at end of experiment	192
Figure B.74	Solids content profile of reed canarygrass 15 at end of experiment	192
Figure B.75	Solids content profile of streambank wheatgrass 7 at end of experiment	193
Figure B.76	Solids content profile of streambank wheatgrass 14 at end of experiment	193
Figure B.77	Solids content profile of streambank wheatgrass 17 at end of experiment	193

---

Figure C.1	Plate load test apparatus	195
Figure C.2	PLT results on three different layers of Altai wildrye 1	196
Figure C.3	PLT results on three different layers of Altai wildrye 2	197
Figure C.4	PLT results on three different layers of Altai wildrye 9	198
Figure C.5	PLT results on two different layers of control 6	199
Figure C.6	PLT results on two different layers of control 8	200
Figure C.7	PLT results on two different layers of control 10	201
Figure C.8	PLT results on three different layers of creeping foxtail 5	202
Figure C.9	PLT results on three different layers of creeping foxtail 12	203
Figure C.10	PLT results on three different layers of creeping foxtail 18	204
Figure C.11	PLT results on three different layers of red top 3	205
Figure C.12	PLT results on three different layers of red top 11	206
Figure C.13	PLT results on three different layers of red top 16	207
Figure C.14	PLT results on three different layers of reed canarygrass 4	208
Figure C.15	PLT results on three different layers of reed canarygrass 13	209
Figure C.16	PLT results on three different layers of reed canarygrass 15	210
Figure C.17	PLT results on three different layers of streambank wheatgrass 7	211
Figure C.18	PLT results on three different layers of streambank wheatgrass 14	212
Figure C.19	PLT results on three different layers of streambank wheatgrass 17	213

---

Figure D.1	Temporal variations in plant height of altai wildrye	215
Figure D.2	Temporal variations in plant height of creeping foxtail	215
Figure D.3	Temporal variations in plant height of red top	216
Figure D.4	Temporal variations in plant height of reed canarygrass	216
Figure D.5	Temporal variations in plant height of streambank wheatgrass	217
Figure D.6	LAI and fitting curve of Altai wildrye	220
Figure D.7	LAI and fitting curve of creeping foxtail	220

Figure D.8	LAI and fitting curve of red top	221
Figure D.9	LAI and fitting curve of creeping foxtail	221
Figure D.10	LAI and fitting curve of streambank wheatgrass	222
Figure D.11	Root biomass of Altai wildrye	223
Figure D.12	Root biomass of creeping foxtail	223
Figure D.13	Root biomass of red top	224
Figure D.14	Root biomass of reed canarygrass	224
Figure D.15	Root biomass of streambank wildrye	225

---

Figure E.1	Measured and fitted Soil Water Characteristic Curve (SWCC) of CT	228
Figure E.2	Unsaturated hydraulic conductivity of CT	228
Figure E.3	Tailings settlement on Altai wildrye	229
Figure E.4	Tailings settlement on control	229
Figure E.5	Tailings settlement on creeping foxtail	230
Figure E.6	Tailings settlement on red top	230
Figure E.7	Tailings settlement on reed canarygrass	231
Figure E.8	Tailings settlement on streambank wheatgrass	231
Figure E.9	Measured and predicted solids content profile of Altai wildrye	232
Figure E.10	Measured and predicted solids content profile of control	233
Figure E.11	Measured and predicted solids content profile of creeping foxtail	234
Figure E.12	Measured and predicted solids content profile of red top	235
Figure E.13	Measured and predicted solids content profile of reed canarygrass	236
Figure E.14	Measured and predicted solids content profile of streambank wheatgrass	237
Figure E.15	Measured and predicted bearing capacity	238

## List of symbols and abbreviations

---

The units used in variables or symbols are defined the first time they occur in each chapter.

ANOVA	analysis of variance
B	boron or width of footing base
$B_R$	biomass of roots per unit volume of soil
$B_{Rtop}$	root biomass at the tailings surface
$B_{Rtopm}$	root biomass at the tailings surface at the time of maturity
Ca	calcium
Cl	chloride
CMT	copper mine tailings
CT	composite tailings, consolidated tailings
c	global cohesion
$c'$	effective cohesion of a saturated soil
$c_p$	specific heat of air
Cu	copper
$c_R$	increased effective soil cohesion due to root matrix reinforcement
$c_v$	increased effective soil cohesion due to suction
$D_f$	depth of footing base
dS	deci-Siemen
$\Delta$	slope of the saturation vapor pressure-temperature curve
$\Delta T_{ai}$	actual root water uptake from compartment i
$\Delta T_{pi}$	plant transpiration in compartment i
e	void ratio
$e_{z_0}$	actual vapor pressure
$e_z$	saturation vapor pressure
$E_a$	actual evaporation
$E_{at}$	aerodynamic transport term
$E_0$	potential evaporation
EC	electrical conductivity
ET	evapotranspiration
$ET_0$	potential evapotranspiration
Fe	iron
f(u)	wind function
f( $u_w$ )	soil suction function
$\phi'$	effective angle of internal friction of a saturated soil
G	soil heat flux
$G_s$	specific gravity
$\gamma$	unit weight of tailings
$\gamma_c$	psychrometric constant
$\gamma_w$	unit weight of water
ha	hectare
$h_d$	displacement height for a crop
$K_a$	dielectric constant
k	von Karman constant
$k_c$	crop coefficient
K	potassium or hydraulic conductivity
$K_{evap}$	evaporation limiting factor
$K_R$	root coefficient
$K_s$	saturated hydraulic conductivity
$K_2O$	potash
LAI	leaf area index
LAW	limited available water

$\lambda$	latent heat of vaporization
MFT	mature fine tailings
Mg	magnesium
Mn	manganese
N	nitrogen
n	porosity
Na	sodium
P	precipitation
$P_a$	atmospheric pressure
$P_0$	surcharge pressure
$P_2O_5$	phosphoric acid
ppm	part per million
q	water flow between compartments
$q_f$	ultimate bearing capacity
$r_a$	aerodynamic resistance
$r_c$	surface resistance
RH	relative humidity
$R_n$	net radiation
$R_s$	solar radiation
$\rho, \rho_a$	air density
$(\sigma_n - u_a)$	net normal stress
$\sigma$	total stress
$\sigma'$	effective stress
SAR	sodium adsorption ratio
$S_e$	effective saturation
$S_r$	degree of saturation
t	time
$t_m$	time to plant maturity
T	temperature, sink term or actual transpiration
$T_{max}$	maximum temperature
$T_{min}$	minimum temperature
TDR	time domain reflectometry
$T_0$	potential transpiration
$T_p$	plant transpiration
$\theta$	volumetric water content
$\theta_r$	residual water content
$\theta_s$	saturated water content
$\theta_{wp}$	water content at wilting point
$\Theta(u_a - u_w)$	normalized water content
$\tau$	shear strength
$(u_a - u_w)$	matric suction
$u, u_z$	wind speed at some reference height z
$u_w$	pore water pressure or matric suction (negative pore water pressure)
$u_{wb}$	bubbling pressure or air entry value
$u_{w1}$	matric suction at which soil water begins to limit plant growth
$u_{w2}$	matric suction at wilting point
$u_s$	velocity of solids
$u_w$	velocity of water
$V_s$	volume of solids in a compartment
$V_w$	volume of water in a compartment
$V_{wr}$	volume of water in a compartment at residual water content
$V_{ws}$	volume of water in a compartment at saturated water content
wk	week
y	vertical spatial coordinate
$y_m$	maximum rooting depth

$y_r$	rooting depth
$z$	level above the surface, reference height
$z_0$	vegetation roughness parameter
$Z$	material coordinate system
$Zn$	zinc
$z_{om}$	roughness length of momentum transfer
$z_{ov}$	roughness length of vapor transfer
$z_p$	height of humidity and temperature measurements
$z_w$	height of wind speed measurement

# Chapter 1

## *Introduction*

---

### 1.1 INTRODUCTION

Large volumes of mine waste tailings are generated yearly in Canada and around the world by the mining industry. After ore extraction, a slurry waste consisting of residual ore, water, sand, silt and fine clay particles is hydraulically transported and stored within surface tailings ponds. Without chemical treatment prior to deposition, the fast-settling sand particles segregate from the slurry upon deposition at the edge of the tailings ponds while the finer fraction, which is known as fine tailings, accumulates in the center of the pond. The different types of fine tailings generated by the mining industry include phosphatic clays, bauxite red muds, fine taconite tailings and slimes from the oil sands tailings (Vick 1983). As an example, the total volume of fine mine waste produced by the Oil sands operating in northern Alberta is expected to exceed 1 billion cubic meters by the year 2020 (Lui et al. 1994). Currently, there is in storage approximately 400 million cubic meters of mature fine tailings (MFT) at a gravimetric water content of 233% deposited in Alberta.

The major geoenvironmental issues associated with the contents of tailings ponds are their instability and incapability of supporting the weight of animals or machines for a long period of time. Reclamation of these tailings to a desired dry landscape will not be possible until the surface of the deposit is capable of supporting human traffic. The slow rate of consolidation of existing tailings is compounded by the continuous addition of new fine tailings from the ongoing extraction process.

There has been a need to find innovative, environmentally acceptable, economic and technically feasible ways to dewater high water content tailings and enhance their surface stability. The adoption and engineering of natural processes to enhance strength and surface stability of tailings has been viewed as achieving environmental and economical harmony. Evaporation, freeze-thaw consolidation, evapotranspiration and plant root reinforcement are the key natural processes that were highlighted by Stahl (1996) as a result of detailed site investigation activities undertaken at two different mine sites.

The freeze-thaw consolidation mechanism has been used to dewater fine tailings and is well understood (Sego et al. 1994). This technique can only be utilized in mine sites located in cold regions. Freezing of saturated high void ratio fine tailings during winter months, followed by spring and summer thaw, encourage structural enhancement including consolidation/volume reduction and strength gain.

The evaporation process has been used to dewater tailings of the Florida phosphate industry (McFarlin et al. 1989) and Alberta oil sands (Cuddy and Lahaie 1993; Johnson et al. 1993; Li and Feng 1995). As tailings surfaces desaturate with evaporation, the evaporative flux decreases and the depth of soil enhancement through dewatering becomes limited. The most characteristic feature of tailings is the development of surficial salt crusts during periods of drying. These crusts interfere with the evaporation process to such an extent that in some cases the evaporation rate can be reduced to 12% of potential evaporation (Qiu and Segó 1998). Burns et al. (1993) highlighted that effective dewatering of oil sands tailings can only occur if thin layers (10 to 20 cm) are placed and dewatered. Therefore, dewatering of tailings by means of pure evaporation is generally not economically feasible because of the vast areas and quantities of tailings involved in land disposal operations.

The use of plants to dewater tailings has been identified as a mechanism, which economically enhances the surface stability of these weak deposits on a large scale. Experimental results by Stahl (1996) and Johnson et al. (1993) have shown that suitable plant species are capable of



increasing the strength of weak tailings deposits. Plants growing in tailings have the ability to remove the water through evapotranspiration, ultimately increasing the matric suction in the deposit. This results in an increase in the shear strength and hence bearing capacity in the root zone. Furthermore, the plant root system provides fiber reinforcement, which also contributes to the increased bearing capacity of the rooted tailings. At present, the literature lacks a theoretical formulation that can describe the plant dewatering mechanism of tailings with large strain consolidation and predict the bearing capacity increased due to matric suction and root reinforcement.

The first priority in the investigation of the plant dewatering of tailings was to identify the suitable plant species that can grow in the extremely adverse conditions characteristic of tailings. Plant species must adapt to the particular chemical and physical conditions of the growth medium, the macro- and microclimates and waterlogged conditions. Species lists of potential dewatering plants must be developed on a regional basis to take general climatic effect into account, but additional screening programs are necessary to determine the response of proposed species to special soil conditions. As suggested by Ripley et al. (1978) the ultimate selection of species must remain site specific; that is, the choice will have to be made at each individual mining site based on greenhouse experiments and/or field trials.

Synchrude Canada Ltd. is currently evaluating a technique for solidifying wet slurries that consists of the addition of phosphogypsum ( $\text{CaSO}_4 \cdot 2\text{H}_2\text{O}$ ) to a mixture of tailings cyclone underflow and MFT. This technique produces a nonsegregating tailings stream known as Composite Tailings or Consolidated Tailings (CT). The full evaluation of this technique must proceed in conjunction with the development of reclamation options such that a suitable long-term waste management disposal program can be implemented. In this research CT was prepared by mixing tailings sand, MFT, tailings pond water and gypsum. The amount of gypsum added was approximately  $1200 \text{ g/m}^3$  and the proportion of sand, MFT and water was such that the CT mixture had 20% fines and an initial solids content (dry weight divided by total weight) of approximately 65%.

## **1.2 RESEARCH OBJECTIVES**

The main objective of this research was to study and evaluate the strength enhancement mechanism of suitable plant species growing on high water content tailings.

Specific objectives are summarized as follows:

- Identify the most suitable plant species for dewatering and reclamation of tailings. Two mine tailings were chosen: Composite Tailings (CT) from Alberta oil sands operated by Syncrude Canada Ltd. and Copper Mine Tailings (CMT) from the Kennecott site in Utah.
- Identify the main physical processes that control the plant dewatering mechanism.
- Formulate a theoretical framework to predict the increase of bearing capacity of tailings due to the plant dewatering mechanism.
- Develop a finite difference solution algorithm of the theoretical formulation.
- Conduct a greenhouse experiment to calibrate and validate the proposed numerical model and evaluate the plant response to mine tailings. Composite Tailings (CT) was used as the growth medium.

## **1.3 ORGANIZATION OF THESIS**

This thesis is organized into a series of five fundamental chapters (Chapters 2 through 6). Successive appendices provide detailed investigation results. Each of the chapters has either been published or is awaiting publication in conference proceedings and/or journals. The chapters have been organized in a chronological fashion with each being unique in focus.

**Chapter 2** presents an initial screening program of plants species that can adapt to the particular chemical and physical conditions of mine waste tailings. A two-phase greenhouse experiment was conducted to identify the most suitable species for dewatering and reclamation of Composite Tailings from Alberta oil sands operated by Syncrude Canada Ltd. and Copper Mine Tailings from the Kenecott site in Utah.

**Chapter 3** describes in detail a physical based model for predicting the contributions to bearing capacity of tailings by the strength enhancement mechanisms of plants. The model simulates one dimensional water flow in a tailings deposit of high water content, including the root zone, by solving a transient flow equation coupled with water extraction from within via transpiration. This chapter also outlines a finite difference solution algorithm of the theoretical formulation.

**Chapter 4** presents the results of a greenhouse experiment conducted to calibrate and validate the model developed to simulate the strength enhancement mechanism of plants. Composite Tailings from the Alberta oil sands operated by Syncrude Canada Ltd. was used as the test material. Five plant species, which were recommended in Chapter 2, were utilized in the experiment. The solids content profile, consolidation and bearing capacities that were measured in the greenhouse experiment were compared with their respective predicted values using the model.

**Chapter 5** includes an evaluation of the plant response to oil sand tailings from the greenhouse experiment described in Chapter 4. This chapter presents important plant parameters like plant height, leaf area, root and shoot biomass, evapotranspiration and symptom scale. The last parameter represents an overall assessment of the behavior and response of the plants to the oil sands tailings.

**Chapter 6** provides the results of a Class A prediction of solids content and bearing capacity on a vegetated tailings deposit. Climatic data of 1997 and 1998 from the Fort McMurray region, physical parameters of a recent CT deposit and plant parameters of reed canarygrass were used

as input data. Different deposit depths were analyzed to determine the depth at which optimum dewatering can be achieved. A sensitivity analysis was performed to identify the tailings parameters whose variations greatly affect the model results and whose values are difficult to determine accurately by laboratory means.

**Chapter 7** provides a synopsis of the key topics discussed, conclusions gathered, and provides recommendation for future research pursuits.

**Appendix A** summarizes the water loss from each lysimeter due to evapotranspiration from the plants in the greenhouse experiment described in Chapter 1. **Appendix B** present the calibration curves for the TDR and the neutron probe used to measure the solids content profile in each lysimeter. **Appendix C** presents the figures of the bearing capacity tests conducted in each lysimeter. **Appendix D** summarizes the plant parameters that were measured or calculated during the greenhouse experiment described in Chapter 4. **Appendix E** presents comparisons of measured and predicted values of surface settlement, solids content profiles and bearing capacities. A summary of climatic data measured to characterize the growth room is also included. **Appendix F** summarizes the daily climatic data of 1997 and 1998 from the Fort McMurray region. **Appendix G** presents samples of input and output data and the source code of the plant dewatering model.

#### 1.4 REFERENCES

- Burns, R., Cuddy, G. and Lahaie, R. 1993. Dewatering of fine tails by natural evaporation. Proceedings of the oil sands - Our petroleum future conference (fine tailings symposium), Edmonton, Alberta, April 4-7, Paper F-16.
- Cuddy, G. and Lahaie, R. 1983. Dewatering of mature fine tails by natural evaporation. Syncrude Canada Ltd. Research and Development Research Report 93-01.
- Johson, R.L., Bork, P., Allen, E.A.D., James, W.H., and Koverny, L. 1993. Oil sands sludge dewatering by freeze-thaw and evapotranspiration. Alberta Conservation and Reclamation Council Report No. RRTAC 93-8. ISBN 0-7732-6042-0.

- Li, X., and Feng, Y. 1995. Dewatering fine tails by evaporation: A mathematical modeling approach. Alberta Environmental Center, Vegreville, Alberta. AECV95-R5.
- Lui Y., Caughill, D. Scott, J.D., and Burns, R. 1994. Consolidation of Suncor nonsegregating tailings. Proceedings, 47<sup>th</sup> Canadian Geotechnical Conference, Halifax, Nova Scotia, September 21-23, 1994, pp. 504-513.
- McFarlin, R.F., Lloyd, G.M., and El-Shall, H. 1989. Tailings management of the Florida phosphate industry. In: Tailings and effluent management. Edited by M.E. Chalkley, B.R. Conrad, V.I. Lakshmanan, V.I., and K.G. Wheeland. Proceedings of the International Symposium on Tailings and Effluent Management, Halifax, Nova Scotia, August 20-24, 1989.
- Qiu, Y. and Segó, D.C. 1998. Engineering properties of mine tailings. Proceedings, 51<sup>st</sup> Canadian Geotechnical Conference, Edmonton, Alberta. October 4-7. Vol. 1. pp. 149-154.
- Ripley, E., Redman, R., and Maxwell, J. 1978. Environmental impact of mining in Canada. Center for Resource Studies, Queen University, Kingston, Ontario.
- Segó, D.C., Dawson, R.F., Dereniwski, T., and Burns, B. 1994. Freeze-thaw dewatering to reclaim oil sand fine tails to a dry landscape. Proceedings, 7<sup>th</sup> International Cold Regions Engineering Specialty Conference, Edmonton, Alberta, March 7-9, 1994, pp. 669-688.
- Stahl, R.P. 1996. Characterization and natural processes enhancing dry landscape reclamation of fine processed mine waste. Ph.D. thesis, University of Alberta, Edmonton, Alberta.
- Vick, S.G. 1983. Planning, design and analysis of tailings dams. John Wiley and Sons, New York, New York.

## Chapter 2

### *Plant selection for dewatering and reclamation of tailings<sup>1</sup>*

#### 2.1 INTRODUCTION

Fine tailings are composed mainly of slow-settling fine mineral particles and a large amount of water. They have little or no sand and include phosphatic clays, bauxite red muds, fine taconite tailings, and slimes from the oil sands tailings (Vick 1983). These materials have very high moisture contents, which leads to very low strengths. Thus the tailings must be stored behind a retaining structure capable of retaining heavy fluids. If the water can be removed, the strength of the material can be greatly enhanced, and the volume of water stored can be reduced potentially reducing the cost of the retaining structures.

There is a need to find innovative, environmentally acceptable, economic and technically feasible ways to dewater fine tailings, enhance their surface stability and reduce their volume to generate additional storage space for continued tailings deposition. The use of plants to dewater tailings has been identified as a mechanism, which may economically enhance the surface stability of these weak deposits. Plants growing in fine tailings will have the ability to remove the water through evapotranspiration, increasing the matric suction in the deposit. This results in an increase in the shear strength and bearing capacity in the root zone. Furthermore, the plant root

---

<sup>1</sup> A version of this chapter has been published.

*Silva, M.J., Naeth, M.A., Biggar, K.W., Chanasyk, D.S., and Segó, D.C. 1998. Plant selection for dewatering and reclamation of tailings. Proceedings, 15<sup>th</sup> Annual National Meeting of the American Society for Surface Mining and Reclamation, St. Louis, Missouri, May 17-21, 1998, pp. 104-117.*

system may provide a fiber reinforcement, which should also contribute to the increased bearing capacity of the rooted tailings. Reclamation activities will be facilitated once tailings are stabilized.

Plant species for dewatering of tailings must adapt to the particular chemical and physical conditions of the growth medium, and to the macro- and microclimates. Species lists of potential dewatering plants must be developed on a regional basis to take general climatic effect into account, but additional screening programs will be necessary to determine the response of proposed species to special soil conditions. As suggested by Ripley et al. (1978) and supported by Stahl (1996) the ultimate selection of species must remain site specific; that is, the choice will have to be made at each individual mining site based on greenhouse experiments and/or field trials.

This paper presents the results of a two-phase greenhouse experiment conducted to identify the most suitable plant species for dewatering and reclamation of Composite Tailings (CT) from Alberta oil sands operated by Syncrude Canada Ltd. and Copper Mine Tailings (CMT) from the Kennecott site located in the State of Utah. The selected species will be used in a future greenhouse experiment to quantify the improvement in tailings deposit behavior due to the plant dewatering mechanism.

Both tailings are not phytotoxic as demonstrated by experiments conducted by Johnson et al. (1993) on oil sands tailings and from information provided by Neilson and Peterson (1978) and Barth (1986) on vegetation established on copper mine tailings.

## **2.2 BACKGROUND**

### **2.2.1 Plant dewatering**

The use of plants to dewater high water content materials is an inexpensive technique, which has been accomplished for many years by the Dutch to dewater lacustrine and marine sediments (Public Relations and Information Department of the Netherlands 1959, Shelling 1960, Volker

1982). This drying of wet soils to shallow depths in short time periods is called *polder reclamation*. The ocean bottom sediments with which polder formation begins have an extremely high water content, are low in hydraulic conductivity, and have a low bearing capacity (Rijniersce 1982). The plants accelerate the dewatering process in polders by using large amounts of water and developing deep root systems. Evapotranspiration by plants allows the construction of thicker polders, whereas when relying only on surface evaporation the maximum thickness will be about 20 cm, because the formation of a desiccated crust will inhibit further evaporation. Wuerz (1986) found that roots of alfalfa (*Medicago sativa*) penetrated more than 2 m into the soil in the polders, thereby loosening the soil and forming air channels, which accelerated drainage and consolidation.

Plant dewatering has also been used in dewatering sludge from wastewater treatment facilities, termed reed beds, which were initially built in Austria and southern Germany (Neurohr 1983). In addition, studies conducted by Lee et al. (1976) demonstrated the feasibility of using selected vegetation to dewater and consolidate fine textured dredged materials.

The dewatering capabilities of plants have also been observed in the reclamation of tailings. Barth (1986) recognized that vegetation transpires large quantities of water, thus reducing water entry into tailings and subsequent seepage. He concluded that vegetation is the most effective and least costly means to stabilize tailings against wind and water erosion.

Dean and Havens (1973) compared the cost of different methods for stabilization of tailings. The principal methods included physical, chemical and vegetative. They reported that the vegetative method was the most economical and recommended that wherever applicable it should be a preferred method.

At present, vegetation is the most common and usually preferred stabilization option for tailings impoundments. If a self-perpetuating vegetative cover can be established, not only can wind and water erosion be minimized, but the impoundment can be returned to some semblance of its



original appearance and land use (Vick 1983, Ludeke 1973). Leroy (1973) estimated that a fully vegetated acre of tailings will transpire from 5,000 to 10,000 gallons of water daily (4.5 to 9 mm/day), and eliminate all previous erosion brought about with every precipitation. Presnell (1988) reported that when alfalfa was planted in phosphate tailings in Florida, the clay began to dry out further and significant cracking and splitting of the soil were evident as the soil moisture was withdrawn by the plants. Chosa and Shreton (1976) established a test on an abandoned mined mill wastes from an iron mining process. The species tested were cattails (*Typha latifolia*), reed canarygrass transplants, and willow cuttings (*Salix sp.*). Of the three local species studied for the stabilization of iron mine slime tailings, willow cuttings proved to be most effective. Their extensive root and branching habit helped to increase water removal from the slimes allowing planting of herbaceous vegetation.

Although plant dewatering of tailings has been recognized for a long time, it was not until recently that researchers showed interest in studying the mechanical effects that plants have on the tailings. Oil sands tailings from northeastern Alberta at 50% solids were planted with reed canary grass in trial pits. The tailings were dewatered to 80% solids in one growing season at which they had a shear strength of 120 kPa (Johnson et al. 1993). Stahl (1996) studied changes in surface stability of an 18.2-hectare coal tailings impoundment undergoing reclamation activities since reaching full capacity in 1989. Natural enhancement processes including dewatering through evaporation, evapotranspiration, and fiber reinforcement of plant root systems increased the shear strength of the surficial soils. Bearing capacity and surface stability of the coal tailings within the impoundment also increased. In some cases, the bearing pressure of the rooted tailings were 50 to 60% greater than that of the unrooted tailings at equivalent strain or relative settlement levels.

The formation of root-bound surfaces causes as much stabilization of weak soils as does the loss of water by evapotranspiration. Therefore, the increase of surface stability and bearing capacity of fine tailings cannot be predicted by only considering the net loss of water as the plants develop.

Evaporation only has been used to dewater tailings of the Florida phosphate industry (McFarlin et al. 1989) and Alberta oil sands (Cuddy and Lahaie 1993, Johnson et al. 1993, Li and Feng 1995). As soil surfaces desaturate with evaporation, the evaporative flux decreases and the depth of soil enhancement through dewatering becomes limited. Newson et al. (1996) reported that the depth of influence of evaporative flux on shear strength of saline gold tailings was limited to 10 cm, and Burns et al. (1993) highlighted that effective dewatering of oil sands tailings can only occur if thin layers (10 to 20 cm) are placed. However, because of the slow consolidation rate of tailings, this method requires a long period of time to reclaim the area and return it to a useful state (Bromwell 1982, McLonden et al. 1983, U.S. Bureau of Mines 1975). For consolidation of tailings to occur, substantial drying must take place. Furthermore, this drying must proceed to a considerable depth rather than be limited to the surface. Therefore dewatering by means of pure evaporation is generally not economically feasible because of the vast areas and quantities of tailings involved in land disposal operations.

### **2.2.2 Plant species selection**

An ongoing debate among some reclamation specialists involves the selection of species, and in particular whether native or introduced plant species should be used. A variety of introduced species is available, allowing the selection of those plants that can quickly stabilize the surface by shallow soil-holding root systems, rapid growth rates, and high seed production. The use of introduced species also offers the opportunity for use of special salt-resistant or metal-resistant varieties; an important and sometimes crucial factor in attempts to revegetate the surface of toxic tailings directly without topsoiling (Bradshaw et al. 1978). Introduced species are often preferred because of flexibility in selecting those plant varieties that have characteristics compatible with initial impoundment soil and microclimate conditions. Johnson and Putwain (1981) provided several case histories of the use of native revegetation on iron, bauxite, manganese, nickel, copper, and other types of tailings, demonstrating that revegetation with native species, while often costly and difficult, can be successful in establishing a self-perpetuating cover. Native species often have sporadically low seed production and slower establishment rates, whereas

species best suited to initial dewatering and stabilization should ideally have deep, water-seeking root systems, spreading roots, rapid growth, and high seed production.

The problem of selecting plant species for vegetating a tailings pond is complicated by the fact that the composition of all ponds is different, as are the climatic conditions. Harwood (1979) described the reclamation criteria that plant species must conform to: potential survival in the local climate; suitability to the soil conditions on the surface; rapid growth; soil conditioning capability; forage quality and aesthetics.

Barth (1986) reported that at a copper tailings impoundment in Utah, Japanese millet (Echinochloa crus-galli) was used as a cover crop in wet areas followed by perennial species including salt cedar (Tamarix spp.) and reedgrass (Phragmites australis), while in drier areas annual rye (Secale cereale) was used as a cover crop followed by perennial species that included rangeland alfalfa and tall wheatgrass (Agropyron elongatum). At a taconite tailings impoundment in Minnesota, a mixture of smooth bromegrass, red top, perennial ryegrass (Lolium perenne), alfalfa, and birdsfoot trefoil (Lotus corniculatus) is often used to revegetate the drier coarse tailings products while rye grain, sweet clover (Melilotus alba), alfalfa, and red top are used to revegetate the wetter fine tailings products (Barr Engineering Company 1980). Other factors often important in species selection include drought tolerance, rooting depth, hardiness, propensity to accumulate metals, palatability, availability of seed, frost resistance, ease of propagation, and longevity of established plants. Commonly, field trials are necessary to determine which species are adapted to the particular substrate and climatic conditions at the site and to what degree the growth medium must be changed chemically and physically to support the desired species.

### **2.2.3 Fertilization of tailings**

When low fertility restricts plant growth, appropriate fertilizers may dramatically improve growth. Berg (1972) measured a seven-fold increase in grass yields and a six-fold increase in herbaceous ground cover following nitrogen fertilization of gold tailings from telluride ores. Fertilization rates are high when soil nutrients are low,. Dickinson (1972) and Sidhu (1979) found

that over 1,100 kg/hectare (1,000 lb/acre) of nitrogen, phosphorus and potassium fertilizer was required for successful tailings revegetation. Leroy (1973) used a rate of 1,100 kg/hectare (1,000 lb/acre) in reclamation of tailings in Eastern Canada. Based on greenhouse experiments, Meecham and Bell (1977) recommended that 400 kg of phosphorus per hectare (355 lb/acre) be applied to alumina tailings. However, over-fertilization must be avoided. Michelutti (1974) reported that excess fertilizer stunted plant growth and was more harmful than no fertilizer in sulfide tailings. Nitrogen in quantities of more than 50 kg per hectare (45 lb/acre) seriously hampered legume germination (Dean and Havens 1973). As little as 100 ppm N, 30 ppm P, and 150 ppm K were sufficient to achieve optimal reed canary grass growth on pure sludge from oil sands in Alberta. However, 300 ppm N was excessive, causing a decrease in biomass and general lack of vigor in the plants (Johnson et al. 1993).

## **2.3 MATERIALS AND METHODS**

A two-phase greenhouse experimental program was conducted to identify the most suitable plant species for dewatering and reclamation of oil sands Composite Tailings (CT) and Copper Mine Tailings (CMT). Phase 1 was formulated to identify the most suitable plant species for dewatering mine tailings and to examine which species would be suitable for use in reclamation of these two surface deposits. Phase 2 had the purpose of identifying the plant species which would be tolerant to high levels of salinity and any toxic compounds in the tailings release water.

### **2.3.1 Plant material**

A wide range of plants is available for use in dewatering of tailings. Because potentially large areas need to be managed, seeds should be readily available from suppliers or grown in the area. The seeds should have a high viability and germinate quickly at low temperatures to get an early start when temperatures rise.

A literature review was conducted to screen for plant species that might adapt themselves to the local climatic conditions of the two sites and to the tailings as growth medium. The criteria used for the selection of possible candidates were: seed availability, survival in the local climate, rapid growth, soil reinforcing capability, and tolerance to flooding, drought, high pH and high level of salinity. The most practical and complete guides to plant selection for critical environments on the Canadian prairies and in the northern boreal forests were consulted (Alberta Agriculture 1978, Best and Looman 1979, Hardy BBT Limited 1989, Smoliak et al. 1976, Watson et al. 1980). A total of 15 and 9 plant species were selected for testing in CT and CMT, respectively (Table 2.1).

### **2.3.2 Tailings material, release and process water**

In the fall of 1996, CT and CMT materials and CT release and CMT process water were shipped to the University of Alberta from Syncrude and Kennecott sites, respectively. Two representative samples were taken from each tailings to determine nutrient status, pH and electrical conductivity (EC) (Table 2.2). In CT nitrate, phosphate and potassium levels were deficient, sulfate was optimal for plant growth. In CMT nitrate and phosphate levels were deficient. Potassium and sulfate were at marginal and optimum level, respectively.

Results of micronutrient analyses are shown in Table 2.3. In CT, levels of iron, boron and manganese were adequate for plant growth. Zinc and copper levels were marginal and deficient, respectively. Chloride was in excess. The calculated value of Sodium Adsorption Ratio (SAR) was 1.9, which is less than 13 (Miller and Donahue 1990), therefore CT can be classified as a non-sodic soil. Based on the combined values of SAR and EC, CT can be classified as a normal soil (non-saline and non-sodic). In CMT, iron, manganese and zinc were adequate for plant growth. Boron was deficient, chloride in excess and copper may be toxic. SAR for CMT was 1.0. SAR and EC also classify CMT as a normal soil.

Chemical compositions of CT release water and CMT process water are shown in Table 2.4. Both waters have high EC, which could cause severe problems to plant growth. In CT release water sodium was extremely high, giving a high SAR of 43.1. This makes the water unsuitable for

irrigation. SAR for CMT process water was 6.6, which is not critical. However, its high EC also makes it unsuitable for plant watering.

### **2.3.3 Amount of fertilizer**

To avoid over-fertilization the amount of fertilizer was based on optimum levels of macronutrients required by agronomic species. For CT the fertilizer was added to give an equivalent of 150 kg N/hectare (134 lb N/acre), 80 kg P<sub>2</sub>O<sub>5</sub>/hectare (71 lb P<sub>2</sub>O<sub>5</sub>/acre), and 105 kg K<sub>2</sub>O/hectare (94 lb K<sub>2</sub>O/acre) for non-leguminous species; and 10 kg N/hectare (9 lb N/acre), 75 kg P<sub>2</sub>O<sub>5</sub>/hectare (67 lb P<sub>2</sub>O<sub>5</sub>/acre), and 140 kg K<sub>2</sub>O/hectare (125 lb K<sub>2</sub>O/acre) for leguminous species. For CMT the fertilizer was added to give an equivalent of 145 kg N/hectare (129 lb N/acre), 65 kg P<sub>2</sub>O<sub>5</sub>/hectare (58 lb P<sub>2</sub>O<sub>5</sub>/acre), and 30 kg K<sub>2</sub>O/hectare (27 lb K<sub>2</sub>O/acre) for non-leguminous species; and 10 kg N/hectare (9 lb N/acre), 55 kg P<sub>2</sub>O<sub>5</sub>/hectare (49 lb P<sub>2</sub>O<sub>5</sub>/acre), and 15 kg K<sub>2</sub>O/hectare (13 lb K<sub>2</sub>O/acre) for leguminous species.

### **2.3.4 Methods**

Twenty liter plastic buckets were used as lysimeters with no drainage at the bottom to prevent any water loss other than evapotranspiration. The lysimeters were filled with tailings to a depth of about 30 cm and settlement was allowed to take place. Any expressed water was siphoned off and extra tailings was added to restore the initial level.

Fifteen plants were placed in each lysimeter. Three replicates were used for each treatment and one treatment was left unplanted as a control. The lysimeters were placed in the greenhouse in two randomized complete block designs, one for each type of tailings. Air temperature and hours of light per day were set at 22 °C and 15 hours, respectively.

#### **2.3.4.1 Phase 1**

In Phase 1, CT was used as received from the site, with a solids content of about 80%. The initial solids content of CMT was reduced from 87%, as received from the site, to about 76% by adding

process water. Plants were started from seeds in root trainers and transplanted to the lysimeters after 5 weeks. Distilled water was added weekly to simulate the average amount of local precipitation from June through August. CT and CMT were watered at a rate of 16 and 5.5 mm per week for the first four weeks and at 20 and 4.0 mm for the fifth week, respectively. From the sixth week to the end of the experiment the water added to each lysimeter had to be increased to about 29 mm per week to prevent a loss of plant turgor. Water loss due to evapotranspiration was measured weekly by weighing the lysimeters.

#### **2.3.4.2 Phase 2**

In Phase 2, the initial solids contents were 65% and 76% for CT and CMT, respectively. Plants were started in root trainers, but transplanted after 3 weeks to the lysimeters. CT release water was added to the CT at a rate of 7 mm per week for the first four weeks, after which the rate was increased to 14 mm. CMT process water was added to the CMT material at 14 mm per week.

Observations of stress symptoms, survival and tillering were conducted chronologically in both phases. Depths of root penetration and plant biomass were measured at the end of each phase. Also, samples of tailings selected at random from each block were analyzed for nutrient levels, pH and EC at the end of each phase.

## **2.4 RESULTS**

### **2.4.1 Phase 1**

#### **2.4.1.1 Composite Tailings (CT)**

Results of Phase 1 obtained from CT are presented in Figures 2.1 to 2.3. Water was lost from the lysimeters through evapotranspiration or by evaporation alone in the case of the controls. The total amount of water lost after 70 days of plant growth is schematically illustrated in Figure 2.1. The species with the highest dewatering capability were red top (258 mm), smooth bromegrass

(250 mm) and Altai wildrye (248 mm). The evaporation in the unplanted treatment (control) was 166 mm.

The roots of all species reached the bottom of the lysimeters by growing along the sides of the pails where water was easier to access. However, only a few plants developed roots inside the tailings. Figure 2.2 shows the depths of the roots which grew inside the tailings. Altai wildrye, creeping foxtail and reed canarygrass had roots developed in the tailings to the bottom of the lysimeters (about 30 cm deep) and would likely have gone further if the tailings deposit had been deeper. Streambank wheatgrass developed roots to 23 cm, and both red top and smooth brome grass grew roots to a depth of 18 cm.

Dry biomasses above and below ground are shown in Figure 2.3. Red top produced the highest above ground biomass followed by smooth brome grass, western dock and reed canarygrass. However, reed canarygrass produced the highest below ground biomass.

#### **2.4.1.2 Copper Mine Tailings (CMT)**

Results obtained are presented in Figures 2.4 to 2.6. Total evapotranspiration after 69 days of plant growth are shown in Figure 2.4. The plant species with the highest dewatering capability were Altai wildrye (190 mm), alfalfa (180 mm), creeping foxtail (180 mm), and smooth brome grass (179 mm). The evaporation in the unplanted treatment was 133 mm.

The roots of all species behaved the same way as in the CT; they reached the bottom of the lysimeters along their sides. However, only a few plants developed roots inside the tailings. Figure 2.5 shows the depth of only the roots that grew inside the tailings. Altai wildrye was the only plant that developed roots to the bottom of the lysimeters. Western dock developed roots to 20 cm, and both creeping foxtail and smooth brome grass grew roots to a depth of 10 cm.

Results of dry biomass are illustrated in Figure 2.6. Western dock produced the highest above ground biomass followed by reed canarygrass, Altai wildrye, and timothy. However, only Altai



wildrye had a high root biomass, resulting in a high root to shoot ratio, whereas timothy produced a low root biomass, giving a very low root to shoot ratio. Smooth bromegrass had the highest root biomass and the highest root to shoot ratio.

## **2.4.2 Phase 2**

Nutrient status, pH, and EC of the tailings at the beginning of Phase 2 are shown in Table 2.5. Fertilizer was again added to the tailings to increase the macronutrients to optimum levels.

### **2.4.2.1 Composite Tailings (CT)**

Three-week-old plants were transplanted to CT with an initial solids content of 65%. All plants were flooded for three days with water that was being released from the tailings due to consolidation. A total of about 40-mm of water was siphoned off from each lysimeter leaving the CT with a solids content of approximately 73 %.

CT release water, with an electrical conductivity of 7.14 dS/m, was used to water the plants every week. The addition of this water increased the level of salinity of the CT to extremely toxic levels. At the end of Phase 2, samples of tailings were taken at the top and bottom of five treatments selected at random. The increase of EC was in the range from 15.2 to 27.0 dS/m at the surface, but it did not change significantly at the bottom (Table 2.6).

Figure 2.7 presents the total evapotranspiration for each plant species after 56 days of growth. Creeping foxtail caused the highest water loss (115 mm), followed by Altai wildrye (104 mm), red top (101 mm) and reed canarygrass (99 mm).

Altai wildrye, creeping foxtail and streambank wheatgrass developed roots to the bottom of the lysimeters (about 30 cm) (Figure 2.8). In Phase 2 water was applied at a lower rate and the preferential growth of roots along the sides of the lysimeters was prevented by pressing the material tightly against the wall. This avoided added water accumulating in the space between the

tailings and the pail walls as occurred in Phase 1. In this manner plants were forced to developed roots inside the tailings.

Figure 2.9 shows plant biomass above and below ground. Red top produced the highest dry above ground biomass, followed by creeping foxtail, Altai wildrye and reed canarygrass. Creeping foxtail, Altai wildrye and reed canarygrass produced the highest below ground biomass.

Assessments of the plant response to salt increase were conducted at the beginning of the third week and the eleventh week after transplanting (Table 2.7). Altai wildrye presented the lowest change in symptoms. Creeping foxtail had the highest survival and very strong tillering (vegetative reproduction).

#### **2.4.2.2 Copper Mine Tailings (CMT)**

CMT process water, with an EC of 6.04 dS/m, was used to water the plants every week. The salinity levels at the end of Phase 2 are shown in Table 2.8. The increase of the EC at the surface of the tailings ranged from 28.2 to 40.0 dS/m, but it did not change significantly at the bottom.

Figure 2.10 presents the amount of water removed from each treatment after 56 days of plant growth. Smooth brome grass caused the highest water loss (119 mm), followed by Altai wildrye (117 mm), and creeping foxtail (112 mm).

Altai wildrye, creeping foxtail and smooth brome grass developed the deepest root systems 28, 27 and 27 cm, respectively, followed by alfalfa (23 cm) and reed canarygrass (21 cm) (Figure 2.11).

Altai wildrye produced the highest total dry biomass, followed by smooth brome grass and creeping foxtail (Figure 2.12).

Altai wildrye presented the lowest change in symptoms and had the highest survival and very strong tillering (Table 2.9).

## **2.5 DISCUSSION**

### **2.5.1 Phase 1**

Fifteen plant species were initially selected for testing in Composite Tailings (CT) in Phase 1. All plants survived after a ten-week period. Many of the plants examined in this experiment showed signs of healthy growth, except cattails and willows, which did not grow well in the tailings. Seeds of cattails were not commercially available and plants were started from roots collected from the field. Willows were started from cuttings taken from the field. Both cattails and willows were shocked in the transplant and their growth was stunted during the whole period of Phase 1. In spite of that, the results obtained clearly demonstrate that CT is not phytotoxic and can be used as a medium for plant growth. This conclusion is supported by the low EC and SAR, which class CT as a normal soil.

All of the nine species tested in CMT grew reasonably well. The plants caused significantly less water loss than those in the CT did. A higher EC and high levels of copper may have contributed to a decrease in plant performance. However, all plants presented a healthy growth during the ten-week period of Phase 1.

### **2.5.2 Phase 2**

The successful results obtained in Phase 1 made all plants good candidates for future reclamation activities when the impoundments reach full capacity. Plants, which had the lowest performance in Phase 1, were eliminated for testing in Phase 2.

The application of CT release water, with EC of 7.14 dS/m, dramatically increased the level of salinity at the surface of the CT (0 to 7.5 cm) reaching toxic levels in the range of 15.2 to 27.0 dS/m. The addition of process water to CMT increased its surface (0 to 7.5 cm) salinity in the range from 28.2 to 40.0 dS/m. The salinity level at the bottom of both tailings did not change significantly.

In Phase 2 many plants showed signs of stress due to the high salinity level reached in the tailings. The increase of salt content in the tailings caused a reduction in the osmotic potential of the pore water in the tailings, making this water unavailable for plant use. In this situation, the level of metabolic activity in the plants was reduced. This was accomplished by reducing their biomass through shedding their leaves, or by going into a dormant stage. These symptoms were observed at the end of Phase 2, where many plants had dry leaves with tips curled and dead, and with dying tillers. The high salinity level reached in the tailings subjected the plants to water stress; even though the tailings had still high water content, the soil water was not available to them. Consequently the amount of evapotranspiration was significantly reduced.

### **2.5.3 Evaluation of plant performance**

Plants with the highest evapotranspiration rates had the highest above and below ground biomass, deeper roots, highest survival and lowest stress symptoms. This supports the statement that the dewatering capability of plants is closely linked to their growth and physiological condition. Plant performance was evaluated by using a percentage index based on the following four parameters: total evapotranspiration, root depth, above and below ground biomass for both study phases. The plant with the highest value in each parameter was assigned the index of 100. The indices for the other plants are fractions of 100 calculated from their relative values. Each parameter and each phase were assigned equal weights in the calculation of the final indices. Plants with the highest indices on CT were creeping foxtail (91%), reed canarygrass (88%), Altai wildrye (85%), and red top (84%). The rest of the plants had indices below 75%. In CMT the plants with the highest indices were Altai wildrye (97%), smooth brome grass (78%), and creeping foxtail (70%). The rest had indices below 60%.

The final selection of the most suitable plants was based on a qualitative analysis of percentage index, symptom scale, survival, tillering and past performance.

The plants which performed the best under both phases in Composite Tailings were creeping foxtail, reed canarygrass, Altai wildrye, and red top; and in Copper Mine Tailings were Altai wildrye, smooth brome grass and creeping foxtail.

## **2.6 CONCLUSIONS**

A two-phase greenhouse experimental program was conducted to identify the most suitable plant species for dewatering and reclamation of Composite Tailings (CT) and Copper Mine Tailings (CMT). Based on values of Sodium Adsorption Ratio (SAR) and Electrical Conductivity (EC) both tailings can be classified as normal soils (non-sodic and non-saline soils). Healthy plant growth obtained in Phase 1 of the experiment led to the conclusion that both tailings are not phytotoxic and plants can be used to implement future reclamation activities when the impoundments reach full capacity. Results obtained from Phase 2 were useful to identify plant species tolerant to high levels of salinity and any toxic component contained in the tailings water. Those plants adapted well to extremely toxic levels of salinity and are recommended for future field research for dewatering and reclamation of CT and CMT tailings.

In conclusion, four plant species proved to be the best candidates for future greenhouse and/or field research in CT: creeping foxtail, reed canarygrass, Altai wildrye, and red top. Three species are recommended for further studies in CMT: Altai wildrye, smooth brome grass and creeping foxtail.

## **2.7 REFERENCES**

- Alberta Agriculture. 1978. Perennial grasses for hay and pasture. Alberta Agriculture, Agdex 127/20-4. Edmonton, Alberta.
- Barr Engineering Company. 1980. Enhancement of fish and wildlife resources in the reclamation of hard rock mined lands in the Upper Midwest. U.S. Fish and Wildlife Service, FWS/OBS-80/64.

- Barth, R.C. 1986. Reclamation technology for tailing impoundments, Part 2: Revegetation. Mineral and Energy Resources. Colorado School of Mines. Vol. 29, No. 2.
- Berg, W.A. 1972. Vegetative stabilization of mine wastes. In: 1972 Mining Yearbook. Colorado Mining Association, Denver, Colorado. pp. 24-26.
- Best, K.F. and Looman, J. 1979. Budd's flora of the Canadian Prairie Provinces. Publication No. 1662. Research Branch, Agriculture Canada.
- Bradshaw, A., Humphreys, M., and Johnson, M. 1978. The value of heavy metal tolerance in the revegetation of metalliferous mine wastes. In Environmental management of mineral wastes. Proceedings, NATO advanced study institute on waste disposal and the renewal and management of degraded environments (1973). Edited by G. Goodman and M. Chadwick. Sijthoff & Noordhoff, Netherlands. pp. 311-334.
- Bromwell, L.G. 1982. Evaluation of alternative processes for disposal of fine-grained waste materials. Florida Institute of Phosphate Reserch Publication # 02-020-012.
- Burns, R., Cuddy, G., and Lahaie, R. 1993. Dewatering of fine tails by natural evaporation. Proceedings of the oil sands – Our petroleum future conference (fine tailings symposium), Edmonton, Alberta, April 4-7, Paper F16.
- Chosa, J.A. and Shreton, S.G. 1976. Use of willow cuttings to revegetate the slime areas of iron mine tailings basin. Research No. 21. Michigan Technological University, Fort Forestry Center, L'Anse, Michigan.
- Cuddy, G. and Lahaie, R. 1993. Dewatering of mature fine tails by natural evaporation. Syncrude Canada Ltd. Research and Development Research Report 93-01.
- Dean, K.C. and Havens, R. 1973. Comparative costs and methods for stabilization of tailings. In Tailings disposal today. Edited by C.L. Aplin and G.O. Argalls. Miller Freeman, San Francisco. pp. 450-476.
- Dickinson, S.K. 1972. Experiments in propagating plant cover at tailings basins. Mining Congress Journal, **58**: 21-26.
- Hardy BBT Limited. 1989. Manual of plant species suitability for reclamation in Alberta. Alberta Conservation and Reclamation Council Report No. RRTAC 89-4.
- Harwood, G. 1979. A guide to reclaiming small tailings ponds and dumps. USDA Forest Service, Intermountain Forest and Range Experiment Station. Report INT-57. Ogden, Utah.
- Johnson, R.L., Bork, P., Allen, E.A.D., James, W.H., and Koverny, L. 1993. Oil sands sludge dewatering by freeze-thaw and evapotranspiration. Alberta Conservation and Reclamation Council Report No. RRTAC 93-8. ISBN 0-7732-6042-0.
- Johnson, M. and Putwain, P. 1981. Restoration of native biotic communities on land disturbed by metalliferous mining. Minerals and the Environment, **3**(3): 67-85.

- Lee, C.R., Hoeppe, R.E., Hunt, P.G., and Carlson, C.A. 1976. Feasibility of the functional use of vegetation to filter, dewater, and remove contaminants from dredged material. USAE, WEST Tech, Report D-76-4.
- Leroy, J.C. 1973. How to establish and maintain growth in Canada-cold winters and short growing seasons. In *Tailings disposal today*. Edited by C.L. Aplin and G.O. Argalls. Miller Freeman, San Francisco. pp. 411-449.
- Li, X. and Feng, Y. 1995. Dewatering fine tails by evaporation: A mathematical modelling approach. Alberta Environmental Center, Vegreville, AB. AECV95-R5.
- Ludeke, K.L. 1973. Vegetation stabilization of copper mine tailings disposal berms of Pima Mining Company. In *Tailings disposal today*. Edited by C.L. Aplin and G.O. Argalls. Miller Freeman, San Francisco. pp. 377-386.
- McFarlin, R.F., Lloyd, G.M., and El-Shall, H. 1989. Tailings management of the Florida phosphate industry. In *Tailings and Effluent Management*. Edited by M.E. Chalkley, B.R. Conrad, V.I. Lakshmanan, and K.G. Wheeland. Proceedings of the International Symposium on Tailings and Effluent Management, Halifax, Nova Scotia, August 20-24, 1989.
- McLonden, J.T., Boyle, J.R., and Sweeney, J.W. 1983. A technical evaluation of conventional versus developing processes of phosphatic clay disposal. Florida Institute of Phosphate Research Publication # 02-017-022.
- Meecham, J.R. and Bell, L.C. 1977. Revegetation of alumina refinery wastes, II, Glasshouse Experiments: *Australian Journal of Experimental Agriculture and Animal Husbandry*, **17**: 689-696.
- Michelutti, R.E. 1974. How to establish vegetation on high iron-sulfur mine tailings. *Canadian Mining Journal*, **95**: 54-58.
- Miller, R.W. and Donahue, R.L. 1990. *Soils. An introduction to soils and plant growth*. Sixth edition. Prentice Hall. New York.
- Neurohr, G.A. 1983. Use of Macrophytes for sludge treatment. Proceedings, 6<sup>th</sup> symposium on wastewater treatment, Montreal, Quebec, November 16-17, 1983. pp. 413-430.
- Newson, T., Fujiyasu, Y., and Fahey, M. 1996. A field study of the consolidation behavior of saline gold tailings. Proceedings, Tailings and Mine Waste '96 Conference, Fort Collins, Colorado, January 16-19. pp. 179-188.
- Nielson, R.F., and Peterson, H.B. 1978. Vegetation mine tailings ponds. In *Reclamation of drastically disturbed lands*. Edited by F. Schaller and P. Sutton. American Society of Agronomy. pp. 645-652.
- Presnell, S. 1988. Experimental reclamation and crop growth on waste clay settling pond using an all-terrain vehicle. Engineering foundation conference on dewatering and flocculation. Palm Coast, Florida.

- Public Relations and Information Department of the Netherlands Ministry of Transport and Waterstat. 1959. *From Fisherman's Paradise to Farmer's Pride*. Netherlands Government Information Service. The Hague, Netherlands.
- Rijniersce, K. 1982. A simulation model for physical soil ripening in the IJsselmeerpolders. In *Proceeding of Overdruk uit: Polders of the world: papers international symposium*, Lelistad, Netherlands. September 1982. pp. 407-417.
- Ripley, E., Redman, R., and Maxwell, J. 1978. *Environmental impact of mining in Canada*, Center for Resource Studies, Queen's University, Kingston, Ontario.
- Shelling, J. 1960. *New Aspects of soil classification with particular reference to reclaimed hydromorphic soils*. Transactions, International Society of Soil Science, Seventh International Congress of Soil Science, Amsterdam, Holland, 4: 218-224.
- Sidhu, S.S. 1979. *Revegetation and chemical composition of mine and mill tailings*. ASARCO. Buchans, Newfoundland. Newfoundland Forest Research Center Information Report N-X-175, Canada.
- Smoliak, S., Ware, R.A., and Johnson, A. 1976. *Alberta range plants and their classification*. Alberta Agriculture, Agdex 134/06. Edmonton, Alberta.
- Stahl, R.P. 1996. *Characterization and natural processes enhancing dry landscape reclamation of fine processed mine wastes*. Ph.D. thesis. University of Alberta, Edmonton, Alberta.
- U.S. Bureau of Mines. 1975. *The Florida phosphate slimes problem - a review and bibliography*. IC No. 8668.
- Vick, S.G. 1983. *Planning, design and analysis of tailings dams*. John Wiley and Sons, New York.
- Volker, A. 1982. *Polders: An ancient approach to land reclamation*. *Nature and Resources*, 18: 2-13.
- Watson, L.E., Parker, R.W., and Polster, D.F. 1980. *Manual of plant species suitability for reclamation in Alberta*. Alberta Land Conservation and Reclamation Council. Report #RRTAC 80-5. Edmonton, Alberta.
- Warncke, D.D. 1979. *Testing greenhouse growing media: Update and Research*, Crop and Soil Science department, Michigan State University, presented at the 7<sup>th</sup> Soil Plant Analysts' Workshop, Bridgeton, Missouri, 1979.
- Wuerz, W. 1986. *Methods of successes in agricultural and forest reclamation in German lignite Mines..* In *The national mined land reclamation conference*. Edited by C. Carlson and J. Swisher. St. Louis, Missouri, October 28-29, 1986. pp. 173-186



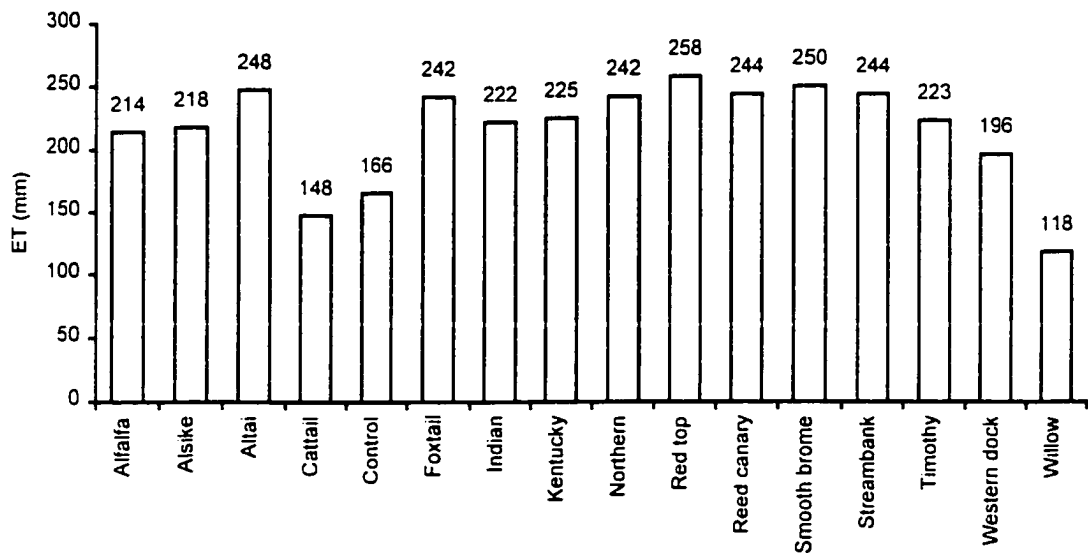


**Figure 2.1** Evapotranspiration of CT phase 1 after 70 days

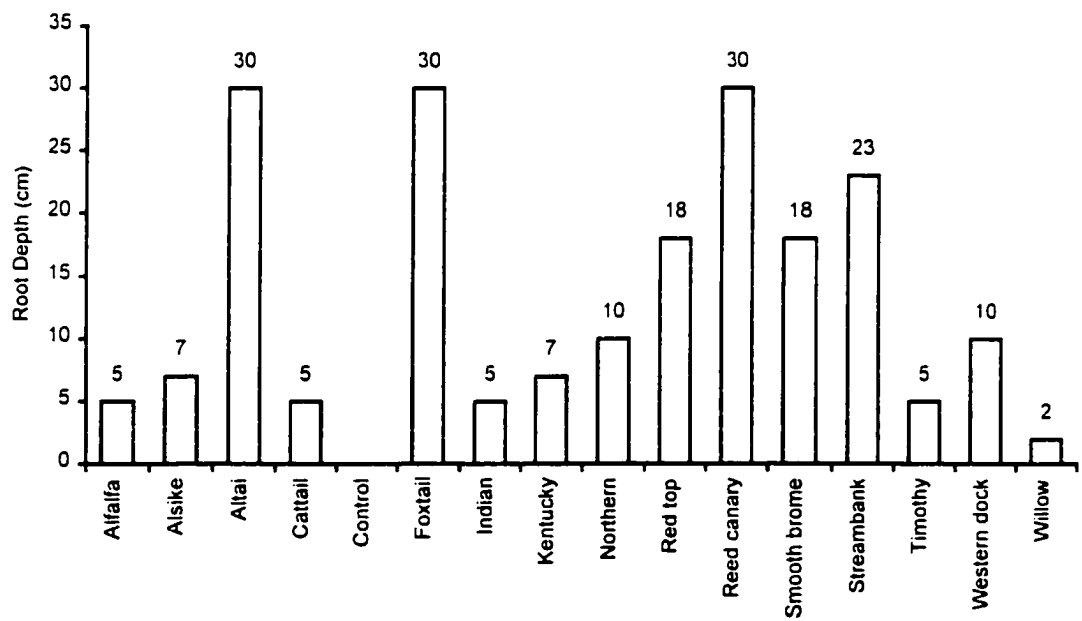


**Figure 2.2** Root depth into CT phase 1

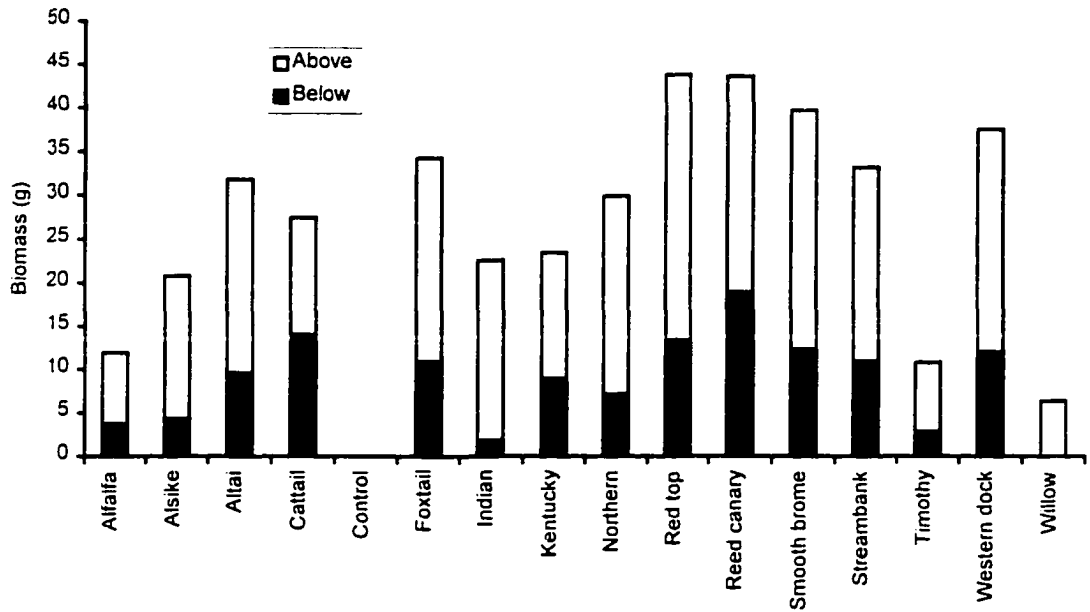


**Figure 2.3 Plant biomass on CT phase 1**

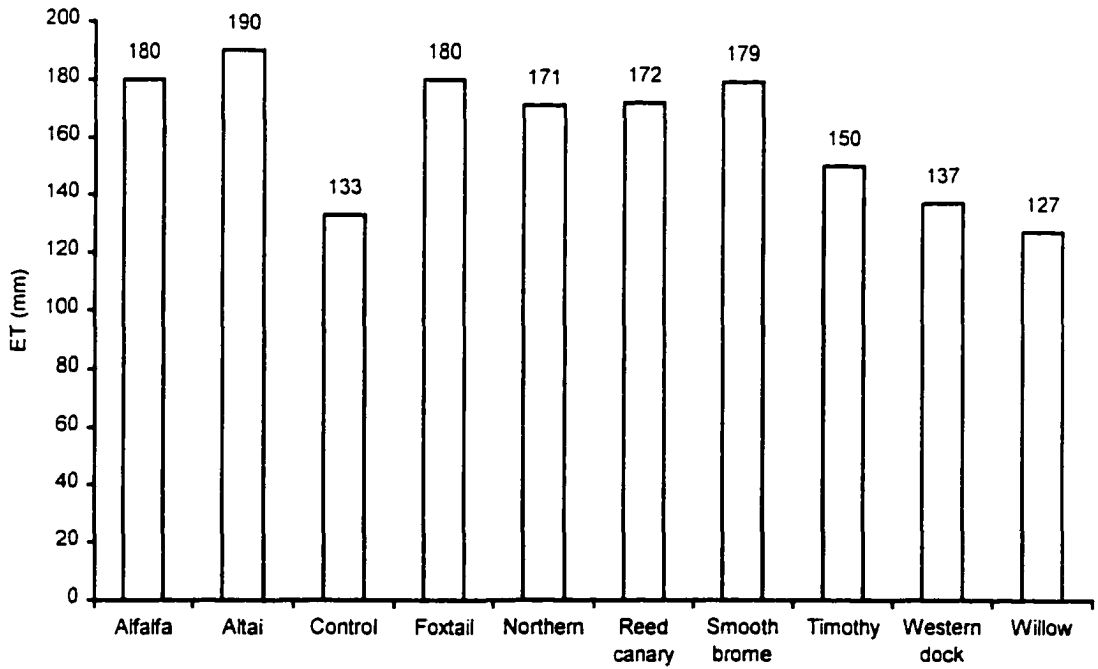


**Figure 2.4 Evapotranspiration of CMT phase 1 after 69 days**

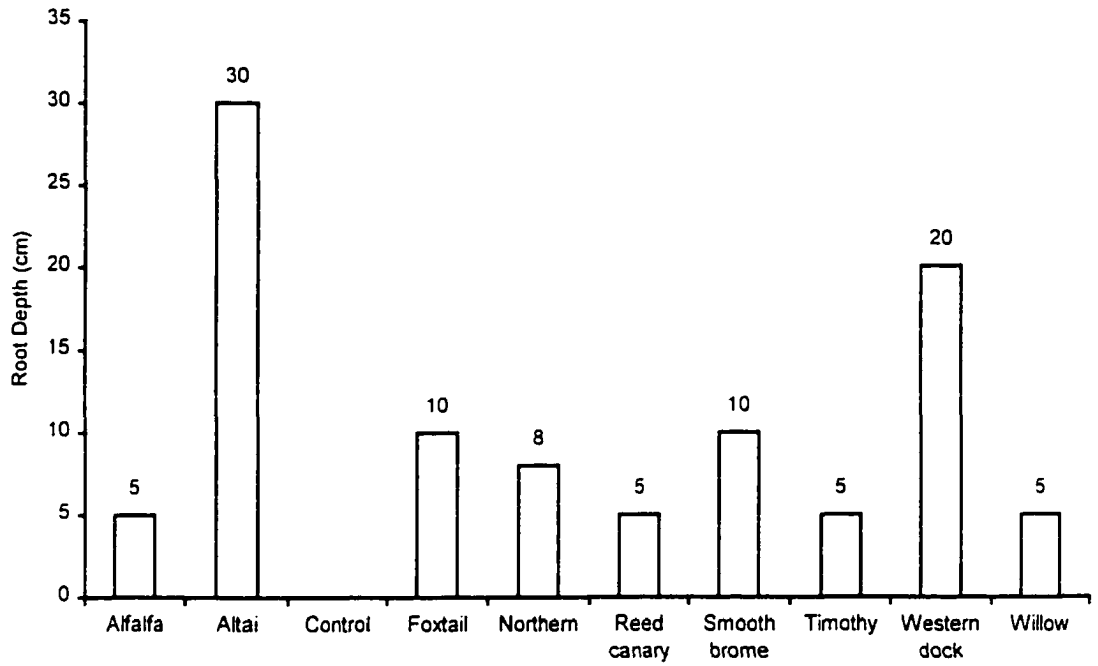


**Figure 2.5 Root depth into CMT phase 1**

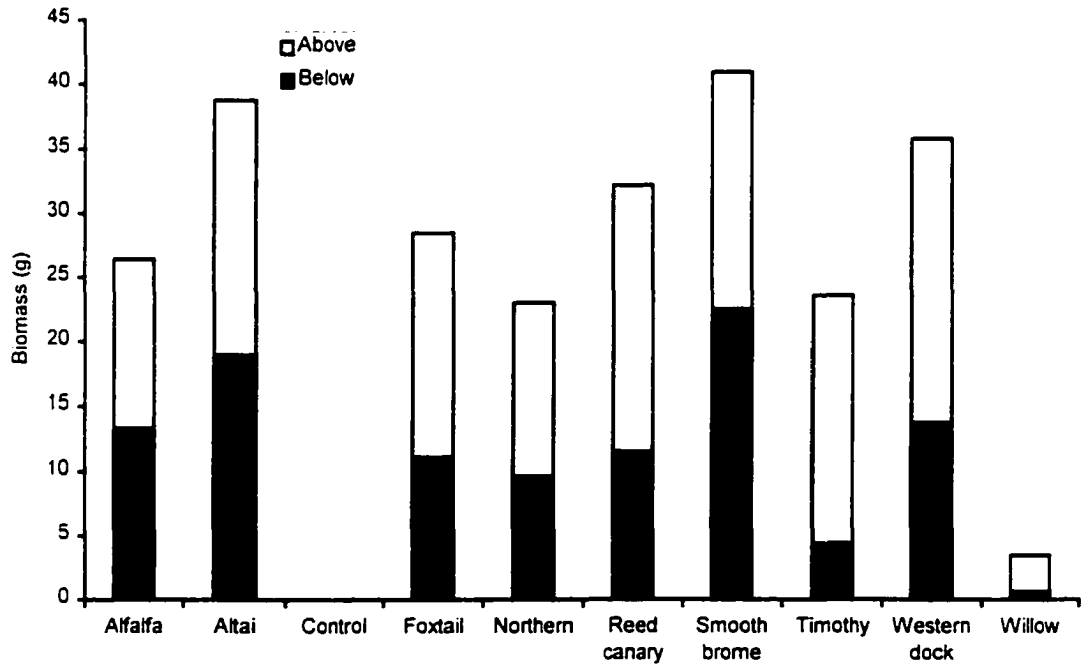


**Figure 2.6 Plant biomass on CMT phase 1**

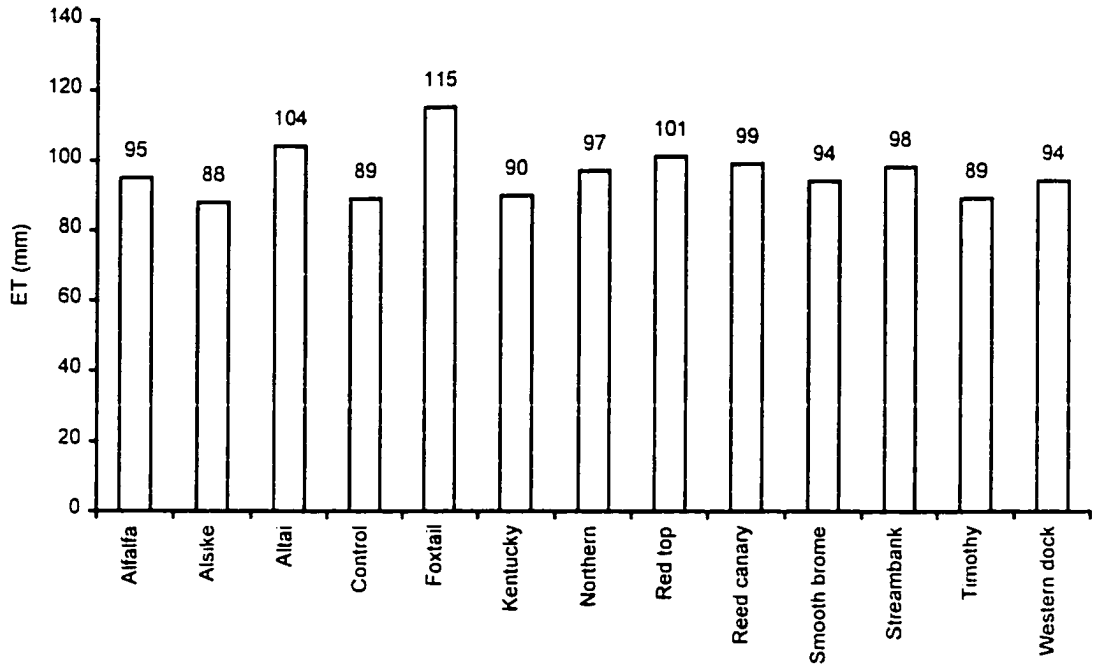


**Figure 2.7** Evapotranspiration of CT phase 2 after 56 days

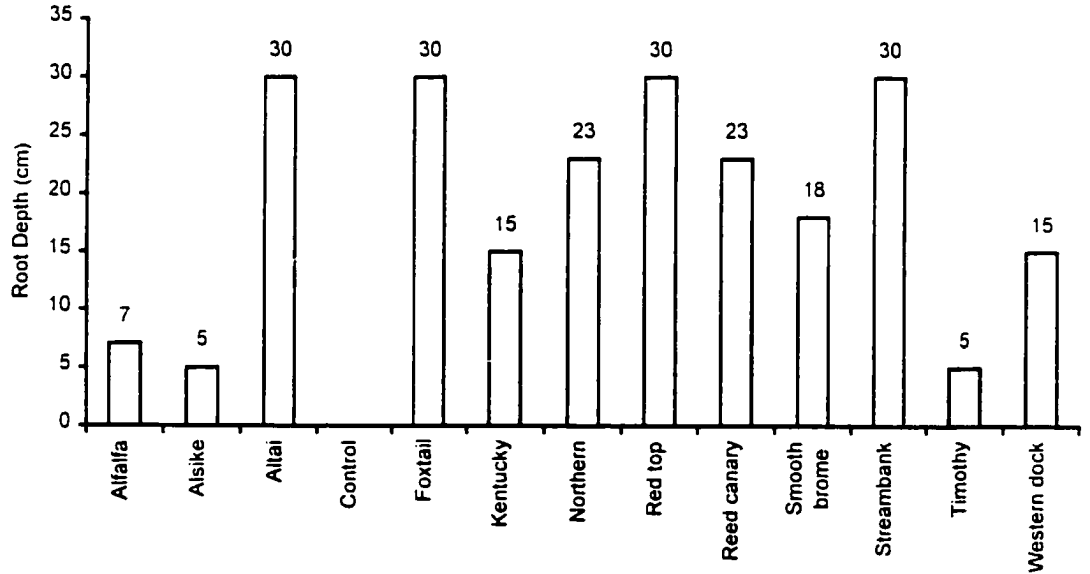


**Figure 2.8** Root depth on CT phase 2

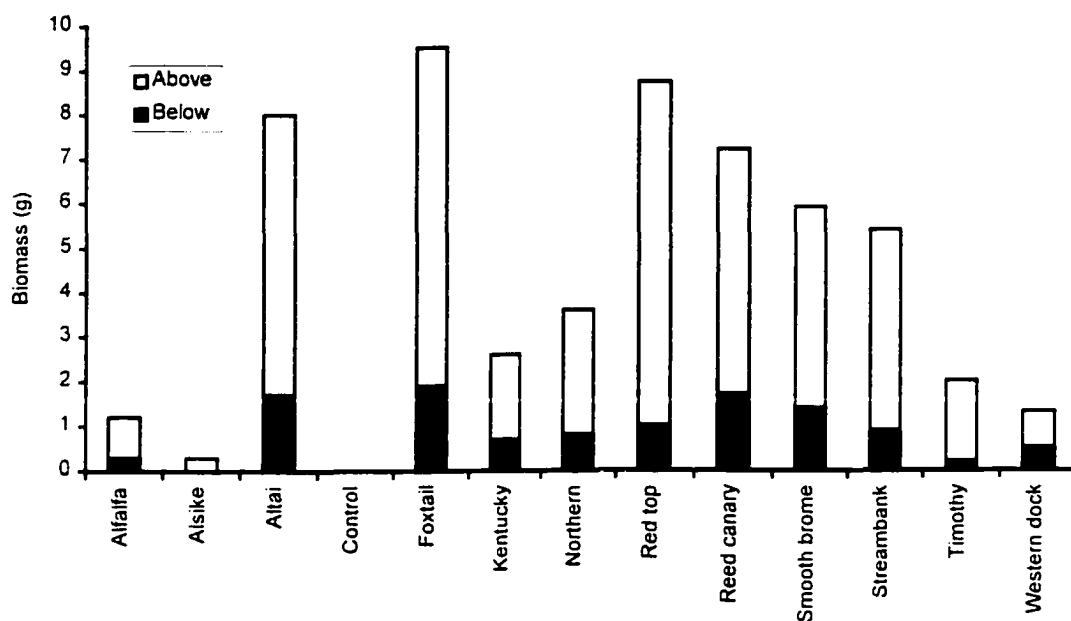


**Figure 2.9 Plant biomass on CT phase 2**

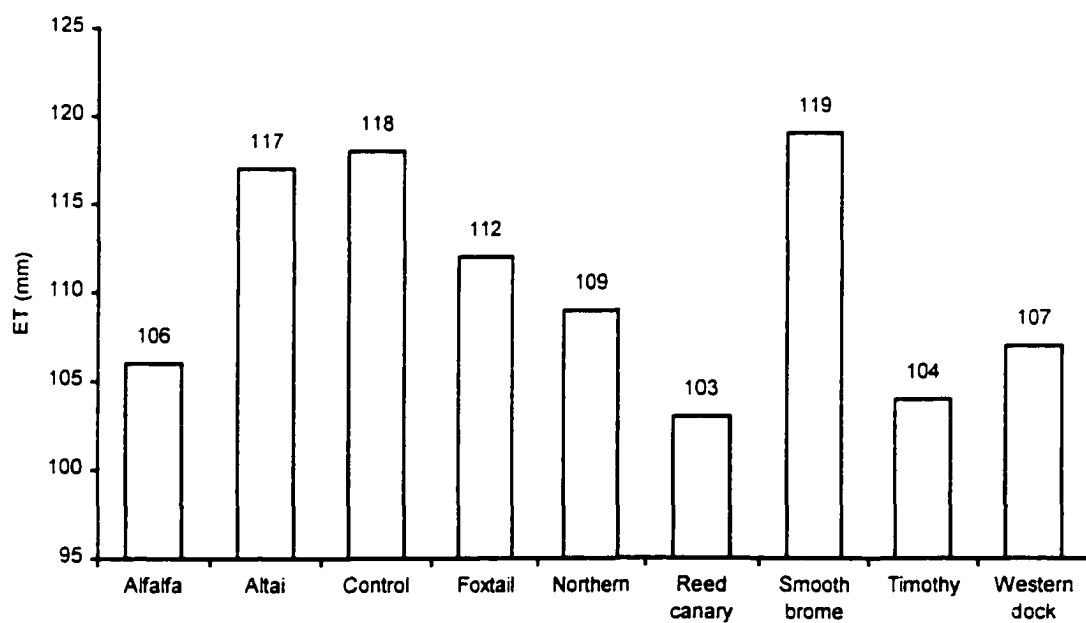


**Figure 2.10 Evapotranspiration of CMT phase 2 after 56 days**

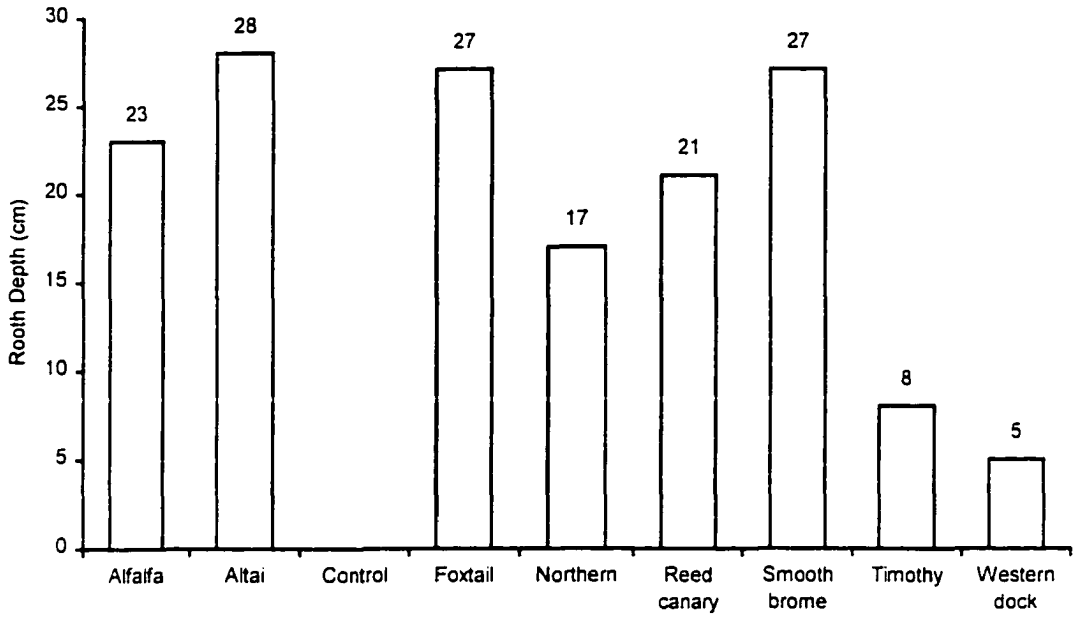


**Figure 2.11 Root depth into CMT phase 2**

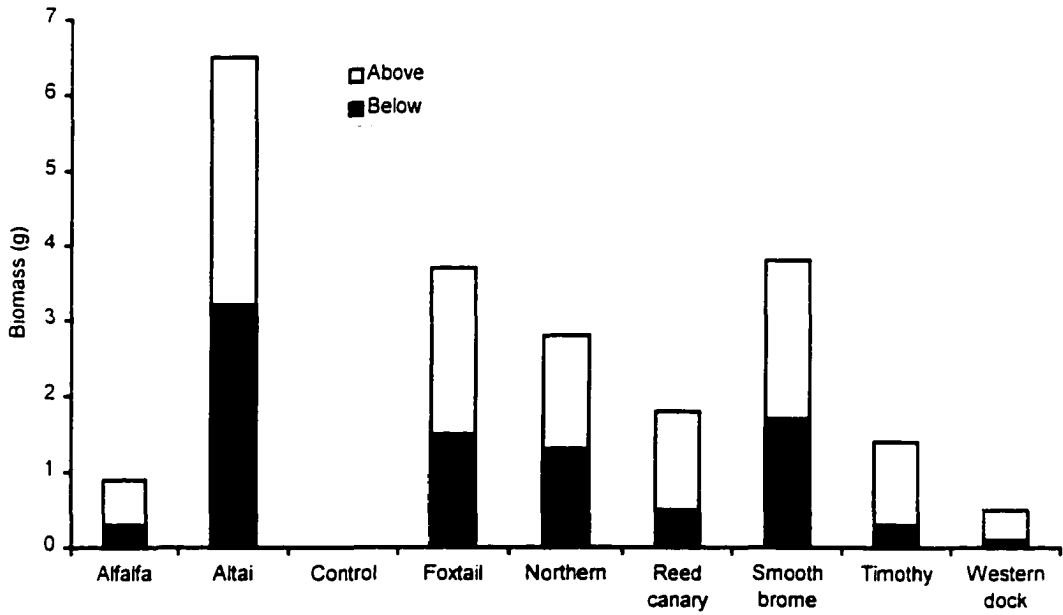


**Figure 2.12 Plant biomass on CMT phase 2**

Common name	Scientific name	CT		CMT	
		Phase		Phase	
		1	2	1	2
Alfalfa	<i>Medicago sativa</i>	✓	✓	✓	✓
Alsike clover	<i>Trifolium hybridum</i>	✓	✓		
Altai wildrye	<i>Elymus angustus</i>	✓	✓	✓	✓
Common cattail	<i>Typha latifolia</i>	✓			
Creeping foxtail	<i>Alopecurus arundinaceus</i>	✓	✓	✓	✓
Indian ricegrass	<i>Oryzopsis hymenoides</i>	✓			
Kentucky bluegrass	<i>Poa pratensis</i>	✓	✓		
Northern wheatgrass	<i>Agropyron dasystachyum</i>	✓	✓	✓	✓
Red top	<i>Agrostis stolonifera</i>	✓	✓		
Reed canarygrass	<i>Phalaris arundinacea</i>	✓	✓	✓	✓
Smooth brome grass	<i>Bromus inermis</i>	✓	✓	✓	✓
Streambank wheatgrass	<i>Agropyron riparian</i>	✓	✓		
Timothy	<i>Phleum pratense</i>	✓	✓	✓	✓
Willow	<i>Salix bebbiana</i>	✓		✓	
Western dock	<i>Rumex occidentalis</i>	✓	✓	✓	✓

**Table 2.1 Plant species selected for testing**

Analysis	CT		CMT		Optimum*
	Sample 1	Sample 2	Sample 1	Sample 2	
pH	9.5	9.6	8.1	8.1	6-8
E.C. (dS/m)	1.1	1.1	3.0	3.3	<1
Nitrate (ppm)	<1	<1	<1	<1	100 – 279
Phosphate (ppm)	1	2	7	9	8 – 13
Potassium (ppm)	39	45	149	163	150 – 249
Sulfate (ppm)	>20	>20	>20	>20	10 - 12

\* Warncke (1979)

**Table 2.2 Chemical analyses of CT and CMT samples**

Element	CT (ppm)	CMT (ppm)
Ca	392	2660
Na	151	190
Mg	58	200
Fe	11	24
Cu	0.23	78.14
Zn	0.7	1.5
B	2.24	0.12
Mn	6.7	3.4
Cl	>50	>50

**Table 2.3 Micronutrient status of CT and CMT**

Parameters and Units	CT	CMT
pH	8.15	6.51
E.C. (dS/m)	7.14	6.04
Ca (mg/L)	54	580
Mg (mg/L)	38.5	155
Na (mg/L)	1700	698
K (mg/L)	38.7	68.1
SO <sub>4</sub> (mg/L)	2360	1920
Nitrate and Nitrite (mg/L)	<0.05	<0.05
PO <sub>4</sub> (mg/L)	<0.05	<0.05
SAR	43.1	6.6

**Table 2.4 Chemical composition of CT release water and CMT process water**



<b>Analysis</b>	<b>CT</b>	<b>CMT</b>
pH	7.5	7.4
E.C. (dS/m)	1.6	2.5
Nitrate (ppm)	<1	7
Phosphate (ppm)	3	12
Potassium (ppm)	44	170
Sulfate (ppm)	>20	>20

**Table 2.5 Chemical analyses of CT and CMT samples at beginning of phase 2**

<b>Analysis</b>	<b>Sample 1</b>		<b>Sample 2</b>		<b>Sample 3</b>		<b>Sample 4</b>		<b>Sample 5</b>	
	Top	Btm	Top	Btm	Top	Btm	Top	Btm	Top	Btm
pH	9.0	8.4	8.8	8.5	9.0	9.0	8.9	8.9	9.1	8.8
E.C. (dS/m)	19.0	1.7	17.3	1.8	27.0	1.5	15.8	1.5	15.2	1.3
Nitrate (ppm)	>75	<1	>75	<1	>75	<1	>75	<1	>75	<1
Phosphate (ppm)	25	17	27	18	32	20	24	20	24	18
Potassium (ppm)	351	59	320	71	548	87	396	80	267	65
Sulphate (ppm)	7	>20	>20	>20	16	>20	>20	>20	>20	>20

**Table 2.6 Chemical analyses of five CT samples at end of phase 2**

Plant species	Symptom scale		No. of tiller				Tillering observed
	3 <sup>rd</sup> Week	11 <sup>th</sup> Week	3 <sup>rd</sup> wk		11 <sup>th</sup> wk		
			Live	Dead	Live	Dead	
Alfalfa	4	3.5	15	1	8	4	No
Alsike clover	4	4	9	7	0	All	No
Altai wildrye	2	2	19	0	23	1	Yes
Creeping foxtail	2	3	29	0	38	0	Yes
Kentucky bluegrass	3	3	24	0	31	2	Yes
Northern wheatgrass	2.5	3	22	1	18	5	Yes
Red top	1	2.5	47	0	54	6	Yes
Reed canarygrass	2	3	24	0	20	11	Yes
Smooth brome grass	2.5	3.5	18	0	18	5	Yes
Streambank wheatgrass	2.5	3	20	1	25	7	Yes
Timothy	2.5	4	24	0	9	15	No
Western dock	1.5	3.5	14	0	4	3	No

Note: tiller means total number of plants and tillering is the ability to develop new plants

Symptom scale is based on degree of plant health

- 1 Very healthy, lush, a few older leaves dying, maybe a few tips browning
- 2 Fairly healthy, many first leaves dying, some symptoms evident, tips dying, a bit of chlorosis
- 3 Looking stressed, dry leaves, chlorosis and necrosis very evident, tips curled and dead, perhaps stunted
- 4 Very stressed, dry, dying tillers

Note: dying refers to mortality

**Table 2.7 Summary of plant behavior assessment for CT phase 2**

Analysis	Sample 1		Sample 2		Sample 3		Sample 4	
	Top	Btm	Top	Btm	Top	Btm	Top	Btm
pH	7.2	8.0	7.3	8.1	7.6	8.1	7.6	8.1
E.C. (dS/m)	35.2	4.9	28.2	4.3	40.0	4.5	36.5	4.8
Nitrate (ppm)	>75	49	>75	43	>75	41	>75	64
Phosphate (ppm)	25	23	21	16	17	17	26	15
Potassium (ppm)	>600	235	>600	198	>600	253	>600	197
Sulphate (ppm)	>20	>20	>20	>20	>20	>20	15	>20

**Table 2.8 Chemical analyses of four CMT samples at end of phase 2**

Plant Species	Symptom Scale		No. of Tiller				Tillering Observed
	3 <sup>rd</sup> Week	11 <sup>th</sup> Week	3 <sup>rd</sup> wk		11 <sup>th</sup> wk		
			Live	Dead	Live	Dead	
Alfalfa	4	3.6	4	10	1	6	No
Altai wildrye	2	2	19	0	22	0	Yes
Creeping foxtail	2.8	3	27	0	24	2	Yes
Northern wheatgrass	2.3	3.7	17	0	9	9	Yes
Reed canarygrass	2.5	4	30	0	0	18	No
Smooth bromegrass	2.7	3.5	16	1	10	5	No
Timothy	2.3	4	27	0	3	24	No
Western dock	1.5	3.7	6	6	2	5	No

**Table 2.9 Summary of plant behavior assessment for CMT phase 2**

## Chapter 3

### **Model for the prediction of bearing capacity on vegetated tailings<sup>1</sup>**

#### 3.1 INTRODUCTION

Fine mine waste tailings are composed mainly of slow-settling fine mineral particles and a large amount of water. They have little or no sand and include phosphatic clays, bauxite red muds, fine taconite tailings, and slimes from the oil sands tailings (Vick 1983). These materials consolidate very slowly. They have a low bearing capacity at the surface for a long period of time and cannot support human traffic. Reclamation of these tailings to a desired dry landscape will not be possible in the short term unless a dewatering mechanism is developed to accelerate the consolidation process. The use of plants to dewater tailings has been identified as such a mechanism, which may economically enhance the surface stability of these weak deposits on a large scale.

Suitable plant species growing in fine tailings have the ability to remove the water through evapotranspiration, increasing the matric suction in the deposit (Silva et al. 1998). This results in an increase in the shear strength and bearing capacity within the root zone. Furthermore, the

---

<sup>1</sup> A version of this chapter has been published.

*Silva, M.J., Biggar, K.W., Segó, D.C., Chanasyk, D.S., and Naeth, M.A. 1998. Plant dewatering of tailings: a theoretical model. Proceedings, 51<sup>st</sup> Canadian Geotechnical Conference, Edmonton, Alberta, October 4-7, 1998. Vol. 2. pp. 631-638.*

A version of this chapter has been submitted for publication.

*Silva, M.J., Biggar, K.W., Segó, D.C., Chanasyk, D.S., and Naeth, M.A. 1999. Model for the prediction of bearing capacity on vegetated tailings. Paper submitted for review to the Canadian Geotechnical Journal, May, 1999. 42 pp.*

plant root system may provide a fiber reinforcement, which should also contribute to the increased bearing capacity of the rooted tailings.

Complex deterministic models have been developed to simulate water movement in and through soils. A thorough review of each of these models, which include microscopic and macroscopic root extraction simulation, was presented by Molz (1981). The water extraction rate is included in the sink term of the Richards equation for soil water flow in the saturated zone. These models have been verified against field data with a reasonable degree of accuracy achieved. However, a major drawback in using any of these models is that they do not account for the effects of volume change of the soil matrix. Most of these models are found outside the traditional area of geotechnical engineering in disciplines such as hydrology, soil physics and agricultural sciences.

The objective of this paper is to present a theoretical model that simulates the vertical movement of water through a rooted tailings system. Bearing capacity can then be predicted from the solids content profile and the root biomass, which grows in the tailings deposit. This model will be an essential tool to identify potentially important parameters needed to understand the complex processes involved in the plant dewatering mechanism and identify the conditions at which optimum dewatering may be achieved. The one-dimensional form of the governing partial differential equation is solved numerically using a Crank-Nicholson finite difference scheme. A computer code of the proposed solution algorithm is tested for accuracy in the solution of two problems. Model predictions will be validated with experimental data.

### **3.2 BACKGROUND**

The use of plants to dewater high water content materials is an inexpensive technique, which has been accomplished for many years by the Dutch to dewater lacustrine and marine sediments (Public Relations and Information Department of the Netherlands 1959; Shelling 1960; Volker 1982). This drying of wet soils to shallow depths in short time periods is called polder reclamation.

Plant dewatering has also been used in dewatering sludge from wastewater treatment facilities, termed reed beds, which were initially built in Austria and southern Germany (Neurohr 1983). In addition, studies conducted by Lee et al. (1976) demonstrated the feasibility of using selected vegetation to dewater and consolidate fine textured dredged materials.

The dewatering capabilities of plants have also been observed in the reclamation of tailings. Barth (1986) recognized that vegetation transpires large quantities of water, thus reducing water entry into tailings and subsequent seepage. At present, vegetation is the most common and usually preferred stabilization option for tailings impoundments. If a self-perpetuating vegetative cover can be established, not only can wind and water erosion be minimized, but the impoundment can be returned to some semblance of its original appearance and land use (Vick 1983; Ludeke 1973).

Although plant dewatering of tailings has been recognized for a long time, it was not until recently researchers showed interest in studying the mechanical effects that plants have on the tailings. Oil sands tailings from northeastern Alberta at 50% solids (equivalent to 100% gravimetric water content) were dewatered to 80% solids in one growing season resulting in a shear strength of 120 kPa (Johnson et al. 1993). Stahl (1996) studied changes in surface stability of an 18.2-hectare coal tailings impoundment undergoing reclamation activities since reaching full capacity in 1989. Natural enhancement processes including dewatering through evaporation, evapotranspiration, and fiber reinforcement of plant root systems increased the shear strength of the surficial soils. Bearing capacity and surface stability of the coal tailings within the impoundment also increased. In some cases, the bearing pressure of the rooted tailings was 50 to 60% greater than that of the unrooted tailings at equivalent strain or relative plate settlements.

Evaporation alone has been used to dewater tailings of the Florida phosphate industry (McFarlin et al. 1989) and Alberta oil sands (Cuddy and Lahaie 1993; Johnson et al. 1993; Li and Feng 1995). As soil surfaces desaturate with evaporation, the evaporative flux decreases and the depth of soil enhancement through dewatering becomes limited. The most characteristic feature of

tailings is the development of surficial salt crusts during periods of drying. Evaporation of water from the tailings induces salt accumulation at the ground surface. These crusts interfere with the evaporation process to such an extent that in some cases the evaporation rate can be reduced to 12% of potential evaporation (Qiu and Segó 1998). Newson et al. (1996) reported that the depth of influence of evaporative flux on shear strength of saline gold tailings was limited to 10 cm, and Burns et al. (1993) highlighted that effective dewatering of oil sands tailings can only occur if thin layers (10 to 20 cm) are placed and dewatered. However, because of the slow consolidation rate of tailings, this method requires a long period of time to reclaim the area and return it to a useful state (Bromwell 1982; McLendon et al. 1983; U.S. Bureau of Mines 1975). For consolidation of tailings to occur, substantial drying must take place. Furthermore, this drying must proceed to a considerable depth rather than be limited to the surface. Therefore, dewatering by means of pure evaporation is generally not economically feasible because of the vast areas and quantities of tailings involved in land disposal operations.

A variety of soil-plant-atmosphere-based models for the evaluation of water flow and moisture redistribution in a soil have been proposed (de Jong and Bootsma 1997; Chang and Corapcioglu 1997). A part of these models deal with flow in the individual plants and their components (Molz 1976; Cushman 1982) and their utility to engineers is limited. Other models use a macroscopic representation of the root extraction process to describe the uptake of water by a crop's root system (Hillel et al. 1976; Feddes et al. 1978; Mariño and Tracy 1988). The water extraction rate is included in the sink term of the Richards equation for soil water flow in the unsaturated zone. These models assume the soil structure to be rigid. Therefore, they are not applicable to tailings, which undergoes large strain consolidation under its own weight (self-weight consolidation). At present, the literature lacks a theoretical formulation that can describe the plant dewatering mechanism of tailings with large strain consolidation and predict the bearing capacity increased due to matric suction and root reinforcement.

### 3.3 MODEL DEVELOPMENT

The plant dewatering mechanism involves primarily the movement of water in the tailings deposit. Three equations of physics are needed to describe the water transport process: continuity of liquid phase, continuity of solids phase and Darcy's law.

#### 3.3.1 Continuity of liquid phase

$$[3.1] \quad \frac{\partial}{\partial t}(nS_r) + \frac{\partial}{\partial y}(nS_r v_w) + T = 0$$

where  $n$  is porosity,  $S_r$  is degree of saturation,  $v_w$  is velocity of water (m/d);  $T$  is sink term (actual plant transpiration, 1/d);  $t$  is time (d); and  $y$  is vertical spatial coordinate (m).

#### 3.3.2 Continuity of solids phase

$$[3.2] \quad \frac{\partial}{\partial t}(1-n) + \frac{\partial}{\partial y}[v_s(1-n)] = 0$$

where  $v_s$  is velocity of solids (m/d)

#### 3.3.3 Darcy's law

$$[3.3] \quad nS_r(v_w - v_s) = -K \frac{\partial h_w}{\partial y}$$

where  $K$  is hydraulic conductivity (m/d); and  $h_w$  is hydraulic head (m).

Combining equations [3.1], [3.2] and [3.3] and presenting the final equation in terms of void ratio, the following is achieved:



$$\begin{aligned}
 [3.4] \quad & \left[ \frac{\partial}{\partial t} \left( \frac{e}{1+e} S_r \right) + u_s \frac{\partial}{\partial y} \left( \frac{e}{1+e} S_r \right) \right] + \frac{e}{1+e} S_r \left\{ -(1+e) \left[ \frac{\partial}{\partial t} \left( \frac{1}{1+e} \right) + u_s \frac{\partial}{\partial y} \left( \frac{1}{1+e} \right) \right] \right\} \\
 & = \frac{\partial}{\partial y} \left( K \frac{\partial h_w}{\partial y} \right) - T
 \end{aligned}$$

The spatial derivatives enclosed in the square brackets in equation [3.4] can be transformed into material derivatives using the following operator:

$$[3.5] \quad \frac{D(\ )}{Dt} = \frac{\partial(\ )}{\partial t} + u_s \frac{\partial(\ )}{\partial y}$$

The resulting equation is

$$[3.6] \quad \frac{D}{Dt} \left( \frac{e}{1+e} S_r \right) - e S_r \frac{D}{Dt} \left( \frac{1}{1+e} \right) = \frac{\partial}{\partial y} \left( K \frac{\partial h_w}{\partial y} \right) - T$$

Equation [3.6] can be transformed in terms of volume of water and volume of solids. This leads to a more convenient equation:

$$[3.7] \quad \frac{1}{V_s(1+e)} \frac{DV_w}{Dt} = \frac{\partial}{\partial y} \left( K \frac{\partial h_w}{\partial y} \right) - T$$

where  $V_w$  is volume of water (m); and  $V_s$  is volume of solids (m), constant. Using the volume of water based approach offers advantages in the numerical solution. Firstly, the volume of water ( $V_w$ ) of a tailings compartment has a clear finite range which encourages numerical stability. Secondly, under saturated conditions any change in the volume of water indicates a consolidation of the same magnitude. Thirdly, a change of volume of water over a certain period of time carries the same units as rainfall, water flow and hydraulic conductivity, which use the units of height of water per unit of time (e.g. m/d). This makes the results easy to visualize and understand.

### 3.3.4 Material coordinate system

The first term of the right side of equation [3.7] uses a spatial derivative. In this case, the coordinate system is fixed in space to a reference point. This system is not ideally suited for deforming materials. This is due, in part, to the need to account continuously for the effect of the deformation on the spatial dependency of  $K$  and  $h_w$ , as well as for the boundary conditions for which equation [3.7] is solved.

For these reasons, it is preferable to describe the transport of water in a coordinate frame (termed referential, material, or Lagrangian) that is associated with the solids phase.

Figure 3.1 shows a representation of a tailings deposit, which undergoes a volume change from time  $t_1$  to time  $t_2$ .  $\Delta y_1$  represents the thickness of a compartment at time  $t_1$ ,  $y_1$  is the depth of the top of the compartment. At time  $t_2$  the compartment undergoes a change in the spatial location ( $y_2$ ), as well as a reduction in its thickness to  $\Delta y_2$ . However, the volume of solids ( $V_s$ ) in the compartment remains constant.

The thickness of the compartment and the volume of solids can be related using the following expression:

$$[3.8] \quad \Delta y = V_s(1 + e)$$

Using

$$[3.9] \quad V_s = \Delta Z$$

the material coordinate  $Z$  is linked to the spatial coordinate  $y$  by the following general relationship:

$$[3.10] \quad \partial y = \partial Z(1 + e)$$

Equation [3.7] can be transformed to a material coordinate system by substituting equation [3.10].

$$[3.11] \quad \frac{DV_w}{Dt} = V_s \frac{\partial}{\partial Z} \left( \frac{K}{1+e} \frac{\partial h_w}{\partial Z} \right) - V_s (1+e)T$$

Equation [3.11] constitutes the governing equation of the plant dewatering model.

### 3.3.5 Saturated condition

The tailings surface is used as the reference point and the downward direction as positive for  $y$  as shown in Figure 3.2. The hydraulic head can be expressed as:

$$[3.12] \quad h_w = \frac{u_w}{\gamma_w} - y$$

where  $u_w$  is pore water pressure (kPa); and  $\gamma_w$  is unit weight of water (9.81 kN/m<sup>3</sup>)

Using the effective stress concept for saturated condition, the pore water pressure can be calculated using the following expression:

$$[3.13] \quad u_w = \sigma - \sigma' = P_0 + \int_0^y \gamma dy - \sigma'$$

where  $\sigma$  is total stress (kPa);  $P_0$  is surcharge pressure (kPa);  $\sigma'$  is effective stress (kPa); and  $\gamma$  is unit weight of tailings (kN/m<sup>3</sup>).

A power relation between  $\sigma'$  and  $e$  is assumed, where

$$[3.14] \quad e = A(\sigma')^B$$

where  $A$  and  $B$  are fitting parameters.

The effective stress of equation [3.14] can be isolated in terms of void ratio and substituted into equation [3.13]. Assuming that no surcharge pressure is applied at the surface of the tailings ( $P_0 = 0$ ) the pore water pressured is

$$[3.15] \quad u_w = \int_0^y \gamma dy - \left( \frac{e}{A} \right)^{\frac{1}{B}}$$

Differentiating equation [3.15] in the spatial coordinate system, with respect to  $y$ , yields

$$[3.16] \quad \frac{\partial u_w}{\partial y} = \gamma - \frac{1}{B} \left( \frac{e}{A} \right)^{\frac{1}{B}-1} \left( \frac{1}{A} \frac{de}{dV_w} \frac{\partial V_w}{\partial y} \right)$$

The unit weight of tailings can be determined using

$$[3.17] \quad \gamma = \frac{G_s + e}{1 + e} \gamma_w$$

where  $G_s$  is the specific gravity of the soil particles. The rate of change of void ratio with respect to the rate of change of volume of water is expressed as

$$[3.18] \quad \frac{de}{dV_w} = \frac{1}{V_s}$$

Substituting equations [3.17] and [3.18] into [3.16] leads to

$$[3.19] \quad \frac{\partial u_w}{\partial y} = \frac{G_s + e}{1 + e} \gamma_w - \frac{1}{ABV_s} \left( \frac{e}{A} \right)^{\frac{1}{B}-1} \frac{\partial V_w}{\partial y}$$

Differentiating equation [3.12] with respect to  $y$  and then substituting equation [3.19], the following expression is obtained

$$[3.20] \quad \frac{\partial h_w}{\partial y} = \frac{G_s + e}{1 + e} - \frac{1}{\gamma_w ABV_s} \left( \frac{e}{A} \right)^{\frac{1}{B}-1} \frac{\partial V_w}{\partial y} - 1$$

Equation [3.20] can be expressed in material coordinates using [3.10]

$$[3.21] \quad \frac{\partial h_w}{\partial Z} = -1 + G_s - \frac{1}{\gamma_w ABV_s} \left( \frac{e}{A} \right)^{\frac{1}{B}-1} \frac{\partial V_w}{\partial Z}$$

### 3.3.6 Unsaturated condition

Differentiating equation [3.12] in the Eulerian coordinate system with respect to  $y$ , and making use of the differential chain law, yields

$$[3.22] \quad \frac{\partial h_w}{\partial y} = \frac{1}{\gamma_w} \frac{\partial u_w}{\partial y} - 1 = \frac{1}{\gamma_w} \frac{\partial u_w}{\partial V_w} \frac{\partial V_w}{\partial y} - 1$$

Rearranging equation [3.22] leads to

$$[3.23] \quad \frac{\partial h_w}{\partial y} = \frac{1}{\gamma_w} \frac{\partial V_w}{\partial u_w} \frac{\partial V_w}{\partial y} - 1 = \frac{1}{\chi(u_w)} \frac{\partial V_w}{\partial y} - 1$$

The function  $\chi(u_w)$  can be derived from the water characteristic curve. The Van Genuchten's (1980) equation is selected because of the documented applicability of this expression to a wide range of soils (Fuentes et al. 1992). In terms of the volumetric water content, Van Genuchten's equation is given by:

$$[3.24] \quad S_e = \frac{\theta - \theta_r}{\theta_s - \theta_r} = \frac{1}{\left[ 1 + |\alpha u_w|^d \right]^m}$$

where  $S_e$  is effective saturation,  $\theta_r$  and  $\theta_s$  are residual and saturated volumetric water contents, respectively, and  $\alpha$  (1/kPa),  $d$ , and  $m$  are empirical parameters. The Mualem (1976) theory states that ( $m = 1 - 1/d$ ).

From equation [3.24] the following expression for  $\chi(u_w)$  is obtained

$$[3.25] \quad \chi(u_w) = \frac{m}{m-1} \alpha (V_{ws} - V_{wr}) S_e^{1/m} (1 - S_e^{1/m})^m$$

where  $V_{wr}$  and  $V_{ws}$  are volume of water at residual and saturated water content, respectively.

Equation [3.23] in material coordinate system is

$$[3.26] \quad \frac{\partial h_w}{\partial Z} = -1 - e + \frac{1}{\chi(u_w)} \frac{\partial V_w}{\partial Z}$$

Equations [3.21] and [3.26] can be generalized in the following way

$$[3.27] \quad \frac{\partial h_w}{\partial Z} = \mathfrak{J} + \mathfrak{R} \frac{\partial V_w}{\partial Z}$$

where  $\mathfrak{J}$  and  $\mathfrak{R}$  are expressed as

$$\text{Saturated} \left\{ \begin{array}{l} \mathfrak{J} = -1 + G_s \\ \mathfrak{R} = -\frac{1}{\gamma_w A B V_s} \left( \frac{e}{A} \right)^{\frac{1}{B}-1} \end{array} \right.$$

$$\text{Unsaturated} \left\{ \begin{array}{l} \mathfrak{J} = -1 - e \\ \mathfrak{R} = \frac{1}{\chi(u_w)} \end{array} \right.$$

### 3.3.7 Root water uptake, sink term

A major difficulty in solving equation [3.11] stems from the function of  $T$  being unknown. Feddes (1981), Molz (1981) and Campbell (1985) gave an overview of possible  $T$ -functions for non-uniform matric potentials. Dirksen (1985, 1987) investigated  $T$ -functions considering the influence of both the osmotic and the matric potential.

Figure 3.3 shows a representation of the water extracted by roots from a compartment. From this figure the following expression is derived

$$[3.28] \quad T = \frac{\Delta T_a}{\Delta y} = \frac{\Delta T_a}{(1+e)V_s}$$

where  $\Delta T_a$  is the actual root water uptake rate (m/d)

Substituting equation [3.28] into equation [3.11], yields

$$[3.29] \quad \frac{DV_w}{Dt} = V_s \frac{\partial}{\partial Z} \left( \frac{K}{1+e} \frac{\partial h_w}{\partial Z} \right) - \Delta T_a$$

The actual root water uptake rate  $\Delta T_a$  can be calculated using the procedure discussed in the following paragraphs.

The plant transpiration ( $T_p$ ) is distributed through the tailings profile which is occupied by the root system ( $y_r$ ). The method of distributing the plant transpiration is presented in Figure 3.4 as a linear decreasing root extraction pattern with depth (Prasad, 1988).

The plant root water uptake in compartment  $i$  is determined using

$$[3.30] \quad \Delta T_{pi} = \frac{T_p}{y_r} (y_{i+1} - y_i) (2y_r - y_{i+1} - y_i)$$

When the water content is low, actual root water uptake is lower than the plant transpiration value. The actual root water uptake is modified by a reducing term LAW (Limited Available Water function), which is dependent upon the tailings matric suction as shown in Figure 3.5.

$$[3.31] \quad \Delta T_{ai} = LAW(u_w) \Delta T_{pi}$$

where  $\Delta T_{ai}$  is the actual root water uptake in compartment  $i$ . The matric suction ( $u_{w1}$ ) at which soil water begins to limit plant growth ranges from -50 to -100 kPa, and the wilting point ( $u_{w2}$ ) for most plants ranges from -1500 to -2000 kPa (Feddes et al. 1978; de Jong et al. 1992).

Plant transpiration ( $T_p$ ) is a component of the evapotranspiration process, which includes the evaporation of liquid water from the soil surface and water intercepted by plants, plus transpiration by plants. To calculate  $T_p$  it is necessary to estimate the potential evapotranspiration ( $ET_0$ ), which is the rate at which water, if available, would be removed from wet soil and plant surfaces (Jensen et al. 1990).  $ET_0$  can be calculated with the Penman equation

$$[3.32] \quad ET_0 = \frac{\Delta(R_n - G)}{\Delta + \gamma_c} + \frac{\gamma_c}{\Delta + \gamma_c} E_{at}$$

where  $ET_0$  is potential evapotranspiration (mm/d);  $\Delta$  is slope of the saturation vapor pressure-temperature curve (kPa/°C);  $\gamma_c$  is psychrometric constant (kPa/°C);  $R_n$  is net radiation expressed in water depth equivalents of energy (mm/d);  $G$  is soil heat flux in water depth equivalents (mm/d); and  $E_{at}$  is given in [3.33]. The aerodynamic transport term  $E_{at}$  has been described in several different forms in which the most common is the Dalton-type equation for the evaporation from a free water surface:

$$[3.33] \quad E_{at} = f(u)(e_z^0 - e_z)$$



where  $f(u)$  is a wind function;  $e_z^0$  and  $e_z$  are saturation and actual vapor pressures (kPa) at the  $z$  level above the surface. Theoretical forms for the wind function expression have been proposed by Monteith (1965) and van Bavel (1966) as

$$[3.34] \quad f(u) = \frac{k^2 \rho c_p u}{\lambda \gamma_c \left\{ \ln \left[ \frac{z - h_d}{z_0} \right] \right\}^2}$$

where  $k$  is von Karman constant (0.41);  $\rho$  is air density ( $\text{kg/m}^3$ );  $c_p$  is specific heat of air ( $\text{J/kg/}^\circ\text{C}$ );  $u$  is wind speed (m/s) at some reference height  $z$ ;  $z$  is reference height (m);  $h_d$  is displacement height for a crop (m) given as  $h_d = 0.67 \times \text{crop height}$ ; and  $z_0$  is the vegetation roughness parameter (m) calculated as  $z_0 = 0.123 \times \text{crop height}$ .

The potential evapotranspiration ( $ET_0$ ) is then distributed into its potential evaporation ( $E_0$ ) and potential transpiration ( $T_0$ ) components using the model proposed by Ritchie (1972), who observed that the transpiration component was dependent on the leaf area index (LAI) according to the following expression:

$$\begin{array}{ll}
 T_0 = 0 & \text{LAI} < 0.1 \\
 [3.35] \quad T_0 = ET_0(-0.21 + 0.7\text{LAI}^{1/2}) & 0.1 \leq \text{LAI} \leq 2.7 \\
 T_0 = ET_0 & \text{LAI} > 2.7
 \end{array}$$

LAI is defined as the area of one side of leaves per unit of soil surface (Jensen et al. 1990). Potential evaporation ( $E_0$ ) is then determined by subtracting  $T_0$  from  $ET_0$ .

Finally, the plant transpiration term is calculated as:

$$[3.36] \quad T_p = k_c T_0$$

where  $k_c$  is an empirical crop coefficient for a particular crop.  $T_0$  characterizes the evaporative demand determined by meteorological conditions and a standard crop surface (grass or alfalfa) and  $k_c$  indicates the relative ability of a specific crop-soil surface to meet that demand.

### 3.3.8 Root growth model

Borg and Grimes (1986) found that the increase in rooting depth  $y_r$  with time ( $t$ ) delineates a sigmoidal curve, which can be described by a single sine function, such that

$$[3.37] \quad y_r = y_m \{ 0.5 + 0.5 \sin [ 3.03 (t / t_m) - 1.47] \}$$

where  $t_m$  is time to plant maturity;  $y_m$  is the maximum rooting depth at  $t = t_m$ ; and  $y_r$  is the current rooting depth.

## 3.4 NUMERICAL APPROACH

Substituting [3.27] into [3.29] the following equation is obtained in discrete form

$$[3.38] \quad \frac{\Delta V_w}{\Delta t} = V_s \frac{\Delta}{\Delta Z} \left[ \frac{K}{1+e} \left( \mathfrak{I} + \mathfrak{R} \frac{\Delta V_w}{\Delta Z} \right) \right] - \Delta T_a$$

Using  $V_s = \Delta Z$  and  $\Phi = \frac{K}{1+e}$  in [3.38], yields

$$[3.39] \quad \frac{\Delta V_w}{\Delta t} = \Delta \left[ \Phi \left( \mathfrak{I} + \mathfrak{R} \frac{\Delta V_w}{\Delta Z} \right) \right] - \Delta T_a$$

Numerical solution of [3.39] is formulated using a Crank-Nicholson finite difference scheme. Figure 3.6 shows the depth-time region occupied by the independent variables  $Z$  (index  $i$ ) and  $t$  (index  $j$ ).

The discretized form of [3.39] is:

$$\begin{aligned}
 [3.40] \quad \frac{V_{w_i}^{j+1} - V_{w_i}^j}{\Delta t^j} &= -\Phi_{i-1/2}^{j+1/2} \left[ \mathfrak{I}_{i-1/2}^{j+1/2} + \mathfrak{R}_{i-1/2}^{j+1/2} \left( \frac{\Delta V_w}{\Delta Z} \right)_{i-1/2}^{j+1/2} \right] \\
 &+ \Phi_{i+1/2}^{j+1/2} \left[ \mathfrak{I}_{i+1/2}^{j+1/2} + \mathfrak{R}_{i+1/2}^{j+1/2} \left( \frac{\Delta V_w}{\Delta Z} \right)_{i+1/2}^{j+1/2} \right] - \Delta T_{ai}^{j+1/2}
 \end{aligned}$$

where  $\Delta V_w / \Delta Z$  can be approximated as

$$[3.41] \quad \left( \frac{\Delta V_w}{\Delta Z} \right)_{i-1/2}^{j+1/2} = \frac{1}{2\text{Dist}_i} (V_{w_i}^{j+1} + V_{w_i}^j - V_{w_{i-1}}^{j+1} - V_{w_{i-1}}^j)$$

$$[3.42] \quad \left( \frac{\Delta V_w}{\Delta Z} \right)_{i+1/2}^{j+1/2} = \frac{1}{2\text{Dist}_{i+1}} (V_{w_{i+1}}^{j+1} + V_{w_{i+1}}^j - V_{w_i}^{j+1} - V_{w_i}^j)$$

Substituting these two terms into [3.40] and rearranging the equation in terms of volume of water, yields

$$\begin{aligned}
 [3.43] \quad &\left( -\frac{\Delta t^j \Phi_{i-1/2}^{j+1/2} \mathfrak{R}_{i-1/2}^{j+1/2}}{2\text{Dist}_i} \right) V_{w_{i-1}}^{j+1} + \left( 1 + \frac{\Delta t^j \Phi_{i-1/2}^{j+1/2} \mathfrak{R}_{i-1/2}^{j+1/2}}{2\text{Dist}_i} + \frac{\Delta t^j \Phi_{i+1/2}^{j+1/2} \mathfrak{R}_{i+1/2}^{j+1/2}}{2\text{Dist}_{i+1}} \right) V_{w_i}^{j+1} \\
 &+ \left( -\frac{\Delta t^j \Phi_{i+1/2}^{j+1/2} \mathfrak{R}_{i+1/2}^{j+1/2}}{2\text{Dist}_{i+1}} \right) V_{w_{i+1}}^{j+1} = \left( 1 - \frac{\Delta t^j \Phi_{i-1/2}^{j+1/2} \mathfrak{R}_{i-1/2}^{j+1/2}}{2\text{Dist}_i} - \frac{\Delta t^j \Phi_{i+1/2}^{j+1/2} \mathfrak{R}_{i+1/2}^{j+1/2}}{2\text{Dist}_{i+1}} \right) V_{w_i}^j + \frac{\Delta t^j \Phi_{i-1/2}^{j+1/2} \mathfrak{R}_{i-1/2}^{j+1/2}}{2\text{Dist}_i} V_{w_{i-1}}^j \\
 &+ \frac{\Delta t^j \Phi_{i+1/2}^{j+1/2} \mathfrak{R}_{i+1/2}^{j+1/2}}{2\text{Dist}_{i+1}} V_{w_{i+1}}^j - \Delta t^j \Phi_{i-1/2}^{j+1/2} \mathfrak{I}_{i-1/2}^{j+1/2} + \Delta t^j \Phi_{i+1/2}^{j+1/2} \mathfrak{I}_{i+1/2}^{j+1/2} - \Delta t^j \Delta T_{ai}^{j+1/2}
 \end{aligned}$$

Equation [3.43] in a simple form can be expressed as

$$[3.44] \quad A_i V_{w_{i-1}}^{j+1} + B_i V_{w_i}^{j+1} + C_i V_{w_{i+1}}^{j+1} = D_i$$

where,

$$A_i = -\frac{\Delta t^i \Phi_{i-1/2}^{j+1/2} \mathfrak{R}_{i-1/2}^{j+1/2}}{2\text{Dist}_i}; \quad C_i = -\frac{\Delta t^i \Phi_{i+1/2}^{j+1/2} \mathfrak{R}_{i+1/2}^{j+1/2}}{2\text{Dist}_{i+1}}; \quad B_i = 1 - A_i - C_i$$

$$D_i = (1 + A_i + C_i)V_{wi}^j - A_i V_{wi-1}^j - C_i V_{wi+1}^j + \Delta t^i \Phi_{i-1/2}^{j+1/2} \mathfrak{J}_{i-1/2}^{j+1/2} - \Delta t^i \Phi_{i+1/2}^{j+1/2} \mathfrak{J}_{i+1/2}^{j+1/2} - \Delta t^i \Delta T_{ai}^{j+1/2}$$

In matrix notation [3.44] can be written as

$$A\bar{V}_w = \bar{D}$$

or as shown in Figure 3.7.

A is a tridiagonal coefficient matrix with zero elements outside the diagonals. In solving this system of equations, a direct method is used by applying the so-called Thomas (tridiagonal) algorithm of the kind discussed by Remson et al. (1971).

### 3.5 BOUNDARY CONDITIONS

The solution of [3.44] requires specification of boundary conditions, which constrain the problem and make solutions unique. Figure 3.8 is a scheme of the conceptual model that shows all sources. The solutions for the top and bottom compartments are obtained by introducing as boundary conditions a flux (Neumann condition) in [3.40].

For the top boundary

$$q_1 = \Phi_{1-1/2}^{j+1/2} \left[ \mathfrak{J}_{1-1/2}^{j+1/2} + \mathfrak{R}_{1-1/2}^{j+1/2} \left( \frac{\Delta V_w}{\Delta Z} \right)_{1-1/2}^{j+1/2} \right]$$

At the tailings surface,  $q_1$  is equal to the actual soil evaporation, rainfall infiltration, or water released from pore pressure dissipation, whichever applies.

The actual soil evaporation can be calculated as

$$[3.45] \quad E_a = K_{\text{evap}} E_0$$

where  $E_a$  is actual evaporation (mm/d);  $K_{\text{evap}}$  is an evaporation limiting factor, which is equal to 1 when the tailings surface is saturated and less than 1 when the surface becomes unsaturated and the supply of water to the surface becomes limited. After the topmost compartment drops to a minimum matric suction, it can dry out no more and the actual evaporation becomes equal to the rate of upward flow of water from the profile. At this stage, the evaporation is no longer set by external and surface conditions, but by internal soil profile hydraulics which determine the flux of soil water delivered to the evaporation zone.

Rainfall infiltration is a function of the soil infiltrability, which is defined according to Hillel (1971) as the downward flux of water through the surface when the surface is maintained under a thin layer of water essentially at atmospheric pressure. Infiltrability is not constant but decreases as the hydraulic gradient decreases throughout the wetted portion of the profile. If rainfall rate does not exceed infiltrability and if no free water is stored on the surface, then the soil absorbs the rain as fast as it falls and the rainfall infiltration is taken to be equal to the rainfall rate. As infiltrability decreases or if rainfall rate is greater than the current infiltrability or free water is present at the soil surface, then the rainfall infiltration is taken to be equal to infiltrability and any excess water will eventually form runoff.

Tailings undergoes a self-weight consolidation process after deposition. Pore water pressure is dissipated creating an upward and a downward flow in the case of double drainage. If the upward flow exceeds the actual evaporation then  $q_1$  is taken to be equal to the upward flow, in the contrary case  $q_1$  is equal to the actual evaporation.

For the bottom boundary

$$q_n = \Phi_{n+1/2}^{j+1/2} \left[ \mathfrak{I}_{n+1/2}^{j+1/2} + \mathfrak{R}_{n+1/2}^{j+1/2} \left( \frac{\Delta V_w}{\Delta Z} \right)_{n+1/2}^{j+1/2} \right]$$

At the lower boundary,  $q_n$  is either free drainage, groundwater recharge or water released from pore pressure dissipation, whichever applies.

### 3.6 HYDRAULIC CONDUCTIVITY

For saturated conditions the hydraulic conductivity is assumed to be a function of the void ratio.

$$[3.46] \quad K = Ce^D$$

where C and D are fitting parameters.

For unsaturated conditions the Brooks and Corey (1964) parametric equation is chosen

$$[3.47] \quad K = K_s \left( \frac{u_{wb}}{u_w} \right)^P \quad \text{for} \quad u_w > u_{wb}$$

where  $K_s$  (m/d) is the saturated hydraulic conductivity;  $u_{wb}$  is the bubbling pressure or air entry value; and P is an empirical parameter.

The unsaturated hydraulic conductivity function is derived from the soil water characteristic curve using the theory developed by Childs and Collis-George (1950) and reformulated by Jackson (1972). The conductivity function is obtained by dividing the soil water characteristic curve into N equal increments of volumetric water content ( $\theta$ ), determining the suction ( $u_w$ ) at the midpoint of each increment, and calculating for each point a value of conductivity according to the equation:

$$[3.48] \quad K_i = K_s \left( \frac{\theta_i}{\theta_s} \right)^{\frac{\sum_{j=1}^M [(2j+1-2i)\mu_{w_j}^{-2}]}{\sum_{j=1}^M [(2j-1)\mu_{w_j}^{-2}]}}$$

where  $K_i$  is the hydraulic conductivity corresponding to any particular value of the soil water content  $\theta_i$ ;  $i$  and  $j$  are summation indices; and  $M$  is the number of  $\theta$  increments for which the calculation is to be made.

### 3.7 BEARING CAPACITY

The ultimate bearing capacity of soil under a shallow strip footing can be expressed by the following general equation (due to Terzaghi):

$$[3.49] \quad q_f = 0.5\gamma B N_\gamma + c N_c + \gamma D_f N_q$$

where  $N_\gamma$ ,  $N_c$  and  $N_q$  are bearing capacity factors depending only on the value of  $\phi$ ;  $B$  and  $D_f$  are the width and depth of the footing base, respectively;  $\gamma$  is the unit weight and  $c$  is the global cohesion coefficient of the tailings, which is calculated as follows

$$[3.50] \quad c = c' + c_v + c_R$$

where  $c'$  is the effective cohesion of saturated soil (kPa),  $c_v$  is the increased effective soil cohesion due to suction (kPa); and  $c_R$  is the increased effective soil cohesion due to root matrix reinforcement (kPa).

### 3.7.1 Calculation of $c_v$

The solution of [3.44] gives the volume of water in every compartment of a tailings deposit. Using this information a moisture profile can be determined and a matric suction profile can be calculated by isolating  $u_w$  from [3.24]

$$[3.51] \quad u_w = -\frac{1}{\alpha} \left[ \left( \frac{\theta_s - \theta_r}{\theta - \theta_r} \right)^{\frac{1}{m}} - 1 \right]^{\frac{1}{d}}$$

The matric suction profile is used to estimate the value of  $c_v$ . Assuming that  $c_v$  is a function of the soil suction the following expression is proposed:

$$[3.52] \quad c_v = f(u_w) \tan \phi' \quad \text{for} \quad u_w > u_{wb}$$

where  $f(u_w)$  is a soil suction (negative pore water pressure) function and  $\phi'$  is the effective angle of internal friction of saturated soil. The function  $f(u_w)$  takes values of  $u_w$  greater than the air entry value  $u_{wb}$ .  $f(u_w) = 0$  when the soil is saturated and for values of  $u_w$  lower than  $u_{wb}$ . This proposed expression somewhat agrees with the model presented by Vanapalli et al. (1996) to predict shear strength with respect to soil suction.

$$[3.53] \quad \tau = c' + (\sigma_n - u_a) \tan \phi' + (u_a - u_w) [\Theta(u_a - u_w)]^\kappa \tan \phi'$$

where  $\tau$  is the shear strength;  $(\sigma_n - u_a)$  is the net normal stress on the plane of failure at failure;  $(u_a - u_w)$  is the matric suction of the soil on the plane of failure;  $\Theta(u_a - u_w)$  is the normalized water content as a function of matric suction; and  $\kappa$  is a fitting parameter.

From [3.53]  $c_v$  and  $f(u_w)$  can be expressed as



$$[3.54] \quad c_v = (u_a - u_w) [\Theta(u_a - u_w)]^k \tan \phi'$$

$$[3.55] \quad f(u_w) = (u_a - u_w) [\Theta(u_a - u_w)]^k$$

### 3.7.2 Calculation of $c_R$

Several researchers agree that the effect of roots is to provide an increase in the effective cohesion of the soil with no effect on the internal angle of friction (Gray and Ohashi 1983; Sotir and Gray 1989).

Coppin and Richards (1990) stated that the magnitude of the mechanical reinforcing effect of plant roots is a function of density, tensile strength, tensile modulus, length/diameter ratio, surface roughness, alignment and orientation. A model that includes all these variables has little use to engineers, who are interested in a simpler relationship to determine  $c_R$ . Endo and Tsuruta (1969) and Ziemer (1981) conducted in-situ direct shear tests on root-permeated soils. Their results showed an approximately linear increase in the root cohesion with increasing root biomass. Laboratory tests conducted by Gray and Sotir (1996) in root-permeated soils show a similar relationship. Therefore, to calculate the root cohesion term the following expression is used:

$$[3.56] \quad c_R = K_R B_R$$

where  $K_R$  is an empirical constant ( $\text{kPa/kg/m}^3$ ) for a specific plant and  $B_R$  is the biomass of roots per unit volume of soil ( $\text{kg/m}^3$ ). Test results for hardwood trees obtained by Nilaweera (1994) showed values of  $K_R$  that ranged from 4 to 15  $\text{kPa/kg/m}^3$ . Gray and Ohashi (1983) conducting laboratory tests in sand using reed fibers obtained a value of  $K_R$  of 3.2  $\text{kPa/kg/m}^3$ . Ziemer (1981) obtained a value of 3.7  $\text{kPa/kg/m}^3$  conducting in situ tests in sand using pine roots.

Coppin and Richards (1990) reported that typical values of  $c_R$  for grasses range from 3 to 5 kPa and for conifers from 3 to 17.5 kPa. Schiechl (1980) presented values of  $c_R$  for grasses from 2.9 to 13.4 kPa.

The root biomass ( $B_R$ ) distribution in the tailings profile is predicted using a linear function

$$(3.57) \quad B_{Ri} = B_{Rtop} \left( \frac{y_r - y_i}{y_r} \right)$$

where  $B_{Ri}$  is the root biomass in the  $i$  compartment ( $\text{kg/m}^3$ );  $B_{Rtop}$  is the root biomass at the tailings surface ( $\text{kg/m}^3$ ); and  $y_i$  is the depth of the  $i$  compartment (m).

$B_{Rtop}$  is predicted using a sine function similar to [3.37]

$$(3.58) \quad B_{Rtop} = B_{Rtopm} \{ 0.5 + 0.5 \sin [ 3.03 (t / t_m) - 1.47 ] \}$$

where  $B_{Rtopm}$  is the root biomass at time of maturity  $t_m$ .

### 3.8 MODEL BEHAVIOR

A computer program of the numerical algorithm has been tested on a variety of problems, only two are presented here. The calculated solutions are compared with the known solutions of the two problems.

The numerical model was first tested using soil input parameters from Pollock (1988) to predict excess pore pressures and tailings-water interface settlement of a sludge-sand mix, which was pumped into a 10-m standpipe and allowed to consolidate under its own weight. The model predicts the measured excess pore pressure very well when neglecting any water uptake by roots (Figure 3.9). The results obtained with the plant dewatering model are identical to those of

Pollock's model. The soil input parameters used in the model were  $A = 28.71 \text{ kPa}^{-1}$ ,  $B = -0.3097$ ,  $C = 7.425 \times 10^{-11}$ ,  $D = 3.847$ ,  $G_s = 2.27$ , initial solids content = 32.4%.

It is evident from Figure 3.10 that the mixture in the standpipe is consolidating faster than the theory predicts. The same behavior was found by Pollock in his evaluation. This more rapid consolidation has been postulated to result from creep (Suthaker 1995), but recent studies have shown that the diameter-to-height ratio of a standpipe influences the initial water release rate for CT (Boratynec et al. 1998). Chan and Masala (1998) suggested that this rapid consolidation may be due to a hindered sedimentation process.

A second example involves the problem of infiltration into Yolo light clay, which was solved by Philip (1957) using a quasianalytical procedure. The model was run using the following boundary and initial conditions:

$$u_w = -58.86 \text{ kPa} \quad t = 0 \quad 40 \text{ cm} \leq y \leq 0 \text{ cm}$$

$$u_w = 0 \quad t > 0 \quad y = 0$$

$$u_w = -58.86 \text{ kPa} \quad t > 0 \quad y = 40 \text{ cm}$$

The moisture retention curve that describes the Yolo light clay was fitted using [3.24] with the following parameters:  $\theta_r = 0.12$ ,  $\theta_s = 0.495$ ,  $\alpha = -0.3$ , and  $d = 1.4$ . The hydraulic conductivity was fitted using [47] with  $u_{wb} = -1.4 \text{ kPa}$  and  $P = 1.75$ . The saturated hydraulic conductivity  $K_s$  is  $1.063 \times 10^{-2} \text{ m/d}$ .

The computed solutions are plotted in Figure 3.11. It is observed that the present model handled the infiltration stage in this example quite well.

The good agreement found in these two examples indicates that the algorithm is correct in terms of its arithmetical operation.

### 3.9 CONCLUSIONS

A mathematical formulation has been developed to predict the bearing capacity increase on initially high water content tailings due to the strength enhancement mechanism of plants. This theoretical model is unique because it brings together formulations available from different disciplines. The model can also be used to predict shear strength with respect to soil suction and root reinforcement. The computer code has been shown to perform well in simulating nonlinear problems under saturated or unsaturated conditions.

The examples presented in this chapter do not test the capability of the model to predict bearing capacity. This issue is addressed in Chapter 4, which describes the greenhouse experiment carried out to gather experimental data to calibrate and validate the predictions of the proposed model.

### 3.10 REFERENCES

- Barth, R.C. 1986. Reclamation technology for tailing impoundments, Part 2: Revegetation. Mineral and Energy Resources. Colorado School of Mines. Vol. 29, No. 2.
- Boratynec, D.J., Chalaturnyk, R.J., and Scott, J.D. 1998. Experimental and fundamental factors affecting the water release rates of CT. Proceedings, 51<sup>st</sup> Canadian Geotechnical Conference, Edmonton, Alberta, October 4-7, 1998. Vol. 2. pp. 607-614.
- Borg, H., and Grimes, D.W. 1986. Depth development of roots with time: an empirical description. Transactions. American Society of Agricultural Engineering, **29**: 194-197.
- Bromwell, L. G. 1982. Evaluation of alternative processes for disposal of fine-grained waste materials. Florida Institute of Phosphate Research, FIPR Publication # 02-020-012.
- Brooks, R.H., and Corey, A.T. 1964. Hydraulic properties of porous media. Hydrology paper 3, Colorado State University, Fort Collins.
- Burns, R., Cuddy, G., and Lahaie, R. 1993. Dewatering of fine tails by natural evaporation. Proceedings of the oil sands – Our petroleum future conference (fine tailings symposium), Edmonton, Alberta, April 4-7, Paper F16.
- Campbell, G.S. 1985. Soil physics with basic transport models for soil-plant systems Development in soil science, 14. Elsevier, Amsterdam.

- Chan, D., and Masala, S. 1998. A time dependent model for sedimentation analysis of fine grained soils. Proceedings, 51<sup>st</sup> Canadian Geotechnical Conference, Edmonton, Alberta, October 4-7, 1998. Vol. 2. pp. 599-606.
- Chang, Y., and Corapcioglu, M.Y. 1997. Effects of roots on water flow in unsaturated soils. *Journal of Irrigation and Drainage Engineering*. **123**(3):202-209.
- Childs, E.C., and Collis-George, N. 1950. The permeability of porous materials. Proceedings of the Royal Society of London, Series A, Mathematical and Physical Sciences, **201A**: 392-405.
- Coppin, N.J., and Richards, I.G. 1990. Use of vegetation in civil engineering. Construction Industry Research and Information Association, Westminster, London.
- Cuddy, G. and Lahaie, R. 1993. Dewatering of mature fine tails by natural evaporation. Syncrude Canada Ltd. Research and Development Research Report 93-01.
- Cushman, J.H. 1982. Nutrient transport inside and outside the root rhizosphere. Theory. *Soil Science Society of America Journal*, **46**(4):704-709.
- de Jong, R. and Bootsma, A. 1997. Estimates of water deficit and surpluses during the growing season in Ontario using the SWATRE model. *Canadian Journal of Soil Science* **77**: 285-294.
- de Jong, R., Topp, G.C., and Reynolds, W.D. 1992. The used of measured and estimated hydraulic properties in the simulation of soil water movement - a case study. In US Salinity Laboratory. Edited by M. Th. van Genuchten, F.J. Leij, and L.J. Lund, US Department of Agriculture and Department of Soil and Environmental Science, University of California, Riverside, CA. pp. 569-585
- Dirksen, C. 1985. Relationship between root uptake-weighted mean soil water salinity and total leaf water potentials of alfalfa. *Irrigation Science*, **6**: 39-50.
- Dirksen, C. 1987. Water and salt transport in daily irrigated root zone. *Netherlands Journal of Agricultural Science*, **35**: 395-406.
- Endo, T. and Tsuruta, T. 1969. The effect of tree roots upon the shearing strength of soil. Annual Report of the Hokkaido Branch, Tokyo Forest Experiment Station, **18**:168-179.
- Feddes, R.A., Kowalik, P.J., and Zaradny, H. 1978. Simulation of field water use and crop yield. Simulation Monographs. Halsted Press, a division of John Wiley & Sons, New York.
- Feddes, R.A. 1981. Water use models for assessing root zone modification. In: Modifying the plant root environment. American Society of Agricultural Engineering, St. Joseph, Monograph **4**:347-390.
- Fuentes, C.R., Haverkamp, and Parlange, J.Y. 1992. Parameter constraint on closed-form soil water relationships. *Journal of Hydrology*, **134**: 117-142.

- Gray, D.H. and Ohashi, H. 1983. Mechanics of fiber reinforcement in sands. *Journal of Geotechnical Engineering (ASCE)*, **109**: 335-353.
- Gray, D.H. and Sotir, R.B. 1996. *Biotechnical and soil bioengineering slope stabilization. A practical guide for erosion control.* John Wiley & Sons. New York.
- Hillel, D. 1971. *Soil and water: physical principles and processes.* Academic Press, New York.
- Hillel, D., Talpaz, H., and Van Keulen, H. 1976. A macroscopic-scale model of water uptake by a nonuniform root system and of water and salt movement in the soil profile. *Soil Science*, **121**: 242-255.
- Jackson, R.A. 1972. On the calculation of hydraulic conductivity. *Soil Science Society of America Journal*, **36**:380-383.
- Jensen, M. E., Burman, R. D., and Allen, R. G., eds. 1990. *Evapotranspiration and irrigation water requirements. Manual of practice No. 70,* ASCE, New York.
- Johnson, R. L., Bork, P., Allen, E. A. D., James, W. H., and Koverny, L. 1993. *Oil sands sludge dewatering by freeze-thaw and evapotranspiration.* Alberta Conservation and Reclamation Council Report No. RRTAC 93-8. ISBN 0-7732-6042-0.
- Lee, C. R., Hoeppel, R. E., Hunt, P. G., and Carlson, C. A. 1976. *Feasibility of the functional use of vegetation to filter, dewater, and remove contaminants from dredged material.* USAE, WEST Tech, Report D-76-4.
- Li, X. and Feng, Y. 1995. *Dewatering fine tails by evaporation: A mathematical modelling approach.* Alberta Environmental Center, Vegreville, Alberta. AECV95-R5.
- Ludeke, K. L. 1973. *Vegetation stabilization of copper mine tailings disposal berms of Pima Mining Company.* In *Tailings disposal today.* Edited by C. L. Aplin, and G. O. Argalls, Miller Freeman, San Francisco. pp. 377-386.
- Mariño, M.A., and Tracy, J.C. 1988. Flow of water through root-soil environment. *Journal of Irrigation and Drainage Engineering*, **114**(4):588-604.
- McFarlin, R. F., Lloyd, G. M., and El-Shall, H. 1989. *Tailings management of the Florida phosphate industry.* In *Tailings and Effluent Management.* Edited by M.E. Chalkley, B.R. Conrad, V.I. Lakshmanan, and K.G. Wheeland. *Proceedings of the International Symposium on Tailings and Effluent Management, Halifax, Nova Scotia, August 20-24, 1989.*
- McLonden, J. T., Boyle, J. R., and Sweeney, J. W. 1983. *A technical evaluation of conventional versus developing processes of phosphatic clay disposal.* Florida Institute of Phosphate Research, FIPR Publication # 02-017-022.
- Monteith, J.L. 1965. *Evaporation and environment.* In *The state and movement of water in living organism.* Edited by G.E. Fogg, Academic Press, New York, N.Y. pp. 205-234.

- Molz, F.J. 1976. Water transport in the soil-root system: transient analysis. *Water Resources Research*, **12**: 805-808.
- Molz, F.J. 1981. Models of water transport in the soil-plant system. A review. *Water Resources Research*, **17**: 1245-1260.
- Mualem, Y. 1976. A new model for predicting the hydraulic conductivity of unsaturated porous media. *Water Resources Research*, **12**(3): 513-522.
- Neurohr, G. A. 1983. Use of macrophytes for sludge treatment. Proceedings, 6<sup>th</sup> symposium on wastewater treatment, Montreal, Quebec, November 16-17, 1983. pp. 413-430.
- Newson, T., Fujiyasu, Y., and Fahey, M. 1996. A field study of the consolidation behavior of saline gold tailings. Proceedings of the tailings and mine waste '96 conference, Fort Collins, Colorado, January 16-19, 1996. pp. 179-188.
- Nilaweera, N.S. 1994. Effects of tree roots on slope stability: The case of Khao Luang Mountain area, So. Thailand. Dissertation No. GT-93-2. Thesis submitted in partial fulfillment of requirements for degree of Doctor of Technical Science, Asian Institute of Technology, Bangkok, Thailand.
- Philip, J.R. 1957. The theory of infiltration, 1, the infiltration equation and its solution. *Soil Science*, **83**(5):345-357.
- Pollock, G.W. 1988. Large strain consolidation of oil sand tailings sludge. M.Sc. Thesis, University of Alberta, Canada.
- Prasad, R. 1988. A linear root uptake model. *Journal of Hydrology*, **99**: 297-306.
- Public Relations and Information Department of the Netherlands Ministry of Transport and Waterstat. 1959. From Fisherman's Paradise to Farmer's Pride. Netherlands Government Information Service. The Hague, Netherlands.
- Qiu, Y. and Sego, D. C. 1998. Engineering properties of mine tailings. Proceedings, 51<sup>st</sup> Canadian Geotechnical Conference, Edmonton, Alberta. October 4-7, 1998. Vol. 1. pp. 149-154.
- Remson, I., Hornberger, G.M., and Molz, F.J. 1971. Numerical methods in subsurface hydrology. Wiley Interscience, New York.
- Ritchie, J.T. 1972. Model for predicting evaporation from a row crop with incomplete cover. *Water Resources Research*, **8**(5): 1204-1213.
- Schiechtl, H.M. 1980. Bioengineering for land reclamation and conservation. Edmonton, Canada: University of Alberta Press.

- Shelling, J. 1960. New aspects of soil classification with particular reference to reclaimed hydromorphic soils. Transactions, International Society of Soil Science, Seventh International Congress of Soil Science, Amsterdam, Holland, Vol. 4. pp. 218-224.
- Silva, M.J., Naeth, M.A., Biggar, K.W., Chanasyk, D.S. and Segó, D.C. 1998. Plant selection for dewatering and reclamation of tailings. Proceedings, 15<sup>th</sup> Annual Meeting of the American Society for Surface Mining and Reclamation. St. Louis, Missouri, May 17-21, 1998. pp. 104-117.
- Stahl, R. P. 1996. Characterization and natural processes enhancing dry landscape reclamation of fine processed mine wastes. Ph.D. thesis, University of Alberta, Edmonton, Alberta.
- Sotir, R.B. and Gray, D.H. 1989. Fill slope repair using soil bioengineering systems. Proceedings, 20th International Erosion Control Association Conference, Vancouver, B.C., February 15-18, 1989. pp. 473-485.
- Suthaker, N. 1995. Geotechnics of oil sand fine tailings. Ph.D. thesis, University of Alberta, Edmonton, Alberta.
- U.S. Bureau of Mines. 1975. The Florida phosphate slimes problem - a review and bibliography. IC No. 8668.
- Van Bavel, C.H.M. 1966. Potential evaporation: the combination concept and its experimental verification. *Water Resources Research*, 2(3):455-467.
- Van Genuchten, M.Th. 1980. A closed-form equation for predicting the hydraulic conductivity of unsaturated soils. *Soil Science Society of America Journal*, 44: 892-898.
- Vanapalli, S.K., Fredlund, D.G., and Pufahl, D.E. 1996. Model for the prediction of shear strength with respect to soil suction. *Canadian Geotechnical Journal*, 33: 379-392.
- Vick, S. G. 1983. Planning, design and analysis of tailings dams. John Wiley and Sons, New York.
- Volker, A. 1982. Polders: An ancient approach to land reclamation. *Nature and Resources* 18: 2-13.
- Ziemer, R. 1981. Roots and shallow stability of forested slopes. International Association of Hydrological Sciences, Publication No. 132, pp. 343-361.



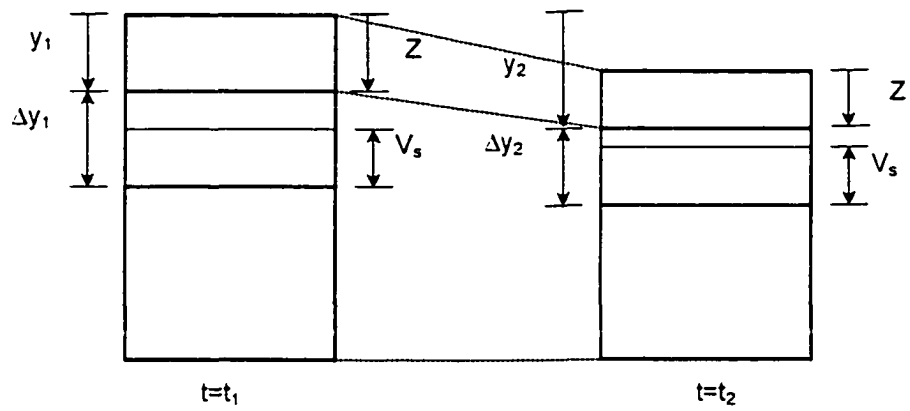


**Figure 3.1** Spatial and material coordinate systems

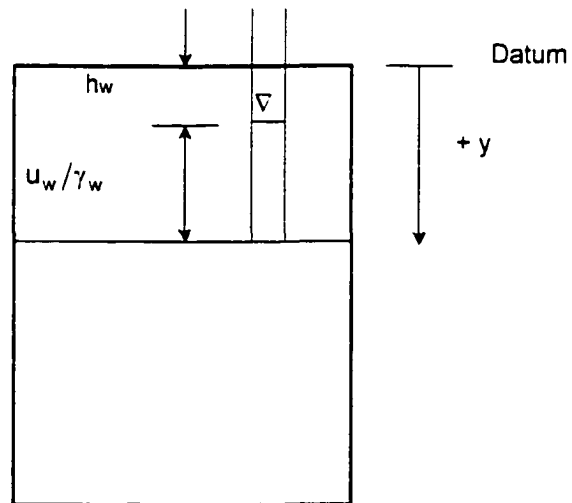


**Figure 3.2** Tailings deposit

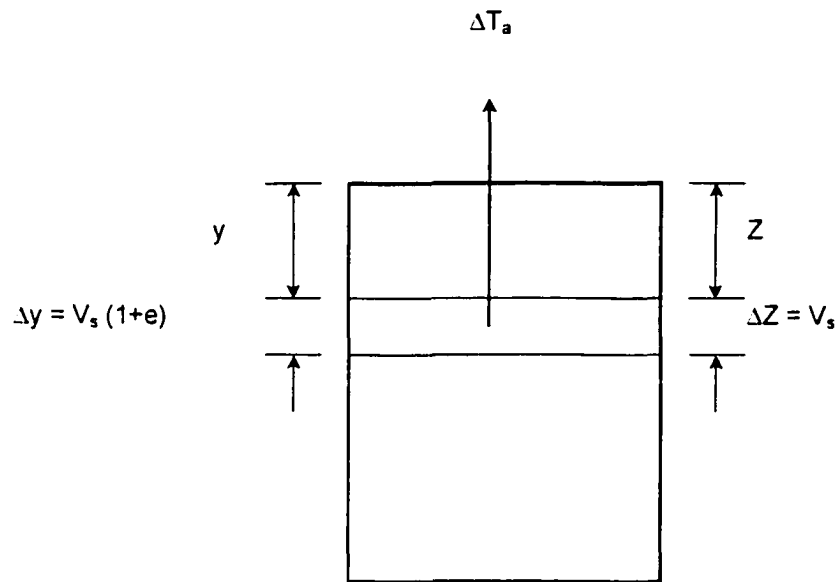


**Figure 3.3** Root water uptake from a compartment

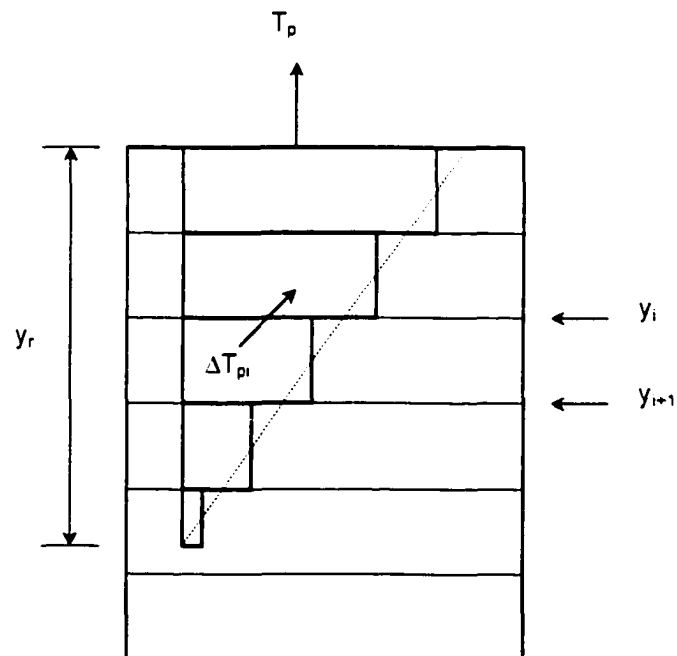


**Figure 3.4** Linear water uptake distribution

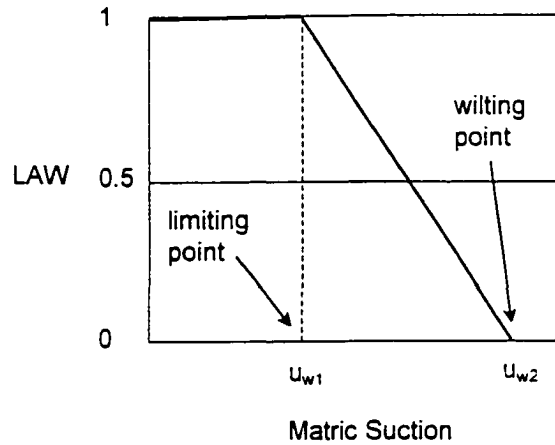


Figure 3.5 Limited available water function

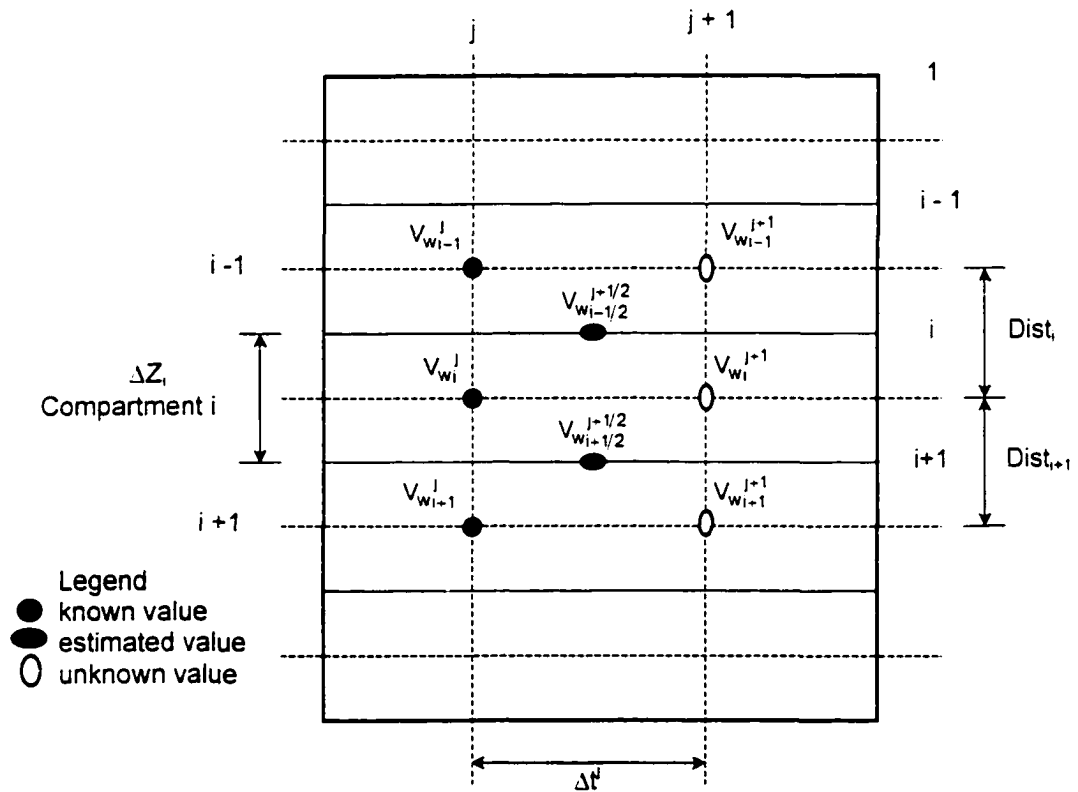
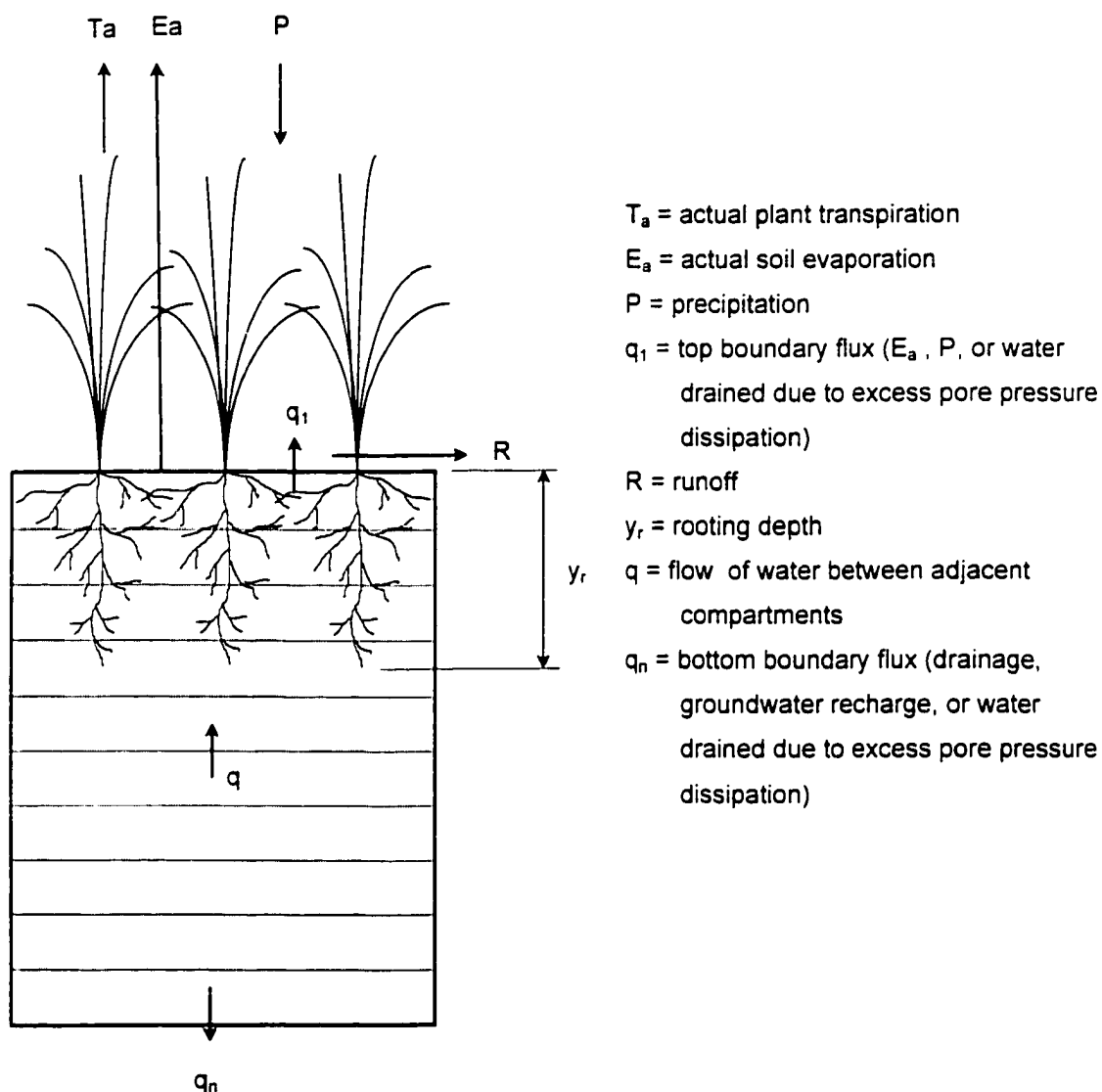


Figure 3.6 Finite difference scheme on the depth-time region

$$\begin{bmatrix} B_1 & C_1 & 0 & \bullet & 0 \\ A_2 & B_2 & C_2 & \bullet & \bullet \\ 0 & \bullet & \bullet & \bullet & 0 \\ \bullet & \bullet & A_{n-1} & B_{n-1} & C_{n-1} \\ 0 & \bullet & 0 & A_n & B_n \end{bmatrix} \times \begin{Bmatrix} V_{w1}^{j+1} \\ V_{w2}^{j+1} \\ \bullet \\ V_{wn-1}^{j+1} \\ V_{wn}^{j+1} \end{Bmatrix} = \begin{Bmatrix} D_1 \\ D_2 \\ \bullet \\ D_{n-1} \\ D_n \end{Bmatrix}$$

**Figure 3.7** System of simultaneous linear equations



**Figure 3.8** Scheme of the plant dewatering model

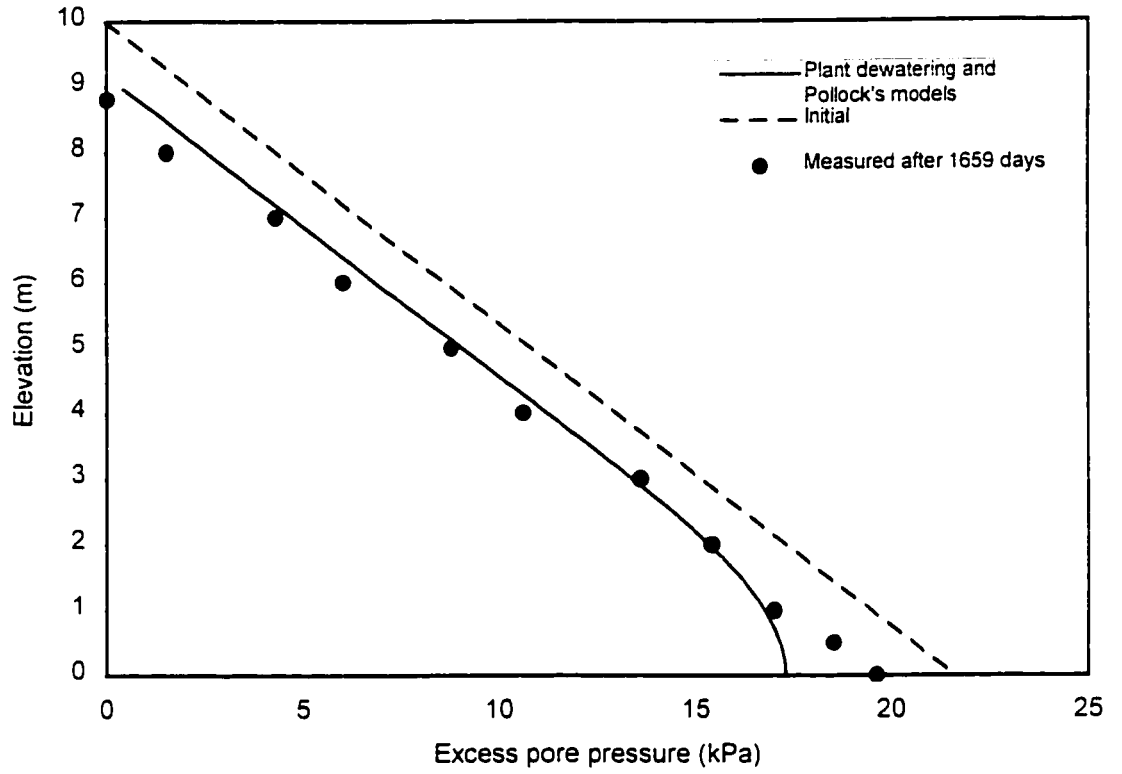


**Figure 3.9 Comparison of excess pore water pressures**

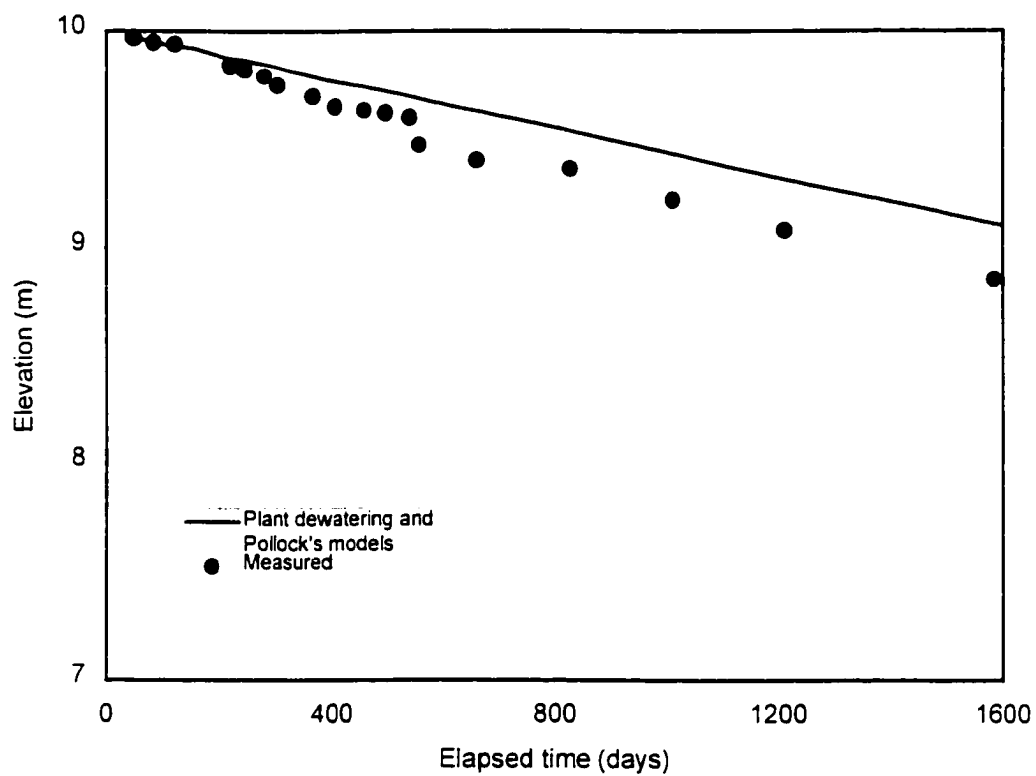


**Figure 3.10 Tailings-water interface settlement**

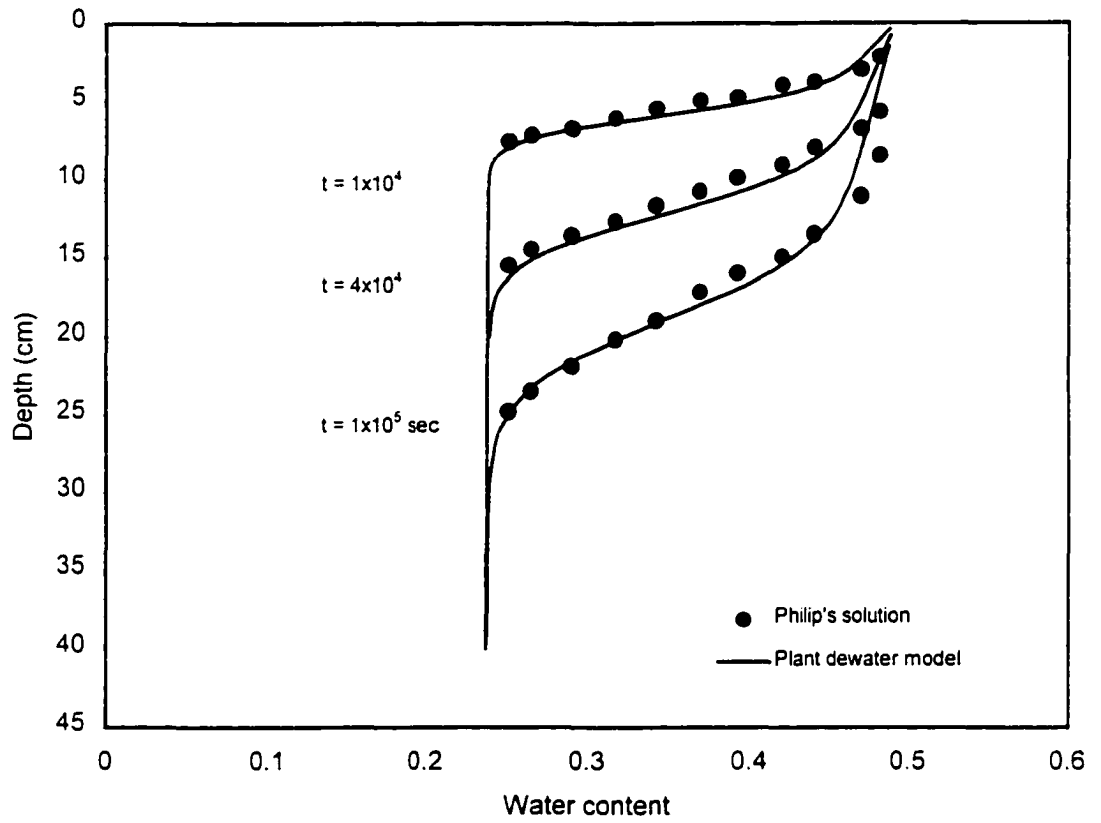


**Figure 3.11 Isothermal infiltration**

## Chapter 4

### **Plant dewatering of tailings: experimental results and model predictions<sup>1</sup>**

#### 4.1 INTRODUCTION

The use of plants to dewater fine tailings has been identified as a mechanism that may economically enhance the surface stability of these weak deposits on a large scale. Plants growing in tailings accelerate the consolidation process and increase their bearing capacity in the root zone through evapotranspiration and root reinforcement.

Prediction of the bearing capacity is essential in the management of tailings. Reclamation of these tailings cannot be initiated until the deposit achieves a trafficable surface. A model capable of predicting the bearing capacity increase due to the strength enhancement mechanism of plants was theoretically described in Silva et al. (1998a). The model was shown to perform well in simulating nonlinear problems under saturated and unsaturated conditions.

This paper presents the experimental validation of the model. Settlement, solids content and bearing capacity profiles, which were measured in a greenhouse experiment, were compared

---

<sup>1</sup> A version of this chapter has been published.

Silva, M.J., Biggar, K.W., Segó, D.C., Chanasyk, D.S., and Naeth, M.A. 1998. *Plant dewatering of tailings: model validation. Proceedings. 51<sup>st</sup> Canadian Geotechnical Conference, Edmonton, Alberta, October 4-7, 1998. Vol. 2. pp. 639-645.*

Silva, M.J., Biggar, K.W., Segó, D.C., Chanasyk, D.S., and Naeth, M.A. 1999. *Plant dewatering and strengthening of tailings: laboratory and computer simulations. Proceedings, Tailings and Mine Waste '99 Conference. Fort Collins, Colorado, January 24-27, pp. 315-323.*

A version of this chapter has been submitted for publication.

Silva, M.J., Biggar, K.W., Segó, D.C., Chanasyk, D.S., and Naeth, M.A. 1999. *Plant dewatering of tailings: experimental results and model predictions. Paper submitted for review to the Canadian Geotechnical Journal, May, 1999. 38 pgs.*



with their respective values predicted by the model. Tailings parameters used in the model were determined from independent laboratory measurements or from data reported in the literature. Parameters that were not available in the literature were back calculated from measured values. A detailed evaluation of the plant response to this mine waste tailings is described in Silva (1999)

## 4.2 BACKGROUND

Experimental results by Stahl (1996) and Johnson et al. (1993) have shown that suitable plants species are capable of increasing the strength of weak tailings deposits. Plants growing in tailings transpire large quantities of water increasing the matric suction in the root zone of the deposit, resulting in an increase in the shear strength and bearing capacity. Furthermore, the plant root system provides a fiber reinforcement, which produces an additional increase in the bearing capacity of the rooted tailings.

The ultimate bearing capacity of soil under a shallow strip footing can be estimated using Terzagui (1943) bearing capacity theory

$$[4.1] \quad q_f = 0.5\gamma BN_\gamma + cN_c + \gamma D_f N_q$$

where  $N_\gamma$ ,  $N_c$  and  $N_q$  are bearing capacity factors depending only on the value of the angle of shearing resistance for a saturated soil ( $\phi'$ );  $B$  and  $D_f$  are the width and depth of the footing base, respectively;  $\gamma$  is the unit weight and  $c$  is the global cohesion coefficient, which is calculated as follows

$$[4.2] \quad c = c' + c_\psi + c_R$$

where  $c'$  is the effective cohesion of saturated soil;  $c_\psi$  is the increased effective soil cohesion due to suction; and  $c_R$  is the increased effective soil cohesion due to root reinforcement. The suction

cohesion  $c_{\psi}$  is determined using the matric suction profile of the tailings deposit and the root cohesion  $c_R$  is calculated using the root biomass distribution (Silva et al. 1999).

The bearing capacity equation [4.1] was further refined to accommodate various shapes of the footing:

$$[4.3] \quad q_f = \lambda_{\gamma} 0.5 \gamma B N_{\gamma} + \lambda_c c N_c + \gamma D_f N_q$$

where  $\lambda_{\gamma}$  and  $\lambda_c$  are shape factors.

For circular footings, the shape factors are  $\lambda_{\gamma} = 0.6$  and  $\lambda_c = 1.3$ .

### 4.3 LABORATORY PROGRAM

A greenhouse experimental program was conducted to evaluate the physical response of tailings to the plant dewatering mechanism as well as to provide a data set for the calibration and validation of the model. Composite Tailings (CT), which is described below, was used as the growth medium and five different plant species were selected for testing. These plant species proved the most viable in CT as a result of greenhouse experiments conducted to identify the most suitable plant species for dewatering CT (Silva et al. 1998).

#### 4.3.1 Materials and method

Composite Tailings (CT) was prepared by mixing tailings sand, Mature Fine Tailings (MFT), tailings pond water and gypsum, which were provided by Syncrude Canada Ltd. The amount of gypsum added was approximately  $1200 \text{ g/m}^3$  and the proportion of sand, MFT and water was such that the CT mixture had 20% fines and an initial solids content of 65%. The mixture was made up in several batches using a  $0.22\text{-m}^3$  cement mixer. The size of the mixer was chosen to

prepare enough volume of CT to fill one lysimeter at a time and to obtain a homogeneous CT mixture in each lysimeter.

When the CT mixture is transferred from the mixer to the lysimeter, some of the water is trapped in the pore spaces. This entrapped water is under an excess pressure, which is caused by the weight of the CT. Thus, some of the water flows out of the deposit relieving this excess pressure, this process is known as self-weight consolidation. The greatest excess pressure occurs at the bottom of the lysimeter and it takes a considerable amount of time for the water to travel from the bottom to the surface of the deposit to relieve this pressure. Figure 4.1 shows a schematic diagram of the lysimeters used in the experiment. This setup, which is described below, accelerated the self-weight consolidation process.

Forty five-gallon drums were lined with a plastic bag and had a 75-mm-thick saturated coarse sand placed at the bottom to act as a filter. One end of a plastic tube, wrapped with geotextile, was inserted into the filter and the other end was located at the top of the lysimeter. This system created double drainage, which accelerated the self-weight consolidation of the CT deposit. The lysimeters had a diameter of 57.2 cm and a height of 84.0 cm. Aluminum tubes, having a diameter of 50 mm and a wall thickness of 1.3 mm, were installed in the center of each lysimeter to allow access for a neutron probe to monitor the solids content within the tailings. The lysimeters were filled with CT to a depth of about 0.8 m and self-weight consolidation was allowed to take place. Any expressed water was siphoned off and additional CT was added to restore the initial level. The plastic tubes were removed from the lysimeters four days later when no more drainage was noticed. Six lysimeters were instrumented with five mini-TDR probes each built at the University of Alberta. The mini-TDR probes measured solids content in a smaller zone compared with that of the neutron probe. The neutron probe and the TDR probes were specially calibrated to measure solids content of the CT in the lysimeters.

The plant species used in the experiment were: Altai wildrye (*Elymus angustus*), Creeping foxtail (*Alopecurus arundinaceus*), Red top (*Agrostis stolonifera*), Reed canary grass (*Phalaris*

arundinacea), and Streambank wheatgrass (Agropyron riparian). Plants were started from seeds in root trainers and transplanted to the lysimeters after 4 weeks with the equivalent to 64 plants/m<sup>2</sup>. At that time, the tailings had some free water at the surface generated by the consolidation process and the small seedlings were under a waterlogged condition. Three lysimeters were used for each species and three were left unplanted as a control. The lysimeters were placed in a growth room in a randomized complete block design. Air temperature and hours of light per day were set at 22 °C and 15 hours, respectively, simulating a typical growing environment in Fort McMurray in June. The average maximum and minimum temperature recorded were 24.7 and 20.6 °C, respectively. The average relative humidity was 52.9%. Water was added weekly to simulate average precipitation at Syncrude Canada's Mildred lake site from June through August. Long-term values of precipitation for this location are 63.9 mm for June, 79.1 mm for July and 71.8 mm for August.

Fertilizer was added cautiously to prevent the total solute load from exceeding the salinity tolerance of the plants. To avoid over-fertilization, the amount of fertilizer was based on optimum levels of macronutrients required by agronomic species. The fertilizer was added to give an equivalent of 150 kg N/ha, 80 kg P<sub>2</sub>O<sub>5</sub>/ha, and 105 kg K<sub>2</sub>O/ha. Refer to Chapter 2 for appropriate analysis and background.

### **4.3.2 Measurements**

The climatic condition of the growth chamber was characterized by measuring the ambient relative humidity, minimum and maximum air temperatures and potential evaporation.

Initial tailings elevations were recorded after transplanting. Thereafter, elevations were recorded in each lysimeter at regular intervals to determine the surface settlement. Solids contents were measured weekly via the neutron probe and TDR probes to obtain information on the water lost due to evapotranspiration in the planted lysimeters and evaporation in the controls. Number of

tillers, number of leaves, plant height and leaf area were determined at regular intervals throughout the experiment.

The leaf area was determined on five different dates using the following procedure. The leaves of a subsample from each lysimeter were carefully traced on paper. The leaf area was then measured using a planimeter. The total leaf area was determined by multiplying the area of the subsample by the total number of leaves. These leaf areas were then used to calculate the leaf area index (LAI), which is defined as the area of one side of leaves per unit of soil surface (Jensen et al. 1990).

After ten weeks of plant growth, reed canary grass and creeping foxtail showed symptoms of water stress. Solids content measurements indicated that indeed the tailings deposit was near the wilting point, which is about 96% solids. This condition dictated the end of the test series. The wilting point was determined from the soil water characteristic curve for CT reported by Qiu and Sego (1998). The solids content of 96% corresponds to a soil suction of about 1500 kPa, which is generally accepted as the wilting point of most plants.

Bearing capacity was measured at two locations in each of three different layers within each barrel by conducting plate load tests (Figure 4.2). A plate with a diameter of 80 mm was chosen to eliminate any boundary effect in the test. Also, the vertical distance between two adjacent test layers was at least two times the plate diameter to avoid overlapping of the zone of influence of the bearing tests.

Samples of tailings were taken every 10 cm to measure the solids content profiles. Root densities below every plate load test were measured by inserting rings of known volume. The roots were washed and oven dried to measure the dry root biomass within this zone.

#### 4.4 EXPERIMENTAL RESULTS

The measured solids content profiles at the end of the greenhouse experiment are presented in Figure 4.3. Reed canarygrass did the best job of water removal followed closely by creeping foxtail. In these samples the low moisture content and high suctions were close to the wilting point (between 1500 and 2000 kPa) and the plants started showing signs of water stress. This condition dictated the termination of the experiment. Pure evaporation (control) caused little dewatering of the CT compared to the plants. Salt accumulations and the presence of a film of bitumen at the surface of the control lysimeters inhibited further water removal by evaporation.

The root biomass profile is presented in Figure 4.4. These curves are the average of six root density profiles measured within each planted treatment. A semi-logarithmic scale was used to provide a better visualization of root biomass differences. Reed canary grass produced the highest root biomass distribution. There appears to be a direct relationship between root biomass and root water uptake, which can be seen by comparing Figures 4.3 and 4.4.

Results of the plate load tests are shown in Figure 4.5. These curves are the average of six bearing tests performed within each treatment. It is evident that matric suction (from solids content profile of Figure 4.3) and root reinforcement (from root biomass of Figure 4.4) had a direct effect on the bearing capacity test results. Reed canarygrass, having the highest solids content profile (hence the highest matric suction profile) and the highest root biomass distribution, produced the highest bearing pressures, which ranged from approximately 975 to 1050 kPa. Plate load tests conducted on the control lysimeters (no plants) resulted in the lowest measured bearing capacities, with an average bearing capacity at the surface of the tailings of approximately 55 kPa. At the middle layer the average bearing capacity was in the order of 15 kPa. At the bottom layer the material was so soft that it was not possible to conduct a test using the test equipment. Comparing the bearing capacities of the planted lysimeters to the control lysimeters, the significance of the strength enhancement mechanism of the plants is evident.

## 4.5 MODEL CALIBRATION/VALIDATION

The model described in Silva et al. (1999) was used to predict the plant dewatering process observed in the greenhouse experiment.

### 4.5.1 Model data input

The Soil Water Characteristic Curve (SWCC) for CT presented by Qiu and Segó (1998) was fitted according to the empirical relationship (Van Genuchten 1980):

$$[4.4] \quad \theta = \theta_r + \frac{\theta_s - \theta_r}{\left[1 + (\alpha u_w)^d\right]^m}$$

where  $\theta$  is volumetric water content;  $u_w$  is pore water pressure (matric suction);  $\theta_r$  (0.01) and  $\theta_s$  (0.38) are the residual and saturated volumetric water contents, respectively;  $\alpha$  (0.15),  $d$  (1.35) and  $m$  (0.26) are regression parameters.

The plot of effective stress versus void ratio for CT presented by Qiu and Segó (1998) was fitted to the following power relationship:

$$[4.5] \quad e = A(\sigma')^B$$

where  $e$  is void ratio;  $\sigma'$  is effective stress (kPa);  $A$  (0.9952 kPa<sup>-1</sup>) and  $B$  (-0.1811) are fitting parameters.

For saturated conditions the hydraulic conductivity is calculated as:

$$[4.6] \quad K = Ce^D$$

where  $K$  is hydraulic conductivity (m/d);  $C$  ( $5.18 \times 10^{-4}$  m/d) and  $D$  (1.3754) are fitting parameters, whose values were taken directly from Qiu and Segó (1998).

The unsaturated hydraulic conductivity versus matric suction relationship was calculated from the SWCC for CT using the theory developed by Childs and Collis-George (1950) and reformulated by Jackson (1972). The resultant plot was then fitted to the expression proposed by Brooks and Corey (1964):

$$[4.7] \quad K = K_s \left( \frac{u_{wb}}{u_w} \right)^P \quad \text{for} \quad u_w > u_{wb}$$

where  $K_s$  is saturated hydraulic conductivity (m/d);  $u_{wb}$  is bubbling pressure or air entry value (-0.6 kPa); and  $P$  is a fitting parameter (0.65).

The limiting point of water extraction ( $u_{w1}$ ) was set as -500 kPa, which correspond to about 20% of the remaining available water (Doorenbos and Kassam 1979) and the wilting point ( $u_{w2}$ ) used was -2000 kPa.

The measured potential evapotranspiration ( $ET_0$ ) was distributed into its evaporation ( $E_0$ ) and transpiration ( $T_0$ ) components using the model proposed by Ritchie (1972), who observed that the transpiration component was dependent on the leaf area index (LAI) according to the following relationship:

$$\begin{array}{ll}
 T_0 = 0 & \text{LAI} < 0.1 \\
 [4.8] \quad T_0 = ET_0 (-0.21 + 0.7 \text{ LAI}^{1/2}) & 0.1 \leq \text{LAI} \leq 2.7 \\
 T_0 = ET_0 & \text{LAI} > 2.7
 \end{array}$$

LAI is defined as the area of one side of leaves per unit of soil surface (Jensen et al. 1990). Potential evaporation ( $E_0$ ) is then determined by subtracting  $T_0$  from  $ET_0$ .



Values of LAI for each plant species were calculated from measured leaf areas and then fitted using an S-shape curve of the form

$$[4.9] \quad \text{LAI} = \frac{x}{x + \exp(c_1 - c_2x)}$$

where  $x$  represents a time fraction;  $y$  represents LAI;  $c_1$  and  $c_2$  are fitting parameters. LAI curves used as input in the model are shown in Figure 4.6. As an example, measured values of LAI of reed canarygrass and red top are presented in the figure to show how well the measured data fit the curves. Fitting parameters  $c_1$  and  $c_2$  for each plant species are presented in Table 4.1.

The actual soil evaporation ( $E_a$ ) is calculated as

$$[4.10] \quad E_a = K_{\text{evap}}E_0$$

where  $K_{\text{evap}}$  is an evaporation limiting factor, which is equal to 1 when the tailings surface is saturated and less than 1 when the surface becomes unsaturated and the supply of water to the surface becomes limited. This limiting factor also accounts for a salt crust formation that inhibits evaporation. The evaporation rate of CT drops to about 0.6 of potential evaporation in approximately 10 days (Qiu and Segó 1998). This result was used in the model as the evaporation limiting factor ( $K_{\text{evap}}$ ).

Crop coefficients ( $K_c$ ) (Silva et al. 1999) for plants growing in CT are not available in the literature. Most of the published crop coefficients were determined under normal soil conditions and cannot be extrapolated to an artificial soil like the tailings. Therefore, values of  $K_c$  were assumed based on plant performance reported by Silva et al. (1998). The following values of  $K_c$  were used: Altai (0.5); Foxtail (0.85); Red top (0.75); Reed canary (1); and Streambank (0 for first four weeks and 0.7 afterwards).

The root growth was predicted using a sine function (Borg and Grimes 1986):

$$[4.11] \quad y_r = y_m \{0.5 + 0.5 \sin[3.03(t/t_m) - 1.47]\}$$

where  $y_r$  is rooting depth (m) at time  $t$  (d);  $t_m$  is time to plant maturity (d);  $y_m$  is the maximum rooting depth at  $t = t_m$ . Values of  $y_m$  and  $t_m$  were estimated from the solids content profiles.

The suction cohesion  $c_v$  was calculated with the equation

$$[4.12] \quad c_v = f(u_w) \tan \phi' \quad \text{for} \quad u_w > u_{wb}$$

where  $f(u_w)$  is a soil suction function and  $\phi'$  is the angle of shearing resistance for a saturated soil, taken as  $30^\circ$  (Qiu and Segoo 1998).

The root cohesion  $c_R$  was determined with the expression

$$[4.13] \quad c_R = K_R B_R$$

where  $K_R$  is an empirical constant ( $\text{kPa/kg/m}^3$ ) for a specific plant and  $B_R$  is the biomass of roots per unit volume of soil ( $\text{kg/m}^3$ )

The function  $f(u_w)$  was estimated together with the root coefficient  $K_R$  using the measured values of bearing pressure, matric suction (determined from solids content) and root biomass from the Control and Red top test results. The Control had no roots and the bearing capacity was affected by only the suction and effective cohesion of the CT. Red top had a wide range of values of bearing capacity, matric suction and root distribution biomass. These two treatments were good candidates for calibrating the model. The global cohesion was back calculated inserting the measured bearing capacities in equation [4.1]. The same global cohesion was again calculated using [4.2], which can be expressed as

$$[4.14] \quad c = c' + K_\psi u_w^\beta \tan \phi' + K_R B_R$$

where  $K_\psi$  and  $\beta$  are fitting parameters. The value of  $K_R$  was taken as 5 kPa/kg/m<sup>3</sup> (Silva et al. 1999); and  $B_R$  is root biomass. A good correlation between measured and calculated values of  $c$  global (Figure 4.7) was found with  $K_\psi = 0.285$  and  $\beta = 0.69$ , which define the suction function as

$$[4.15] \quad f(u_w) = K_\psi u_w^\beta$$

#### 4.5.2 Settlement predictions

The tailings profile was divided in 13 compartments, each one having an initial thickness of 0.05 m. The size of each time step was restricted to a maximum variation in the volume of water of the compartments (Max  $\Delta V_w = 1 \times 10^{-5}$  m). Additionally, a maximum time step was prescribed (Max  $\Delta t^{n+1} = 1$  hour).

The measured and predicted surface settlements for only reed canarygrass and streambank wheatgrass are presented in Figure 4.8 and Figure 4.9, respectively. These two planted treatments present the extremes of solids content profiles (Figure 4.3). Similar curves were obtained for the other treatments. The model matches very well the trend of the measured settlements, however the model predicted slightly higher values in all cases. No significant difference was found in the settlements which occurred in the planted and the unplanted treatments.

#### 4.5.3 Solids content profile predictions

The measured and simulated solids content profiles are presented in Figures 4.10 to 4.15. Day 1 represents the initiation of the modeling time. Samples of tailings were taken from the lysimeters using a mini-piston sampler built at the University of Alberta. These values were used as initial conditions in the model.

The model predictions generate a smooth curve matching very well the trend of the measured values. The profile trends in the planted lysimeters indicate the influence of plant transpiration

and root growth. Physical measurements of solids content at the end of the experiment matched very well with TDR and neutron probe measurements carried out throughout the growth period.

#### **4.5.4 Bearing capacity predictions**

Predicted and measured values of bearing capacity are presented in Figure 4.16. Two treatments (Control and Red top) were used to calibrate the model for predicting both the suction cohesion ( $c_v$ ) and the root cohesion ( $c_R$ ). The values of bearing capacity predicted by the model are inside or very close to the 95% confidence interval of the measured values of the remaining treatments. This range comprises six bearing capacity tests conducted on each layer of every treatment. These results validate the model for predicting bearing capacity increase due to the strength enhancement mechanism of plants.

The root cohesion component (Table 4.2) is very small compared with the suction cohesion component. However, in practice, the suction cohesion component will vary in response to climatic or environmental conditions such as evaporation, plant transpiration, and precipitation. Whereas, the root cohesion will be somewhat stable when the plants reach maturity and the rooting depth will be at its maximum value.

#### **4.6 PRACTICAL IMPLICATIONS**

The suction and root components of the global cohesion coefficient can be reduced or eliminated in nature. As an example, the suction component can be reduced by precipitation and the root component can be eliminated by root decay. Taking  $c' = 3$  kPa,  $\phi' = 30^\circ$  (Qiu and Sego 1998) and  $c_v = 20$  kPa,  $c_R = 5$  kPa (Reed canary grass, Table 4.2) and using only the cohesion component of equation [4.2] the bearing capacity obtained is approximately 1008 kPa. The contributions of each component to the total bearing capacity are 11% due to the saturated cohesion, 18% due to the root reinforcement, and 71% due to the matric suction. If matric suction reaches zero after a

heavy rainfall, the bearing capacity will be 288 kPa, from that 37% will be due to the saturated cohesion and 63% will be accredited to the root reinforcement.

The worst case scenario will be when the roots and the matric suction do not make any contributions (root decay and zero matric suction) to the bearing capacity. In this case the bearing capacity will be solely due to the saturated cohesion (108 kPa ). This value of bearing capacity is higher than the average bearing capacity measured in the control lysimeters, 55 kPa at the surface and 15 kPa in the middle layer. To compensate for this discrepancy a conservative value of  $c' = 0.2$  kPa was used in the model to calculate bearing capacity.

#### **4.7 CONCLUSIONS**

A greenhouse experiment was conducted to validate the strength enhancement mechanism of plants growing on tailings. Measured values were compared with values predicted by the plant dewatering model. The model slightly over-predicts the surface settlement, but a good match was found in the trend. Good agreement was found between the measured and predicted solids content profile. The theoretical formulation simulates very well the plant dewatering mechanism regarding the dynamics of the soil moisture. Back-calculation was conducted to determine the parameters, which define the suction cohesion function and root cohesion coefficient. These parameters were inserted in the model and bearing capacities were predicted for the remaining treatments. Predicted values of bearing capacity are in good agreement with measured values.

The bearing capacity increase caused by the plant dewatering mechanism exceeded expectations. The evaporation process, which was acting on the controls, did not cause any significant dewatering of the CT compared to the plants.

The model is considered appropriate for predicting solids content profile and bearing capacity increase due to the plants for one growing season.

#### 4.8 REFERENCES

- Borg, H., and Grimes, D.W. 1986. Depth development of roots with time: an empirical description. *Transactions, American Society of Agricultural Engineering*, **29**: 194-197.
- Brooks, R.H., and Corey, A.T. 1964. Hydraulic properties of porous media. Hydrology paper 3, Colorado State University, Fort Collins.
- Childs, E.C., and Collis-George, N. 1950. The permeability of porous materials. *Proceedings Royal Society*. Vol. 201A, pp. 392- 405.
- Doorenbos, J. and Kassam, A.M. 1979. Yield response to water. Food and Agriculture Organization of the United Nations, Rome, FAO Irrigation and drainage paper 33.
- Jackson, R.A. 1972. On the calculation of hydraulic conductivity. *Soil Science Society of America Proceedings*, **36**: 380-383.
- Jensen, M. E., Burman, R. D., and Allen, R. G., eds. 1990. Evapotranspiration and irrigation water requirements. ASCE Manuals and Reports of Engineering Practice No. 70, New York.
- Johnson, R. L., Bork, P., Allen, E. A. D., James, W. H., and Koverny, L. 1993. Oil sands sludge dewatering by freeze-thaw and evapotranspiration. Alberta Conservation and Reclamation Council Report No. RRTAC 93-8. ISBN 0-7732-6042-0.
- Qiu, Y. and Segó, D. C. 1998. Engineering properties of mine tailings. *Proceedings, 51<sup>st</sup> Canadian Geotechnical Conference*, Edmonton, Alberta, October 4-7, 1998. Vol. 1. pp. 149-154.
- Ritchie, J. T. 1972. Model for predicting evaporation from a row crop with incomplete cover. *Water Resources Research*, **8**(5): 1204-1213.
- Silva, M.J. 1999. Plant dewatering and strengthening of mine waste tailings. Ph.D. thesis, University of Alberta, Edmonton, Alberta.
- Silva, M. J., Biggar, K. W., Segó, D. C., Chanasyk, D. S., and Naeth, M. A. 1999. Model for the prediction of bearing capacity on vegetated tailings. Paper submitted for review to the *Canadian Geotechnical Journal*, March 1999.
- Silva, M. J., Naeth, M. A., Biggar, K. W., Chanasyk, D. S., and Segó, D. C. 1998. Plant selection for dewatering and reclamation of tailings. *Proceedings, 15th Annual National Meeting of the American Society for Surface Mining and Reclamation*, St. Louis, Missouri, May 17-21, 1998. pp. 104-117.
- Stahl, R. P. 1996. Characterization and natural processes enhancing dry landscape reclamation of fine processed mine wastes. Ph.D. thesis, University of Alberta, Edmonton, Alberta.
- Terzagui, K. 1943. Theoretical soil mechanics. John Wiley & Sons, New York.

Van Genuchten, M.Th. 1980. A closed-form equation for predicting the hydraulic conductivity of unsaturated soils. *Soil Science Society of America Journal*, **44**: 892-898.

-

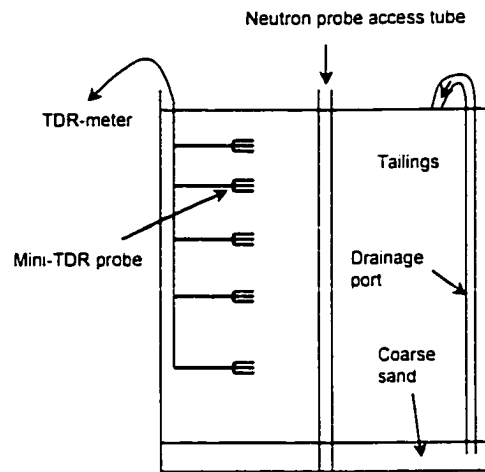


**Figure 4.1 Lysimeter layout**

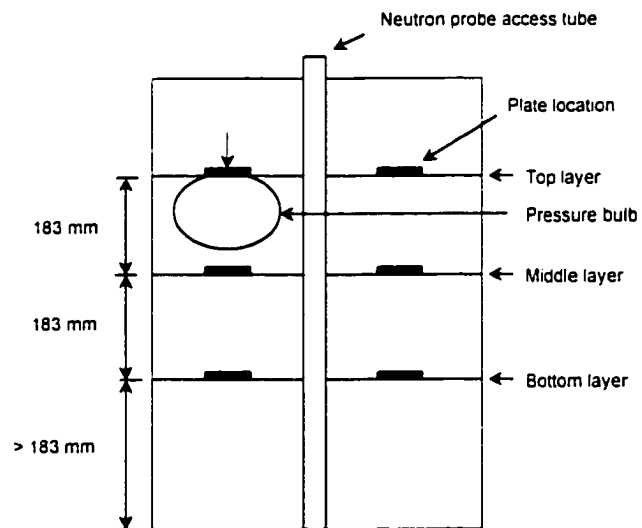


**Figure 4.2 Bearing capacity tests**



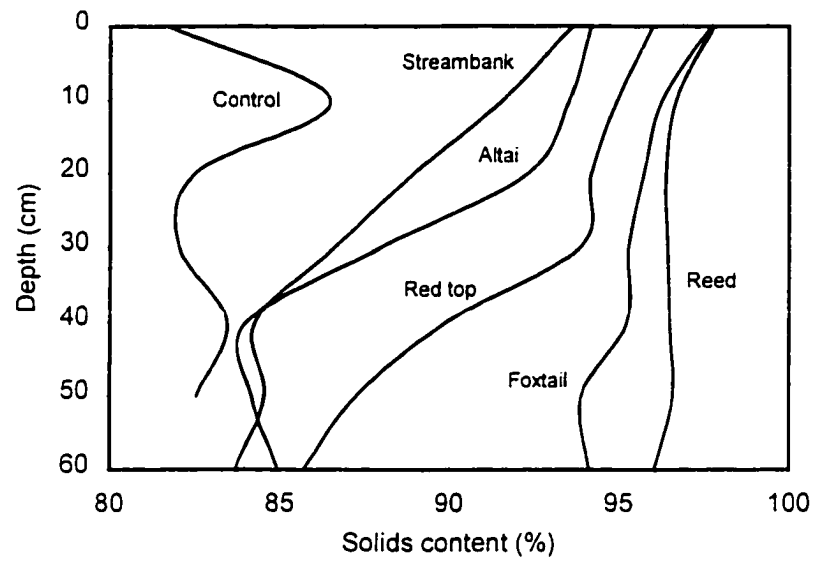


**Figure 4.3** Mean measured solids content profiles at the end of the tests

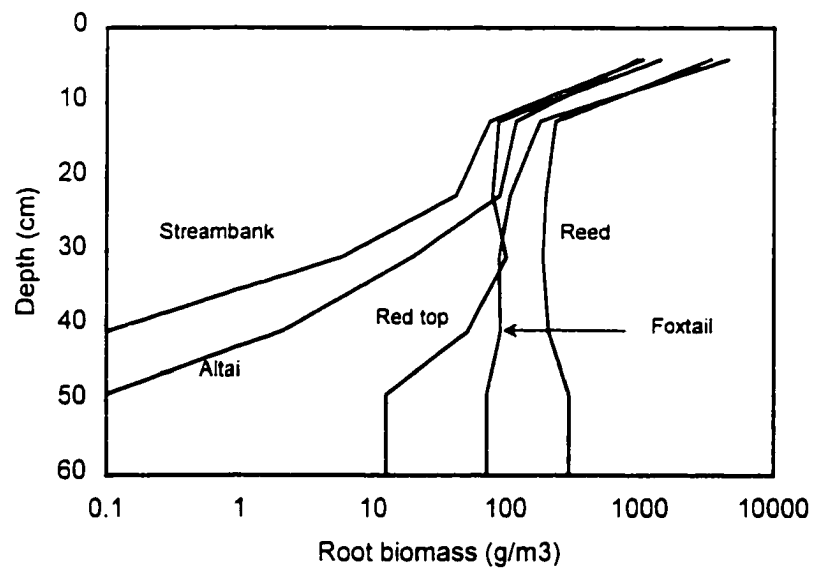


**Figure 4.4** Root biomass profile

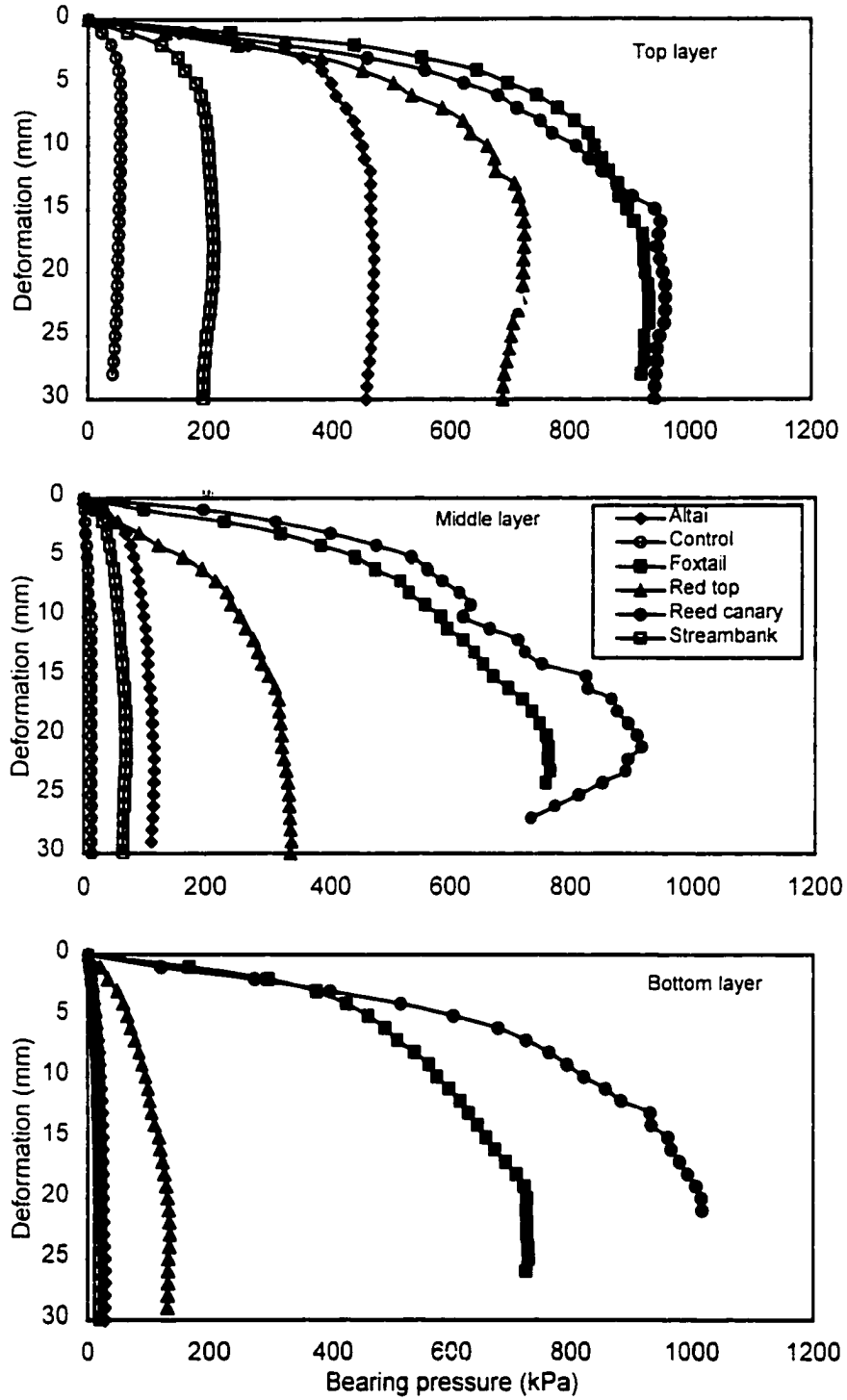


**Figure 4.5 Average bearing capacity test results**

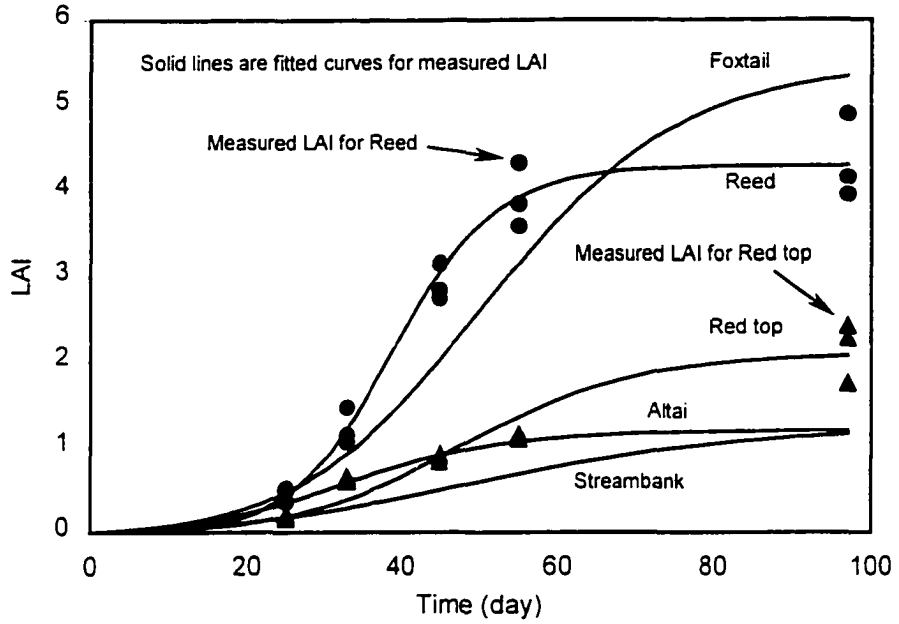


Figure 4.6 Leaf area index

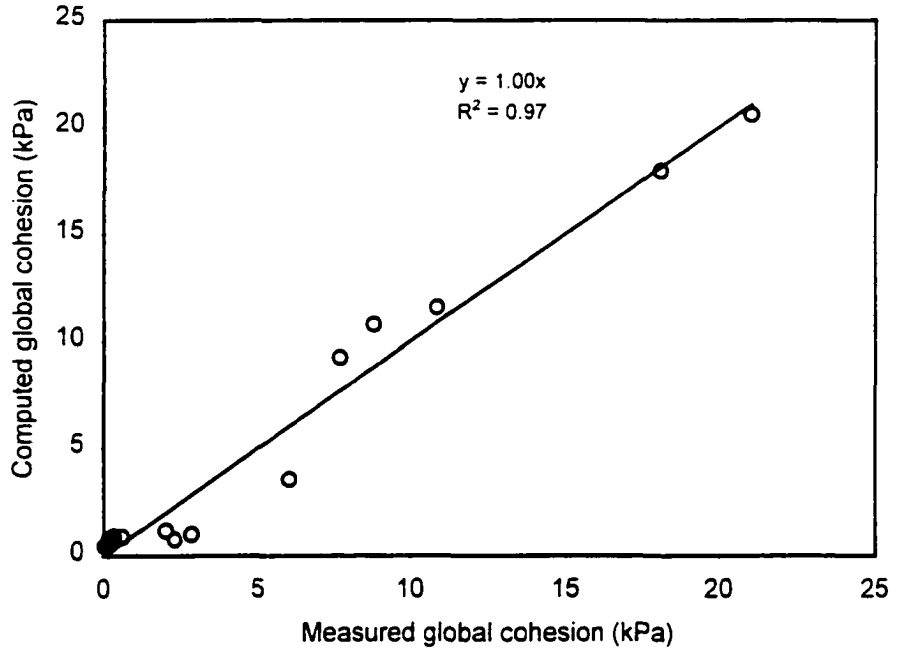
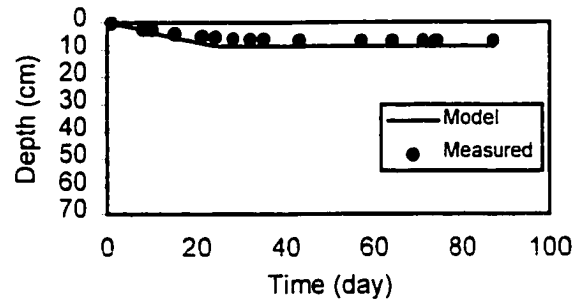
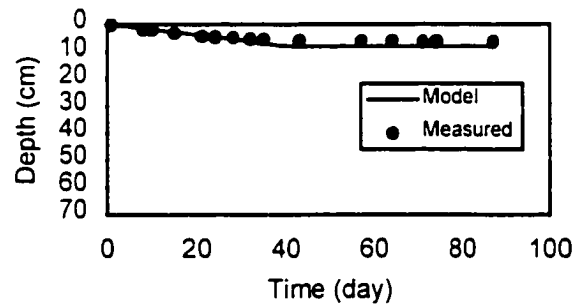


Figure 4.7 Correlation of global cohesion



**Figure 4.8 Tailings settlement (reed canarygrass)**



**Figure 4.9 Tailings settlement (streambank wheatgrass)**

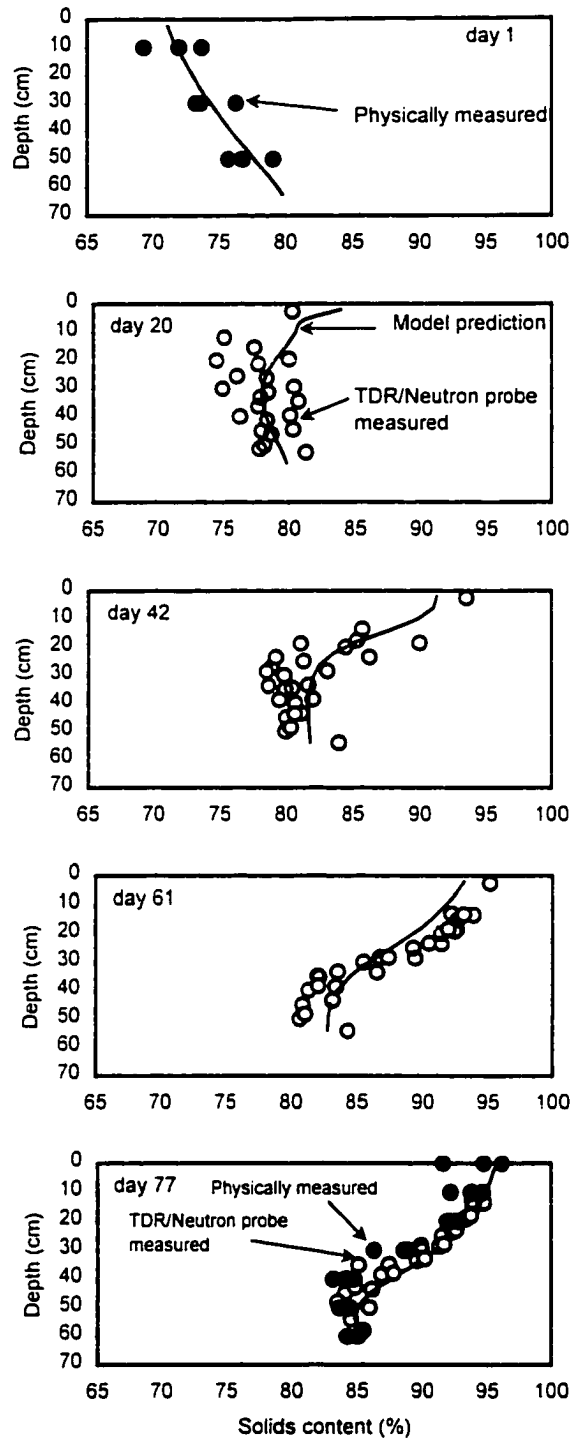


**Figure 4.10 Solids content profile (Altai wildrye)**

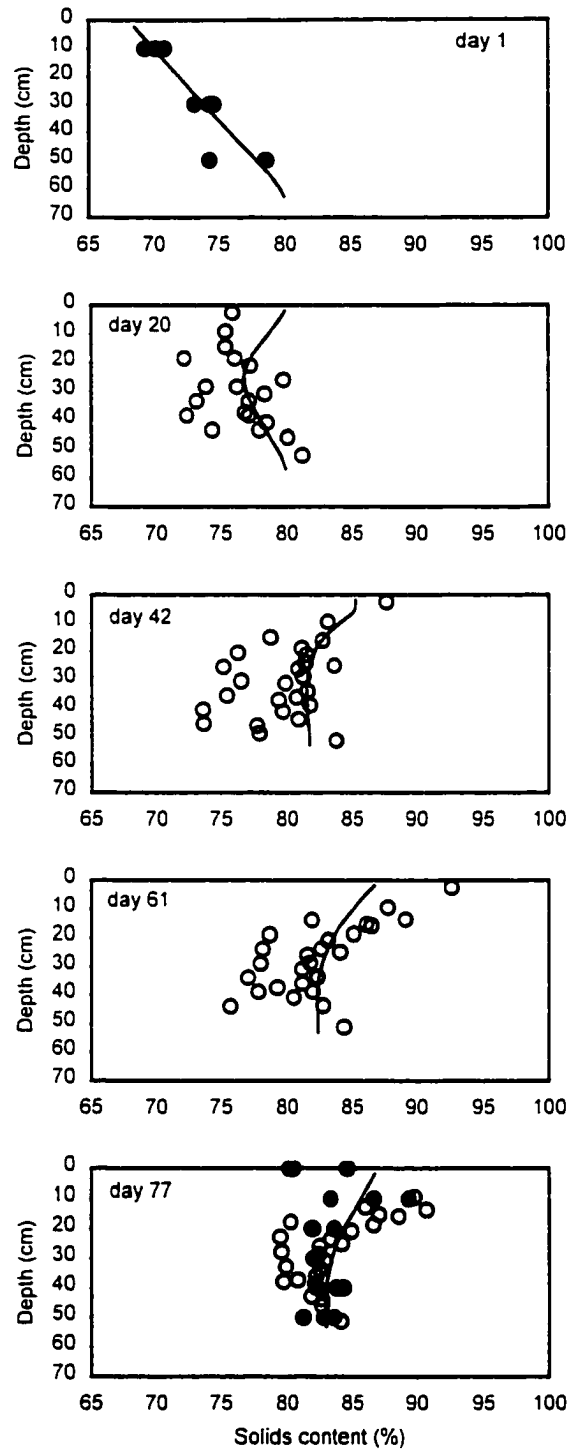


**Figure 4.11 Solids content profile (control)**

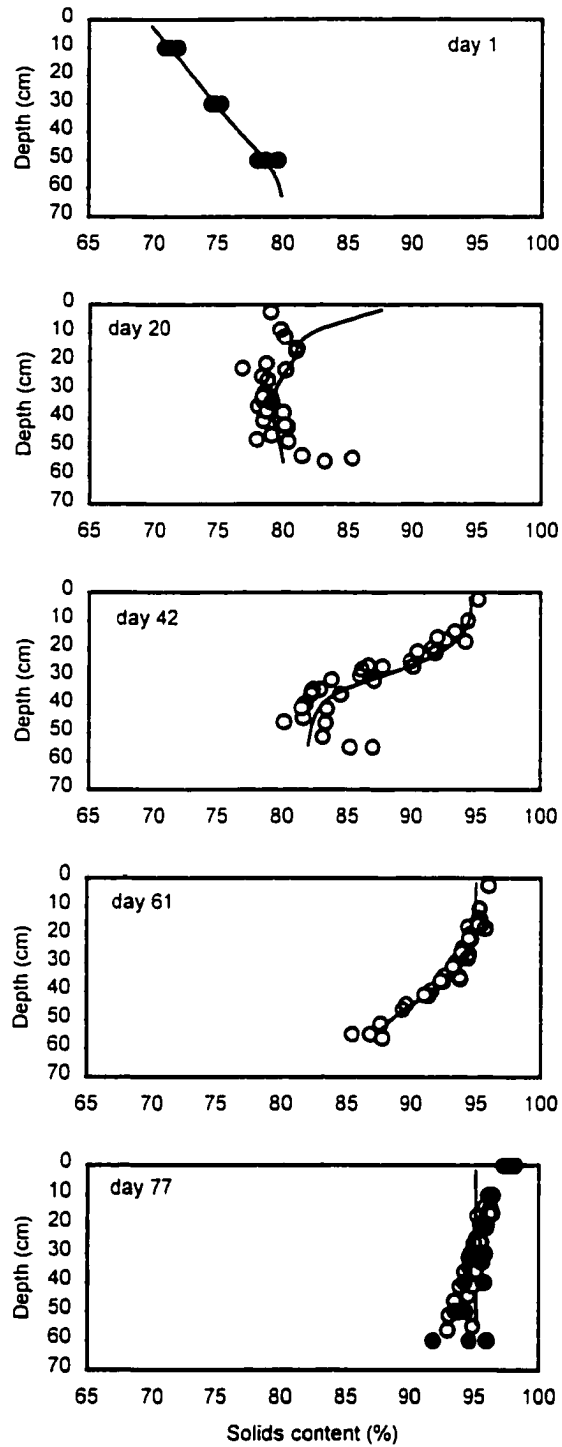


**Figure 4.12 Solids content profile (creeping foxtail)**

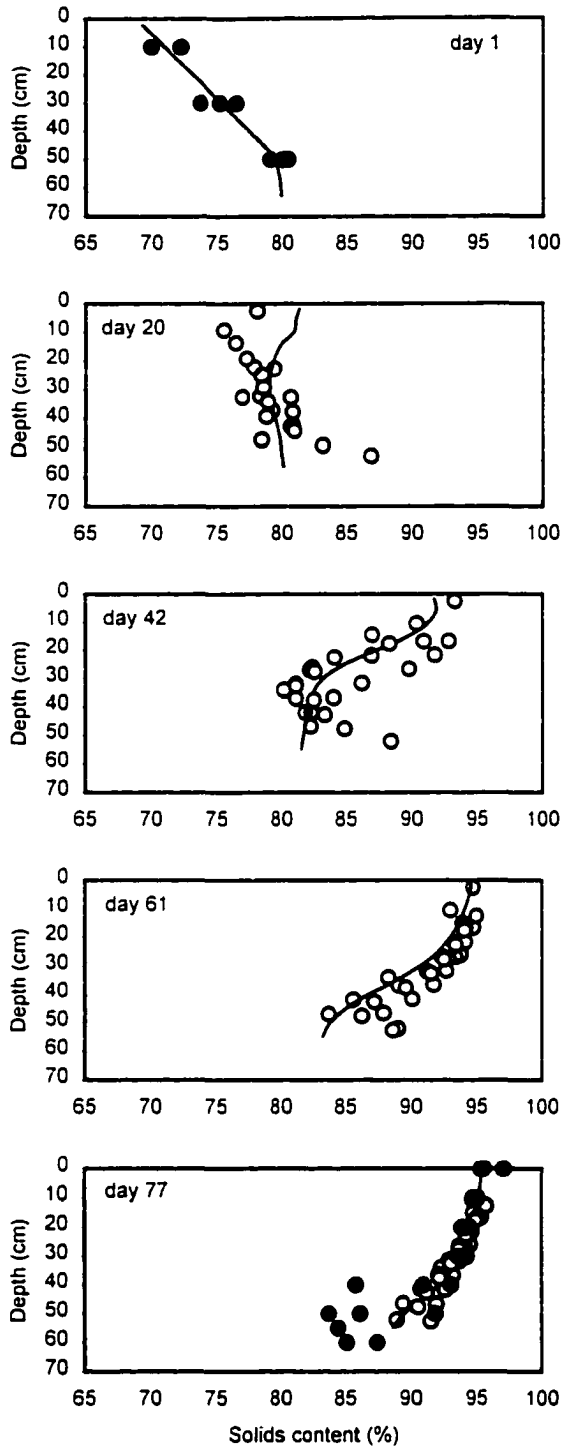


**Figure 4.13 Solids content profile (red top)**



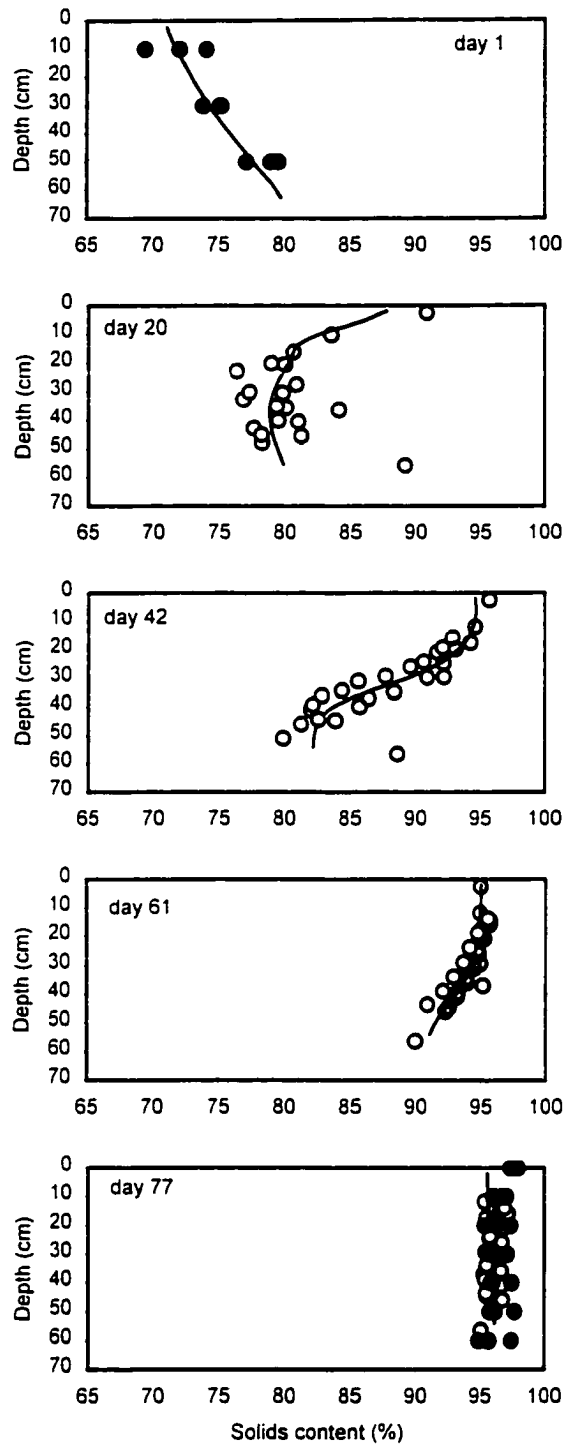


**Figure 4.14 Solids content profile (reed canarygrass)**

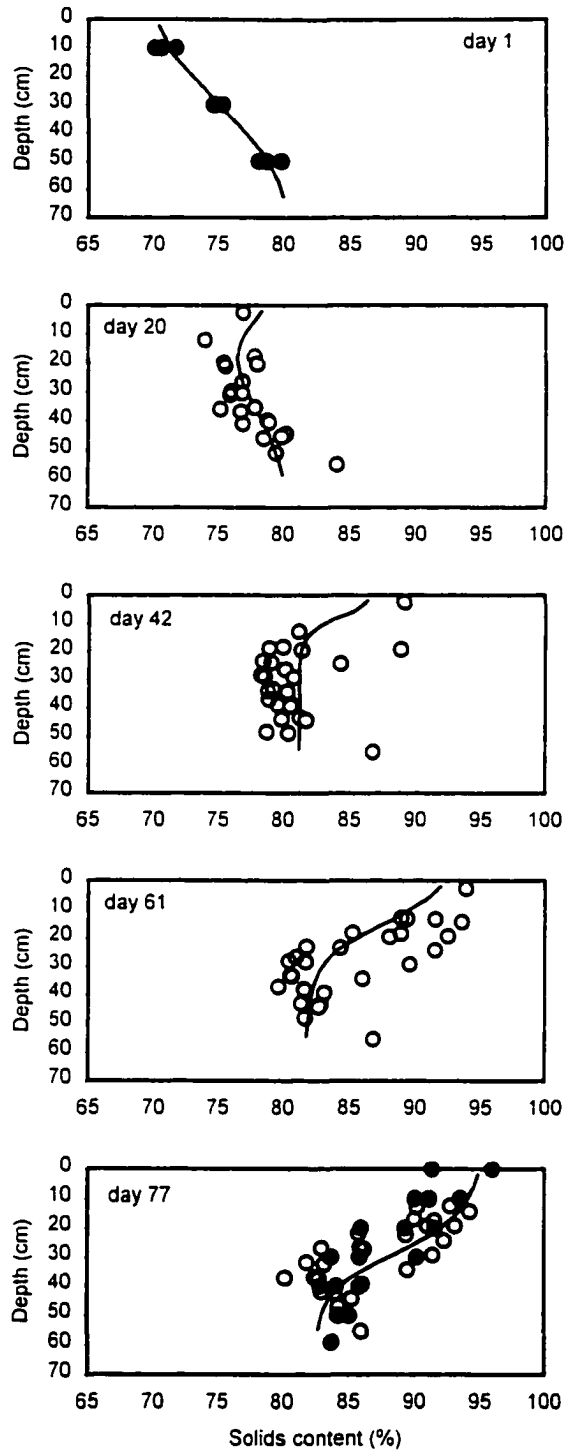


**Figure 4.15 Solids content profile (streambank wheatgrass)**

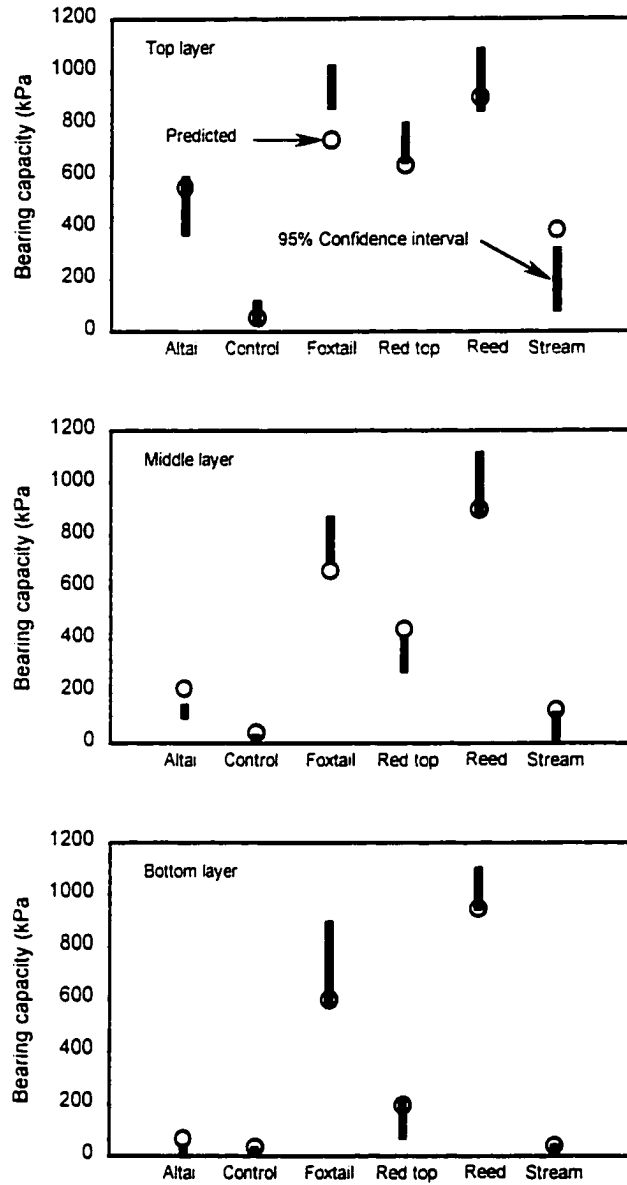


**Figure 4.16 Bearing capacity results**

Plant species	$c_1$	$c_2$
Altai wildrye	1.35	7.0
Creeping foxtail	2.6	6.1
Red top	2.8	7.0
Reed canarygrass	4.0	12.2
Streambank wheatgrass	1.5	4.0

**Table 4.1 Fitting parameters of the S-shape curve that describes the LAI of plants**

Treatments	Layer	Model predictions			Measured bearing capacities	
		$c_w$	$c_R$	$q_f$	95% Confidence interval	Mean (n = 6)
Altai	Top	13.8	1.2	556	384 to 582	483
	Middle	5.4	0	210	108 to 134	121
	Bottom	1.4	0	67	23 to 31	27
Control	Top	1.1	0	54.5	39 to 107	73
	Middle	0.7	0	40.2	15 to 19	17
	Bottom	0.5	0	34.5	*	*
Foxtail	Top	15	5	736	870 to 1006	938
	Middle	15	3	663	712 to 858	785
	Bottom	15.3	0.9	598	585 to 881	733
Red top	Top	15.8	1.6	641	660 to 787	723
	Middle	10.9	0.8	438	285 to 388	337
	Bottom	4.9	0.1	196	81 to 199	140
Reed	Top	19.6	5	900	859 to 1071	965
	Middle	21.3	3.2	897	896 to 1104	1000
	Bottom	24.5	1.3	944	954 to 1092	1025
Streambank	Top	9.7	0.7	390	93 to 307	200
	Middle	3.2	0	129	26 to 104	65
	Bottom	0.7	0	41	20	20

\* not measured

**Table 4.2 Predicted and measured bearing capacity results**

## Chapter 5

### ***Response of plants to oil sands tailings***<sup>1</sup>

---

#### **5.1 INTRODUCTION**

The Athabasca deposit, which has an average thickness of 38 m, is the largest of four oil sands deposits located in Alberta, Canada and is the only deposit in the province that can be recovered through surface mining. The Athabasca oil sands of Northern Alberta have been commercially mined by Syncrude Canada Limited and Suncor Inc. since 1978 and 1967, respectively. The two major types of material generated by the oil sands mining and extraction process include overburden and tailings. The overburden consists of all materials lying above the economically minable oil sands. Tailings are a byproduct of the oil sand extraction process. After extracting the bitumen, a slurry waste consisting of residual bitumen, water, sand, silt and fine clay particles is hydraulically transported and stored within surface tailings ponds. Without chemical treatment prior to deposition, the fast-settling sand particles segregate from the slurry upon deposition at the edge of the tailings ponds while the finer fraction accumulates in the center of the pond. Currently, there are approximately 400 million m<sup>3</sup> of mature fine tailings (MFT) at a gravimetric water content of 233% in storage and if current discharge methods continue 1 billion m<sup>3</sup> will require storage and future reclamation by 2020 (Liu et al. 1994). The major environmental issues associated with the tailings ponds are their instability and incapability of supporting the weight of animals or machines for a long period of time. Reclamation of these tailings to a desired dry

---

<sup>1</sup> A version of this chapter has been submitted for publication.

Silva, M.J., Naeth, M.A., Chanasyk, D.S., Biggar, K.W., and Segó, D.C. 1999. *Response of plants to oil sands tailings. Paper submitted for review to the Journal of Environmental Quality, May, 1999. 26 pp.*

landscape will not be possible until the surface of the deposit is capable of supporting human traffic. The slow rate of consolidation of the existing fine tails is compounded by the continuous addition of new fine tails from the ongoing extraction process.

Synchrude Canada Ltd. is currently evaluating a technique for solidifying wet slurries that consists of the addition of phosphogypsum ( $\text{CaSO}_4 \cdot 2\text{H}_2\text{O}$ ) to a mixture of tailings cyclone underflow and MFT. This technique produces a nonsegregating tailings stream known as composite tailings or consolidated tailings (CT). The full evaluation of this technique must proceed in conjunction with the development of reclamation options such that a suitable long-term waste management disposal program can be implemented.

Plant species for reclamation of tailings must adapt to the particular chemical and physical conditions of the growth medium, and to the macro- and microclimates. Species lists must be developed on a regional basis to take the general climatic effect into account, but additional screening programs will be necessary to determine the response of proposed species to special soil conditions. As suggested by Ripley et al. (1978) the ultimate selection of species must remain site specific; that is, the choice will have to be made at each individual mining site based on greenhouse experiments and/or field trials. Experimental results by Johnson et al. (1993) and Silva et al. (1998) have shown that oil sands tailings are not phytotoxic. Selected plants should tolerate extremely adverse conditions characteristic of oil sands tailings. Of particular interest will be a tolerance to high pH, high salinity level, water logging, residual bitumen, and a short growing season. This paper presents part of a research program whose main objective is to study and evaluate the strength enhancement mechanism of suitable plant species growing on initially high water content tailings. This paper presents the results of a greenhouse experiment conducted to evaluate the response of five agronomic species on composite tailings from Alberta oil sands operated by Synchrude Canada Ltd. These plant species proved the most viable in CT as a result of greenhouse experiments conducted to identify the most suitable plant species for dewatering and reclamation of CT (Silva et al. 1998).

## 5.2 MATERIALS AND METHOD

### 5.2.1 Composite tailings

Composite Tailings (CT) was prepared by mixing tailings sand, Mature Fine Tailings (MFT), tailings pond water and gypsum, which were provided by Syncrude Canada Ltd. The amount of gypsum added was approximately  $1200 \text{ g/m}^3$  and the proportion of sand, MFT and water was such that the CT mixture had 20% fines and an initial solids content of approximately 65%. The mixture was made up in several batches using a  $0.22\text{-m}^3$  cement mixer. The size of the mixer was chosen to prepare enough volume of CT to fill one lysimeter at a time and to obtain a homogenous CT mixture in each lysimeter.

When the CT mixture is transferred from the mixer to the lysimeter, some of the water is trapped in the pore spaces. This entrapped water is under an excess pressure, which is caused by the weight of the CT. Thus, some of the water flows out of the deposit relieving this excess pressure; this process is known as self-weight consolidation. The greatest excess pressure occurs at the bottom of the lysimeter and it takes a considerable amount of time for the water to travel from the bottom to the surface of the deposit to relieve this pressure. Figure 5.1 shows a schematic diagram of the lysimeters used in the experiment. This setup, which is described below, accelerated the consolidation process.

Forty-five gallon drums were lined with a plastic bag and had a 75-mm-thick saturated coarse sand placed at the bottom to act as a filter. One end of a plastic tube, wrapped with geotextile, was inserted into the filter and the other end was located at the top of the lysimeter. This system created double drainage, which accelerated the self-weight consolidation of the CT deposit. The lysimeters had a diameter of 57.2 cm and a height of 84.0 cm. Aluminum tubes with a diameter of 50 mm were installed in the center of each lysimeter to allow access for a neutron probe to monitor the solids content within the tailings. The lysimeters were filled with CT to a depth of about 0.8 m and self-weight consolidation was allowed to take place. Any expressed water was siphoned off and additional CT was added to restore the initial level. The plastic tubes were

removed from the lysimeters four days later when no more drainage was noticed. Six lysimeters were instrumented with five mini-TDR probes, each built at the University of Alberta. The mini-TDR probes measured solids content in a smaller zone compared with that of the neutron probe. The neutron probe and the TDR probes were specially calibrated to measure solids content of the CT in the lysimeters.

The CT mixture consists of about 80% sand, 10% silt and 10% clay (Qui and Sego 1998). Values of nutrient concentrations, pH and electrical conductivity (EC) for the CT mixture used in this study are presented in Table 5.1. Nitrate, phosphate and potassium levels were deficient for plant growth, whereas sulfate was at an optimal level. Levels of iron, boron and manganese were adequate for plant growth, but zinc and copper levels were deficient. Chloride was in excess. The mean Sodium Adsorption Ratio (SAR) was  $8.2 \pm 1.2$ , which is less than 13 (Miller and Donahue 1990); therefore CT can be classified as a non-sodic soil. Based on the combined values of SAR and EC, CT can be classified as a normal soil (non-saline and non-sodic).

### **5.2.2 Plant material and growth room conditions**

The plant species used in the experiment were: Altai wildrye (*Elymus angustus*), Creeping foxtail (*Alopecurus arundinaceus*), Red top (*Agrostis stolonifera*), Reed canarygrass (*Phalaris arundinacea*), and Streambank wheatgrass (*Agropyron riparian*). Plants were started from seeds in root trainers and transplanted to the lysimeters after 4 weeks with the equivalent of 64 plants/m<sup>2</sup>. At that time, the tailings had some free water at the surface generated by the consolidation process and the small seedlings were under a waterlogged condition. Three lysimeters were used for each species and three were left unplanted as a control. The lysimeters were placed in a growth room in a completely randomized design. Air temperature and hours of light per day were set at 22 °C and 15 hours, respectively, simulating a typical growing environment in Fort McMurray in June. The average maximum and minimum temperatures recorded were 24.7 and 20.6 °C, respectively. The average relative humidity was 52.9%. Water was added weekly to simulate average precipitation at Syncrude Canada's Mildred Lake site from



June through August. Long-term average values of precipitation for this location are 63.9 mm for June, 79.1 mm for July and 71.8 mm for August.

Fertilizer was added cautiously to prevent the total solute load from exceeding the salinity tolerance of the plants. To avoid over-fertilization, the amount of fertilizer was based on optimum levels of macronutrients required by agronomic species. The fertilizer was added to give an equivalent of 150 kg N/ha, 80 kg P<sub>2</sub>O<sub>5</sub>/ha, and 105 kg K<sub>2</sub>O/ha.

### **5.2.3 Measurements**

Solids contents were measured weekly via the neutron probe and TDR probes to obtain information on the water lost due to evapotranspiration in the planted lysimeters and evaporation in the controls. Observation of stress symptoms, survival and tillering were conducted chronologically. Number of tillers, number of leaves, plant height, and leaf area were determined at regular intervals throughout the experiment.

The leaf area was determined on five different dates using the following procedure. The leaves of a subsample from each lysimeter were carefully traced on paper. The leaf area was then measured using a planimeter. The total leaf area was determined by multiplying the area of the subsample by the total number of leaves. These leaf areas were then used to calculate the leaf area index (LAI), which is defined as the area of one side of leaves per unit of soil surface (Jensen et al. 1990).

After ten weeks of plant growth, reed canarygrass and creeping foxtail showed symptoms of water stress. Solids content measurements indicated that indeed the tailings deposits were near the wilting point, which is about 96% solids content. This condition dictated the end of the test series. The plants were then cut to measure the dry shoot biomass. The wilting point was determined from the soil water characteristic curve for CT reported by Qiu and Segó (1998). The solids content of 96% corresponds to a soil suction of about 1500 kPa, which is generally accepted as the wilting point of most plants.

At the end of the experiment samples of tailings were taken in 10-cm increments to measure the solids content profiles. Root densities were measured at six different depths by inserting rings of known volume. The roots were washed and oven dried to measure the dry root biomass profile. The total root biomass from each lysimeter was then calculated by extrapolation. EC and pH profiles were measured on only six lysimeters, chosen at random from each treatment. EC was measured using a EC/pH meter apparatus (Accumet from Fisher) on a 2:1 solution:soil ratio. The laboratory procedure is described in the United State Salinity Laboratory Staff (1954)

#### **5.2.4 Statistical Analyses**

Statistical testing of biomass production by species within a treatment was performed using single factor analysis of variance (ANOVA) followed by multiple comparison testing utilizing Duncan's multiple range test as described in Little and Hills (1972).

### **5.3 EXPERIMENTAL RESULTS**

Mean height growth over time is shown in Figure 5.2. Plant height generally increased with time reaching maximum height at approximately 100 days. Creeping foxtail and reed canarygrass demonstrated a high degree of tolerance of the harsh growing conditions in the tailings. However, it appears that the growth of streambank wheatgrass was dramatically delayed and maximum height was reduced. Transplant shock and initial waterlogged conditions likely contributed to this poor growth.

Values of LAI (Figure 5.3) for each plant species were calculated from measured leaf areas. The time used in the horizontal axis is from the date of germination, which on average occurred about 7 days after seeding. The ability of a plant canopy to intercept energy and subsequently to transpire varies with LAI. As an emerging seedling develops leaves and its roots permeate the soil, the plant increases in effectiveness as a conduit for transferring water from the soil profile to the atmosphere. The ground is considered completely covered when the LAI reaches the value of

2.7. At this value the plant canopy also becomes complete (Ritchie 1974). LAI after 98 days was greatest for creeping foxtail and reed canarygrass. Reed canarygrass appeared to have leveled at about day 55. Altai wildrye had reached their maximum LAI by about day 55.

Creeping foxtail and reed canarygrass produced the highest shoot and root dry weights (Table 5.2), which were not significantly different between them, but were significantly different from the other species. Altai wildrye and streambank wheatgrass generated the lowest shoot and root dry weights. Creeping foxtail and streambank wheatgrass produced the highest root to shoot ratio (0.93), followed by reed canarygrass (0.75).

The root biomass profile is presented in Figure 5.4. These curves are the average of six root density profiles measured within each planted treatment. A semi-logarithmic scale was used to provide a better visualization of root biomass differences. Reed canarygrass had the highest root biomass with depth.

The profiles of the electrical conductivity (EC) were similar in the different treatments (Figure 5.5). EC was highest at the surface and ranged from 2.2 to 3.9 dS/m. Salt accumulations were more evident in the control lysimeters where a white film of salt was present at the surface. The pH was uniform along the tailings profile with an average value of 8.1 (Figure 5.6).

Assessments of the plant response were conducted at seven different dates using a symptom scale, which was based on the degree of plant healthiness (Table 5.3). Altai wildrye and streambank wheatgrass presented signs of stress since transplanting. It appears that these two plants are not tolerant of waterlogged conditions at their early stage of growth. Approximately 25% of older leaves of streambank wheatgrass slowly turned chlorotic, then started to die on Day 57. Altai wildrye presented a poor growth; small necrotic spots on many leaf tips were evident during the initial stage of the experiment. However, both Altai wildrye and streambank wheatgrass displayed a strong propensity for regrowth following initial leaf loss. Creeping foxtail and reed canarygrass presented a healthy growth during the whole experiment; plants started showing

signs of water stress after Day 65. The water stress symptom was more notable on reed canarygrass, leaf tips were curled and dying, many first leaves were dying as well. Later solids content measurements confirmed that indeed the soil was close to the wilting point and insufficient water was available to the plants.

Water was lost from the lysimeters through evapotranspiration or by evaporation alone in the case of the controls. The water loss in each lysimeter was calculated from the measured solids content profiles. The cumulative water loss from the lysimeters is shown in Figure 5.7. On Day 28 the seedlings, which were grown in root trainers, were transplanted to the lysimeters. For the first two weeks after transplanting, there was little difference in the cumulative water loss among treatments. When the creeping foxtail and reed canarygrass plants increased in height and LAI, their evapotranspiration increased over the controls and other species. In spite of smaller heights and lower end LAI than creeping foxtail, reed canarygrass had the highest evapotranspiration. Streambank wheatgrass lost less water than the controls until Day 85. Because of its poor physiological state, it transpired little water, and the presence of the leaf cover on the surface of the tailings in the lysimeter reduced the evaporative losses. The controls lost little water from day 60 on.

The cumulative evapotranspiration at the end of the greenhouse experiment is directly reflected in the final solids content profile (comparing Figures 5.7 and 5.8). Also, there appears to be a direct relationship between root biomass and root water uptake, which can be seen by comparing Figures 5.6 and 5.8. Reed canarygrass and creeping foxtail significantly lowered the moisture content of the CT mixture, and as a result had the highest solids content at the end of the experiment. Solids content was fairly uniform with depth for these two treatments. For all others except the controls, it generally decreased with depth, averaging about 83 to 85% at the bottom of the profile. Roots of reed canarygrass and creeping foxtail plants reached the bottom of the lysimeters and may have gone further if the containers had been deeper. In these lysimeters the moisture contents were close to the wilting point and the plants started showing signs of water stress. This condition dictated the termination of the experiment. Pure evaporation (control) did

not cause any significant dewatering of the CT compared to the plants. Salt accumulations and the presence of a film of bitumen at the surface of the control lysimeters inhibited further evaporation.

#### **5.4 DISCUSSION**

Five agronomic species were selected to evaluate their response on composite tailings from Alberta oil sands operated by Syncrude Canada Ltd. All plants survived after an eleven-week period. Creeping foxtail, red top and reed canarygrass plants showed signs of healthy growth, whereas Altai wildrye and streambank wheatgrass did not grow well in the tailings in the initial period when the tailings had free water at the surface. These plants were shocked in the transplant and their growth was stunted at the beginning. Stress symptoms were more evident in streambank wheatgrass. It appears that the level of metabolic activity in the plants was reduced. This was accomplished by reducing their biomass through shedding their leaves, or by going into a dormant stage. The stress was observed in many plants, which had dry leaves with tips curled and dead. Low plant height increase, low leaf area index, low evapotranspiration and low shoot and root biomass are evidences of poor plant growth. However, both Altai wildrye and streambank wheatgrass displayed a propensity for regrowth. This capacity can be an important attribute for species used in reclamation, and may reduce replanting cost (Fedkenheuer et al. 1980). Macyk et al. (1998) reported that streambank wheatgrass exhibited good growth and initial establishment in tailings sands. They concluded that this plant is suitable for revegetation on the Syncrude tailings dike, especially for the purpose of erosion control.

Creeping foxtail and reed canarygrass had the highest evapotranspiration, the highest above and below ground biomasses, the greatest plant heights and leaf area indexes, the deepest roots and the lowest stress symptoms. These plant parameters are linked to the healthy plant growth and physiological conditions.

Red top plants had a fairly healthy growth during the whole period. However, at the end of the experiment, the plants showed signs of water stress. Their roots were not as deep as those of creeping foxtail and reed canarygrass plants and the stress was caused by moisture deficiency near the surface of the tailings. The results indicate that red top is a short plant with shallow roots for the conditions tested.

The results obtained clearly confirm that CT is not phytotoxic and can be used as a medium for plant growth. This conclusion is supported by the low EC and SAR, which class CT as a normal soil.

## **5.5 CONCLUSIONS**

A greenhouse experimental program was conducted to evaluate the response of five agronomic species on high water content tailings. Based on values of Sodium Adsorption Ratio (SAR) and Electrical Conductivity (EC), composite tailings (CT) can be classified as normal soils (non-sodic and non-saline). Healthy plant growth confirmed that CT is not phytotoxic and suitable plants can be used to implement future reclamation activities when the impoundment reaches full capacity.

Reed canarygrass, creeping foxtail and red top plants proved to be the best candidates for future field research in dewatering CT when there is free water at the surface of the tailings. Altai wildrye and streambank wheatgrass plants are not tolerant of waterlogged conditions; however, they are also good candidates for future field research in CT without free water at the surface.

## **5.6 REFERENCES**

Fedkenheuer, A.W., Heacock, H.M., and Lewis, D.L. 1980. Early performance of native shrubs and trees planted on amended Athabasca oil sand tailings. *Reclamation Review*, **3**: 47-55.

Johnson, R. L., Bork, P., Allen, E. A. D., James, W. H., and Koverny, L. 1993. Oil sands sludge dewatering by freeze-thaw and evapotranspiration. Alberta Conservation and Reclamation Council Report No. RRTAC 93-8. ISBN 0-7732-6042-0.

- Jensen, M.E., Burman, R.D., and Allen, R.G., eds. 1990. Evapotranspiration and irrigation water requirements. Manual of practice No. 70, ASCE. New York.
- Little, T.M., and Hills, F.J. 1972. Statistical methods in agricultural research. Agricultural extension. University of California.
- Lui, Y., Caughill, D., Scott, J.D., and Burns, R. 1994. Consolidation of Suncor nonsegregating tailings. Proceedings, 47<sup>th</sup> Canadian Geotechnical Conference, Halifax, Nova Scotia, September 21-23, 1994, pp. 504-513.
- Macyk, T.M., Fung, M.Y.P., and Pauls, R.W. 1989. Reclamation research for various land uses in the oil sands region of Alberta, Canada. Proceedings, 15<sup>th</sup> Annual National Meeting of the American Society for Surface Mining and Reclamation, St. Louis, Missouri, May 17-21, 1998, pp. 593-602.
- Miller, R.W. and Donahue, R.L. 1990. Soils. An introduction to soils and plant growth. Sixth edition. Prentice Hall.
- Qiu, Y. and Sego, D.C. 1998. Engineering properties of mine tailings. Proceedings, 51<sup>st</sup> Canadian Geotechnical Conference, Edmonton, Alberta, October 4-7, 1998. Vol. 1. pp. 149-154.
- Ripley, E., Redman, R., and Maxwell, J. 1978. Environmental impact of mining in Canada. Center for Resource Studies, Queens University, Kingston, Ontario.
- Ritchie, J.T. 1972. Model for predicting evaporation from a row crop with incomplete cover. Water Resources Research, 8: 1204-1213.
- Silva, M.J., Naeth, M.A., Biggar, K.W., Chanasyk, D.S., and Sego, D.C. 1998. Chapter 2. Plant selection for dewatering and reclamation of tailings. Proceedings, 15th Annual National Meeting of the American Society for Surface Mining and Reclamation, St. Louis, Missouri, May 17-21, 1998. pp. 104-117.
- United State Salinity Laboratory Staff. 1954. Diagnosis and improvement of saline and alkali soils. United State Department of Agriculture, handbook No. 60, Chapter 2, pp. 7-17.

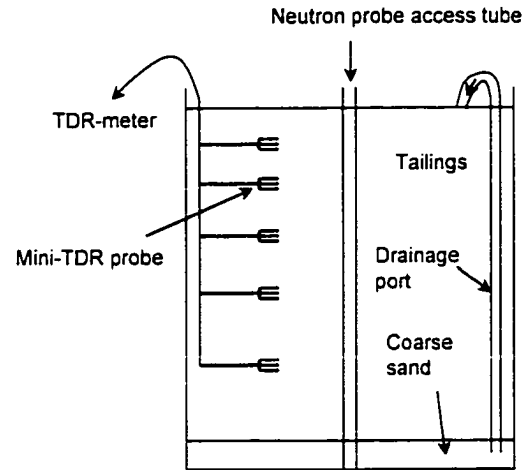


**Figure 5.1** Lysimeter layout

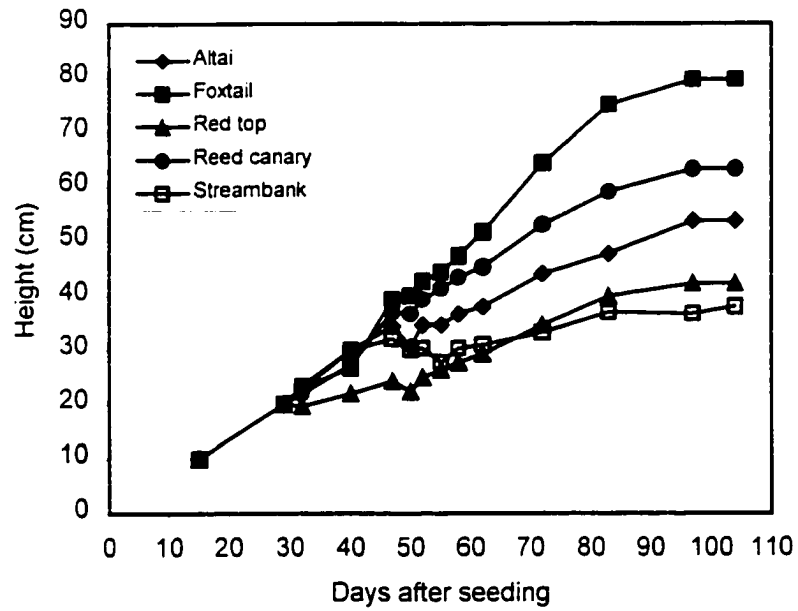


**Figure 5.2** Temporal variations in plant height



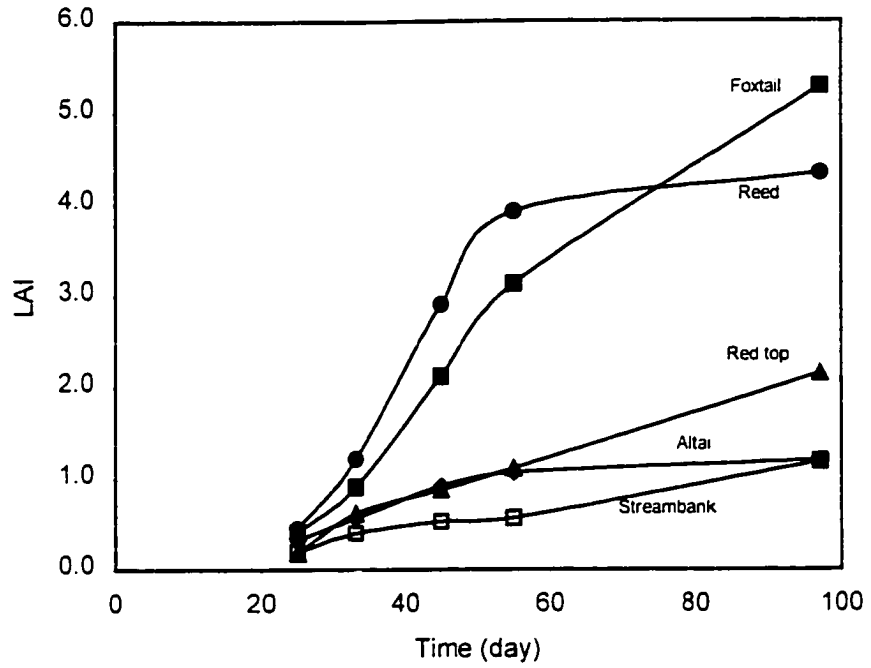


**Figure 5.3** Temporal variations in Leaf Area Index (LAI)

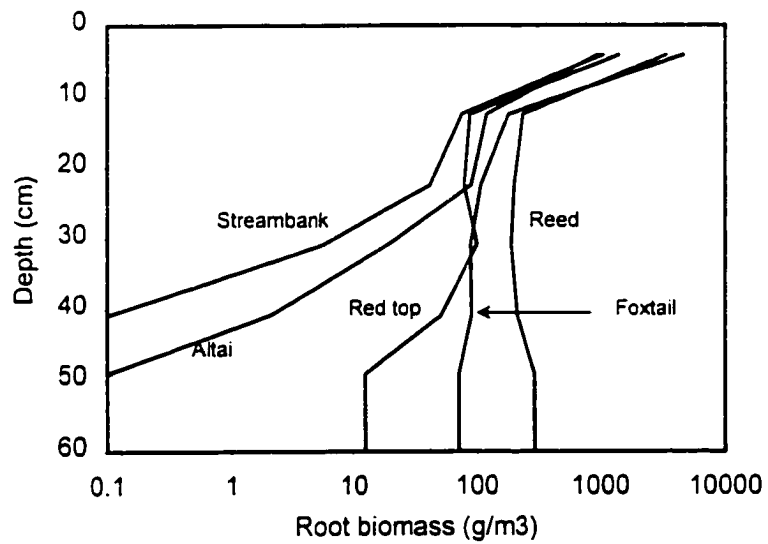


**Figure 5.4** Root biomass profile

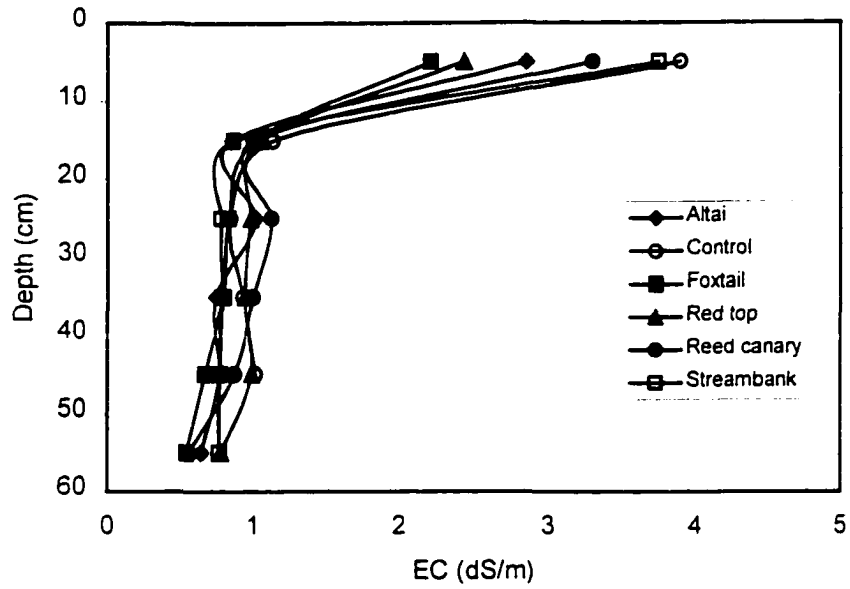


**Figure 5.5** Electrical conductivity profile at end of experiment

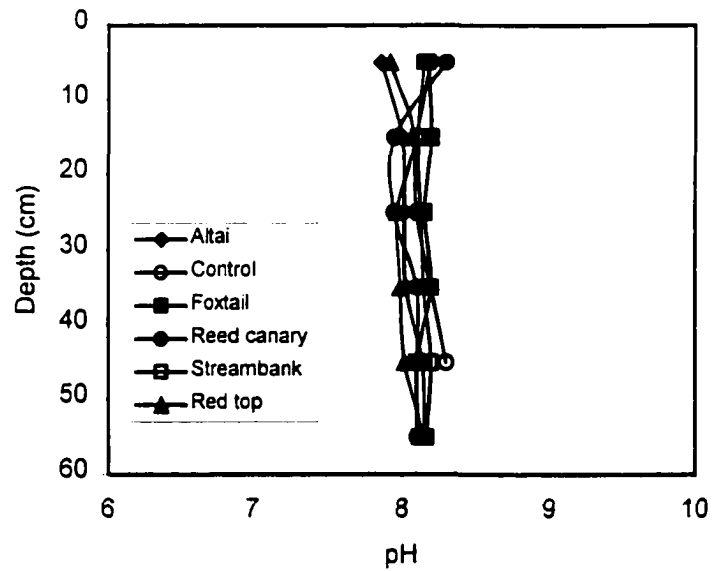


**Figure 5.6** pH profile at end of experiment

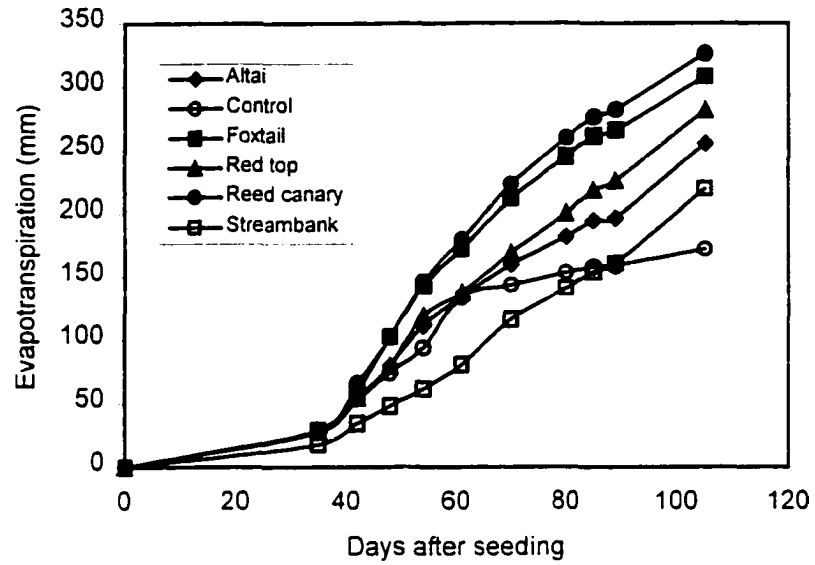


**Figure 5.7 Cumulative evapotranspiration**

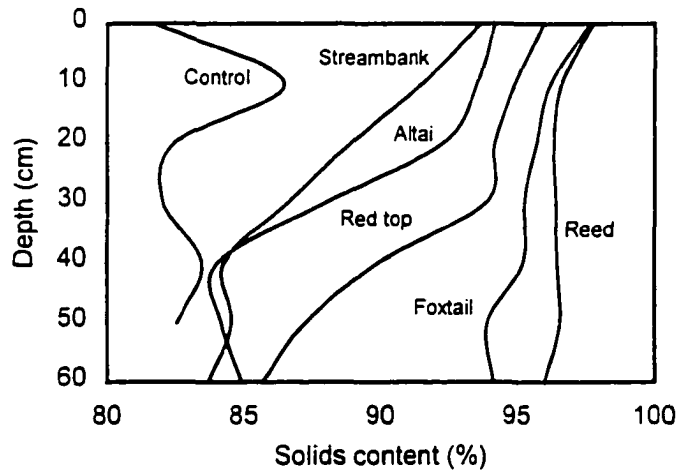


**Figure 5.8 Mean measured solids content profiles at end of the tests**

Analysis	CT
pH	7.7 ± 0.3 <sup>*</sup>
E.C. (dS/m)	3.1 ± 0.3
Nitrate (ppm)	1.0 ± 0.0
Phosphate (ppm)	4.0 ± 2.9
Potassium (ppm)	43 ± 3
Sulfate (ppm)	>20
Ca (ppm)	437 ± 40
Na (ppm)	681 ± 93
Mg (ppm)	65 ± 7
Fe (ppm)	17 ± 0.8
Cu (ppm)	0.13 ± 0.0
Zn (ppm)	0.3 ± 0.0
B (ppm)	3.0 ± 0.1
Mn (ppm)	5.4 ± 0.4
Cl (ppm)	>50

<sup>\*</sup> Means (n = 4) ± standard deviation

**Table 5.1 Chemical composition of CT**

Species	Shoot dry weight (g)	Root dry weight (g)	Root : shoot ratio
Altai wildrye	37.7 c <sup>*</sup>	24.5 b	0.65
Creeping foxtail	120.0 a	111.4 a	0.93
Red top	86.7 b	37.3 b	0.43
Reed canarygrass	134.3 a	100.8 a	0.75
Streambank wheatgrass	26.9 c	24.9 b	0.93

<sup>\*</sup> Means (n = 3) within a column followed by a common letter are not significantly different at the 5% level.

**Table 5.2 Shoot and root dry weights**

Plant species	Symptom scale						
	Day 38	Day 41	Day 48	Day 57	Day 65	Day 83	Day 90
Altai wildrye	1.5	1.5	2	2	2	2	2.5
Creeping foxtail	1	1	1	1	1.5	1.5	2
Red top	1	1.5	1.5	1.5	1.5	2	2
Reed canarygrass	1	1	1	1.5	2	2	2
Streambank wheatgrass	1.5	1.5	2	2.5	2.5	2.5	3

Day number is the number of days after seeding

**Table 5.3 Summary of plant behavior assessment**

Symptom scale is based on degree of plant health

- 1 Very healthy, lush, a few older leaves dying, maybe a few tips browning
- 2 Fairly healthy, many first leaves dying, some symptoms evident, tips dying, a bit of chlorosis
- 3 Looking stressed, dry leaves, rolling leaves, chlorosis and necrosis very evident, tips curled and dead, perhaps stunted
- 4 Very stressed, dry, dying tillers

Note: dying refers to mortality

## Chapter 6

### ***Prediction of bearing capacity of vegetated composite tailings<sup>1</sup>***

---

#### **6.1 INTRODUCTION**

The Athabasca oil sands, located in the Fort McMurray area of Northeastern Alberta, is the Province's largest and most accessible source of bitumen. They have been commercially mined by Syncrude Canada Limited and Suncor Inc. since 1978 and 1967, respectively. The oil sands industry is heading into an extensive expansion period, putting increased pressure on current land uses, reclamation planning and the creation of reclaimed landscapes that address local and regional land and resource use needs over long periods of time.

The two major types of waste material generated by the oil sands mining and extraction process include overburden and tailings. The overburden consists of all materials lying above the economically minable oil sands. Numerous studies have been conducted for the reclamation of these dry wastes (Macyk et al. 1998). Tailings are a byproduct of the oil sand extraction process. After extracting the bitumen, a slurry waste consisting of residual bitumen, water, sand, silt and fine clay particles is hydraulically transported and stored within surface tailings ponds. Without chemical treatment prior to deposition, the fast-settling sand particles segregate from the slurry upon deposition at the edge of the tailings ponds while the finer fraction accumulates in the center of the pond. Currently, there are approximately 400 million m<sup>3</sup> of mature fine tailings (MFT) at a

---

<sup>1</sup> A version of this chapter has been submitted for publication.

Silva, M.J., Biggar, K.W., Segó, D.C., Chanasyk, D.S., and Naeth, M.A. 1999. *Prediction of bearing capacity of vegetated composite tailings*. Paper submitted for review to the *Canadian Geotechnical Journal*, May, 1999, 31 pp.

solids content of 30% (gravimetric water content of 233%) in storage, and future predictions estimate that 1 billion m<sup>3</sup> will require storage and future reclamation by 2020 if current discharge methods continue (Liu et al. 1994). The oil sands operations, through annual production of 85 million barrels of high quality synthetic crude (Sheeran 1993) generate 160 million m<sup>3</sup> of fluid tailings with a solids content of 40 to 60% (Suthaker 1995).

The major environmental issues associated with the contents of the fine tailings ponds are their instability and incapability of supporting the weight of animals or machines for a long period of time. Reclamation of these tailings to a desired dry landscape will not be possible until the surface of the deposit is capable of supporting human traffic. The slow rate of consolidation of the existing fine tails is compounded by the continuous addition of new fine tails from the extraction process.

Synchrude Canada Ltd. is currently evaluating a technique for solidifying wet slurries that consists of the addition of phosphogypsum ( $\text{CaSO}_4 \cdot 2\text{H}_2\text{O}$ ) to a mixture of sand from the tailings cyclone underflow and MFT. This technique produces a nonsegregating tailings stream known as composite tailings or consolidated tailings (CT). The full evaluation of this technique must proceed in conjunction with the development of reclamation options such that a suitable long term waste management disposal program can be implemented.

The use of plants to dewater CT has been identified as a mechanism that may economically enhance the surface stability of these weak deposits on a large scale. Plants growing in tailings accelerate the consolidation process and increase their bearing capacity in the root zone through evapotranspiration and root reinforcement.

Prediction of the bearing capacity is essential in the management of tailings. Reclamation of these tailings cannot be initiated until the deposit achieves a trafficable surface. A theoretical model capable of predicting the bearing capacity increase due to the strength enhancement mechanism of plants was described in Silva et al. (1999a). The model was shown to perform well

in simulating nonlinear problems under saturated and unsaturated conditions. The model was then calibrated and validated in a greenhouse experiment using five different agronomic species (Silva et al. 1999b). The model is considered appropriate for predicting solids content profile and bearing capacity increase due to the plants for one growing season.

This paper presents the results of a Class A prediction of the bearing capacity of vegetated tailings using daily climatic data of 1997 and 1998 from the Fort McMurray region. Different deposit depths were analyzed to determine the depth at which an optimum dewatering can be achieved using the plant parameters of reed canarygrass. A sensitivity analysis was performed to identify the tailings parameters whose variations greatly affect the model results and whose values are difficult to determine accurately by laboratory means.

## **6.2 SETTING**

The Athabasca oil sands area has a cool temperature climate with relatively long, cold winters and short, cool summers. January has a mean daily temperature of  $-20\text{ }^{\circ}\text{C}$  and July a mean daily temperature of  $17\text{ }^{\circ}\text{C}$ . An extended period of over 17 hours of daylight occurs during June and July, and the average growing season from May through August is about 95 days.

The mean annual precipitation (1944 to 1990) is 335 mm of rainfall and 172 cm of snowfall with average potential evapotranspiration of 500 mm/year.

## **6.3 POTENTIAL EVAPOTRANSPIRATION**

The model described in Silva et al. (1999a) was modified to include the Penman-Monteith equation. This combination equation (Monteith 1981) is used to calculate the potential daily evapotranspiration. This equation not only reconciles thermodynamics and aerodynamics aspects, but also includes the aerodynamic resistance to sensible heat and vapor transfer,  $r_a$ , and



the surface resistance to vapor transfer,  $r_c$ . The resulting equation represents a basic general description of the evaporation process from vegetation:

$$[6.1] \quad \lambda ET_0 = \frac{\Delta}{\Delta + \gamma_c(1 + r_c / r_a)} (R_n - G) + \frac{\gamma_c}{\Delta + \lambda_c(1 + r_c / r_a)} K_1 \frac{0.622\lambda_c\rho_a}{P_a} \frac{1}{r_a} (e_z^0 - e_z)$$

where  $ET_0$  is potential evapotranspiration (mm/d);  $\lambda$  is latent heat of vaporization (MJ/kg);  $\Delta$  is slope of the saturation vapor pressure-temperature curve (kPa/°C);  $\gamma_c$  is psychrometric constant (kPa/°C);  $R_n$  is net radiation (MJ/m<sup>2</sup>/d);  $G$  is soil heat flux (MJ/m<sup>2</sup>/d);  $r_c$  is the surface resistance (s/m);  $r_a$  is the aerodynamic resistance (s/m);  $\rho_a$  is air density (kg/m<sup>3</sup>);  $P_a$  is atmospheric pressure (kPa);  $e_z^0$  and  $e_z$  are saturation and actual vapor pressures (kPa) at the  $z$  level above the surface. The aerodynamic resistance is calculated using the following expression:

$$[6.2] \quad r_a = \frac{\ln[(z_w - h_d) / z_{om}] \ln[(z_p - h_d) / z_{ov}]}{k^2 u_z}$$

where  $z_w$  is the height of the wind speed measurement;  $z_p$  is the height of the humidity (psychrometer) and temperature measurements;  $u_z$  is the wind speed at height  $z_w$ ;  $k$  is von Karman constant (0.41);  $z_{om}$  is roughness length of momentum transfer (m) and  $z_{ov}$  is roughness length for vapor transfer (m) calculated as 0.123 x crop height, and 0.1 x  $z_{om}$ , respectively (Jensen et al. 1990);  $h_d$  is displacement height for a crop (m) calculated as  $h_d = 2/3$  x crop height (Monteith 1981);  $K_1$  is a dimension coefficient needed to assure that both terms have the same units. The value of  $K_1$  is  $8.64 \times 10^4$  for  $u_z$  in m/s to give the aerodynamic term the same dimensions as  $R_n$  and  $G$  (MJ/m<sup>2</sup>/d). The value of  $(K_1 0.622\lambda_c\rho_a)/P_a$  is calculated using (Jensen et al. 1990):

$$[6.3] \quad \frac{K_1 0.622\lambda_c\rho_a}{P_a} = 1710 - 6.85T$$

where  $T$  is air temperature (°C).

Climatic data for 1997 and 1998 were provided by Syncrude Canada Ltd. from their site to calculate daily values of potential evapotranspiration from May through October. The data used in the model were: daily maximum and minimum temperatures, daily maximum and minimum relative humidities, mean daily wind velocity, mean daily solar radiation and altitude.

The daily soil heat flux ( $G$ ) was neglected since its magnitude under a crop canopy over 10- to 30-day periods or longer is relatively small (Jensen et al. 1990). The surface resistance ( $r_c$ ) was also neglected. Since  $r_c$  and  $r_a$  are coupled in series,  $r_a$  is relatively important in annual crops in determining the total resistance, while in perennial tree crops,  $r_c$  may be of greater importance. Field crops tend to have greater aerodynamic resistance than forests (Radersma and de Ridder 1996). The net radiation ( $R_n$ ) was determined with a simple linear equation using the solar radiation ( $R_s$ ) as the independent variable (Polavarapu 1970)

$$[6.4] \quad R_n = 0.6R_s - 2.5$$

A comparison of climatic data for 1997 and 1998 to a long-term average (1944 to 1990) is presented in Table 6.1. Temperatures in 1997 and 1998 were a little higher than usual for the months of June, July and August. The precipitation values were lower in 1997 and 1998 than those of the long-term-average, excepting those of August and September of 1997. The wind speed and relative humidity did not appear to be significantly different from the long-term-average. In general, 1997 and 1998 can be considered a little warmer-than-usual Fort McMurray summer.

#### **6.4 BOUNDARY AND INITIAL CONDITIONS**

The calculated daily values of evapotranspiration were divided into its evaporation and transpiration components (Silva et al. 1999a). These two values together with the daily values of rainfall ( $P$ ) were used as the top boundary conditions in the model (Figure 6.1). A zero flux ( $q_n =$

0) was used at the bottom of the tailings deposit. The initial solids content in all simulations was assumed to increase linearly from 72% at the surface to 80% at the bottom.

The plant parameters used in the model correspond to reed canarygrass. It was assumed that the plants started to grow from small seedlings and were then transplanted to the CT deposit at the beginning of May 1997. In 1998 it was assumed that plants had a full growth (complete canopy and maximum rooting depth). Freeze-thaw dewatering for the winter of 1997/1998 was neglected. The tailings and plant parameters used in the present simulation are summarized in Table 6.2. A description of these parameters can be found in Silva et al. (1999b).

The tailings profile was divided in compartments, each one having an initial thickness of 0.05 m. The size of each time step was restricted to a maximum variation in the volume of water of the compartments ( $\text{Max } \Delta V_w = 1 \times 10^{-5} \text{ m}$ ). Additionally, a maximum time step was prescribed ( $\text{Max } \Delta t^{*1} = 1 \text{ hour}$ ).

## 6.5 MODEL RESULTS

### 6.5.1 Tailings deposit 5 m deep

The purpose of the first simulation was to examine the performance of the strength enhancement mechanism of plants on a deep CT deposit. The initial deposit depth was taken as 5 m. This initial depth is the depth of the CT deposit after the rapid consolidation process has occurred (right after tailings deposition).

The maximum effective rooting depth of fully grown grasses ranges from 0.5 to 1.5 m (Jensen et al. 1990). An average maximum rooting depth of 1 m was used in this evaluation. The deposit was divided in 100 compartments of equal thickness. The solids content profiles for the initial conditions, end of 1997 and end of 1998 are shown in Figure 6.2. Although the roots reached a depth of only 1 m into the deposit, a gradient was established and water flowed from the bottom

of the deposit to the root zone, where water was being extracted continuously via plant transpiration. At the end of 1997 and 1998 the average solids contents at the surface (0 to 70 cm) were about 90 and 95%, respectively.

To obtain a graphical view of the soil bearing capacity generated by the plant dewatering mechanism and the fiber reinforcement of the root system the tailings profile was divided in layers, each one comprising five compartments. The bearing capacity was calculated assuming an 80-mm-diameter circular footing at the top of each layer and using the average matric suction and average root biomass calculated for the five compartments contained in each layer. In this way the depth of influence of each bearing capacity ranged from 20 to 25 cm. This bearing capacity calculation is consistent with the calibration and validation of the plant dewatering model described in Silva et al. (1999b). At the end of 1997 the bearing capacity at the tailings surface (0-70 cm) was greater than 100 kPa (Figure 6.3), reaching a maximum value of 206 kPa in the second layer, whose surface was located at a depth of about 22 cm. At the end of 1998 the bearing capacity at the surface (0-70 cm) was greater than 500 kPa. The top layer has the maximum bearing capacity of 960 kPa.

The bearing capacity values obtained after one year (1997) of plant growth on this deep tailings deposit are lower than those measured at the end of the greenhouse experiment. Plants remove the water from the root zone reducing the hydraulic gradient; the water removed is replaced by water flowing upwards from a high hydraulic gradient at the bottom to a low hydraulic gradient at the top of the deposit. A deep tailings deposit has a larger volume of water than an 0.8-m lysimeter. The plants were able to remove all available water from the lysimeter. However, in a deep deposit one year of plant growth is not enough to remove all available water and generate a significant increase in solids content and bearing capacity.

These results indicate that at the end of the first year (1997) the surface of this deep deposit will be strong enough to allow human or animal traffic. The tailings surface will be stronger at the end of the second year (1998). If the deposit is left planted with these grasses, the bottom material will

be gaining strength with time due to the gradient caused by the soil suction due to the plants at the surface of the deposit. However, this process is extremely slow. The best solution for deep dewatering will be the planting of deep root trees, which will extract the water directly and reinforce the bottom material with the root system. If time is a limiting factor then shallow deposits, which are allowed to dewater can be seen as the best solution. However, larger areas of land will need to be utilized if shallow deposits are used.

### **6.5.2 Optimum CT deposit depth**

The model was run using different initial deposit depths in order to determine the depth at which optimum dewatering can be achieved. Initial deposit depths of 1, 1.5, 2, 2.5, and 3 m were analyzed using one and two growing seasons.

Using just one growing season (1997) the optimum initial deposit depth was found to be equal or less than 1.5 m. The solids content at the end of 1997 was greater than 90% in the whole profile (Figure 6.4) and the bearing capacity was around 250 kPa (Figure 6.5).

Using two growing seasons (1997 and 1998) the optimum initial deposit depth was found to be 2 m. The final solids content was around 95% (Figure 6.6) and the final bearing capacity varied from 906 kPa at the surface to 317 kPa at the bottom layer (Figure 6.7). The selection of the optimum deposit depth will depend upon the final desirable bearing capacity.

## **6.6 SENSITIVITY ANALYSIS**

A sensitivity analysis was conducted to identify the parameters that have a significant effect in the model results. For this task the 1997 climatic data were selected and the initial deposit depth was chosen as 1 m. The parameters were increased and reduced by a certain amount and then inserted in the model. Solids content and bearing capacity profiles were plotted and the variations in results were examined against the results obtained with no change in the parameter value. As result of this evaluation the parameters of the equations of the saturated and unsaturated

hydraulic conductivity and soil water characteristic curve were found to be the most sensitive.

Details are given as follows:

The expression of the saturated hydraulic conductivity used in the model is

$$[6.5] \quad K = Ce^D$$

where  $K$  is hydraulic conductivity (m/d),  $e$  is void ratio,  $C$  (m/d) and  $D$  are fitting parameters. The parameter  $C$  has the value of  $5.18 \times 10^{-4}$  m/d and was increased and reduced by one order of magnitude. An increase in the value of  $C$  caused a reduction in the final solids content (Figure 6.8) and bearing capacity (Figure 6.9). Low hydraulic conductivity tailings cause a low infiltration rate at the surface and less water from rainfall enters the deposit. However, for deeper deposits water will flow at a lower velocity from the bottom to the root zone. The parameter  $D$ , which was increased and reduced by 10%, did not cause any significant variation in the model results.

The expression for the unsaturated hydraulic conductivity used in the model is the parametric equation of Brooks and Corey (1964)

$$[6.6] \quad K = K_s \left( \frac{u_{wb}}{u_w} \right)^P \quad \text{for} \quad u_w > u_{wb}$$

where  $K_s$  is saturated hydraulic conductivity (m/d),  $u_w$  is pore water pressure (matric suction when negative, kPa),  $u_{wb}$  is the bubbling pressure or air entry value (kPa), and  $P$  is an empirical parameter. This parameter was increased and reduced by 10%. The final solids content show some small variations (Figure 6.10), but there are very significant differences in the bearing capacity results (Figure 6.11). A higher value of  $P$  will increase the bearing capacity at the bottom of the deposit.

The soil water characteristic curve was fitted using the Van Genuchten's equation (1980)

$$[6.7] \quad \frac{\theta - \theta_r}{\theta_s - \theta_r} = \frac{1}{\left[1 + |\alpha u_w|^d\right]^m}$$

where  $\theta_r$  and  $\theta_s$  are residual and saturated volumetric water contents, respectively, and  $\alpha$  (1/kPa),  $d$ , and  $m$  are empirical parameters. The Mulaem (1976) theory relates  $d$  and  $m$  as  $m = 1 - 1/d$ .

The parameters  $\alpha$  and  $d$  were increased and reduced by 10%. The parameter  $\alpha$  did not cause any significant changes in the final solids content and bearing capacity. The solids content and bearing capacity profiles variations caused by the changes in the parameter  $d$  are shown in Figure 6.12 and Figure 6.13, respectively. An increase in the value of the parameter  $d$  causes a reduction in the final solids content and bearing capacity profiles.

## 6.7 CONCLUSIONS

Grasses have the ability to remove water from a CT deposit, increasing the matric suction in the root zone and reinforcing the soil with the root system. Although the roots were assumed to reach a maximum depth of 1 m, the matric suction in the root zone established a gradient causing water to flow from the bottom of the tailings to the root zone. A CT deposit with a 5-m-initial depth subjected to one or two years of plant dewatering will have water removed from a depth of as much as 2 m. If deep tailings deposits are necessary, then grasses can be used to dewater the surface, making it strong enough to allow human traffic and after that, trees can be planted to dewater deeper layers.

The optimum initial deposit depths are equal to or less than 1.5 and 2 m for one and two growing seasons, respectively.

The sensitivity analysis indicated that the tailings parameters that require careful determination are those that characterize the saturated and unsaturated hydraulic conductivity and the parameters that control the equation that defines the soil water characteristic curve.

## 6.8 REFERENCES

- Brooks, R.H., and Corey, A.T. 1964. Hydraulic properties of porous media. Hydrology paper 3, Colorado State University, Fort Collins.
- Jensen, M. E., Burman, R. D., and Allen, R. G., eds. 1990. Evapotranspiration and irrigation water requirements. ASCE Manuals and Reports of Engineering Practice No. 70, New York.
- Lui, Y., Caughill, D., Scott, J.D., Burns, R. 1994. Consolidation of Suncor nonsegregating tailings, Proceedings, 47<sup>th</sup> Canadian Geotechnical Conference, Halifax, Nova Scotia, September 21-23, 1994, pp. 504-513.
- Macyk, T.M., Fung, M.Y.P., and Pauls, R.W. 1998. Reclamation research for various land uses in the oil sands region of Alberta, Canada. Proceedings, 15<sup>th</sup> Annual National Meeting of the American Society for Surface Mining and Reclamation, St. Louis, Missouri, May 17-21, 1998, pp. 593-602.
- Monteith, J.L. 1981. Evaporation and surface temperature. Quarterly Journal of the Royal Meteorological Society, **107**: 1-27.
- Mualem, Y. 1976. A new model for predicting the hydraulic conductivity of unsaturated porous media. Water Resources Research, **12**(3): 513-522.
- Polavarapu, R.J. 1970. A comparative study of global and net radiation measurements at Guelph, Ottawa and Toronto. Journal of Applied Meteorology, **9**: 809-814.
- Radersma, S., and de Ridder, Nico. 1996. Computed evapotranspiration of annual and perennial crops at different temporal and spatial scales using published parameter values. Agricultural Water Management, **31**: 17-34.
- Sheeran, D.D. 1993. An improved understanding of fine tailings structure and behavior. Fine tailings symposium, Proceedings of the oil sands - Our petroleum future, Edmonton, Alberta, April 4-7, 1993. Paper F1.
- Silva, M. J., Biggar, K. W., Segó, D. C., Chanasyk, D. S., and Naeth, M. A. 1999a. Model for the prediction of bearing capacity on vegetated tailings. Paper submitted for review to the Canadian Geotechnical Journal, April 1999.
- Silva, M. J., Biggar, K. W., Segó, D. C., Chanasyk, D. S., and Naeth, M. A. 1999b. Plant dewatering of tailings: experimental results and model predictions. Paper submitted for review to the Canadian Geotechnical Journal, April 1999.
- Suthaker, N.N. 1995. Geotechniques of oil sands fine tailings. Ph.D. thesis, University of Alberta, Edmonton, Alberta.
- Van Genuchten, M.Th. 1980. A closed-form equation for predicting the hydraulic conductivity of unsaturated soils. Soil Science Society of America Journal, **44**: 892-898.



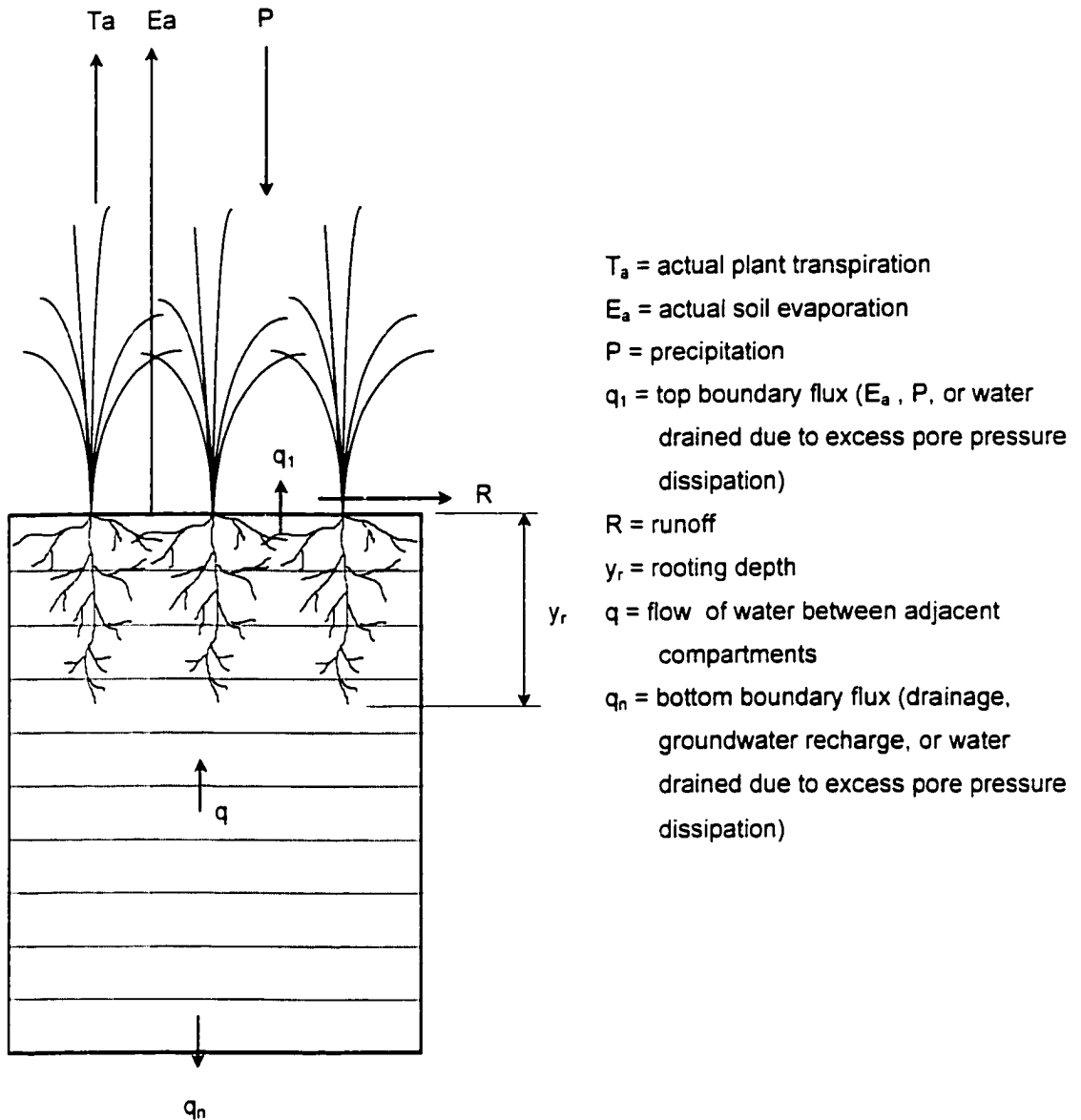


**Figure 6.1 Conceptual model with boundary conditions**

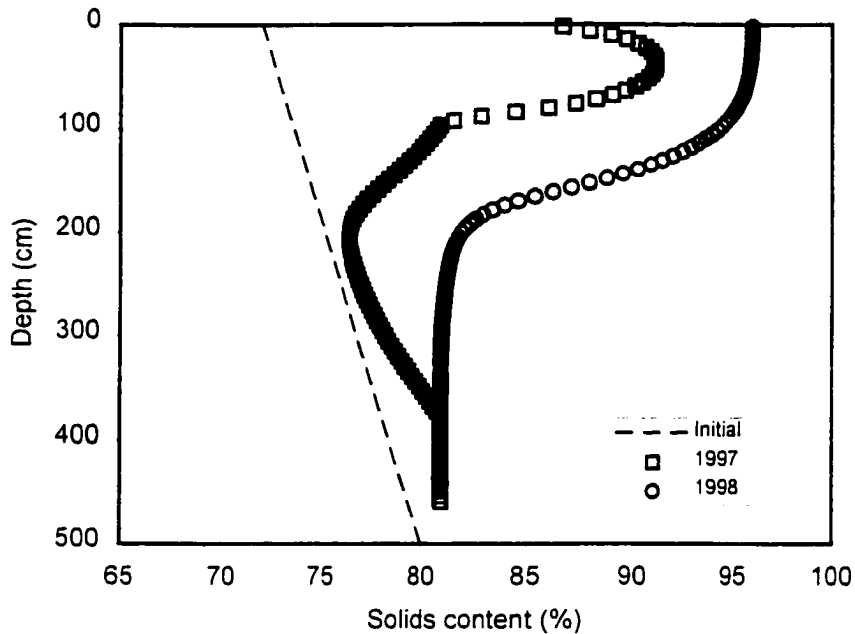


**Figure 6.2 Solids content profile on a 5-m-initial deposit depth**

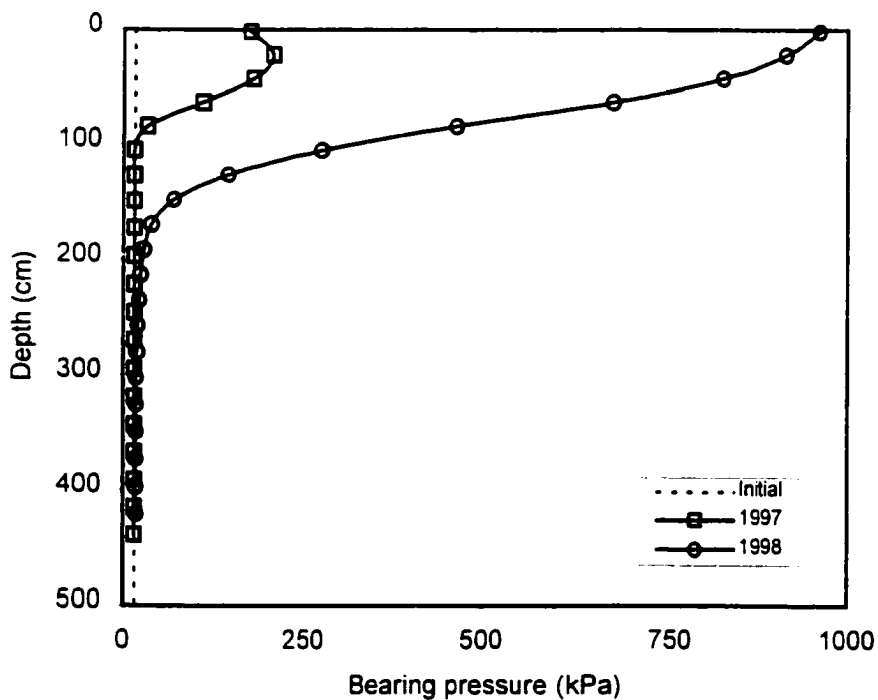


**Figure 6.3 Bearing capacity profile on a 5-m-initial deposit depth**

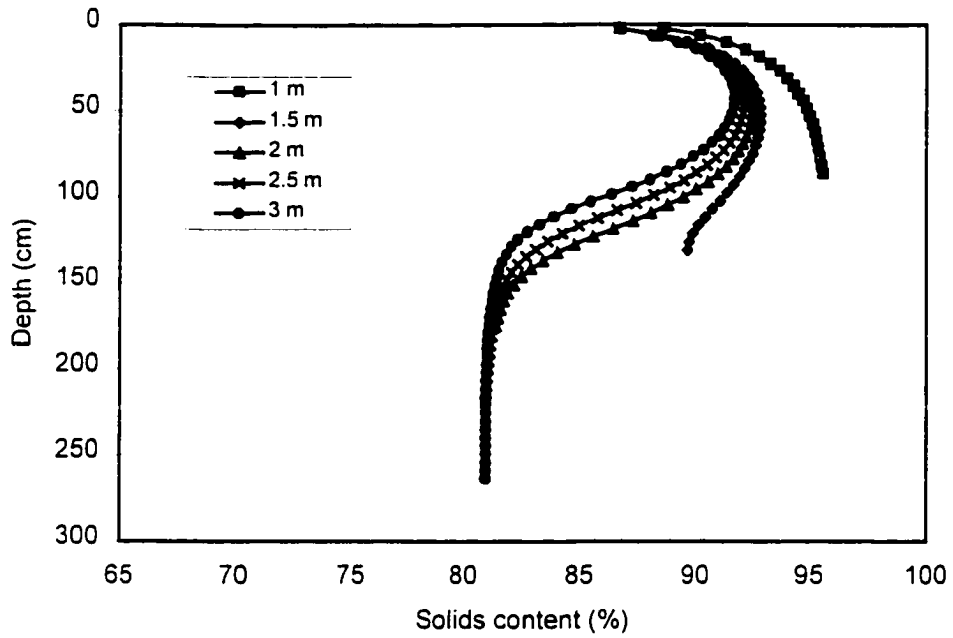


**Figure 6.4 Solids content profiles for different initial deposit depths at end of 1997 (1 year of plant growth)**

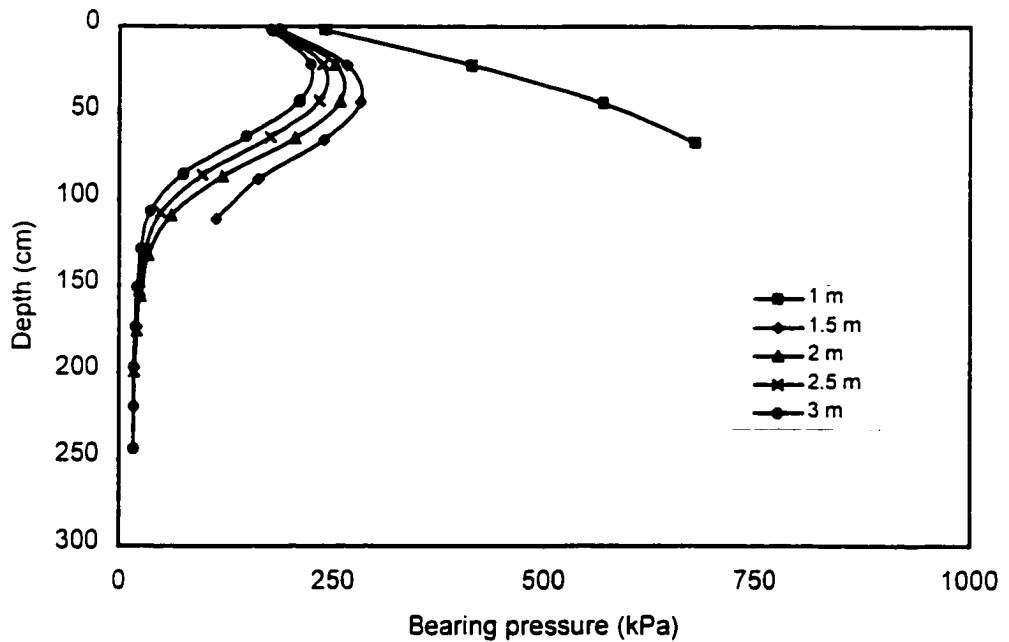


**Figure 6.5 Bearing capacity profiles on different initial deposit depths at end of 1997 (1 year of plant growth)**

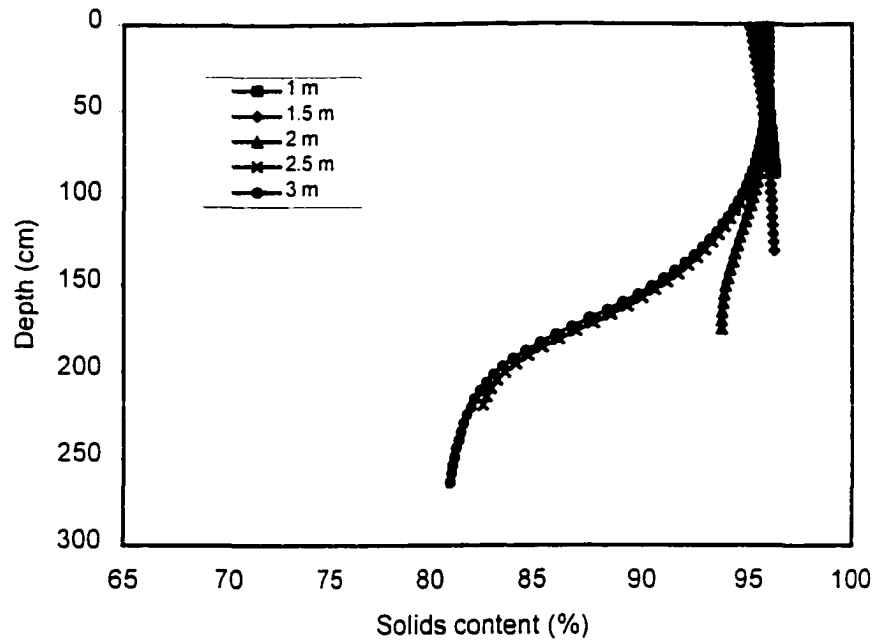


**Figure 6.6 Solids content profiles for different initial deposit depths at end of 1998 (2 years of plant growth)**

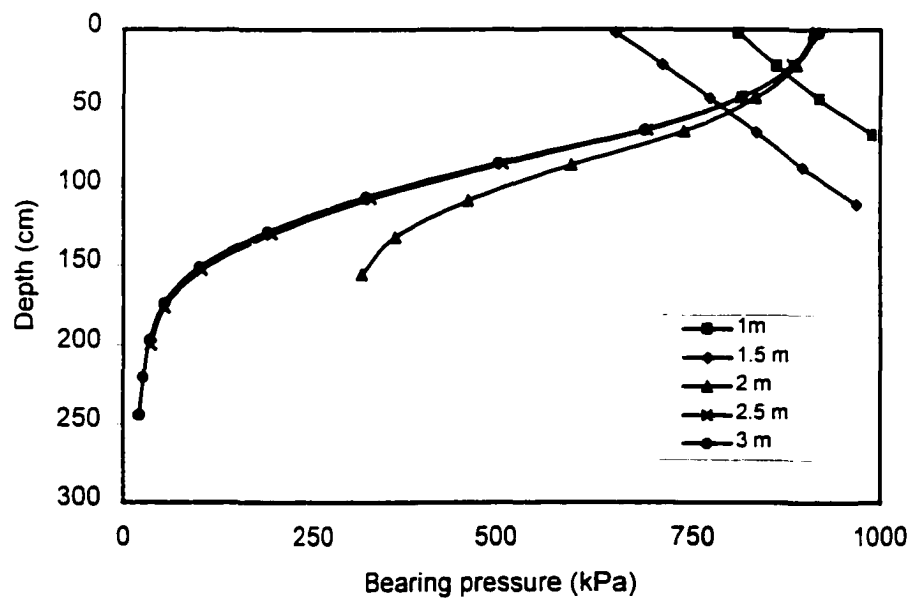


**Figure 6.7 Bearing capacity profiles on different initial deposit depths at end of 1998 (2 years of plant growth)**

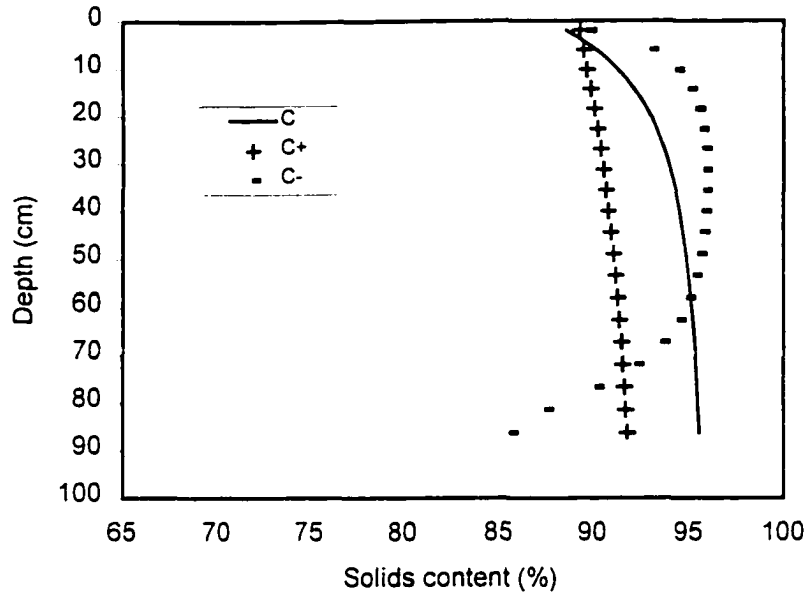


**Figure 6.8 Solids content profile variations caused by changes in the saturated hydraulic conductivity parameter C**

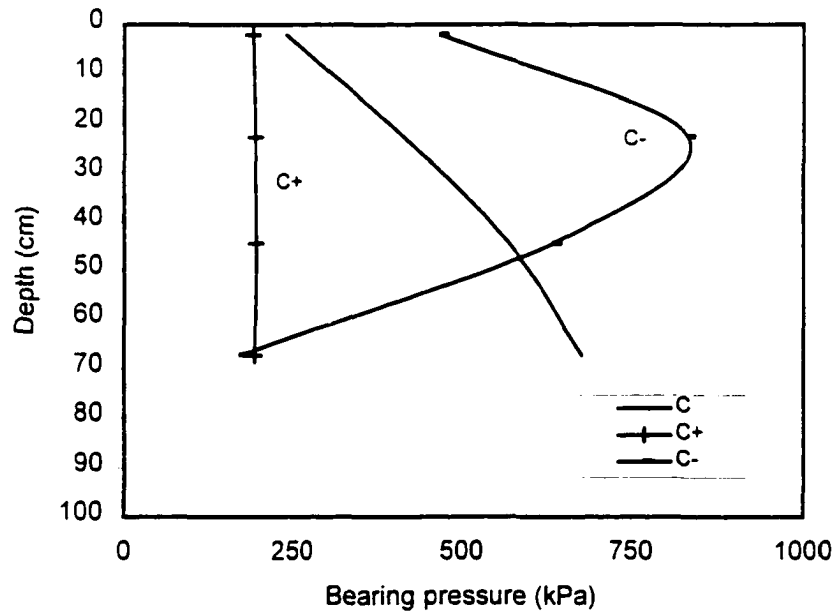


**Figure 6.9 Bearing capacity profile variations caused by changes in the saturated hydraulic conductivity parameter C**

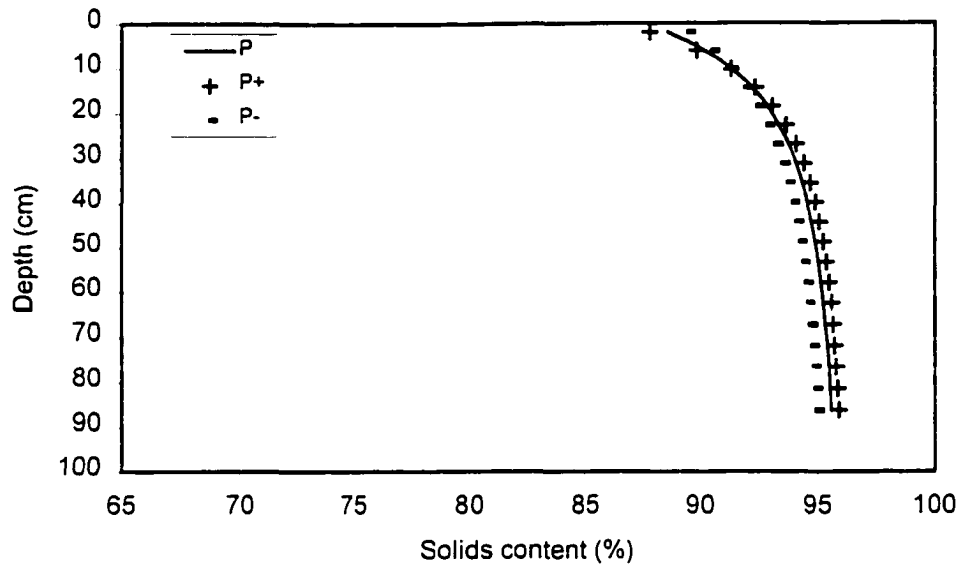


**Figure 6.10 Solids content profile variations caused by changes in the unsaturated hydraulic conductivity parameter P**

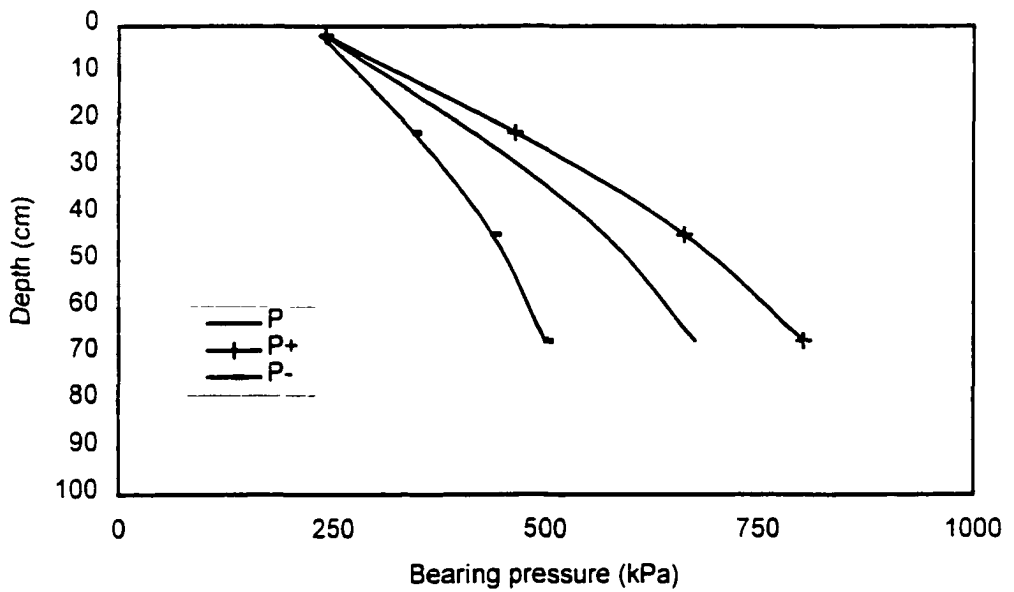


**Figure 6.11 Bearing capacity profile variations caused by changes in the unsaturated hydraulic conductivity parameter P**

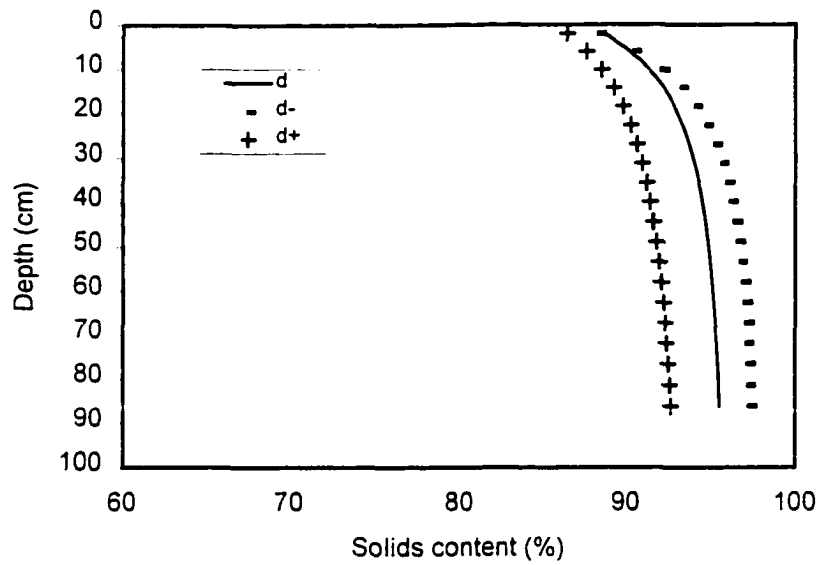


**Figure 6.12 Solids content profile variations caused by changes in the parameter  $d$  of the equation of the SWCC**

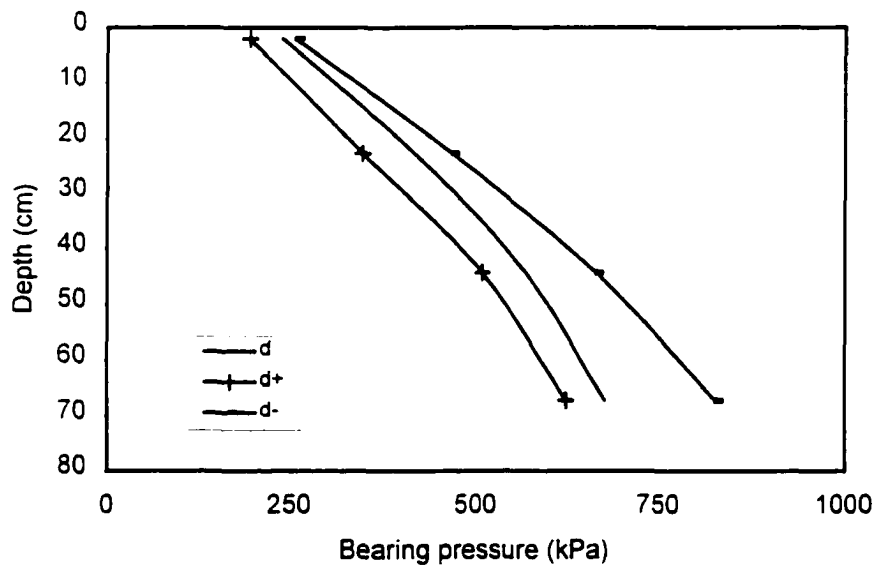


**Figure 6.13 Bearing capacity profile variations caused by changes in the parameter  $d$  of the equation of the SWCC**

Month	T <sub>max</sub> (°C)	T <sub>min</sub> (°C)	P (mm)	u <sub>z</sub> (m/s)	RH (%)
May 97	15.6 ± 1.6	3.7 ± 1.0	13.8	3.1 ± 0.4	65.0
May 98	21.3 ± 1.8	6.4 ± 1.3	16.0	2.8 ± 0.3	64.6
May avg	17.1	3.0	37.2	3.1	57.5
Jun 97	22.1 ± 1.2	11 ± 0.9	46.0	2.5 ± 0.2	70.9
Jun 98	22.9 ± 1.8	10.5 ± 1.5	48.0	2.7 ± 0.3	69.7
Jun avg	21.5	7.7	63.9	2.8	63.0
Jul 97 <sup>2</sup>	26.1 ± 1.5	13.3 ± 1.1	29.2	2.9 ± 0.5	61.1
Jul 98	26.1 ± 1.5	13.3 ± 1.1	29.2	2.9 ± 0.5	61.1
Jul avg	23.2	10.0	79.1	2.5	68.0
Aug 97	23.2 ± 1.8	11.3 ± 1.0	91.4	2.3 ± 0.3	75.8
Aug 98	26.3 ± 1.6	12.0 ± 1.0	14.2	2.9 ± 0.3	57.0
Aug avg	21.8	8.5	71.7	2.5	70.5
Sep 97	16.8 ± 2.5	7.1 ± 1.3	96.2	2.8 ± 0.4	83.0
Sep 98	17.3 ± 1.9	5.4 ± 1.3	13.4	2.4 ± 0.3	64.6
Sep avg	15.1	3.2	48.1	2.8	72.5
Oct 97	5.4 ± 1.9	-0.7 ± 1.2	28.8	2.9 ± 0.3	86.3
Oct 98	9.8 ± 2.0	1.2 ± 1.4	2.8	3.4 ± 0.5	69.3
Oct avg	8.4	-1.9	20.0	2.8	71.5

95% confidence interval; <sup>2</sup> Data were not available, Jul 98 data were used in its place

**Table 6.1 Comparison of climatic data for 1997 and 1998 to a long term average**



<b>Tailings Parameters</b>	<b>Symbol</b>	<b>value</b>
Wilting point	$\theta_{wp}$	6.5%
Saturation point	$\theta_s$	38%
Residual water content	$\theta_r$	1%
Limited Available Water	LAW	- 1000 kPa
Evaporation limiting factor	$K_{evap}$	0.6
Tailings strength parameters	A	0.9952 1/kPa
	B	- 0.1811
	C	$5.18 \times 10^{-4}$
Saturated hydraulic conductivity parameters	D	1.3754
Specific gravity	$G_s$	2.6
Cohesion	$c'$	0.2 kPa
Angle of shearing resistance	$\phi'$	30°
Unsaturated hydraulic conductivity parameters	P	0.65
	$u_{wb}$	- 0.6 kPa
Soil Water Characteristic Curve parameters	$\alpha$	- 0.15
	m	0.259
	d	1.35
<b>Plant parameters</b>		
Leaf Area Index parameters	$C_1$	4
	$C_2$	12.2
Time to plant maturity	$t_m$	98 days
Root biomass at the surface at maturity	$B_{Rtopm}$	0.5 kg/m <sup>3</sup>
Maximum rooting depth	$y_m$	1 m

**Table 6.2 Tailings and plant parameters used in the model**

## Chapter 7

### ***Summary and conclusions***

---

#### **7.1 RESEARCH OBJECTIVES**

The main objective of this thesis was to study and evaluate the strength enhancement mechanism of suitable plant species growing on high water content tailings.

Specific objectives of this thesis as stated in Chapter 1 were as follows:

- Identify the most suitable plant species for dewatering and reclamation of tailings. Two mine tailings were chosen: Composite Tailings (CT) from Alberta oil sands operated by Syncrude Canada Ltd. and Copper Mine Tailings (CMT) from the Kennecott site in Utah.
- Identify the main physical processes that control the plant dewatering mechanism.
- Formulate a theoretical framework to predict the increase of bearing capacity of tailings due to the plant dewatering mechanism.
- Develop a finite difference solution algorithm of the theoretical formulation.
- Conduct a greenhouse experiment to calibrate and validate the proposed numerical model and evaluate the plant response to mine tailings. Composite Tailings (CT) was used as the growth medium.

The results of the theoretical and greenhouse laboratory research carried out indicate the research objectives have been met.

The research objectives were achieved in a progressive manner. The initial plant screening program described in Chapter 2 provided information of suitable plant species for dewatering and reclamation of Composite Tailings (CT) from Alberta oil sands operated by Syncrude Canada Ltd. and Copper Mine Tailings (CMT) from the Kennecott site in Utah. In Chapter 3 a theoretical framework was formulated to predict the increase in bearing capacity of tailings due to the plant dewatering mechanism, the main physical processes that control the plant dewatering mechanism were identified and a finite difference solution algorithm of the theoretical formulation was developed. Chapters 4 and 5 described the greenhouse experiment conducted to calibrate and validate the proposed numerical model and evaluate the plant response to oil sands tailings. The proposed model predicts measured values of solids content and bearing capacity quite well as described in Chapter 5. The theory was applied to a practical field problem to predict bearing capacity of CT deposits as described in Chapter 6.

## **7.2 CONCLUSIONS**

The strength enhancement mechanism of suitable plant species growing on high water content tailings has been studied. A theoretical framework was established and applied to simulate results measured in a greenhouse experiment. The specific conclusions of the research program are:

- Plants growing in weak high water content tailings have the ability to remove the water through evapotranspiration, increasing the matric suction in the deposit. This results in an increase in the shear strength and bearing capacity in the root zone. Furthermore, the plant root system provides a fiber reinforcement, which also contributes to the increased bearing capacity of the rooted tailings.

- Composite Tailings (CT) from Alberta oil sands operated by Syncrude Canada Ltd. and Copper Mine Tailings (CMT) from the Kennecott site in Utah are not phytotoxic and plants can be used to implement future reclamation activities when the impoundments reach full capacity. Based on values of Sodium Adsorption Ratio (SAR) and Electrical Conductivity (EC) both tailings can be classified as normal soils (non-sodic and non-saline soils). Fifteen plant species, which were tested in CT, showed signs of healthy growth. All of the nine species tested in CMT grew reasonably well. These plants adapted well to extremely adverse conditions characteristic of those mine waste tailings.
- Five plant species proved the best candidates for future field plant dewatering and reclamation research in CT: reed canarygrass, creeping foxtail, red top, Altai wildrye and streambank wheatgrass. Three species are recommended for further studies in CMT: Altai wildrye, smooth brome grass and creeping foxtail.
- A second greenhouse experiment using CT as growth medium showed that creeping foxtail, red top and reed canarygrass presented signs of healthy growth, whereas Altai wildrye and streambank wheatgrass did not grow well in the CT in the initial period. Creeping foxtail and reed canarygrass had the highest evapotranspiration, the highest above and below ground biomasses, the greatest plant heights and leaf area indexes, the deepest roots and the lowest stress symptoms. These plant parameters are linked to the healthy plant growth and physiological conditions.
- Reed canarygrass, creeping foxtail and red top plants are tolerant of waterlogged conditions. Altai wildrye and streambank wheatgrass, although not tolerant of waterlogged conditions, are also good candidates for future field research in dewatering CT without free water at the surface.
- A physically based model for predicting the contributions to bearing capacity of tailings by the strength enhancement mechanism of plants was described. The model simulates one

dimensional water flow in a tailings deposit of high initial water content, including the root zone, by solving a transient flow equation coupled with water extraction from within via evapotranspiration. The governing equation of the plant dewatering model is:

$$[3.11] \quad \frac{DV_w}{Dt} = V_s \frac{\partial}{\partial Z} \left( \frac{K}{1+e} \frac{\partial h_w}{\partial Z} \right) - V_s(1+e)T$$

Under saturated conditions the term  $\frac{\partial h_w}{\partial Z}$  includes the theory of self weight consolidation as:

$$[3.21] \quad \frac{\partial h_w}{\partial Z} = -1 + G_s - \frac{1}{\gamma_w ABV_s} \left( \frac{e}{A} \right)^{\frac{1}{B}-1} \frac{\partial V_w}{\partial Z}$$

The evapotranspiration is calculated using the Penman-Monteith equation

$$[6.1] \quad \lambda ET_0 = \frac{\Delta}{\Delta + \gamma_c(1+r_c/r_a)} (R_n - G) + \frac{\gamma_c}{\Delta + \lambda_c(1+r_c/r_a)} K_1 \frac{0.622\lambda_c\rho_a}{P_a} \frac{1}{r_a} (e_z^0 - e_z)$$

Equation [3.11] is non-linear with respect to space and time. The solution algorithm for this equation was successfully obtained using a Crank-Nicholson finite difference scheme. The matric suction and root distribution profiles were used to calculate the increased bearing capacity due to the plants.

- The theoretical model was used to simulate the results of a greenhouse experiment using five plant species, which proved to be the best candidates for dewatering CT from a previous plant-screening program. The model slightly over-predicted the surface settlement, but a good match was found in the trend. Good agreement was found between the measured and predicted solids content profile. Predicted values of bearing capacity were in good agreement with measured values, as well.

- It is predicted that a CT deposit with a 5-m-initial depth subjected to one or two years of plant dewatering will have water removed from a depth of as much as 2 m. If a deep tailings deposit is necessary, then grasses can be used to dewater the surface making it strong enough to allow human traffic and after that, trees can be planted to dewater deeper layers.
- It is predicted that the optimum initial deposit depths are equal to or less than 1.5 and 2 m for one and two growing seasons, respectively.
- The sensitivity analysis conducted on the plant dewatering model indicated that the tailings parameters that require careful determination are those that characterize the saturated and unsaturated hydraulic conductivity and the parameters that control the equation that defines the soil water characteristic curve.

### **7.3 SUGGESTED FUTURE RESEARCH**

Although the main objectives of this thesis have been achieved, several exciting issues were encountered during the course of this research that possibly deserve further investigation. Some of these issues are:

- Conduct a plant-screening program to identify native plant species suitable for dewatering and reclamation of high water content tailings. Utilization of native plant species in dewatering and reclamation of mine sites may be desirable for restoration. If the management objective is to restore the existing natural plant community, then the introduction of exotic species is to be avoided. Native plant species adapted to the climatic conditions of the area, or adapted to lower nutrient requirements, may have advantages over agronomic species in revegetation efforts. It is recommended to test native plant species that can develop a high leaf area index in a short period of time. In this way, the transpiration component of the evapotranspiration process will be greater than the evaporation and the plant dewatering mechanism will be at its maximum capability.

- Conduct experiments to evaluate the possibility of growing plants from seeds planted directly on the surface of the tailings. This will avoid the costly process of transplanting.
- In the particular case of CT, it is necessary to conduct more studies to understand the rapid consolidation process or hindered sedimentation of CT after deposition. In this process, a large volume of water travels from the bottom to the top of the deposit relieving some of the excess pore water pressure generated by the self-weight of the tailings. If seeds or plants are planted on the tailings before this process is complete they may wash out of the mixture and will be floating on the surface. Consequently there will be little chance that they would then germinate and root into the mineral materials.
- In this thesis the contribution of the plant root system to the increased bearing capacity was taken from average values published in the literature. However, many of these reported values take implicitly into account the contribution of the matric suction. A laboratory program to measure independently the contribution to bearing capacity from root reinforcement and matric suction should be conducted for selected plant species.
- The effect of hysteresis with respect to the moisture retention curve must also be addressed. Laboratory tests including infiltration and dewatering events should also be conducted to verify the results of the simulations. The plant dewatering model can easily be modified to include the effect of hysteresis if a theoretical model is available.
- Incorporate in the model (1) the rapid consolidation (*hindered sedimentation*) process that occurs in the tailings right after deposition, and (2) the freeze-thaw consolidation that take place during the winter months. In this way, all natural processes will be included in the model making an all-year-round dewatering process and more realistic predictions of solids content and bearing capacity. Conduct experiments to verify and validate the complete theoretical formulation.

- The unsaturated hydraulic conductivity curve of CT was calculated from the soil water retention curve. The results of the plant dewatering model proved to be very sensitive to the parameters that characterize this tailings property. A more accurate curve should be determined by conducting laboratory tests.
- Validation of the proposed theoretical model should be carried out in a field setting. An appropriate site should be selected for instrumentation. Predicted values of solids content profiles and bearing capacity would be compared with field measurements.

Numerous applications of the plant dewatering model exist, only those related to the geotechnical engineering discipline will be described. For example, the model could be used for the design of long-term cover systems with surface vegetation to minimize the infiltration of water through the hazardous waste material below it. The model may also aid in the analysis of the stability of vegetated slopes. The stability of many slopes depends upon the strength provided by the soil matric suction and the fiber reinforcement provided by the plant root systems. The model can be modified to calculate the shear strength of vegetated slopes.



## **Appendix A**

### **Summary of results of the greenhouse experiment Phase 1 and Phase 2**

#### **A.1 INTRODUCTION**

Chapter 2 of the thesis presents the results of a two-phase greenhouse experiment conducted to identify the most suitable plant species for dewatering and reclamation of Composite Tailings (CT) from the Alberta oil sands operated by Syncrude Canada Ltd. and Copper Mine Tailings (CMT) from the Kennecott site located in the State of Utah. A detailed description of the methodology was given in that chapter. Most of the results were also presented. This appendix presents the remaining results and some additional information related to this greenhouse experiment.

#### **A.2 SEEDING**

Seeds of selected plant species were supplied by Prairie Seeds Inc. A first trial was conducted to obtain information about the germination capability and growth potential of the seeds. Root trainer trays, having ten containers each, were filled with moist compost. Seeds were spread over the compost covering the total surface of the tray. The seeds were then covered with dry compost and the trays were closed with plastic leads and placed inside the greenhouse. Most seeds germinated after one week. All seeds showed excellent germination potential.

Based on the previous trial, a large amount of seeds were sown to obtain the seedlings to be used in Phase 1 of the greenhouse experiment. Trays with 48 small containers were used for this

task. About 4 to 5 seeds were used in each root trainer. A total of 90 plants were needed for this experiment. The same seeding procedure was utilized for Phase 2 of the experiment.

### **A.3 FERTILIZER CALCULATIONS**

The calculations involved in the application of fertilizers were a necessary part of the greenhouse experimental research. The first step in comprehending fertilizer calculations is to understand some of the terms associated with fertilizer materials.

#### **A.3.1 Ratio**

Ratio refers to the relative quantities of the nutrients. A 10-10-10 fertilizer has a ratio of 1-1-1, as would a 20-20-20. A 20-5-10 fertilizer has a ratio of 4-1-2. Ratio provides little information about the actual amount of nutrients in the container. It is the analysis that provides the most useful information about the fertilizer. The fertilizer formulas used in all greenhouse experiments were 15.5-0-0, 0-20-0, and 0-0-60.

#### **A.3.2 Analysis**

Analysis refers to the percentage by weight of the fertilizer nutrients. The analysis is usually listed on the container, either in prominent numbers across the front of the package, or as a part of the label. Nitrogen (N) is expressed on an elemental basis, whereas Phosphorous (P) and Potassium (K) are generally expressed as phosphoric acid ( $P_2O_5$ ) and potash ( $K_2O$ ). A 10-10-10 fertilizer contains by weight 10% N, 10%  $P_2O_5$  and 10%  $K_2O$ . A 100-lb bag would contain 10 lbs. N, 10 lbs.  $P_2O_5$  and 10 lbs.  $K_2O$ .

A frequent mistake is to interpret the analysis as though the last two numbers referred to percentage by weight of elemental P and K. This can lead to large errors, and care should be taken that the following conversions are always used when fertilizer calculations involving P and K are made:  $P_2O_5$  contains 44% P and  $K_2O$  contains 83% K.

Example: A 50-lb bag of fertilizer has the analysis of 20-5-10. How much N, P and K does this bag contain?

The analysis lists the percentage by weight of N,  $P_2O_5$  and  $K_2O$ . First determine the amount of these materials by multiplying the percentage of each of the materials by the total weight of the fertilizer in the bag:  $(50 \text{ lb.} \times 0.20) = 10 \text{ lb. N}$ ,  $(50 \text{ lb.} \times 0.05) = 2.5 \text{ lb. } P_2O_5$ , and  $(50 \text{ lb.} \times 0.10) = 5 \text{ lb. } K_2O$ . The amount of elemental N has been calculated to be 10 lb., but another step will be required to determine the amount of P and K:  $(2.5 \text{ lb. } P_2O_5 \times 0.44) = 1.1 \text{ lb. P}$ , and  $(5 \text{ lb. } K_2O \times 0.83) = 4.15 \text{ lb. K}$ . The bag contains 10 lb. of N, 1.1 lb. of P and 4.15 lb. of K.

#### **A.4 EVAPOTRANSPIRATION**

Water loss due to evapotranspiration was measured weekly by weighing the lysimeters. This appendix presents a summary of the amount of water that was lost from each lysimeter and a summary of the temporal variations of the average ET on CT and CMT.

Treatment	ETcum 26-Nov 13-Dec	Mean	ETcum 26-Nov 27-Dec	Mean	ETcum 26-Nov 14-Jan	Mean	ETcum 26-Nov 4-Feb	Mean
Alfalfa-1	4000		6815		10520		15400	
Alfalfa-2	3925	3918	6785	6687	10350	10183	15565	14935
Alfalfa-3	3830		6460		9680		13840	
Alsike-2	4405		8310		12850		17930	
Alsike-1	785	2148	4080	5682	8310	10042	13630	15203
Alsike-1	1255		4655		8965		14050	
Altai-1	4140		7645		12215		17370	
Altai-2	4270	4175	7600	7588	11995	12017	17290	17280
Altai-3	4115		7520		11840		17180	
Control-1	2570		5280		8225		12585	
Control-2	2585	2585	4770	4993	7820	8082	12110	12528
Control-3	2600		4930		8200		12890	
Foxtail-1	5055		9150		13245		17705	
Foxtail-2	3395	4383	7115	8222	11150	12287	15775	16882
Foxtail-3	4700		8400		12465		17165	
Indian-1	3515		6310		9925		14155	
Indian-2	3740	3668	7125	6833	11700	10908	16570	15440
Indian-3	3750		7065		11100		15595	
Kentucky-1	3475		6235		9970		14820	
Kentucky-2	3945	3705	7765	6955	11330	10715	16375	15685
Kentucky-3	3695		6865		10845		15860	
Northern-1	3640		6930		11010		16315	
Northern-2	4490	3932	8270	7395	12780	11673	17905	16873
Northern-3	3665		6985		11230		16400	
Red top-1	4895		8930		13235		17710	
Red top-2	5520	5200	9685	9252	13755	13483	18185	17982
Red top-3	5185		9140		13460		18050	
Reed-1	5170		8920		12920		17455	
Reed-2	5165	5062	9090	8840	13155	12852	16645	17022
Reed-3	4850		8510		12480		16965	

**Table A.1 Summary of ET measured on CT in Phase 1 (ET is in grams)**

<b>Treatment</b>	<b>ETcum 26-Nov 13-Dec</b>	<b>Mean</b>	<b>ETcum 26-Nov 27-Dec</b>	<b>Mean</b>	<b>ETcum 26-Nov 14-Jan</b>	<b>Mean</b>	<b>ETcum 26-Nov 4-Feb</b>	<b>Mean</b>
Smooth-1	4305		7885		11835		16505	
Smooth-2	5035	4833	8750	8598	12805	12693	17370	17403
Smooth-3	5160		9160		13440		18335	
Streambank-3	4150		7920		12410		17495	
Streambank-1	3670	3890	6915	7412	11100	11732	16465	17000
Streambank-1	3850		7400		11685		17040	
Timothy-1	4075		7035		10655		15245	
Timothy-2	4585	4270	7860	7412	11220	10887	15815	15532
Timothy-3	4150		7340		10785		15535	
Willow-1	2900		5290		8170			
Willow-2	2635	2917	5060	5273	8010	8207		
Willow-3	3015		5470		8440			
	13-Dec				13-Dec		13-Dec	
	27-Dec				14-Jan		4-Feb	
Western dock-1	3540				8435		13105	
Western dock-2	4170	3977			9600	9158	14125	13683
Western dock-3	4220				9440		13820	
	16-Dec				16-Dec		16-Dec	
	27-Dec				14-Jan		4-Feb	
WillowB-1	1740				4500		7780	
WillowB-2	2210	1978			5310	4965	8810	8422
WillowB-3	1985				5085		8675	
Cattail-1	2810				5892		9675	
Cattail-2	2645	2745			6300	6104	11055	10320
Cattail-3	2780				6120		10230	

Table A.1 (Cont.)

Summary of ET measured on CT in Phase 1 (ET is in grams)



**CT ET in mm**

<b>Days</b>	<b>17</b>	<b>31</b>	<b>49</b>	<b>70</b>
Alfalfa	56	96	146	214
Alsike	31	82	144	218
Altai	60	109	172	248
Control	37	72	116	166
Foxtail	63	118	176	242
Indian	53	98	156	222
Kentucky	53	100	154	225
Northern	56	106	167	242
Red top	75	133	193	258
Reed canary	73	127	184	244
Smooth brome	69	123	182	250
Streambank	56	106	168	244
Timothy	61	106	156	223
Willow	42	76	118	
<b>Days</b>	<b>14</b>	<b>32</b>	<b>53</b>	
Western dock	57	131	196	
<b>Days</b>	<b>11</b>	<b>29</b>	<b>50</b>	
Willow-B	28	71	121	
Cattail	39	88	148	

**CMT ET in mm**

<b>Days</b>	<b>16</b>	<b>30</b>	<b>48</b>	<b>69</b>
Alfalfa	52	89	122	180
Altai	53	88	124	190
Control	36	59	90	133
Foxtail	60	94	123	180
Northern	43	76	113	171
Reed	54	87	114	172
Smooth	53	86	119	179
Timothy	45	74	103	150
Willow	29	49	76	127
<b>Days</b>	<b>14</b>	<b>32</b>	<b>53</b>	
Western duck-2	35	76	137	

**Table A.3 Temporal variations of average ET on CT and CMT in Phase 1**

**CT ET in mm**

<b>Plant Species</b>	<b>Time (days)</b>					
	<b>14</b>	<b>21</b>	<b>28</b>	<b>25</b>	<b>42</b>	<b>56</b>
Alfalfa	17	34	48	63	69	95
Alsike	16	30	43	57	62	88
Altai	17	33	49	65	74	104
Control	15	30	44	58	63	89
Foxtail	18	39	56	74	83	115
Kentucky	15	30	44	58	64	90
Northern	17	32	47	62	68	97
Reed	18	34	50	65	72	99
Red top	18	34	49	65	72	101
Smooth	17	32	46	61	67	94
Streambank	16	32	47	62	70	98
Timothy	16	31	44	58	64	89
Western dock	16	31	45	60	67	94

**CMT ET in mm**

<b>Plant Species</b>	<b>Time (days)</b>						
	<b>7</b>	<b>14</b>	<b>21</b>	<b>28</b>	<b>25</b>	<b>42</b>	<b>56</b>
Alfalfa	19	34	46	58	78	82	106
Altai	19	36	51	64	85	91	117
Control	29	44	57	69	90	94	118
Foxtail	19	36	50	63	83	88	112
Northern	20	36	49	62	81	85	109
Reed	19	34	51	58	77	81	103
Smooth	20	36	49	62	81	86	119
Timothy	19	34	47	59	78	81	104
Western dock	18	34	47	59	79	83	107

**Table A.4 Temporal variations of average ET on CT and CMT in Phase 2**



## **Appendix B**

### **TDR and neutron probe calibrations and measurements of solids contents**

#### **B.1 INTRODUCTION**

The methods selected to measure the solids content profile in the lysimeters were the time domain reflectometry (TDR) and the neutron probe.

TDR is a remote sensing electrical measurement technique that has been used to determine the spatial location and nature of different objects. TDR works by emitting an electromagnetic step pulse that travels along a transmission line and remains unaltered if the characteristics of the line remain the same. Probes of various shapes and geometry are used at the end of the line to alter the pulse and return a waveform back to the TDR receiver. This waveform is then used to determine the apparent dielectric constant  $K_a$  of the material surrounding the probe. The apparent dielectric constant is dependent on the soil water content and for this reason TDR has been mainly used in the monitoring of soil moisture in agricultural soils. TDR measurements are dependent of soil type, temperature, salinity and density (Dirksen and Dasberg 1993).

The neutron probe is a device that has been used for many years in agriculture to monitor the soil moisture. The neutron probe is a source of fast or high energy neutrons and a detector of slow or thermal neutrons. The fast neutrons are slowed down by collisions with the nucleus of matter in the soil and then absorbed by the soil matter. Since the mass of the nucleus of hydrogen is the same as that of a free neutron, the presence of hydrogen will result in a high field of thermal neutrons. The thermal neutrons are continually being absorbed by the matter in the soil. The

neutron probe may thus be used as a measuring device for moisture in the soil but it may require calibration for local soil conditions.

The mini TDR probes were developed and constructed at the University of Alberta. The dimensions are approximately 50 mm long and 25 mm in diameter. The neutron probe used was a neutron depth moisture gauge, model 503 DR HYDROPROBE, manufactured by Campbell Pacific Nuclear Corporation (CPN) of Martinez (California).

## **B.2 TDR AND NEUTRON PROBE CALIBRATION CURVES**

Calibration of the TDR probe involved determining the apparent dielectric constant correlation with solids content for CT. Salinity was a potential factor affecting measurement of the apparent dielectric constant, therefore the CT samples used in the calibration had a salinity level close to real conditions. The Tektronic 1502C TDR unit supplied by Syncrude Canada Ltd. was connected to an IBM PC via RS-232 cable to download waveform data. A Windows based TDR waveform analysis algorithm developed by Lefebvre (1997) was used to calculate the apparent dielectric constant of the tailings. The laboratory procedure outlined in Lefebvre (1997) was used to calibrate the mini TDR probes to measure solids content of CT. The resultant calibration curve is presented in Figure B.1.

The neutron probe involved determining the count ratio correlation with solids content. Neutron probes are usually calibrated using the volumetric water content, which can only be derived from gravimetric values if the soil bulk density is known or measured. Silvestri et al. (1991) found that the factory linear calibration curve is satisfactory for volumetric water content not exceeding 40%. However, for volumetric water contents in the range from 40% to 100%, they found that the relationship between probe readings and volumetric water contents is nonlinear. The same behavior was found in the calibration of the neutron probe using Composite Tailings (CT). As shown in Figure B.2, the calibrations provided very consistent results. The methodology followed to calibrate the neutron probe is outlined in the manual that comes with the instrument.

### **B.3 SOLIDS CONTENT MEASUREMENTS**

The solids content profiles, which have been partially presented in the chapters of the thesis, are included in entirety in this appendix. Both TDR and neutron probe measurements of solids content are included in the figures.

Figure B.3 to B.62 present the solids content measured with the TDR probes and the neutron probe. At the beginning of the experiment and before transplanting tailings samples were taken with a mini-piston sampler. These solids contents represent the initial conditions for the modeling evaluation. Figure B.63 to B.77 present the solids content measured at the end of the experiment. The phrase "physically measured" means that the samples were taken at 10-cm increment. The words "Ring 1" and "Ring 2" represent the samples that were taken from ring of known volume to determine the root biomass distribution in the tailings. After the root were removed from the tailings in the rings, samples were taken to determine the solids content.

### **B.4 REFERENCES**

- Lefebvre, M.E. 1997. The feasibility of coaxial time domain reflectometry as an in-situ site characterization tool for determining the moisture content of mine tailings. M.Sc. thesis, University of Alberta, Edmonton, Alberta.
- Dirksen, C. and Dasberg, S. 1993. Improved calibration of time domain reflectometry soil water content measurements. *Soil Science Society of America Journal*, **57**(3), 660-667.
- Silvestri, V., Sarkis, G, Bekkouche, N., Soulie, M., and Tabib, C. 1991. Laboratory and field calibration of a neutron depth moisture gauge for use in high water content soils. *ASTM Geotechnical Testing Journal*, **14**(1): 64-70.

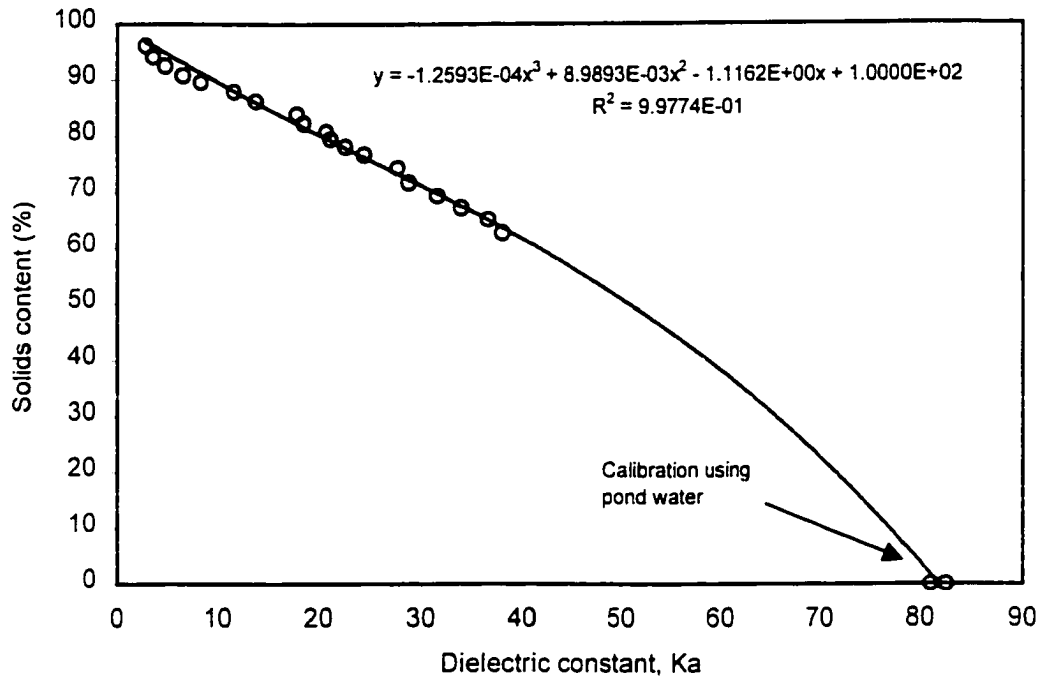


Figure B.1 TDR calibration curve

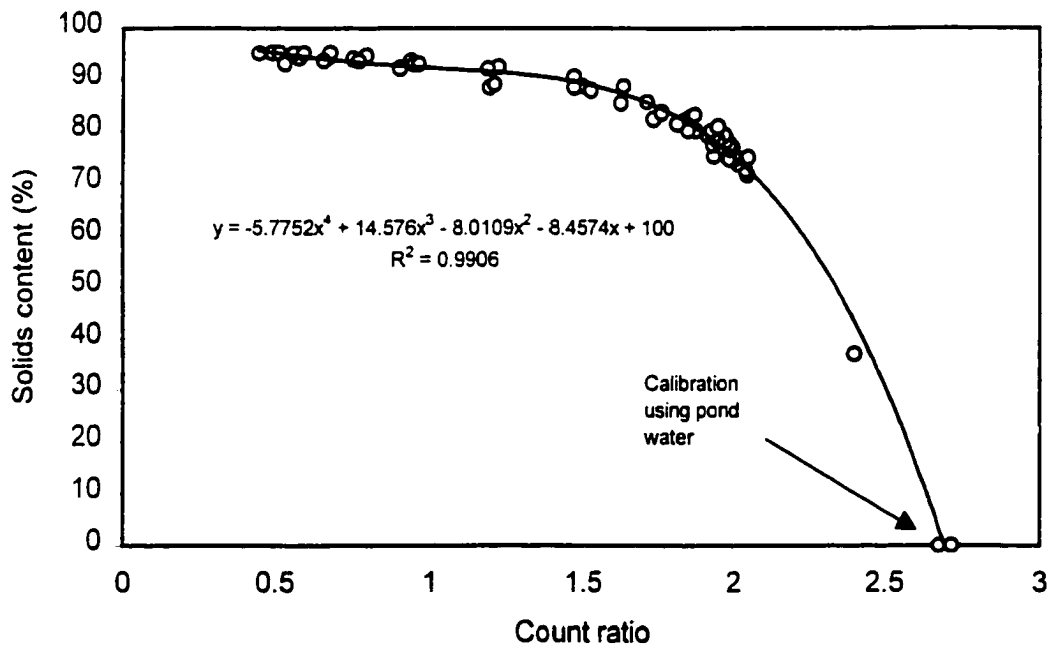
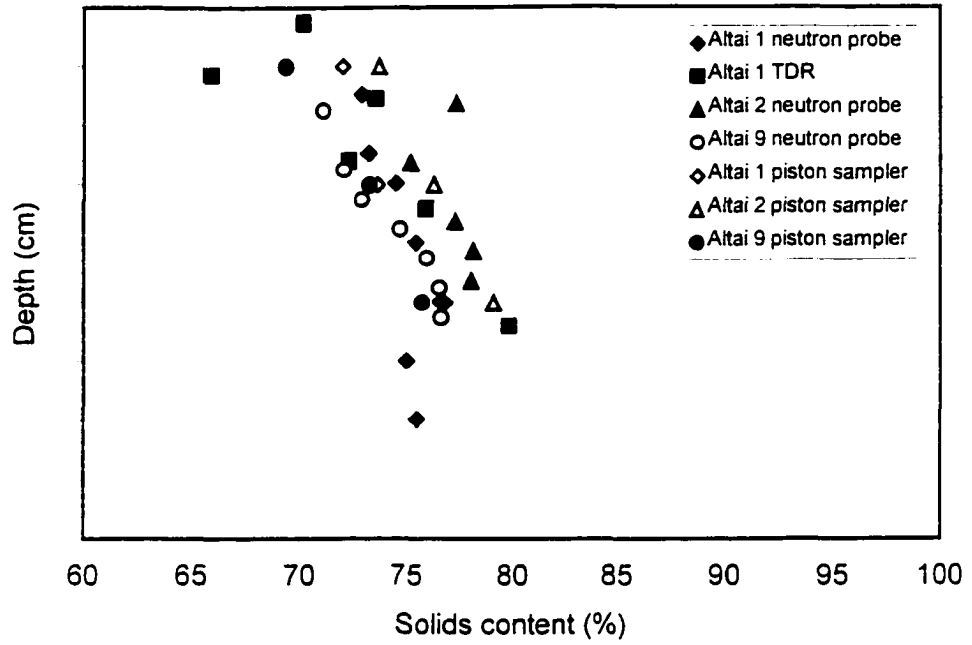
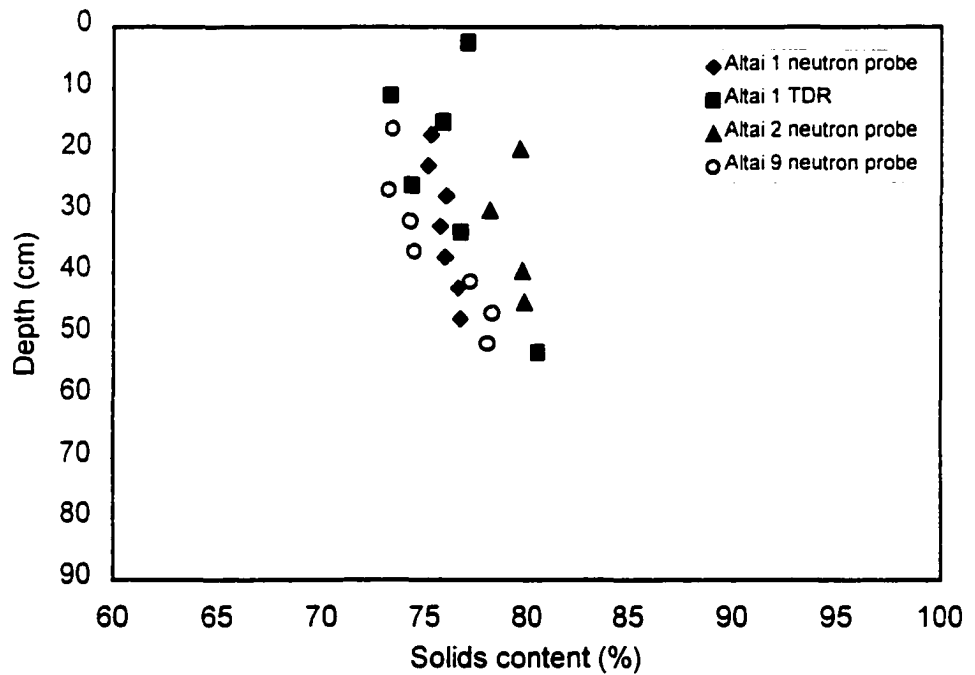


Figure B.2 Neutron probe calibration curve



**Figure B.3 Solids content profile of Altai wildrye measured on February 24, 1998**



**Figure B.4 Solids content profile of Altai wildrye measured on March 3, 1998**

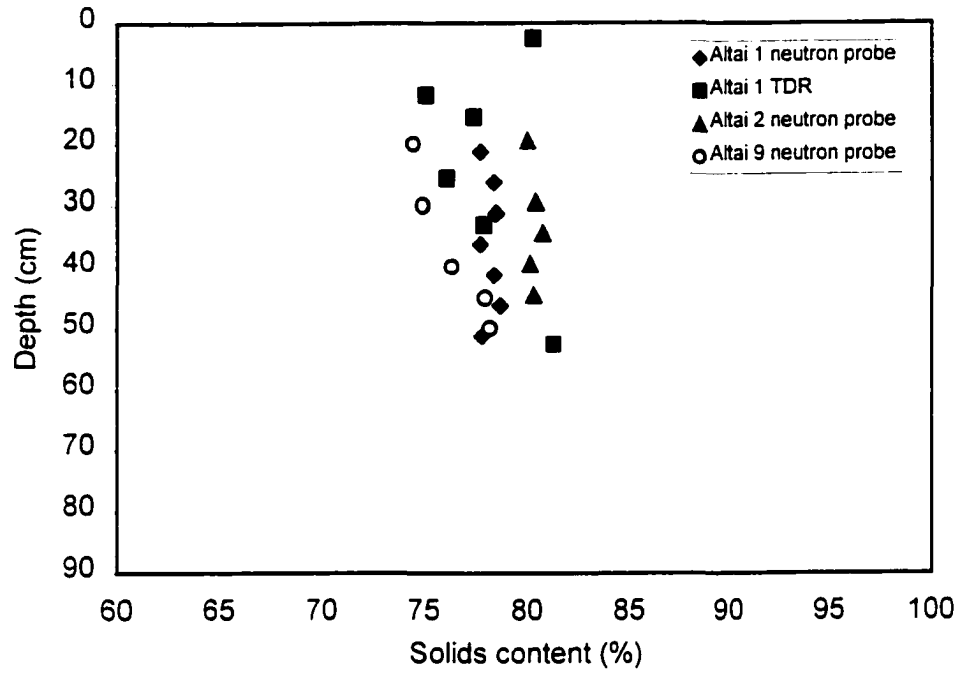


**Figure B.5 Solids content profile of Altai wildrye measured on March 10, 1998**

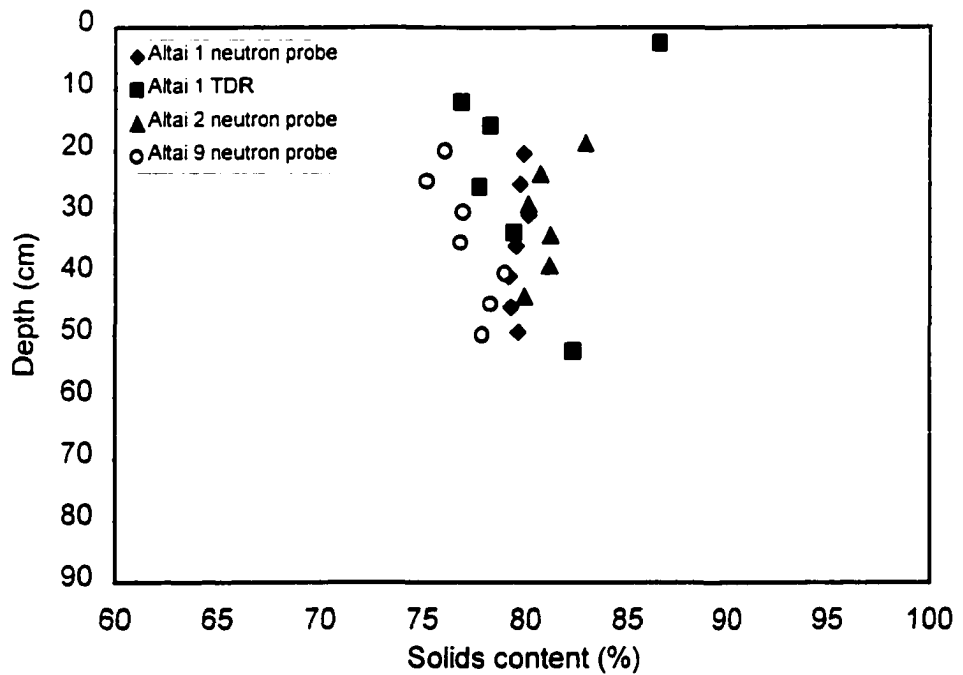


**Figure B.6 Solids content profile of Altai wildrye measured on March 16, 1998**

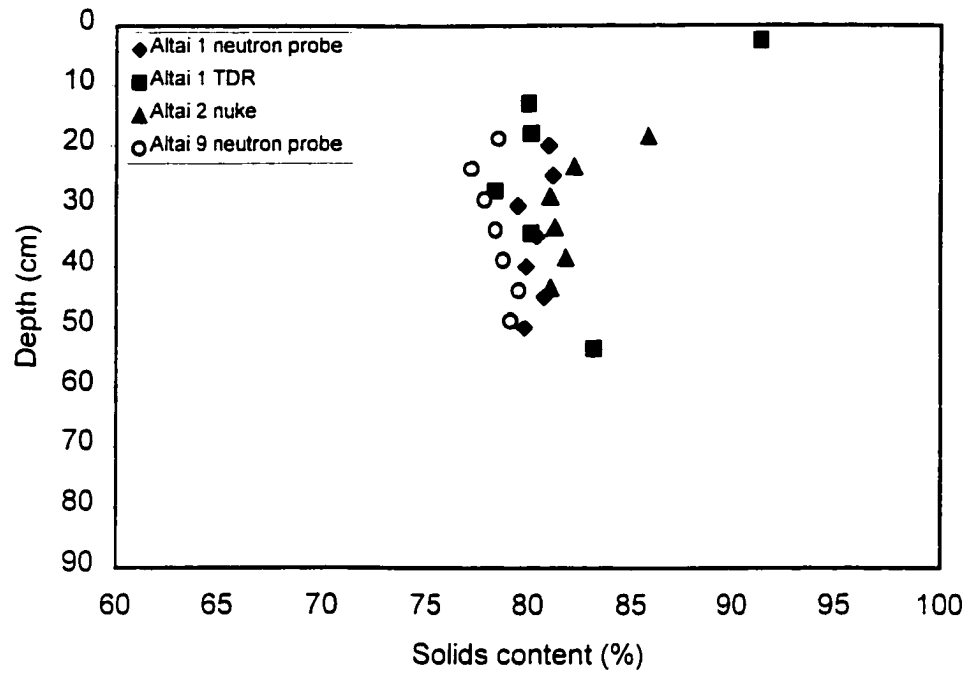


**Figure B.7 Solids content profile of Altai wildrye measured on March 23, 1998**

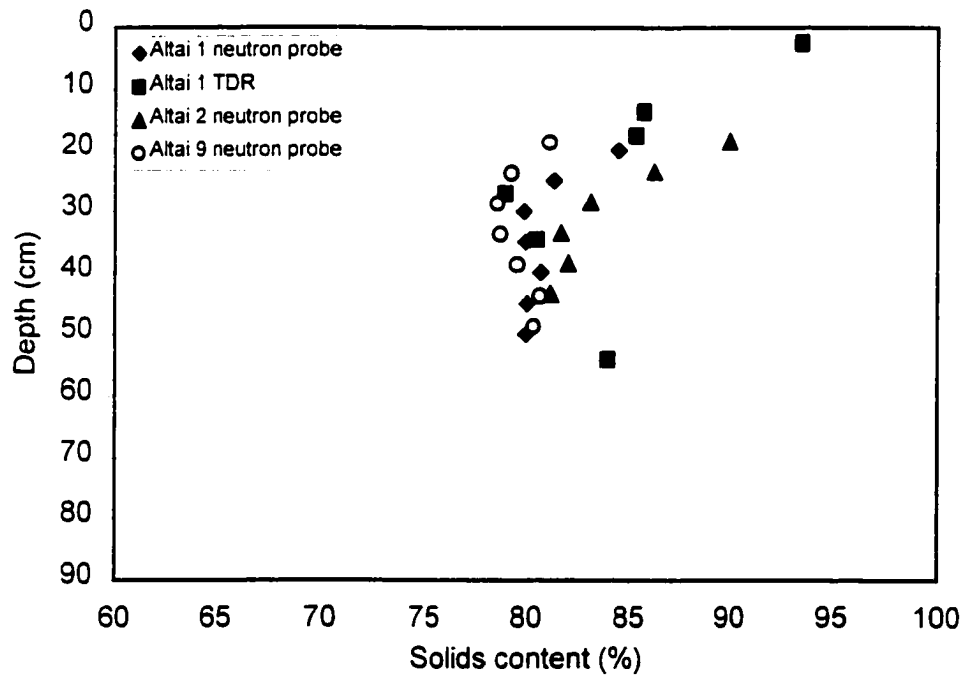


**Figure B.8 Solids content profile of Altai wildrye measured on March 31, 1998**

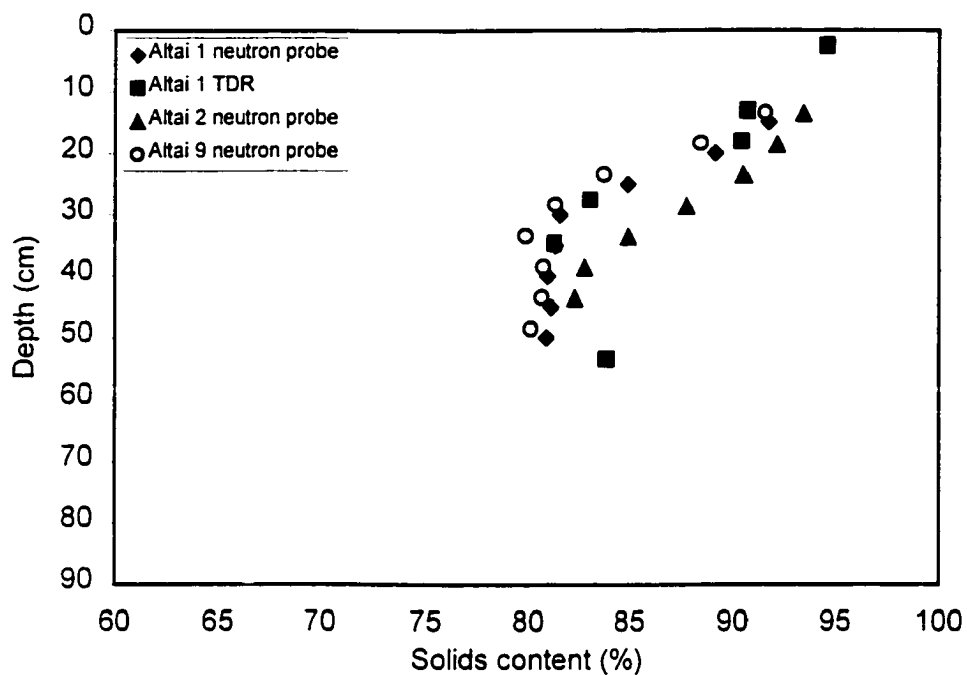


**Figure B.9 Solids content profile of Altai wildrye measured on April 10, 1998**

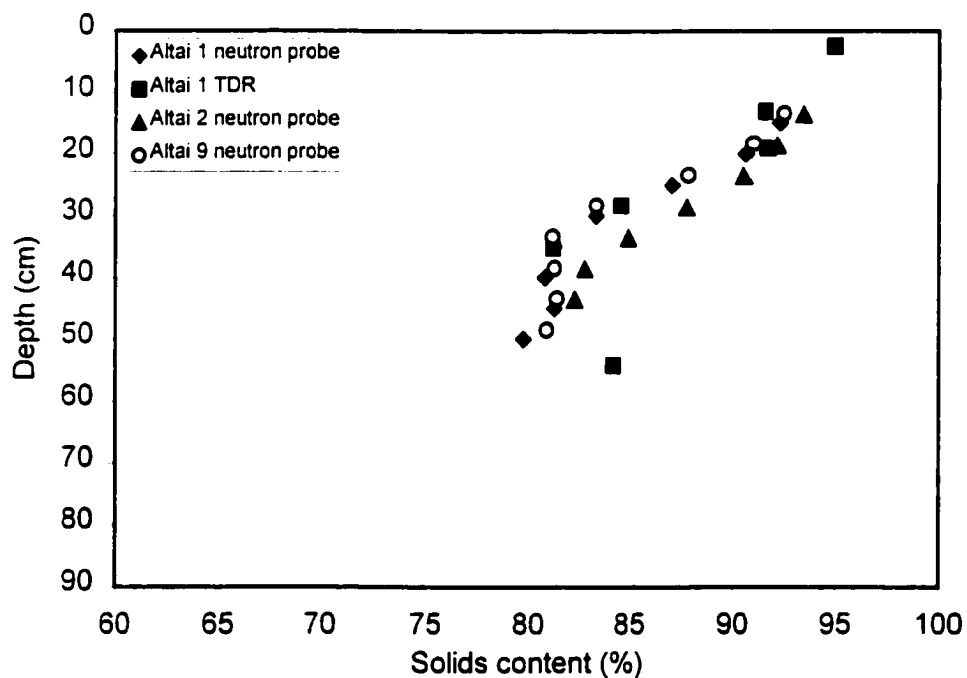


**Figure B.10 Solids content profile of Altai wildrye measured on April 15, 1998**



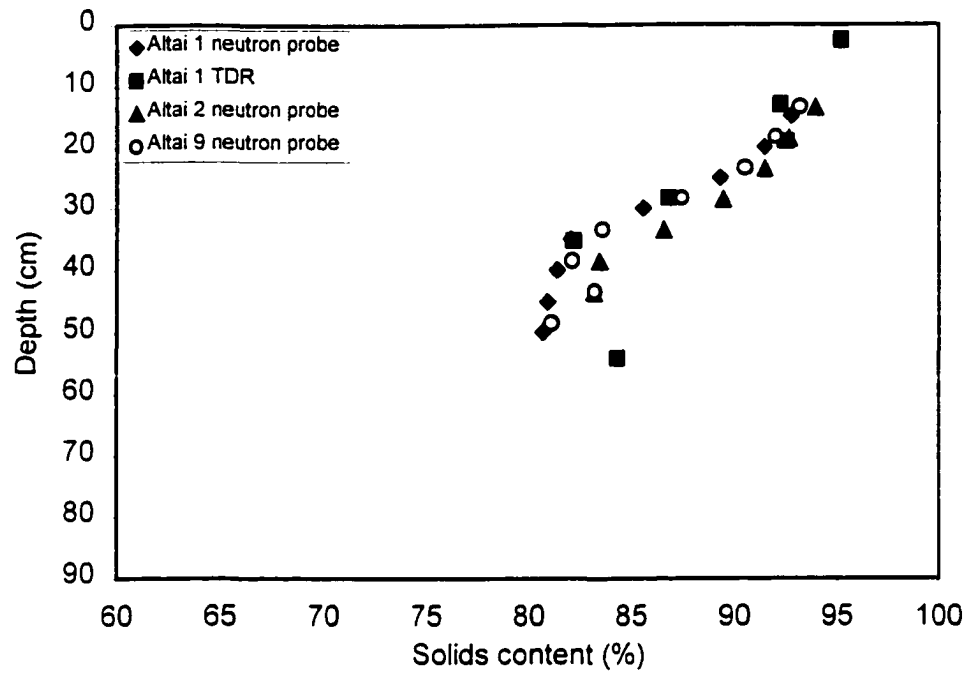


**Figure B.11 Solids content profile of Altai wildrye measured on April 20, 1998**

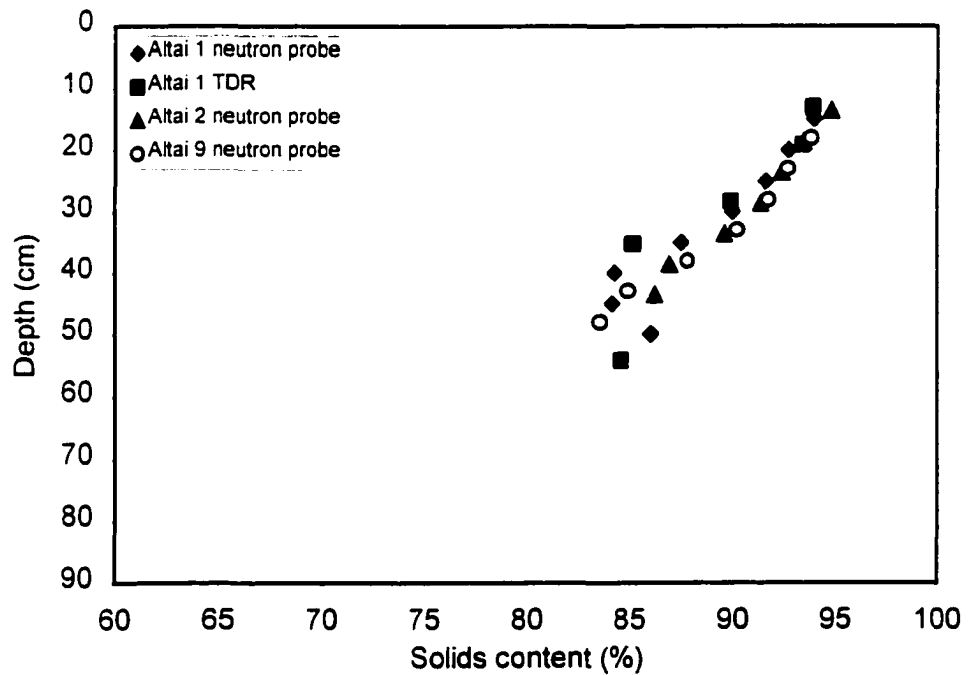


**Figure B.12 Solids content profile of Altai wildrye measured on May 12, 1998**

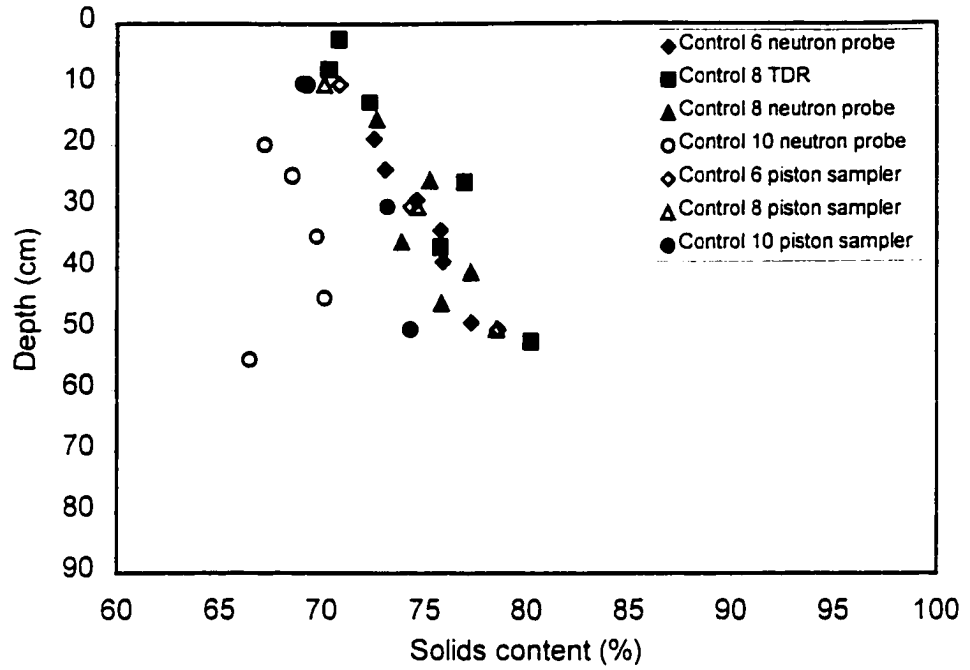


**Figure B.13 Solids content profile of control measured on February 19, 1998**

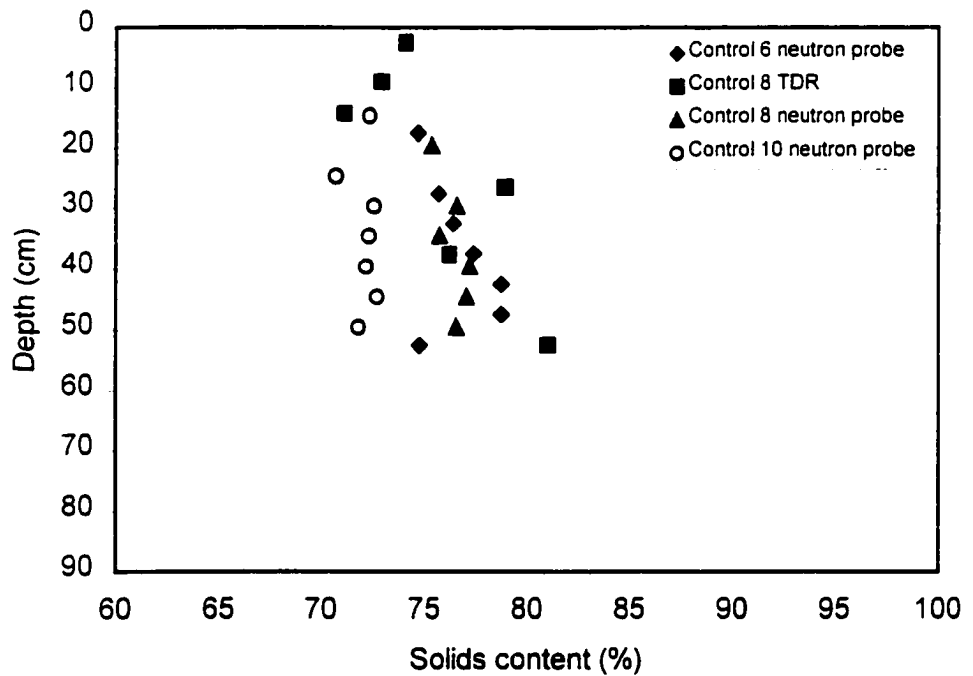


**Figure B.14 Solids content profile of control measured on March 3, 1998**

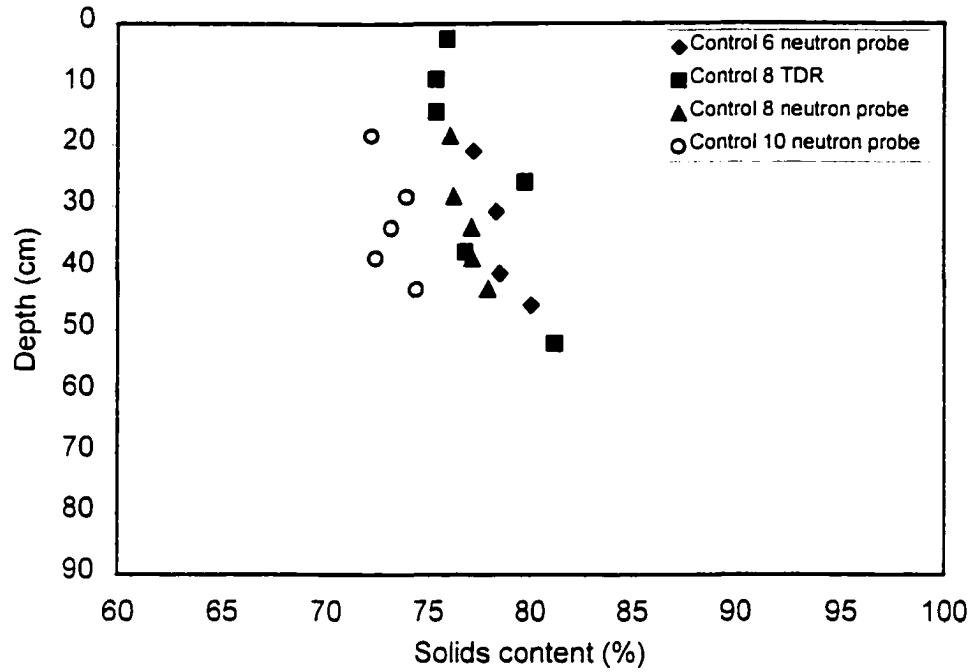


**Figure B.15 Solids content profile of control measured on March 10, 1998**

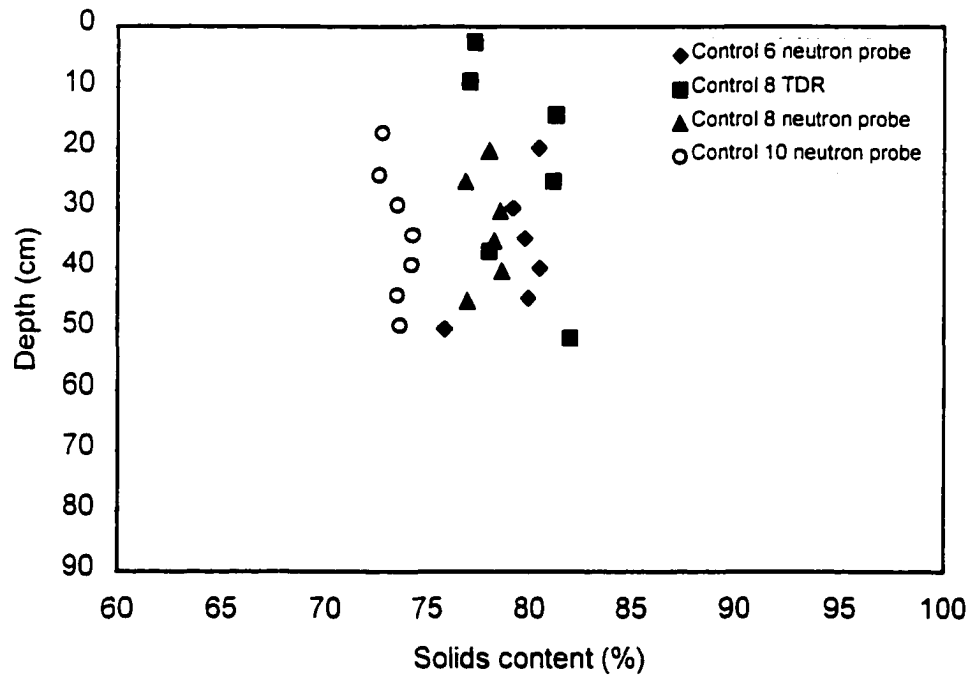


**Figure B.16 Solids content profile of control measured on March 16, 1998**

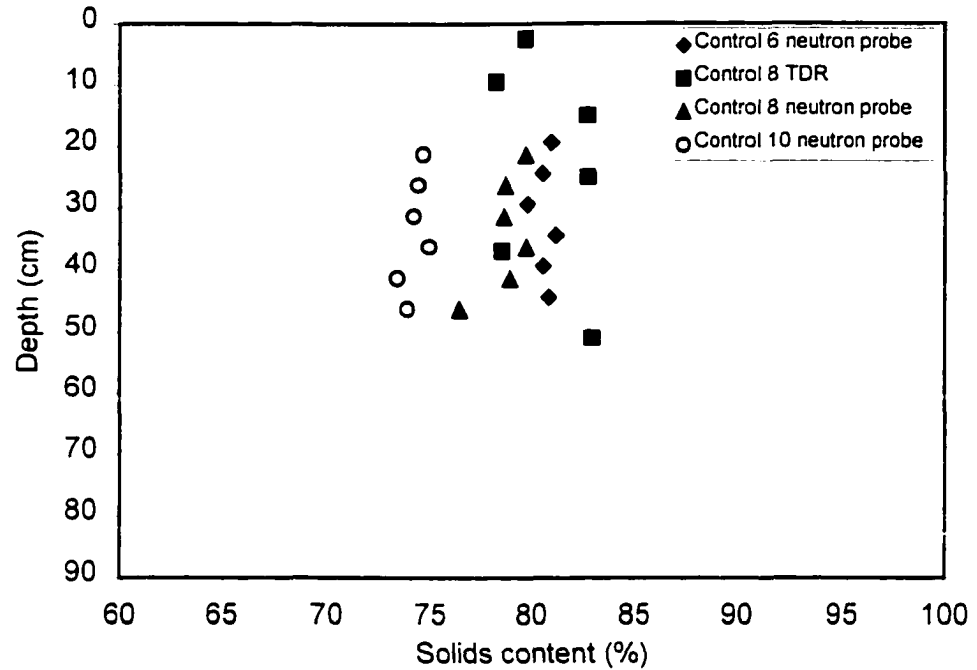


**Figure B.17 Solids content profile of control measured on March 23, 1998**

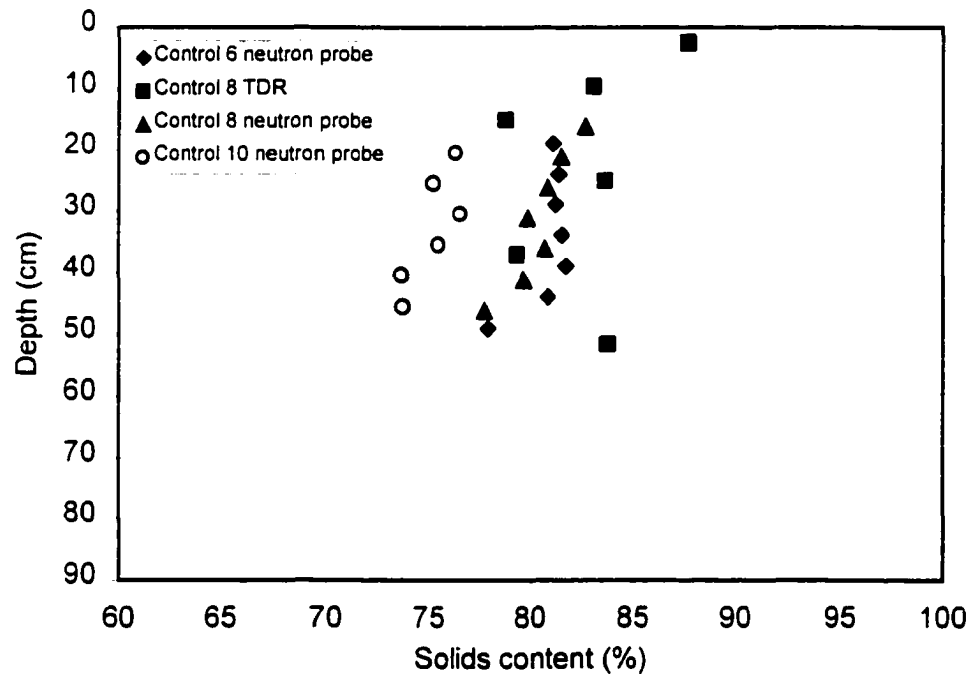


**Figure B.18 Solids content profile of control measured on March 31, 1998**

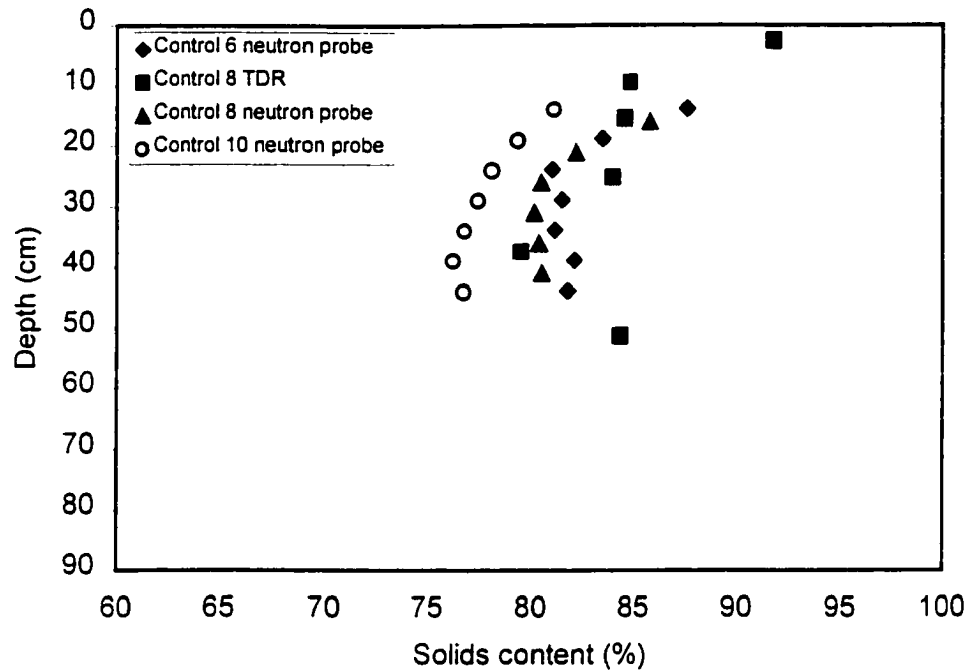


**Figure B.19 Solids content profile of control measured on April 10, 1998**

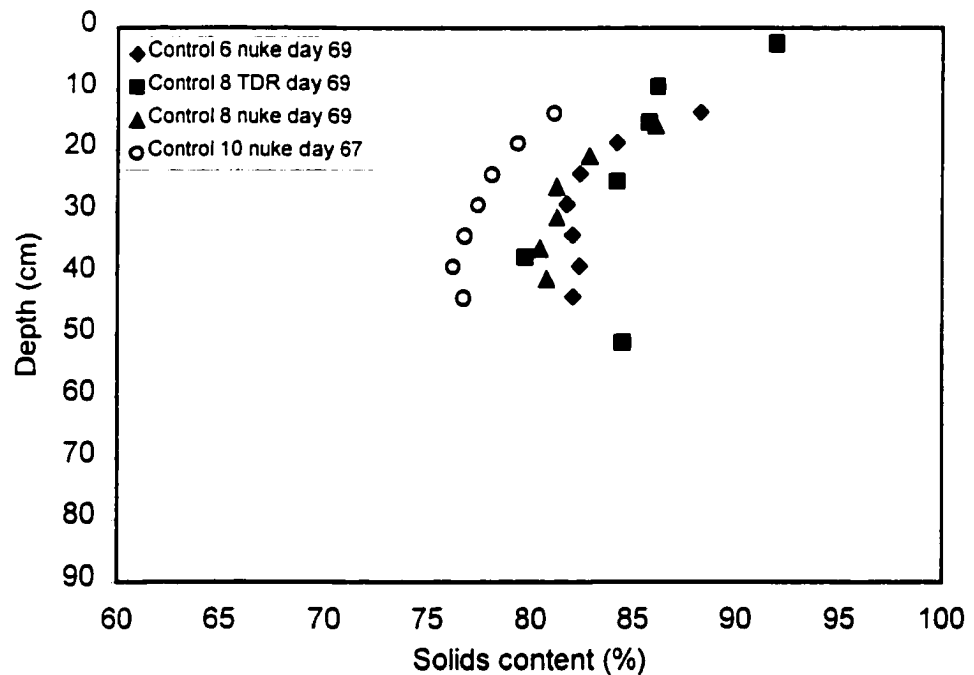


**Figure B.20 Solids content profile of control measured on April 15, 1998**

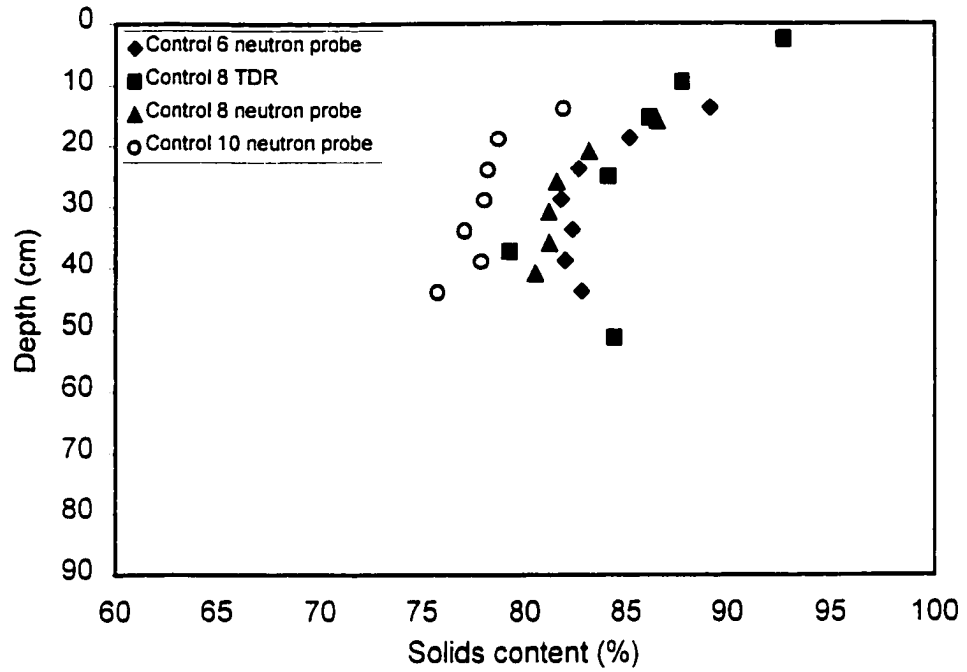


**Figure B.21 Solids content profile of control measured on April 20, 1998**

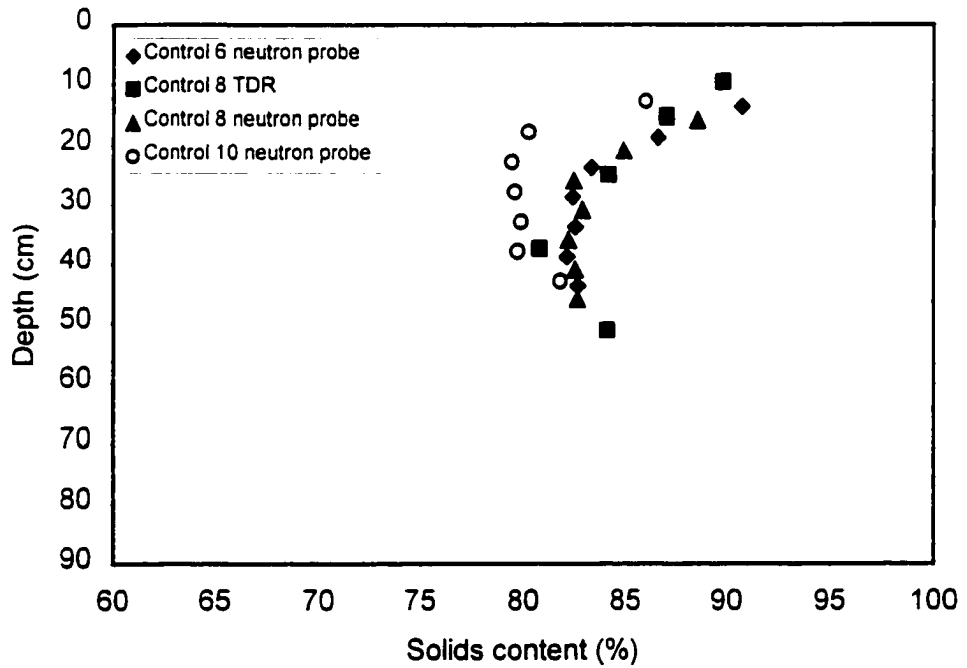


**Figure B.22 Solids content profile of control measured on May 12, 1998**

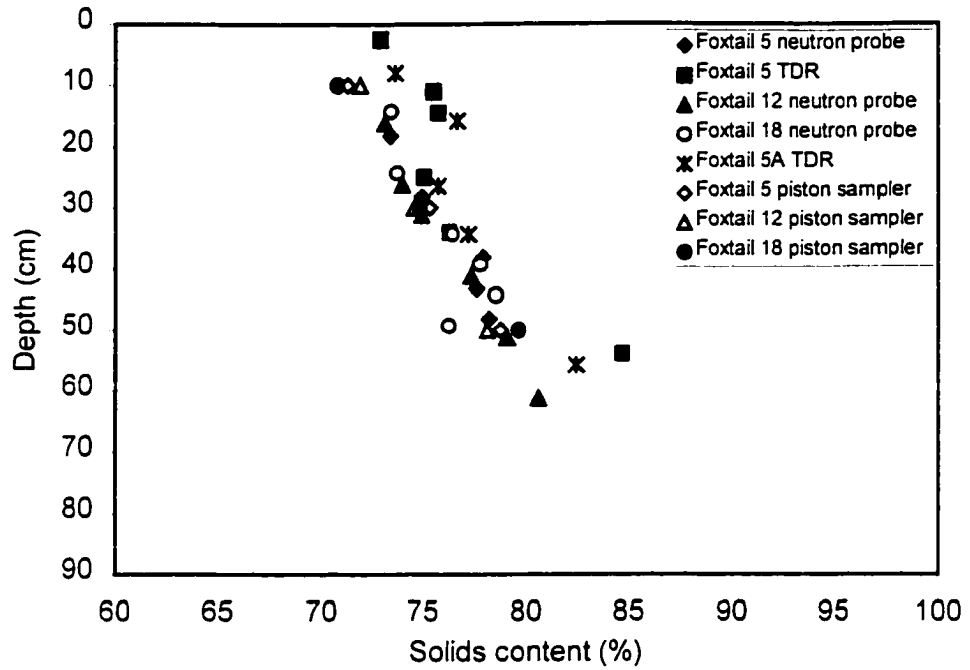


**Figure B.23 Solids content profile of creeping foxtail measured on February 19, 1998**

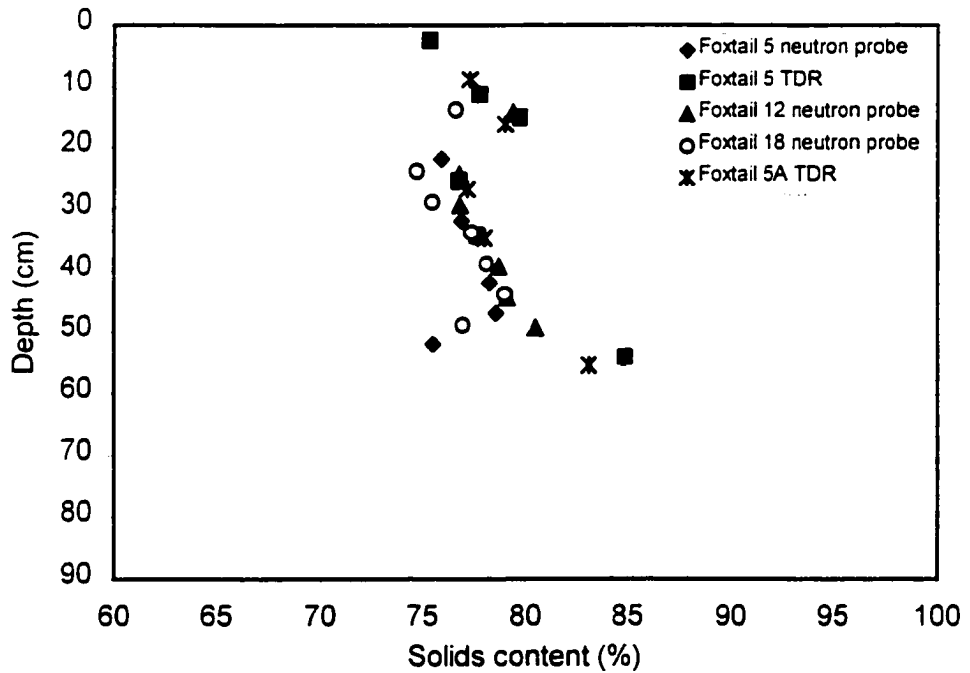


**Figure B.24 Solids content profile of creeping foxtail measured on March 3, 1998**

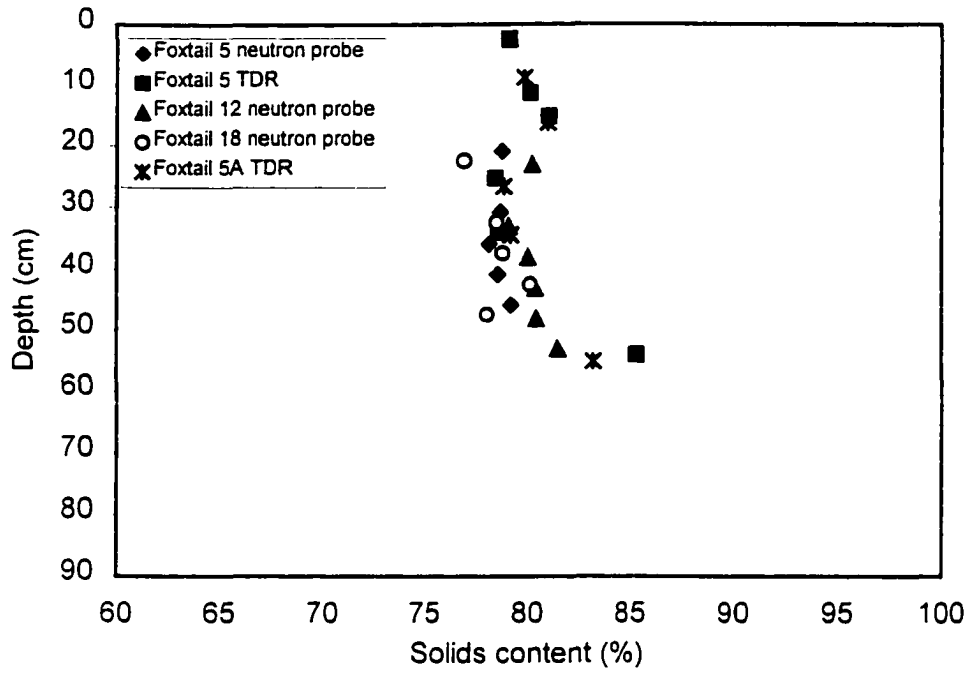


Figure B.25 Solids content profile of creeping foxtail measured on March 10, 1998

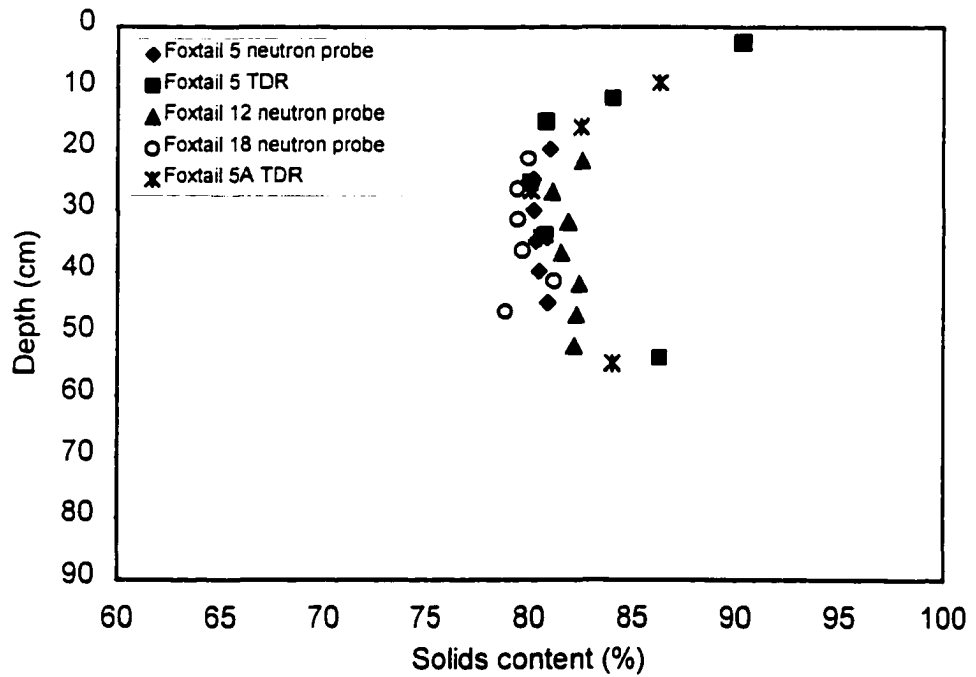
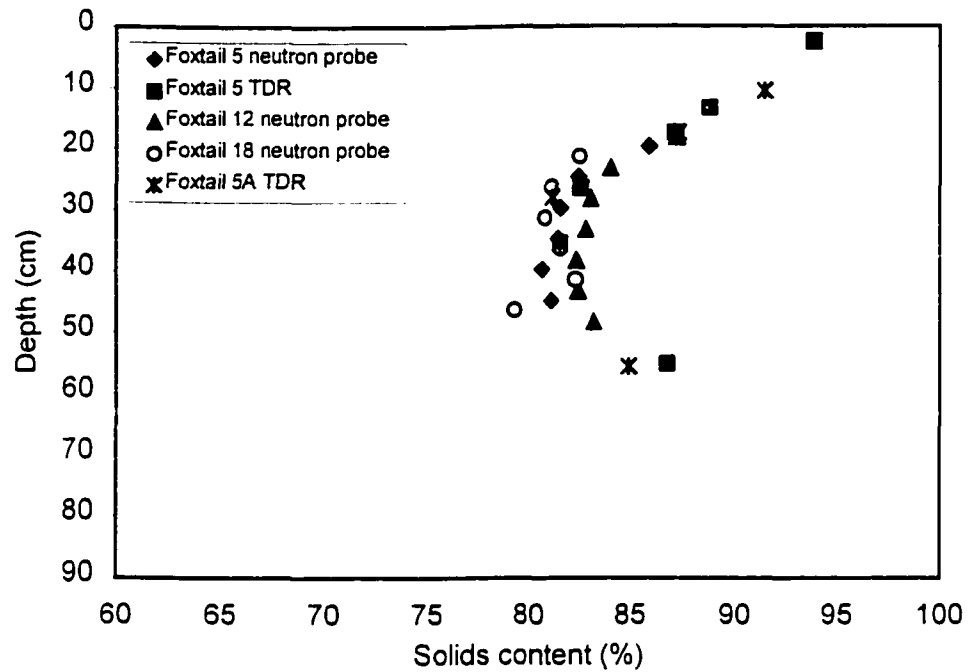
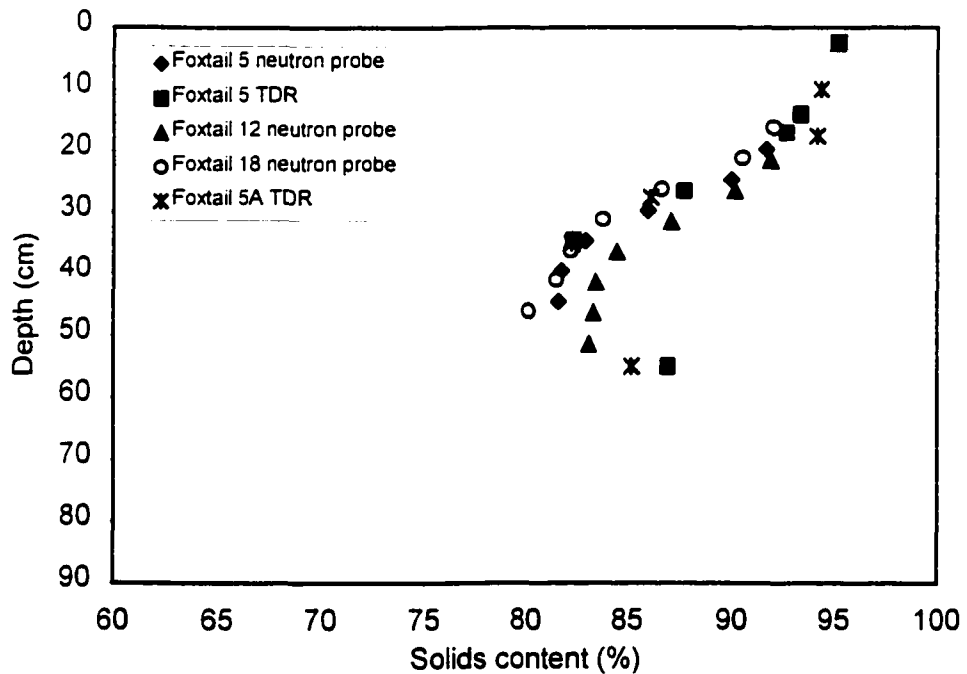


Figure B.26 Solids content profile of creeping foxtail measured on March 16, 1998





**Figure B.27 Solids content profile of creeping foxtail measured on March 23, 1998**



**Figure B.28 Solids content profile of creeping foxtail measured on March 31, 1998**

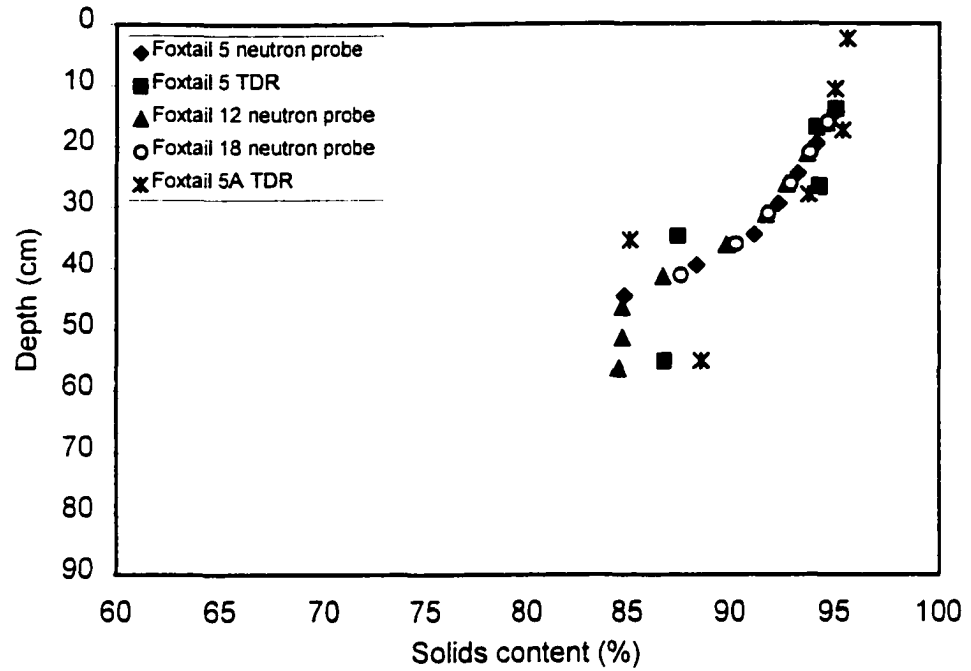


Figure B.29 Solids content profile of creeping foxtail measured on April 10, 1998

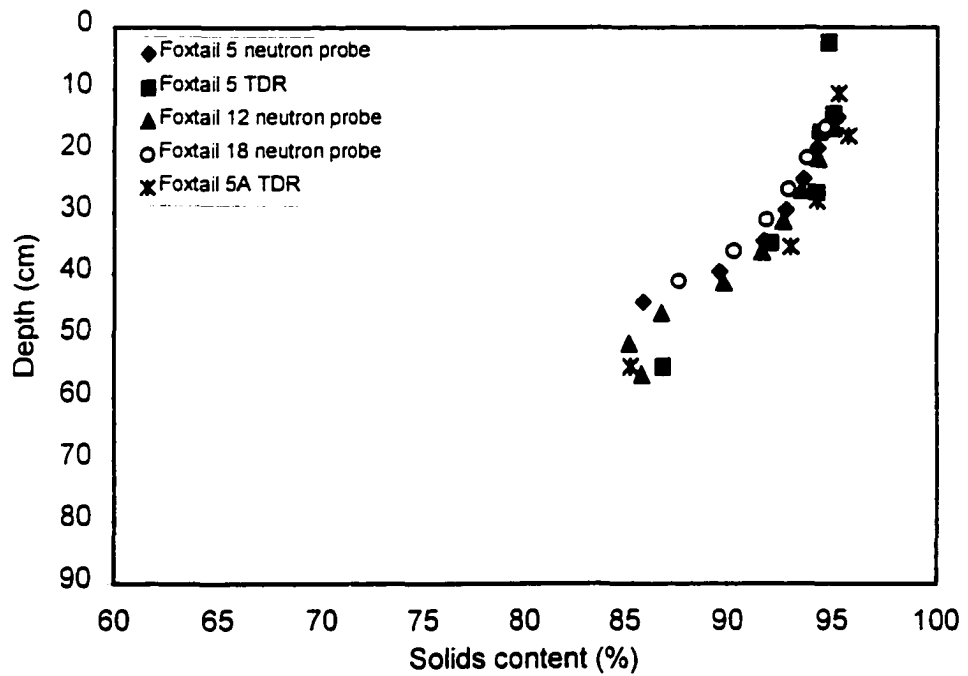


Figure B.30 Solids content profile of creeping foxtail measured on April 15, 1998

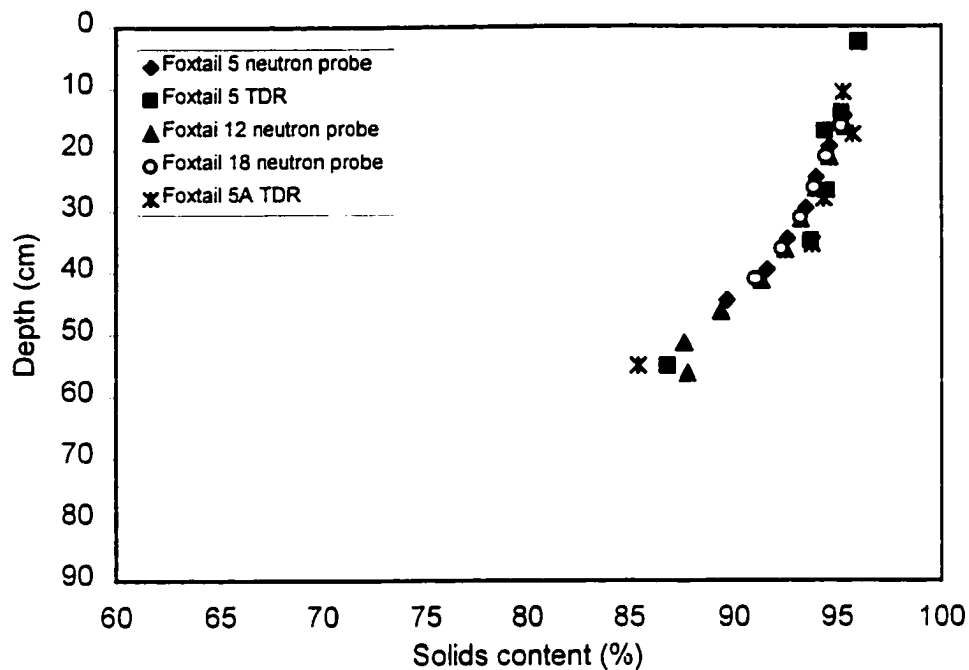


Figure B.31 Solids content profile of creeping foxtail measured on April 20, 1998

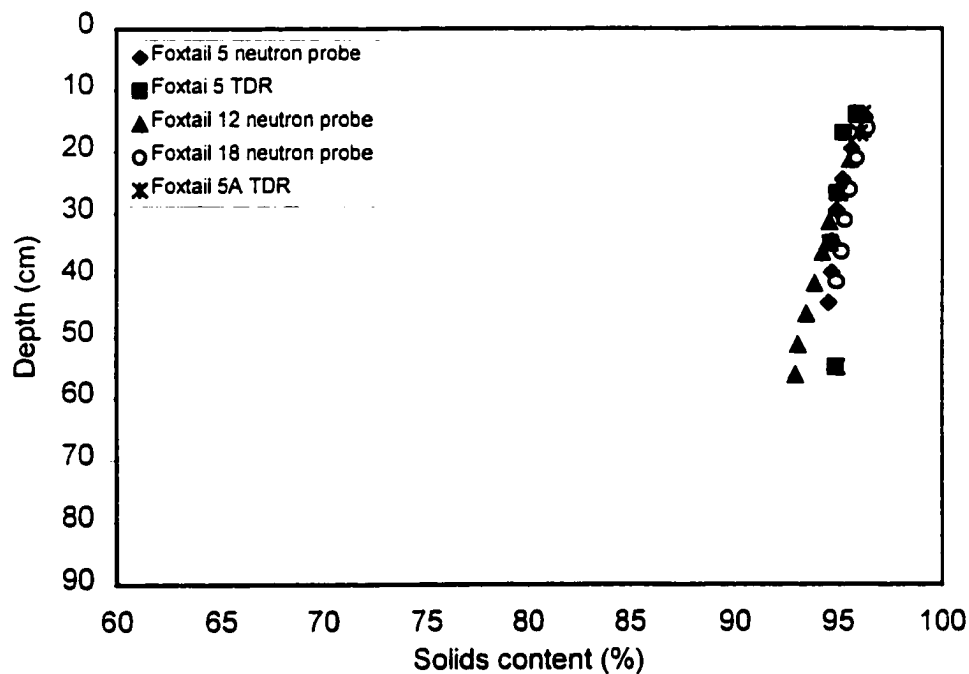


Figure B.32 Solids content profile of creeping foxtail measured on May 12, 1998

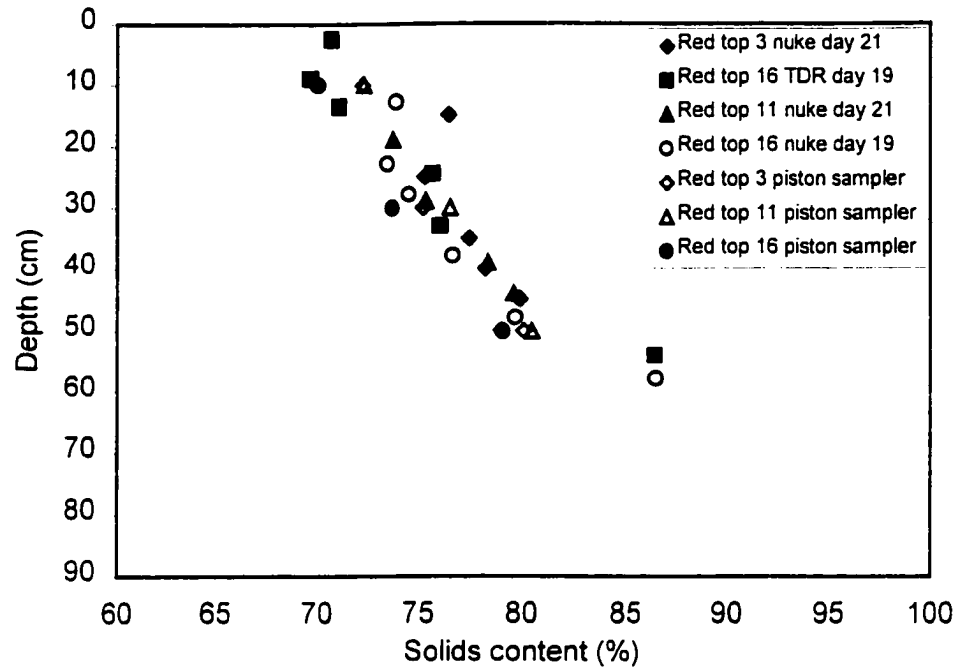


Figure B.33 Solids content profile of red top measured on February 19, 1998

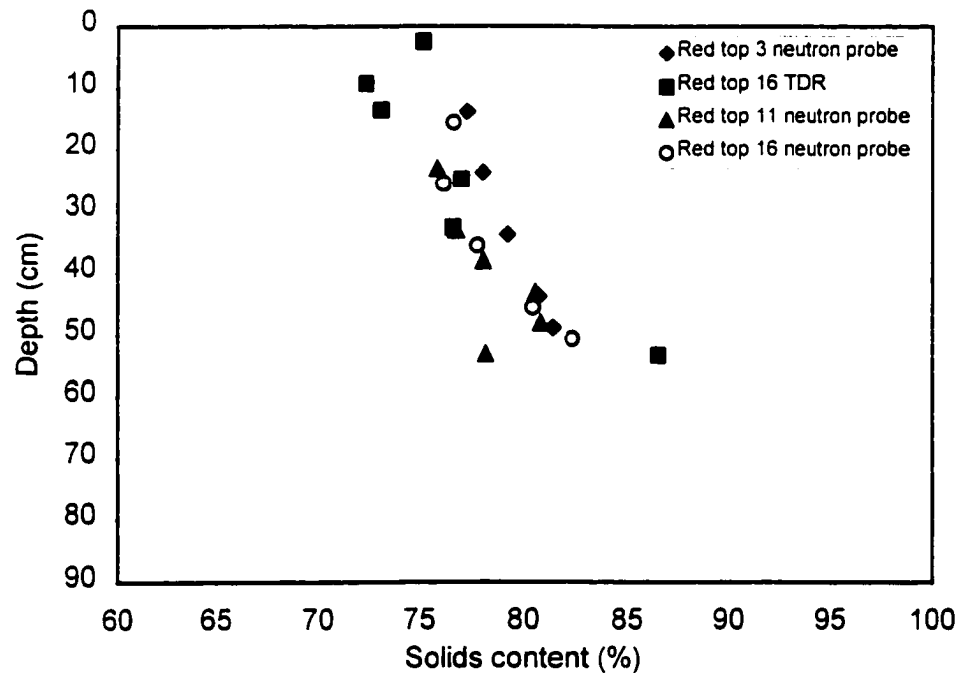


Figure B.34 Solids content profile of red top measured on March 3, 1998

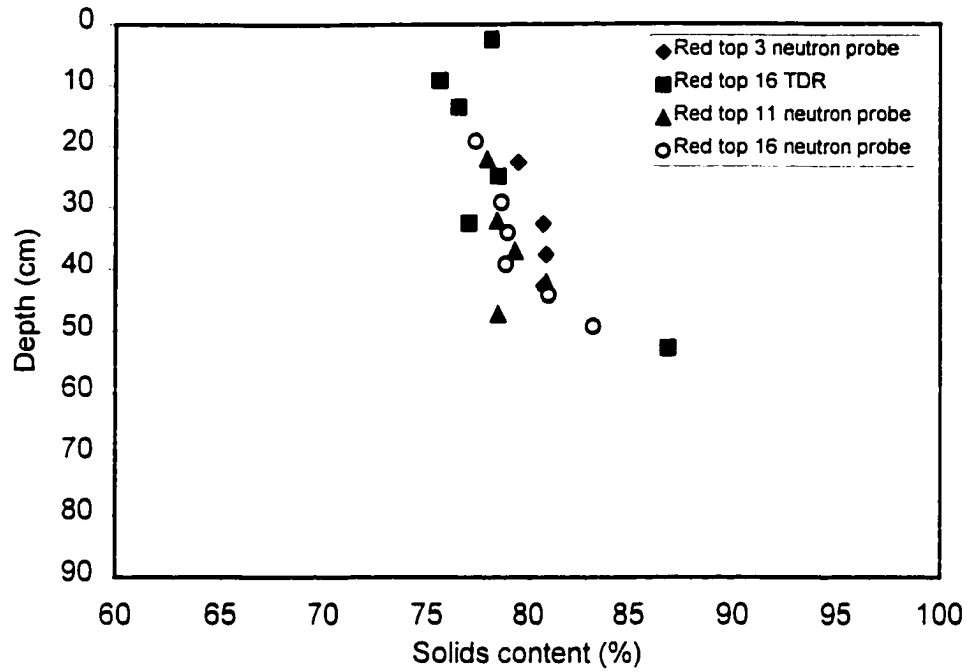


Figure B.35 Solids content profile of red top measured on March 10, 1998

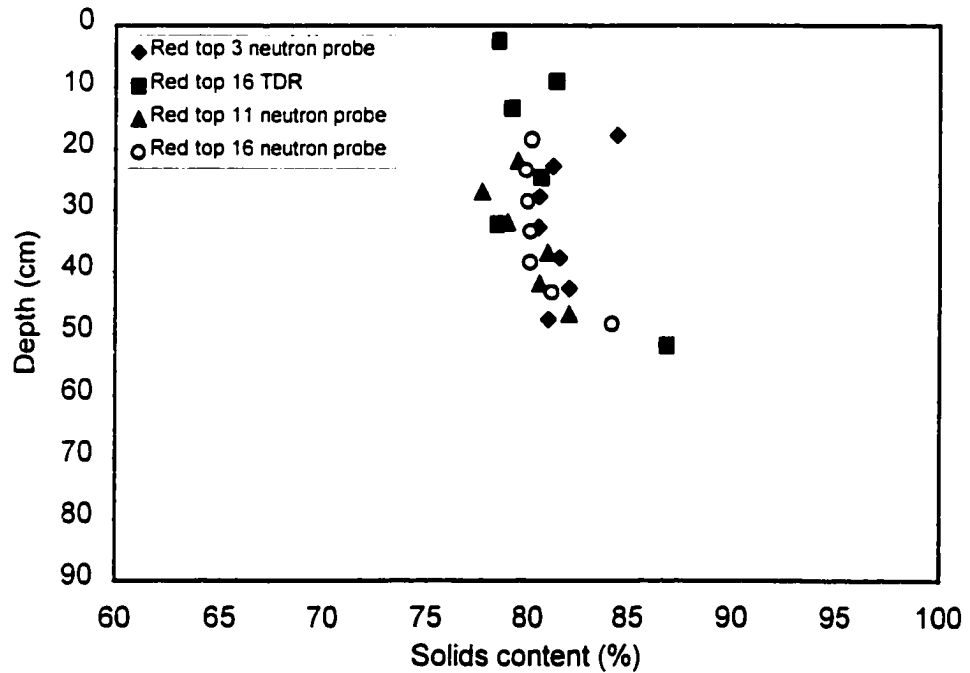
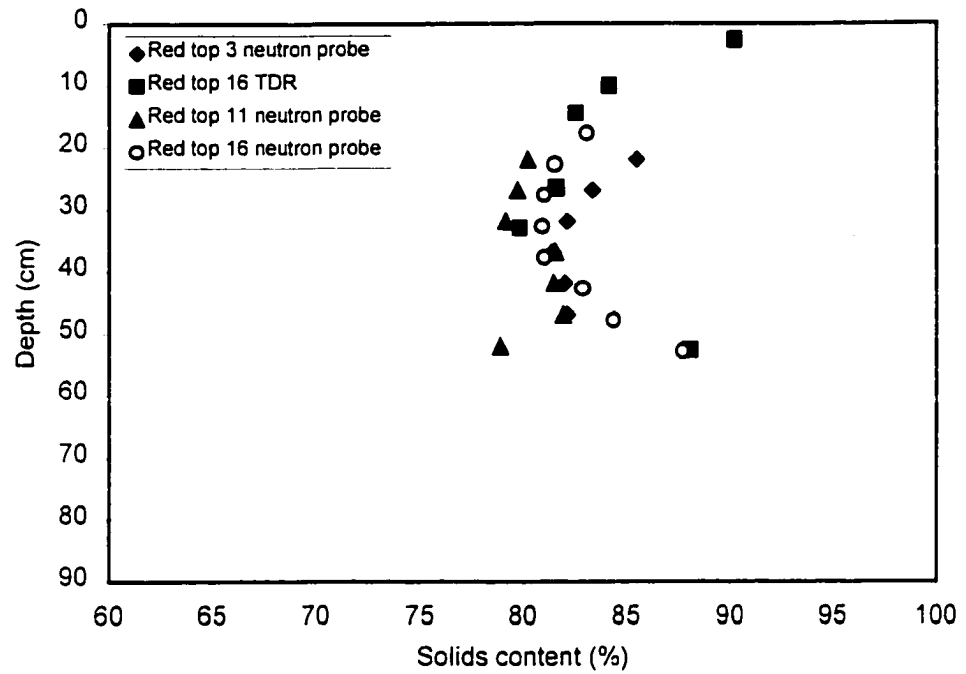
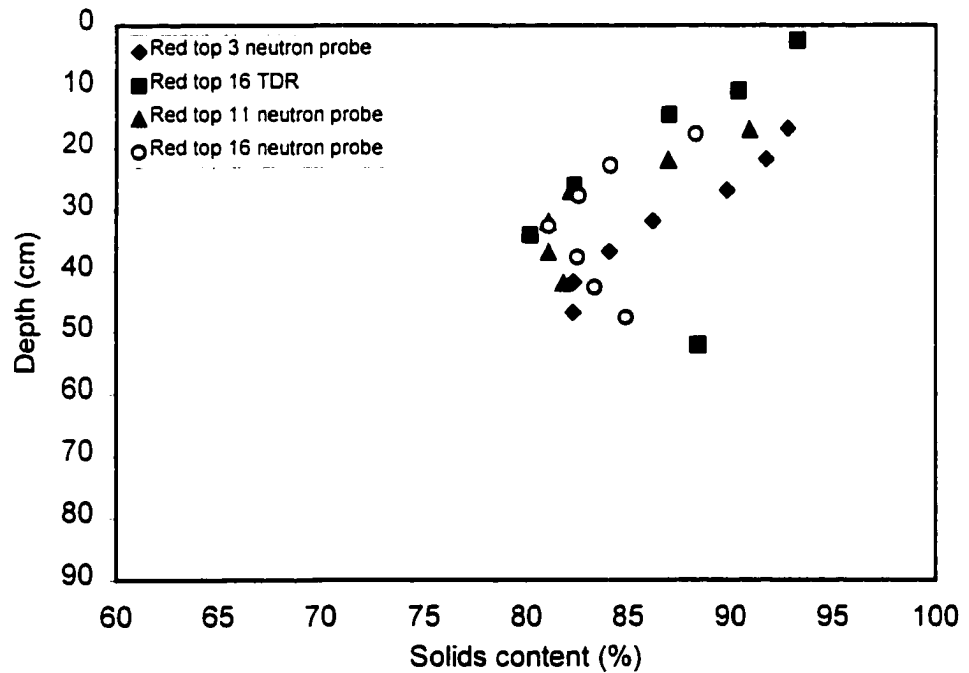


Figure B.36 Solids content profile of red top measured on March 16, 1998



**Figure B.37 Solids content profile of red top measured on March 23, 1998**



**Figure B.38 Solids content profile of red top measured on March 31, 1998**

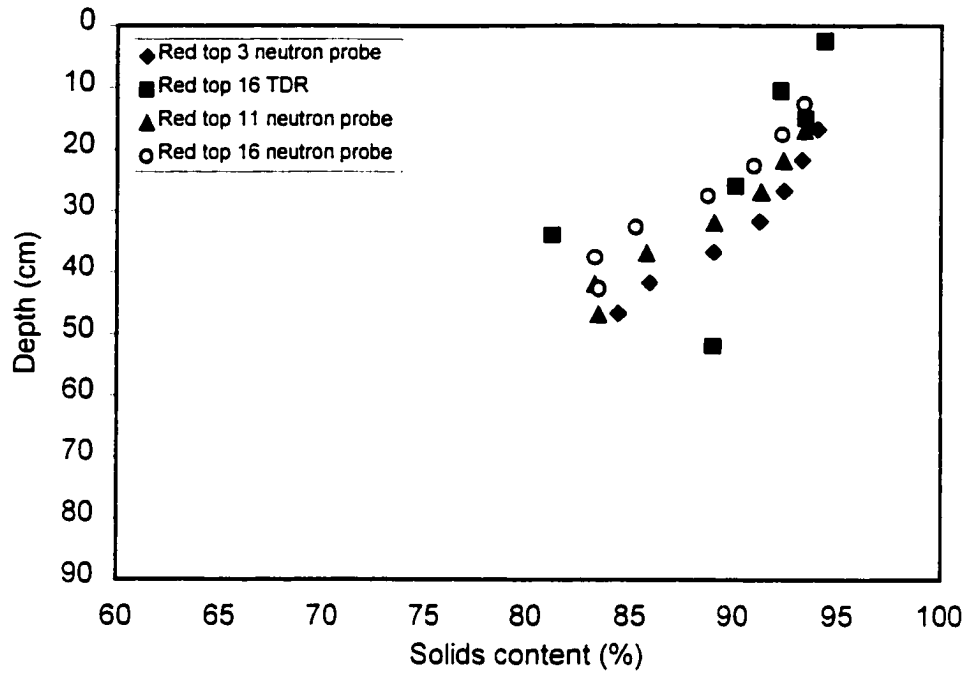


Figure B.39 Solids content profile of red top measured on April 10, 1998

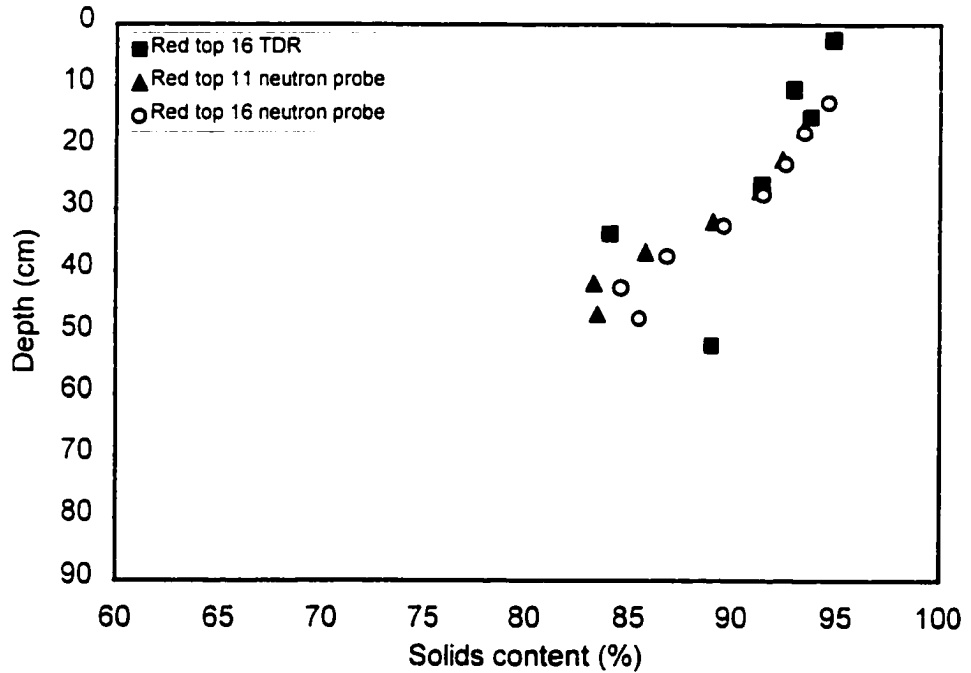
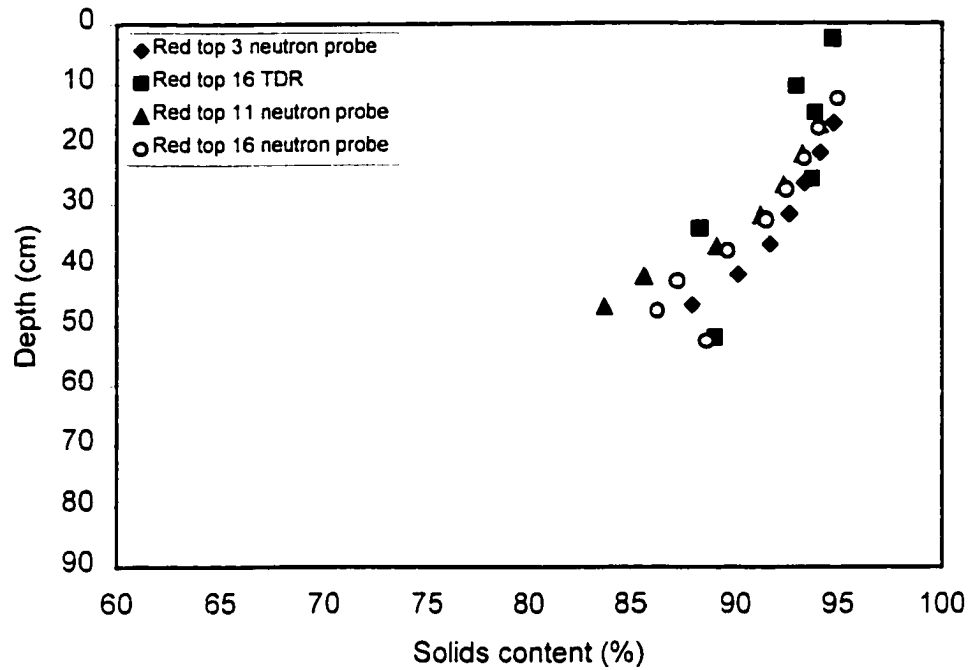
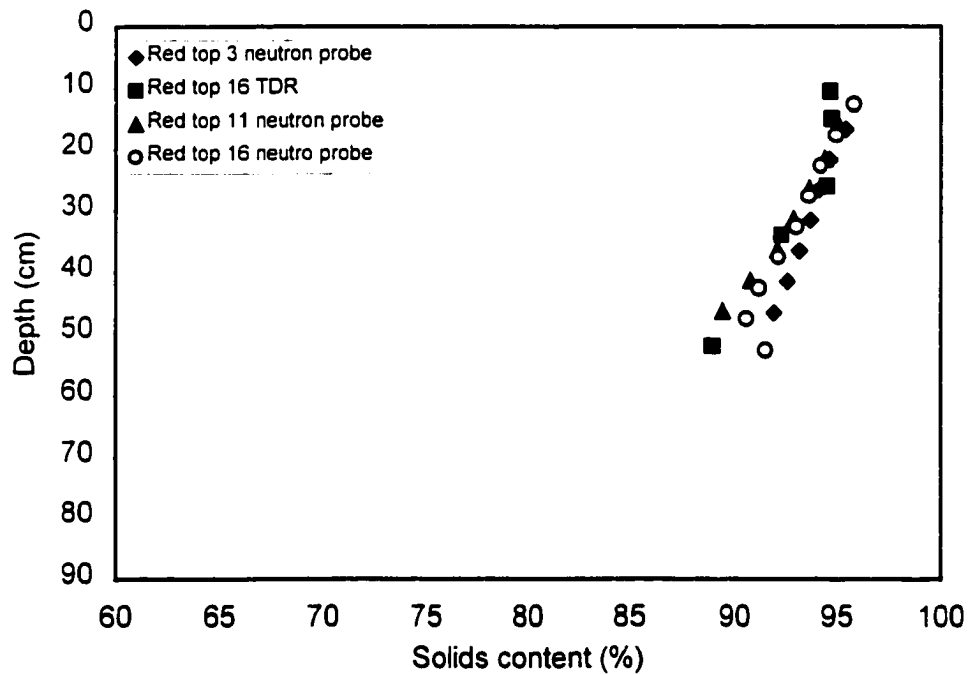


Figure B.40 Solids content profile of red top measured on April 15, 1998



**Figure B.41 Solids content profile of red top measured on April 20, 1998**



**Figure B.42 Solids content profile of red top measured on May 12, 1998**



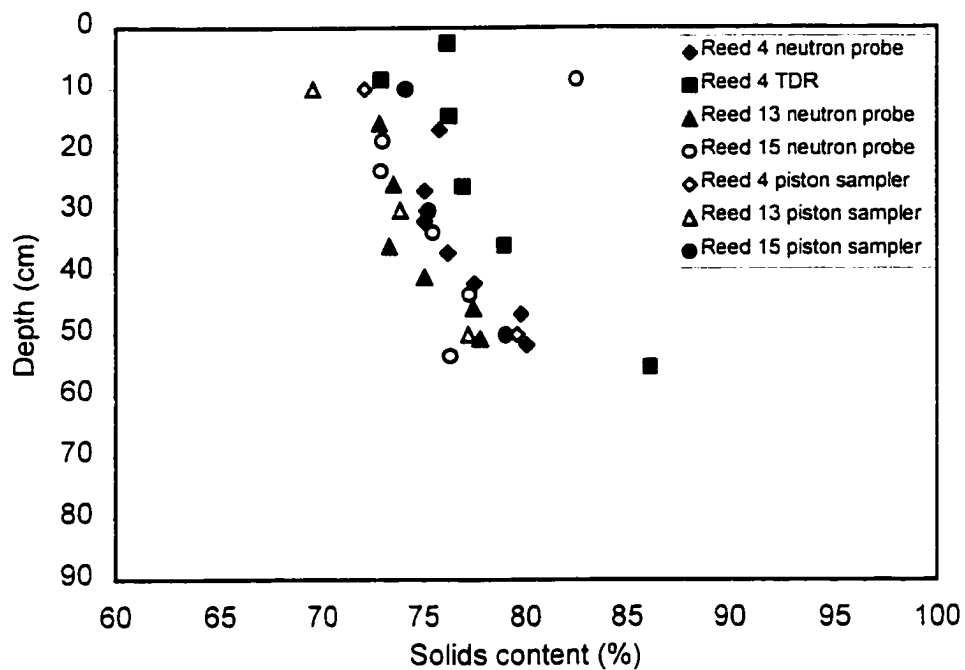


**Figure B.43 Solids content profile of reed canarygrass measured on February 19, 1998**

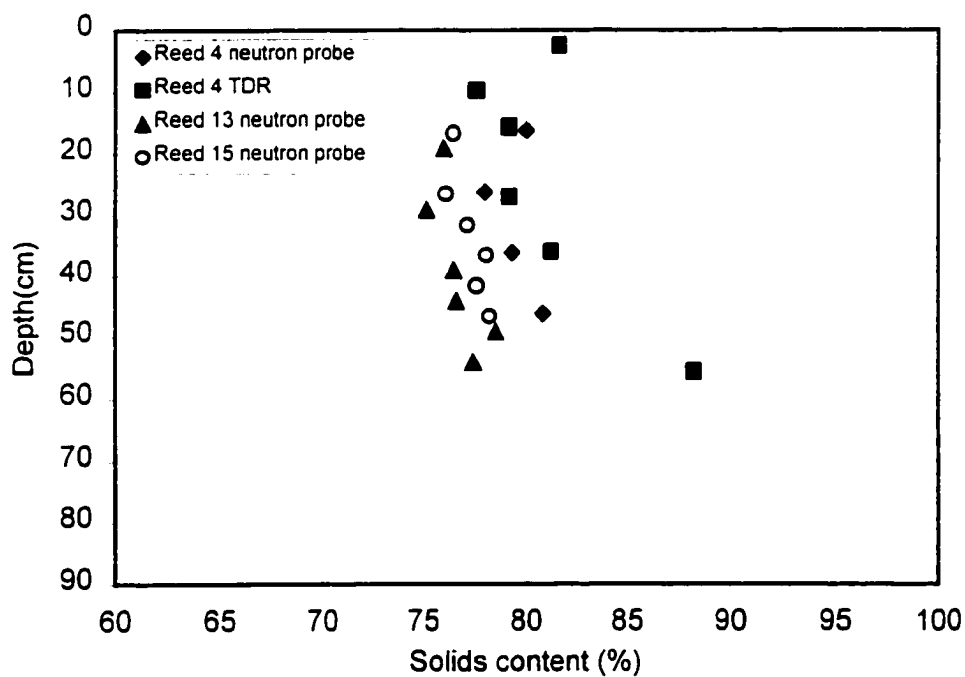


**Figure B.44 Solids content profile of reed canarygrass measured on March 3, 1998**

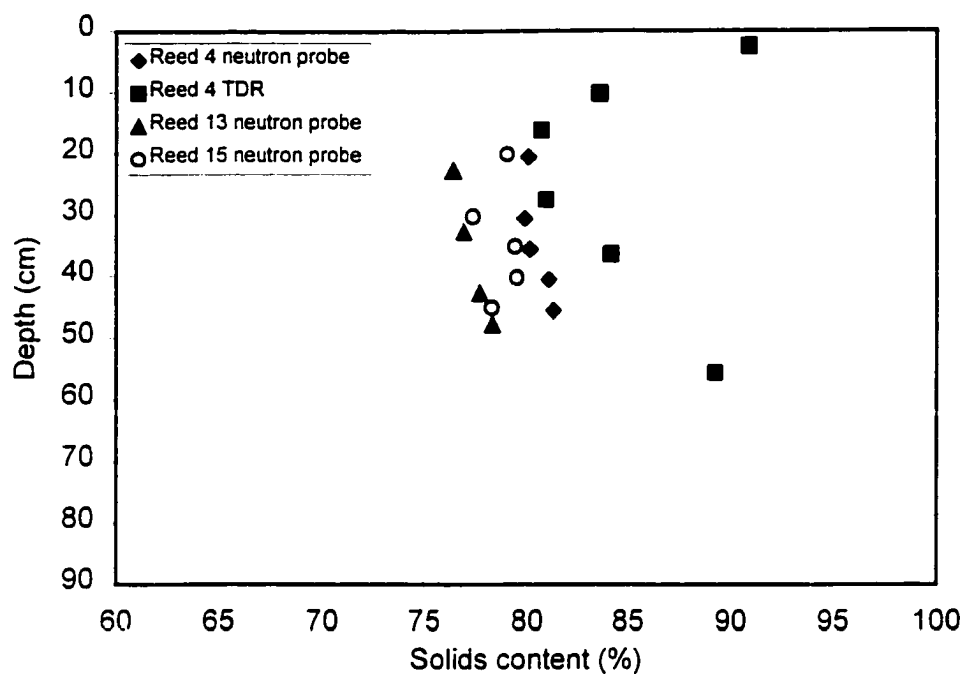


Figure B.45 Solids content profile of reed canarygrass measured on March 10, 1998

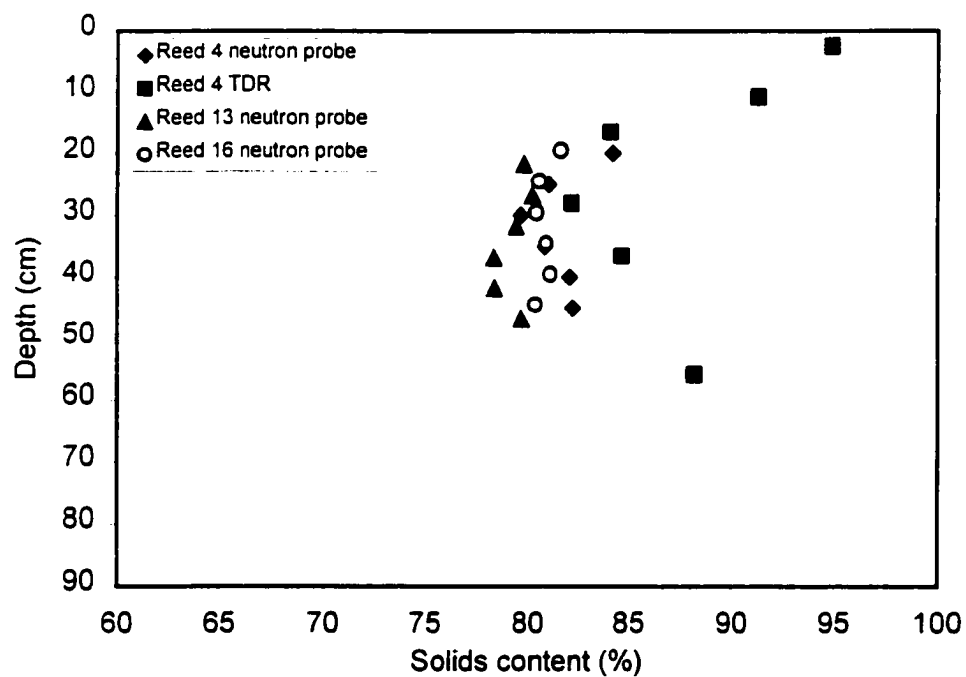
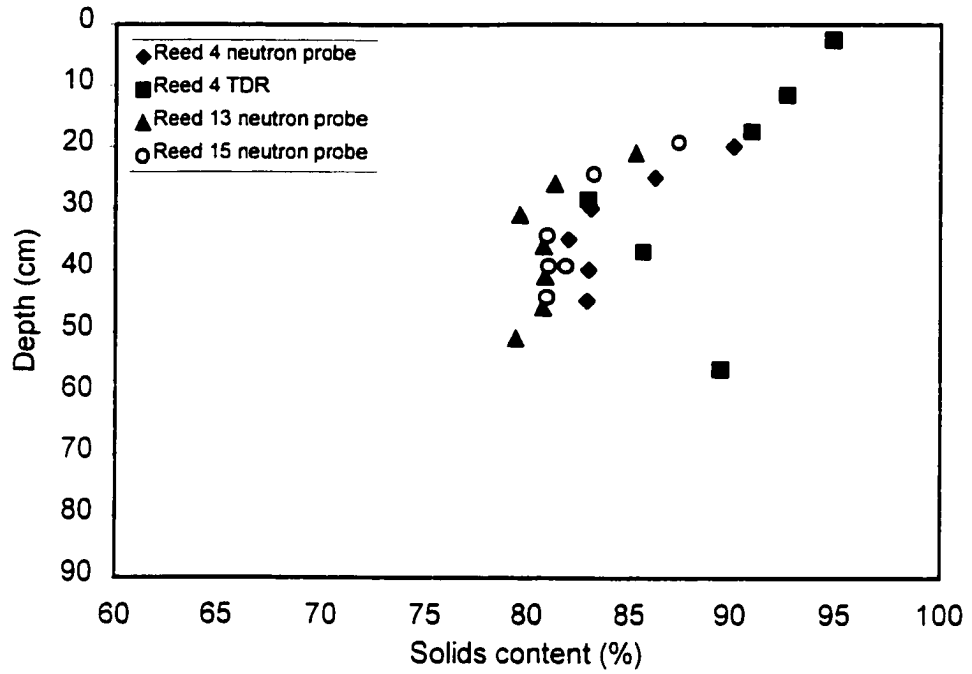
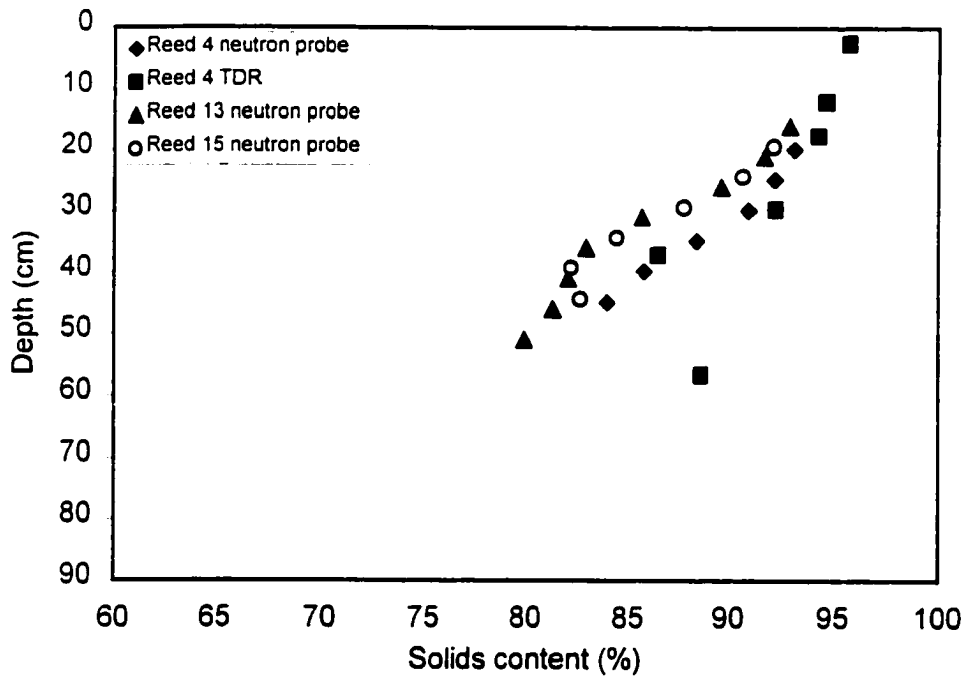


Figure B.46 Solids content profile of reed canarygrass measured on March 16, 1998



**Figure B.47 Solids content profile of reed canarygrass measured on March 23, 1998**



**Figure B.48 Solids content profile of reed canarygrass measured on March 31, 1998**

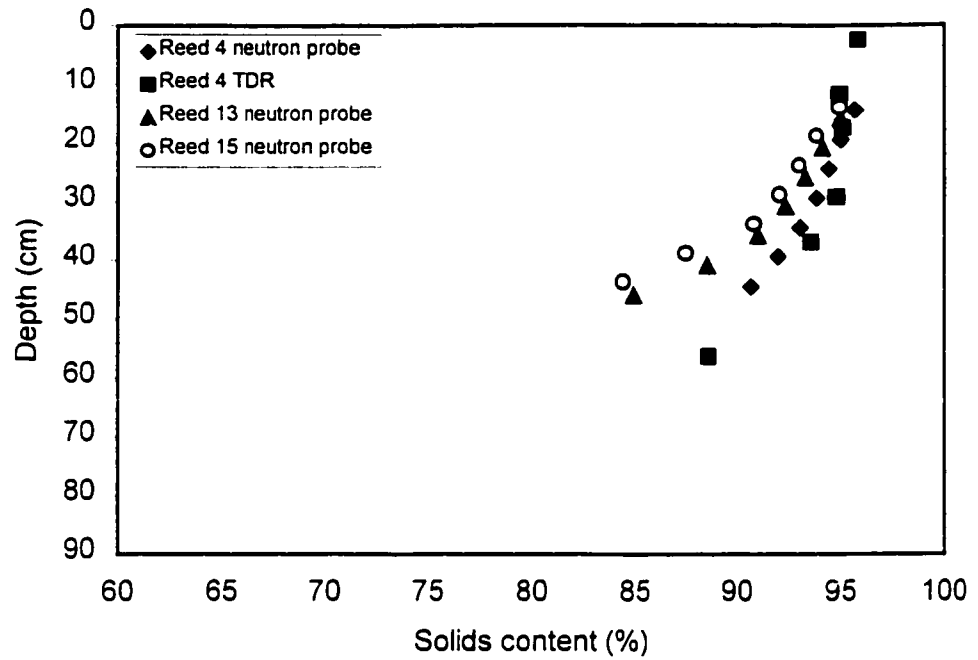


**Figure B.49 Solids content profile of reed canarygrass measured on April 10, 1998**

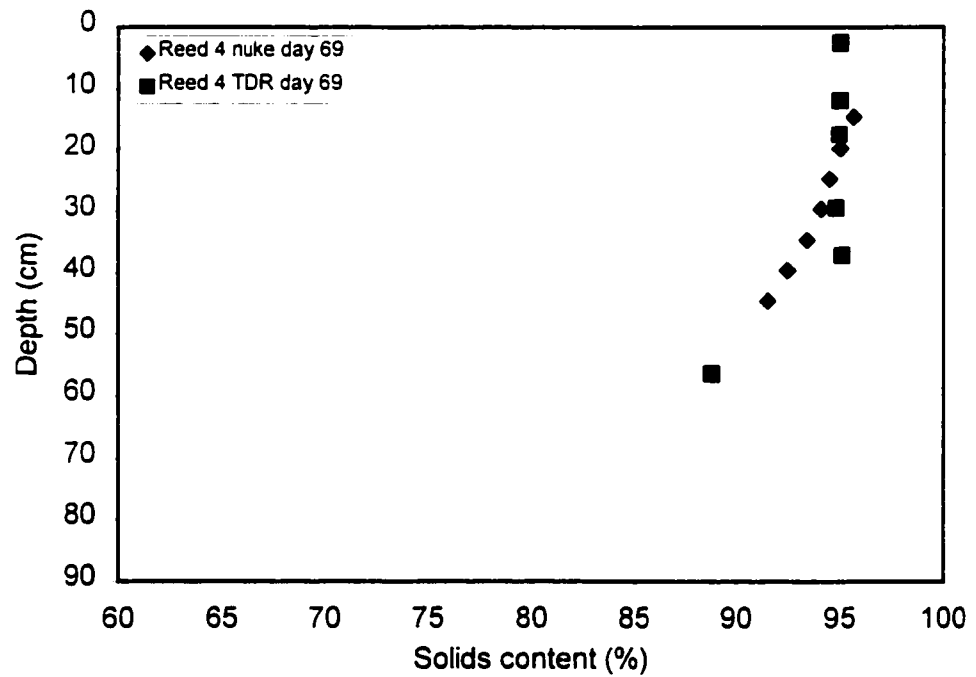


**Figure B.50 Solids content profile of reed canarygrass measured on April 15, 1998**

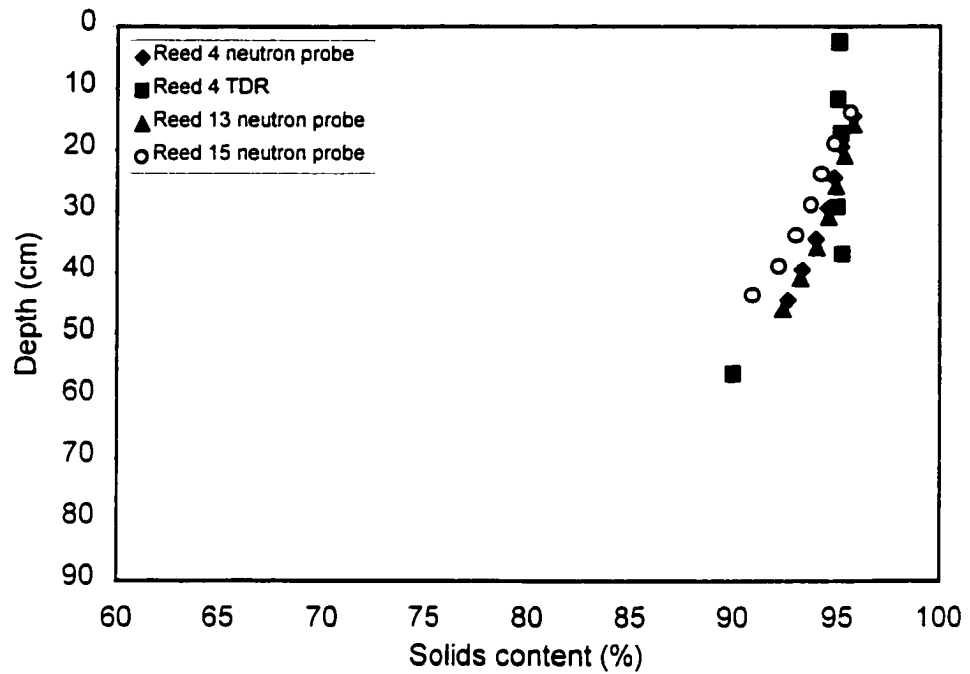


**Figure B.51 Solids content profile of reed canarygrass measured on April 20, 1998**

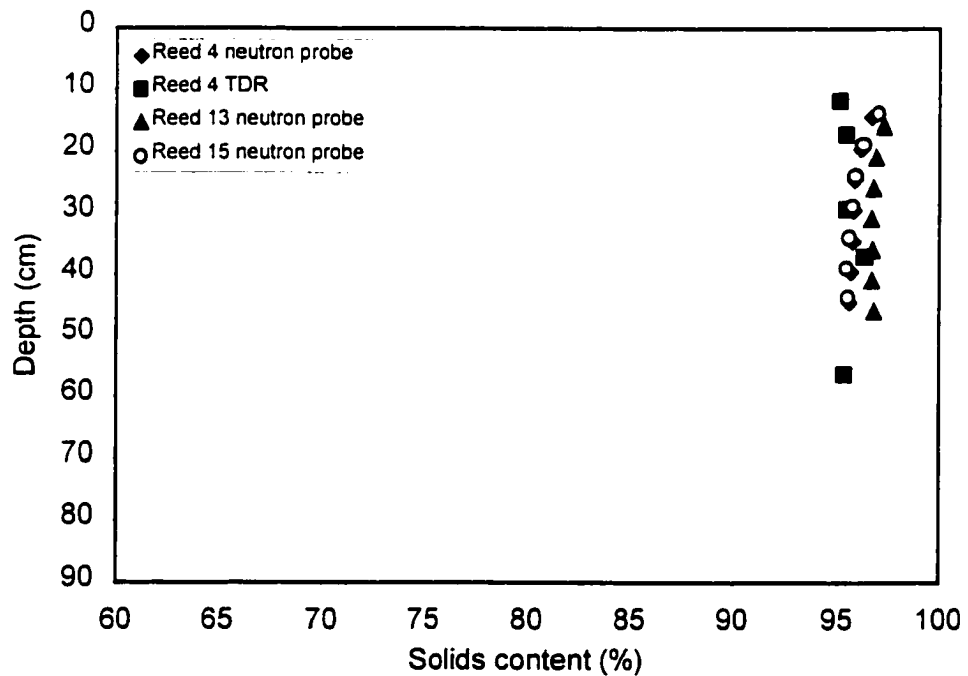


**Figure B.52 Solids content profile of reed canarygrass measured on May 12, 1998**

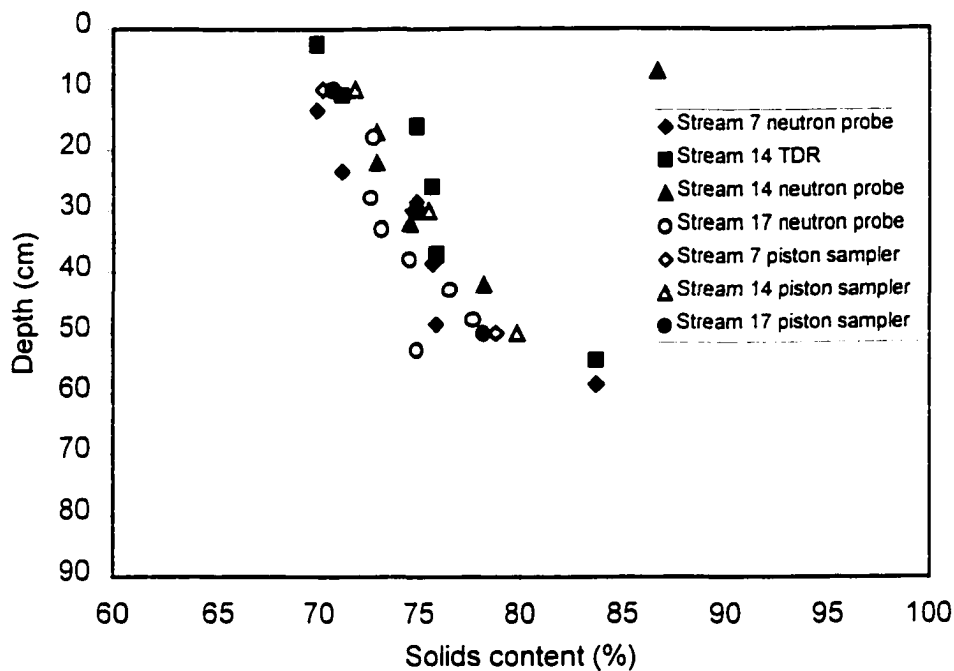


Figure B.53 Solids content profile of streambank wheatgrass measured on February 19, 1998

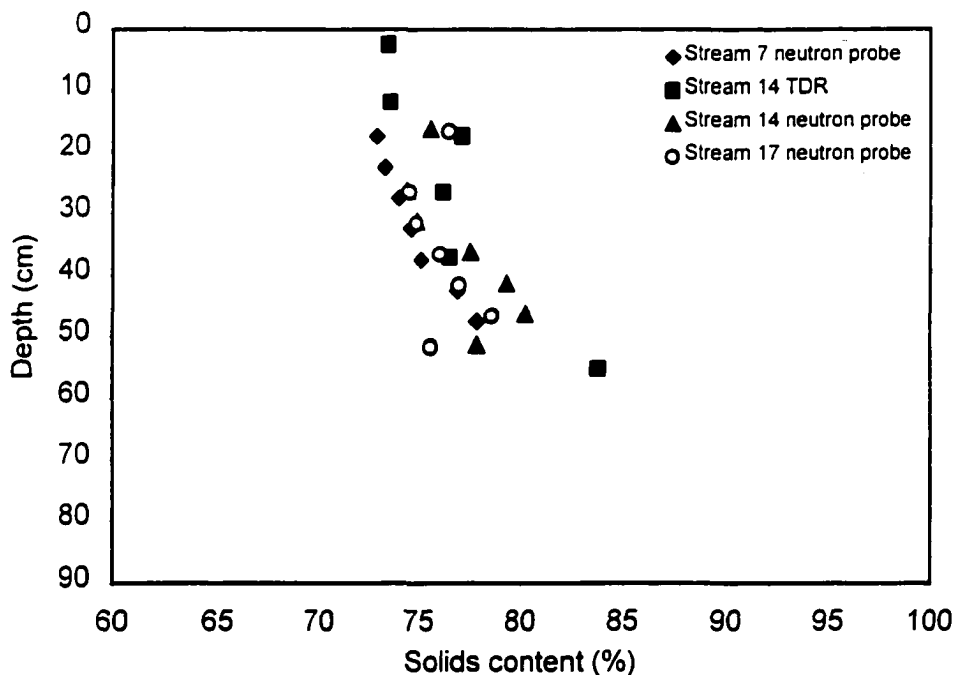
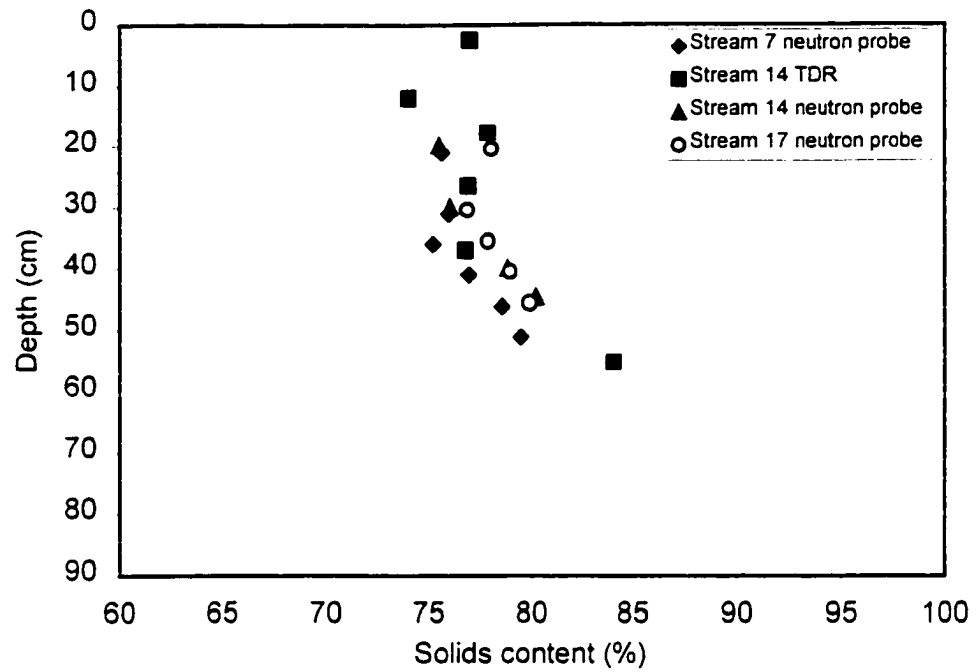
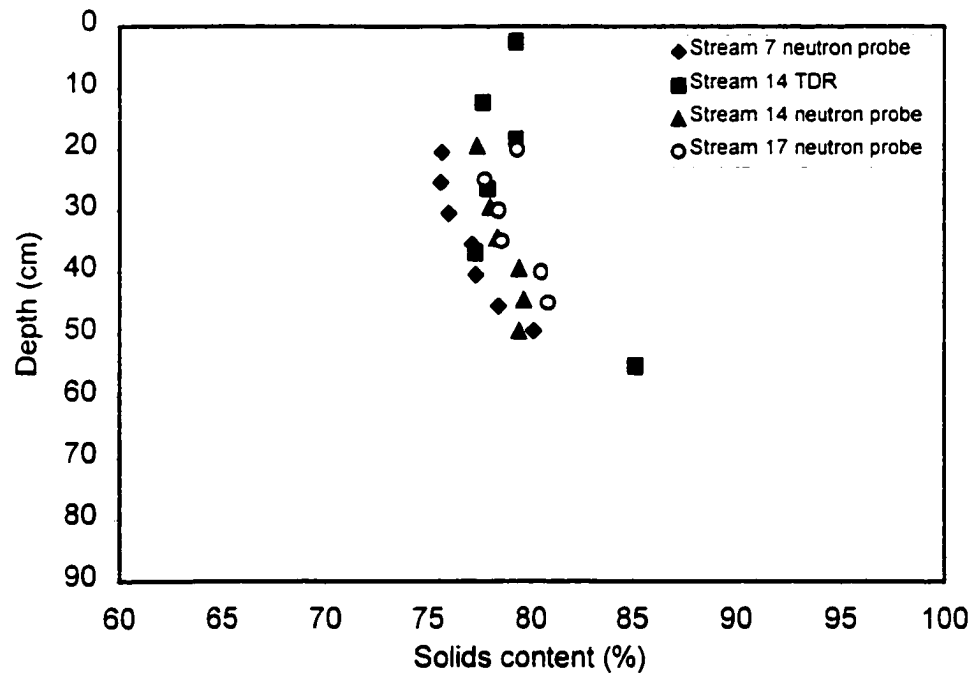


Figure B.54 Solids content profile of streambank wheatgrass measured on March 3, 1998



**Figure B.55 Solids content profile of streambank wheatgrass measured on March 10, 1998**



**Figure B.56 Solids content profile of streambank wheatgrass measured on March 16, 1998**

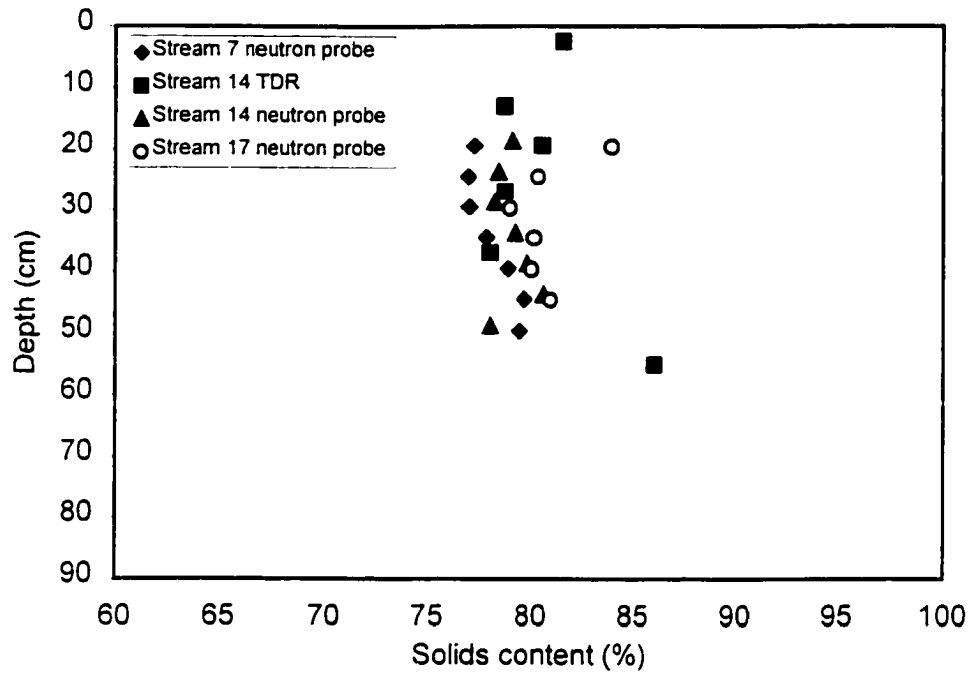


**Figure B.57 Solids content profile of streambank wheatgrass measured on March 23, 1998**

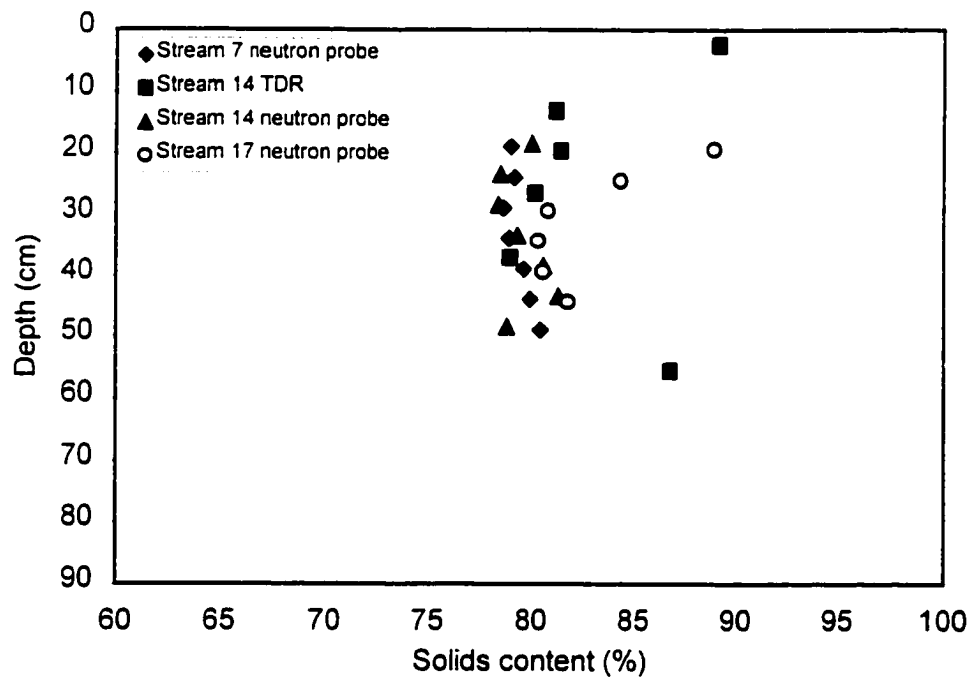


**Figure B.58 Solids content profile of streambank wheatgrass measured on March 31, 1998**



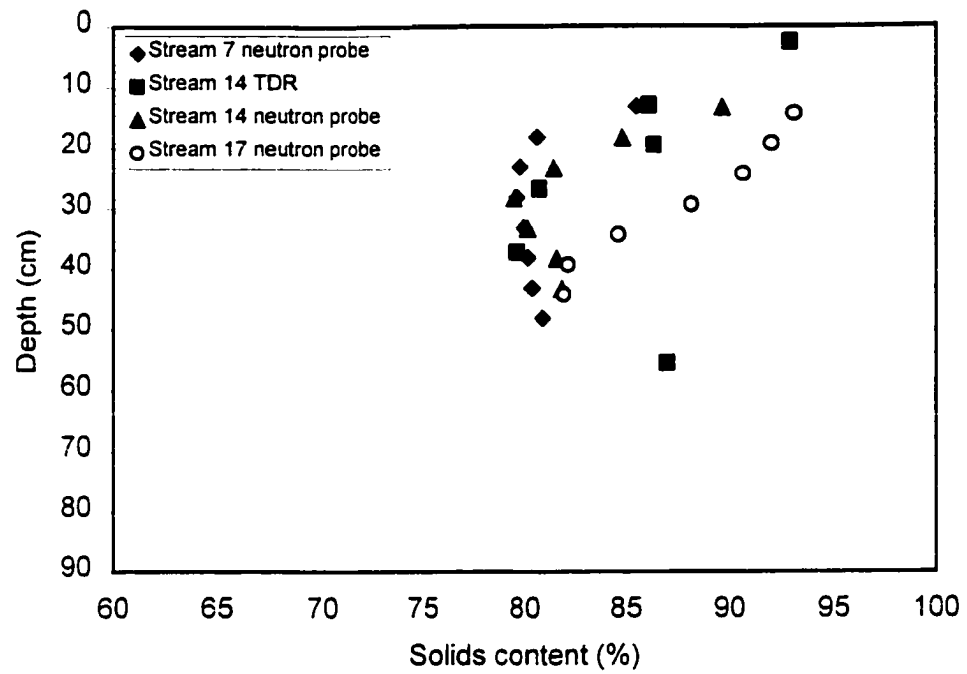


Figure B.59 Solids content profile of streambank wheatgrass measured on April 10, 1998

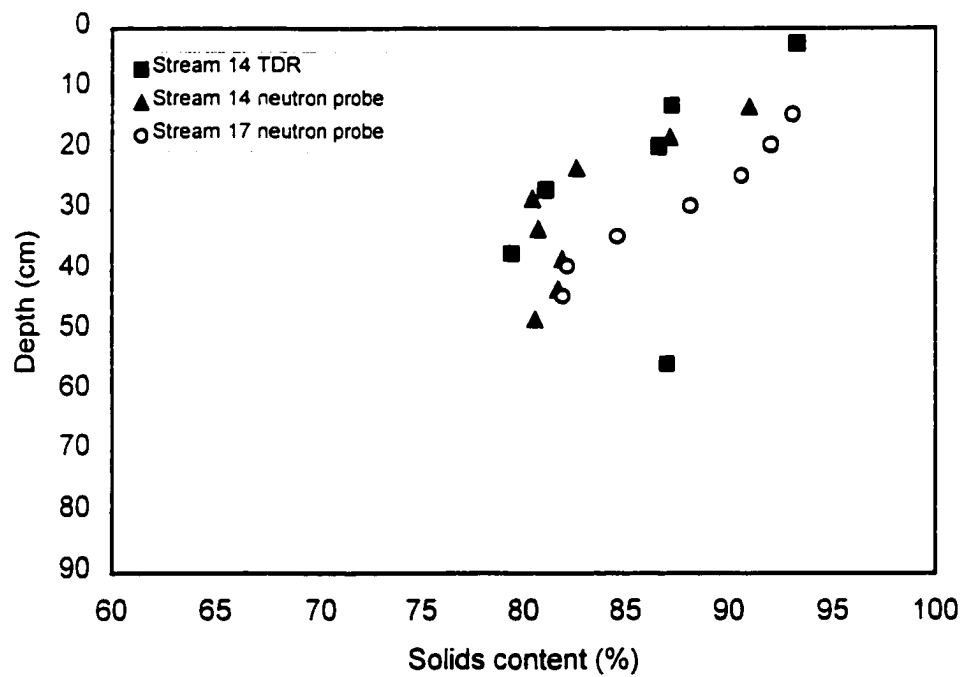
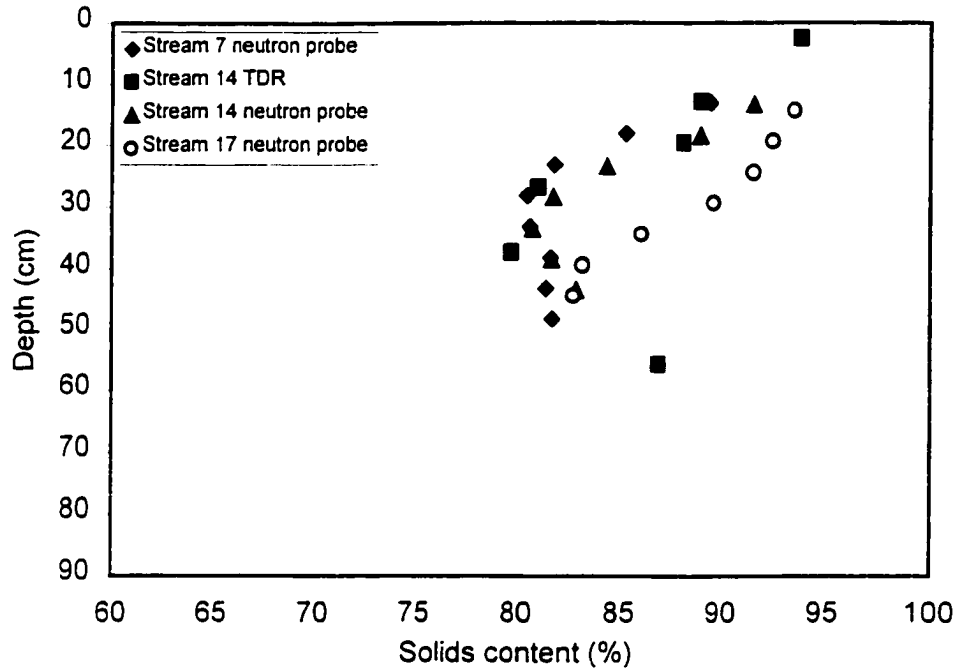
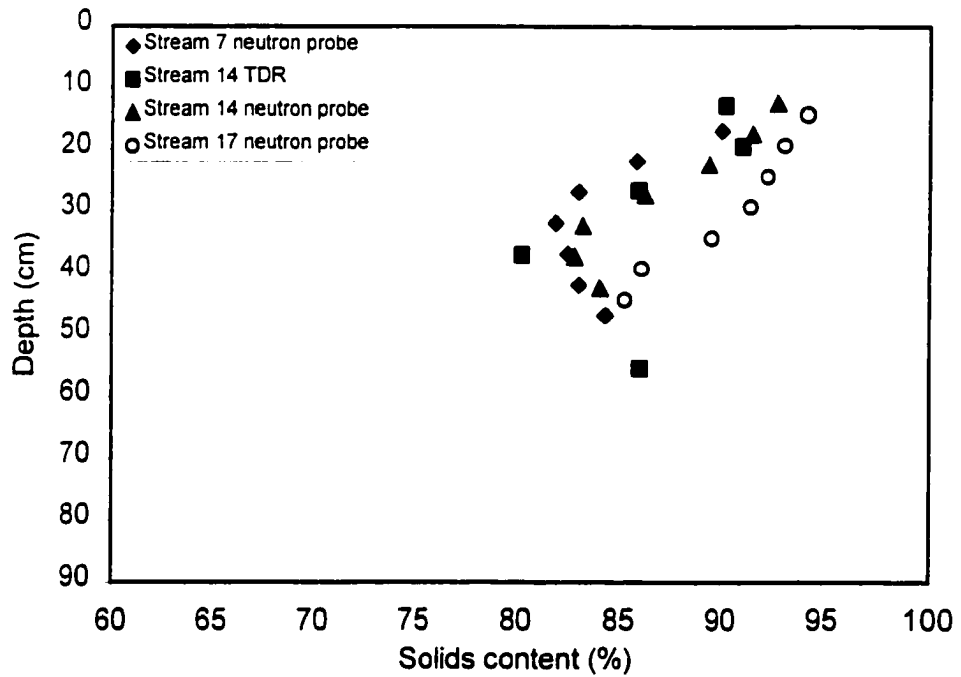


Figure B.60 Solids content profile of streambank wheatgrass measured on April 15, 1998



**Figure B.61 Solids content profile of streambank wheatgrass measured on April 20, 1998**



**Figure B.62 Solids content profile of streambank wheatgrass measured on May 12, 1998**

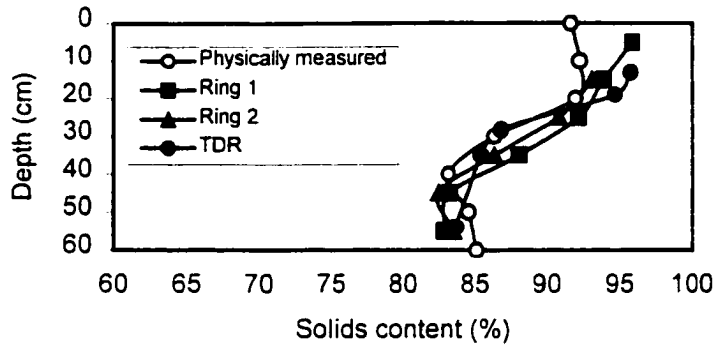


**Figure B.63 Solids content profile of Altai wildrye 1 at end of experiment**

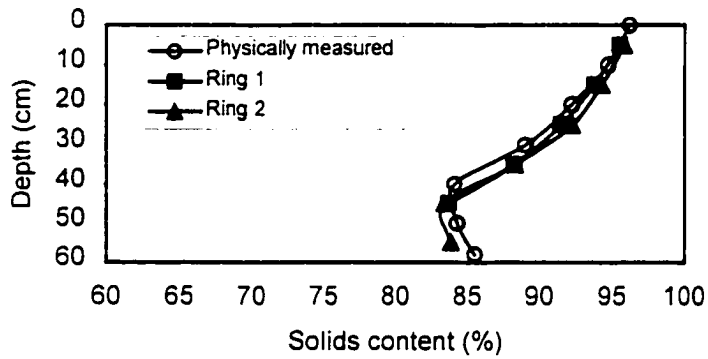


**Figure B.64 Solids content profile of Altai wildrye 2 at end of experiment**

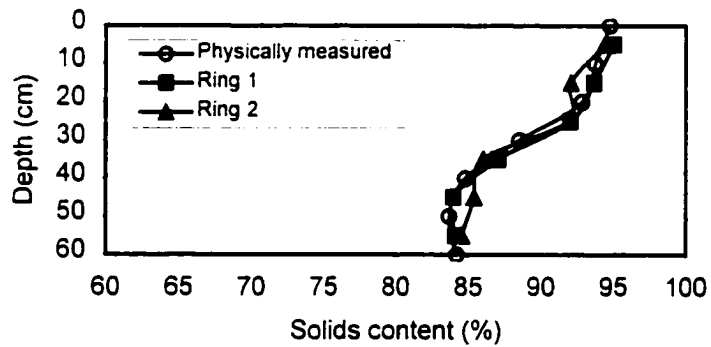


**Figure B.65 Solids content profile of Altai wildrye 9 at end of experiment**

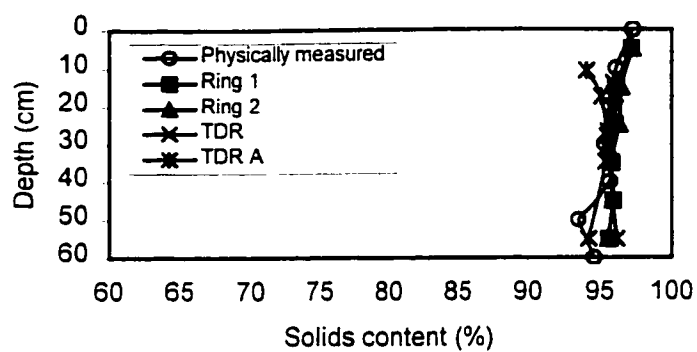


**Figure B.66 Solids content profile of creeping foxtail 5 at end of experiment**

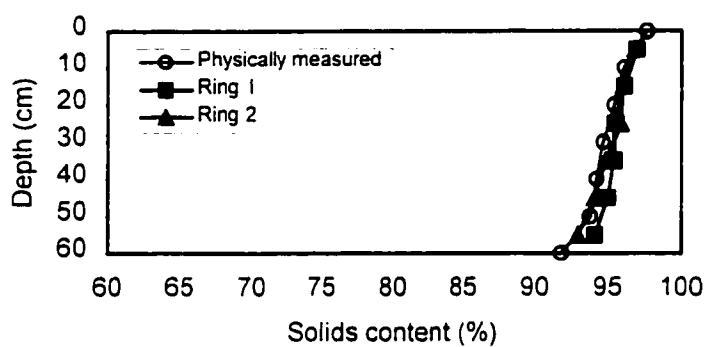


**Figure B.67 Solids content profile of creeping foxtail 12 at end of experiment**

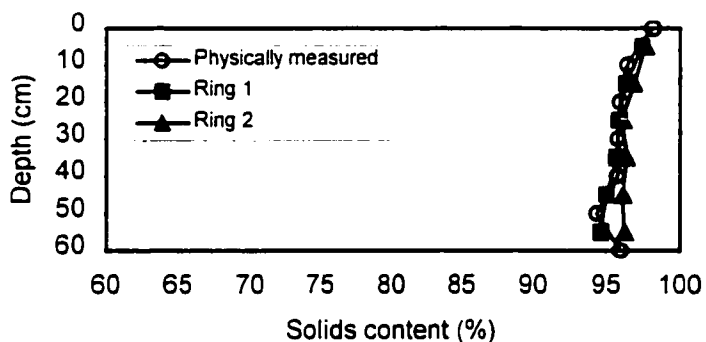


**Figure B.68 Solids content profile of creeping foxtail 18 at end of experiment**

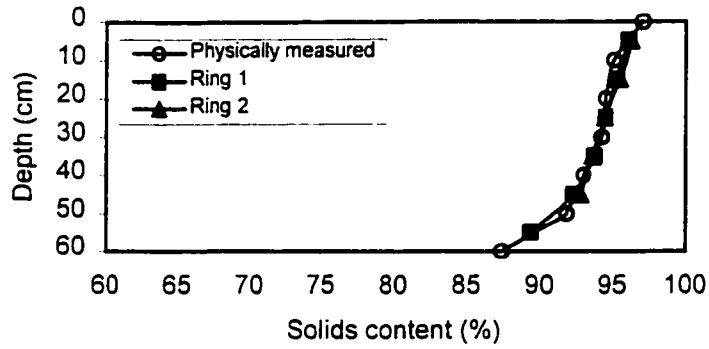


**Figure B.69 Solids content profile of red top 3 at end of experiment**

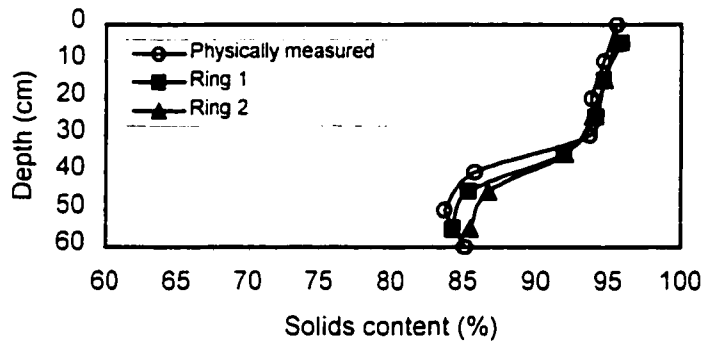


**Figure B.70 Solids content profile of red top 11 at end of experiment**

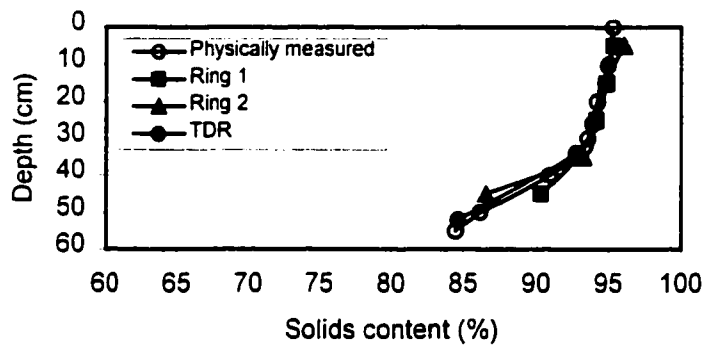


**Figure B.71 Solids content profile of red top 16 at end of experiment**

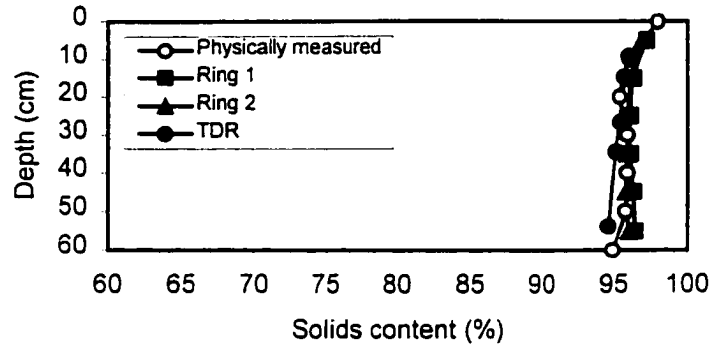


**Figure B.72 Solids content profile of reed canarygrass 4 at end of experiment**

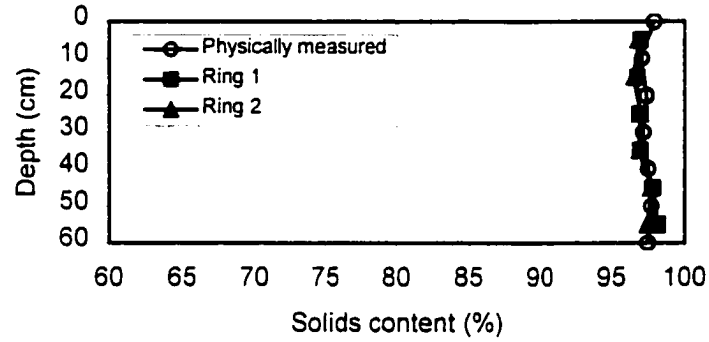


**Figure B.73 Solids content profile of reed canary 13 at end of experiment**

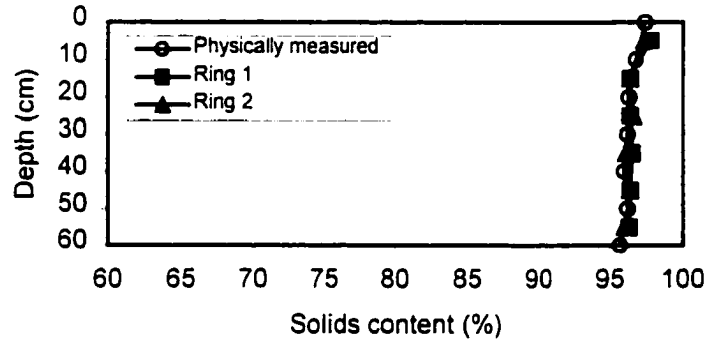


**Figure B.74 Solids content profile of reed canarygrass 15 at end of experiment**

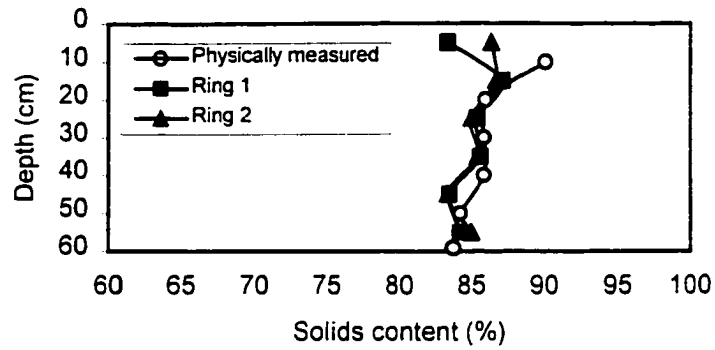


**Figure B.75 Solids content profile of streambank wheatgrass 7 at end of experiment**

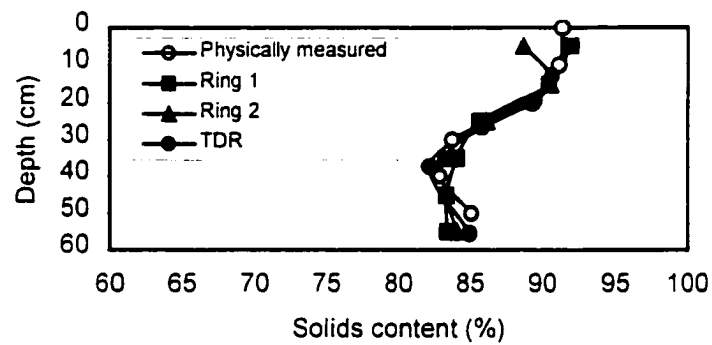


**Figure B.76 Solids content profile of streambank wheatgrass 14 at end of experiment**

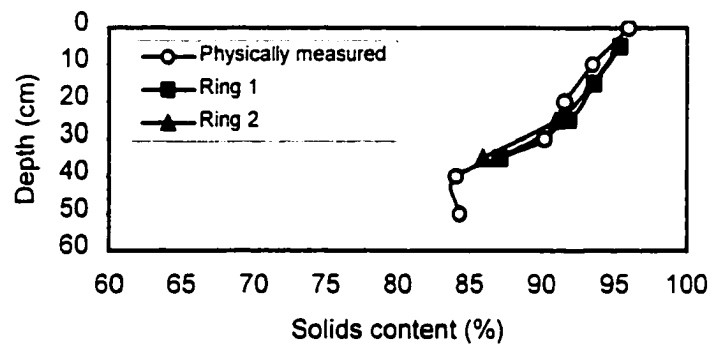


**Figure B.77 Solids content profile of streambank wheatgrass 17 at end of experiment**

## **Appendix C**

### ***Plate Load Test results***

---

#### **C.1 INTRODUCTION**

Bearing capacity was measured at two locations in each of three different layers within each lysimeter by conducting Plate Load Tests (PLT). A plate with a diameter of 80 mm was chosen to eliminate any boundary effect in the test. Also, the vertical distance between two adjacent test layers was at least two times the plate diameter to avoid overlapping of the zone of influence of the bearing tests. PLT locations are illustrated in Chapter 4. A diagram of the plate load apparatus is shown in Figure C.1.

The methodology followed to conduct this test is described in ASTM D 1194 - 72 with small modifications to adjust the test to the unique conditions presented by the tailings in the lysimeters. But, in general, the principle of the test was the same.

#### **C.2 RESULTS**

Results of the Plate Load Tests, which have been partially presented in the chapters of the thesis, are included in entirety in this appendix. These figure include plots of pressure versus settlement presented in arithmetic scale. The bearing capacities at failure in most of the tests are clearly defined in the plots.



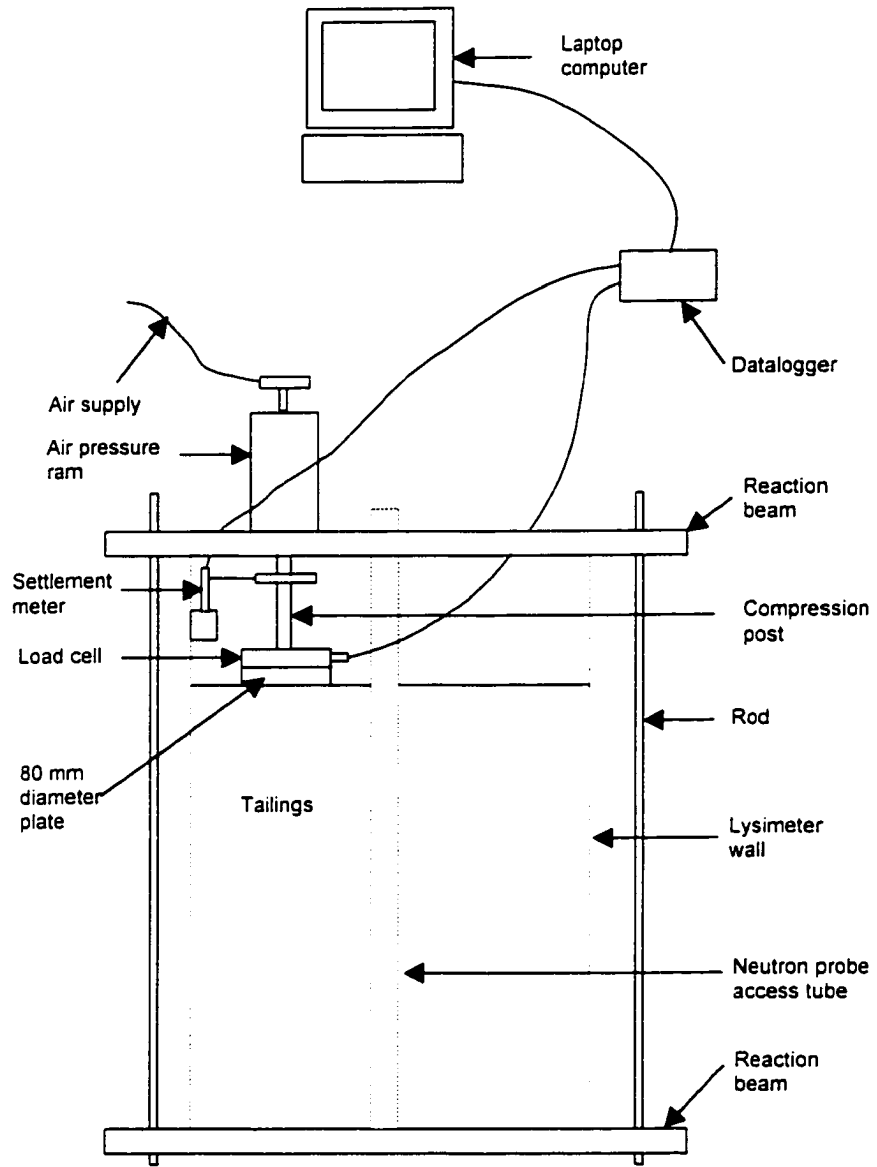


**Figure C.1 Plate Load Test apparatus**

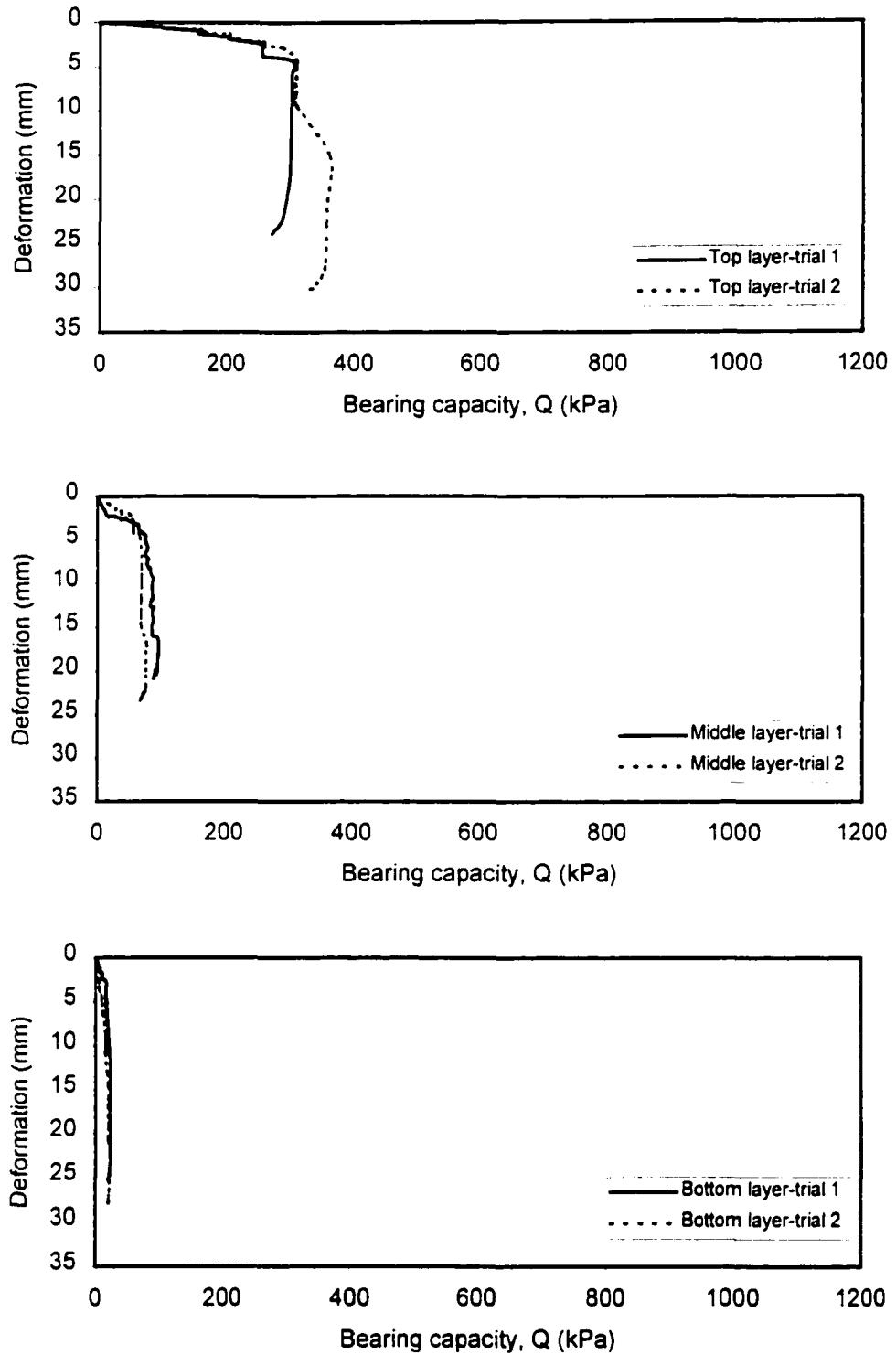


**Figure C.2** PLT results on three different layers of Altai wildrye 1

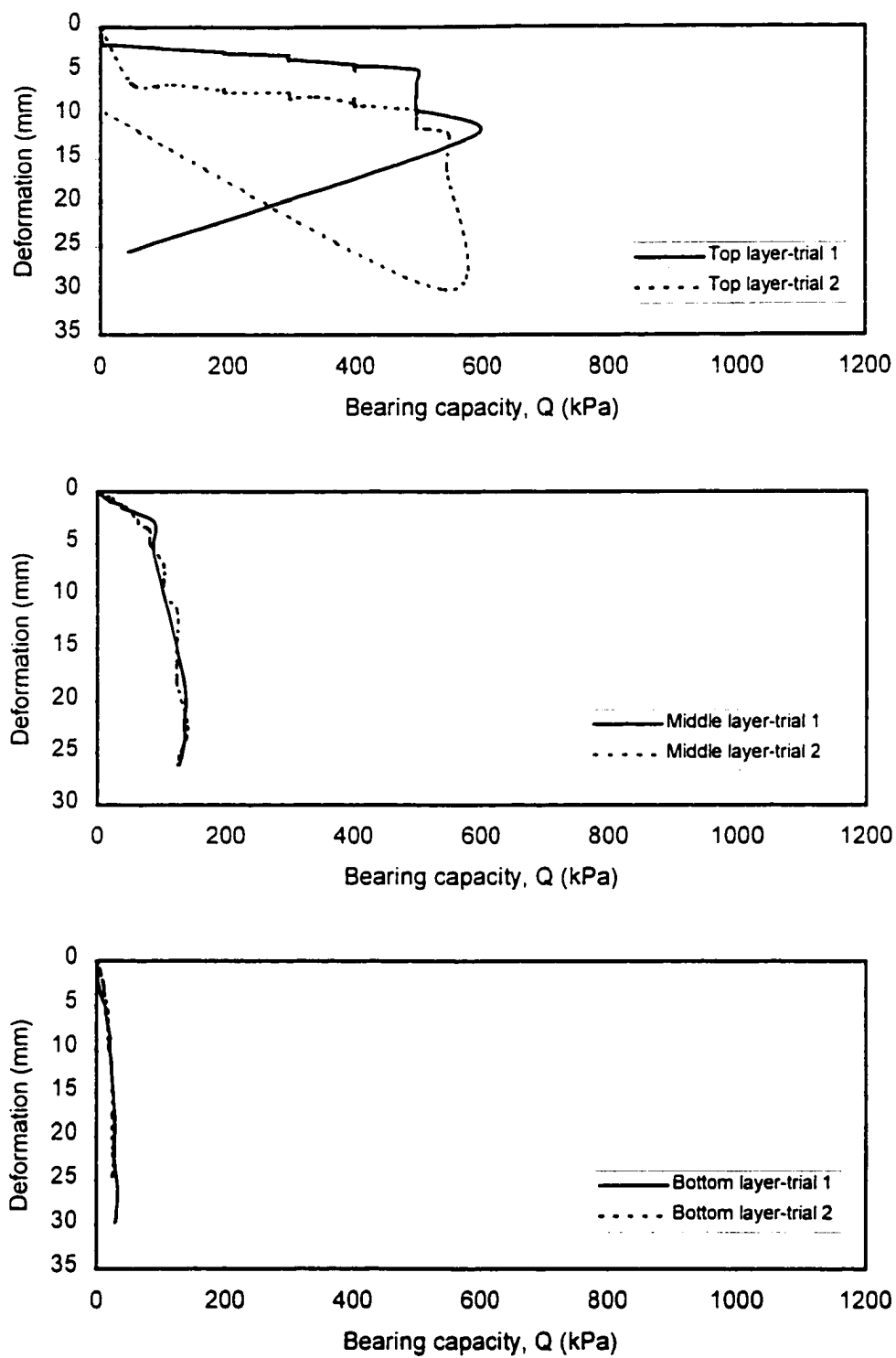


**Figure C.3 PLT results on three different layers of Altai wildrye 2**

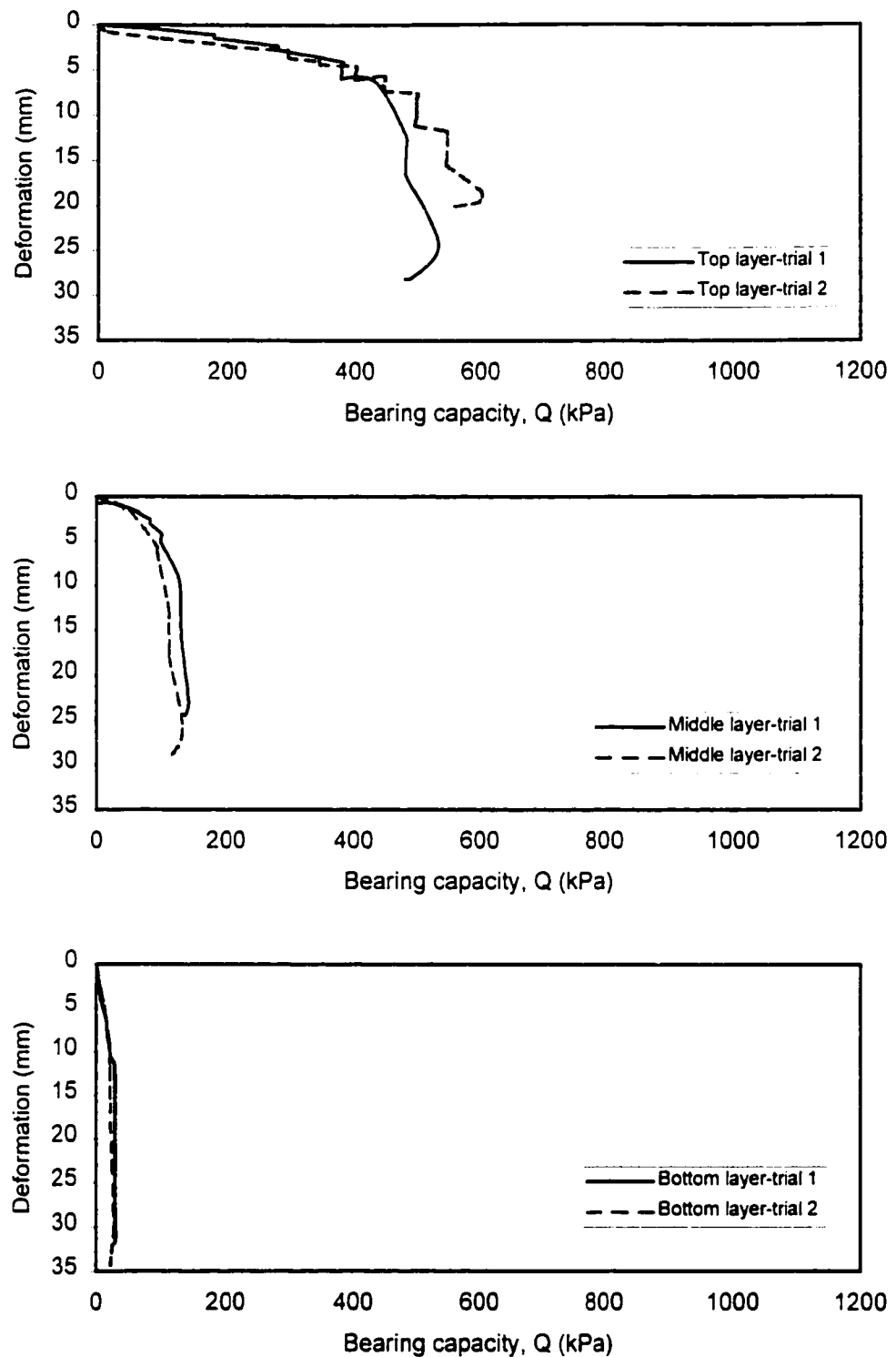


**Figure C.4** PLT results on three different layers of Altai wildrye 9

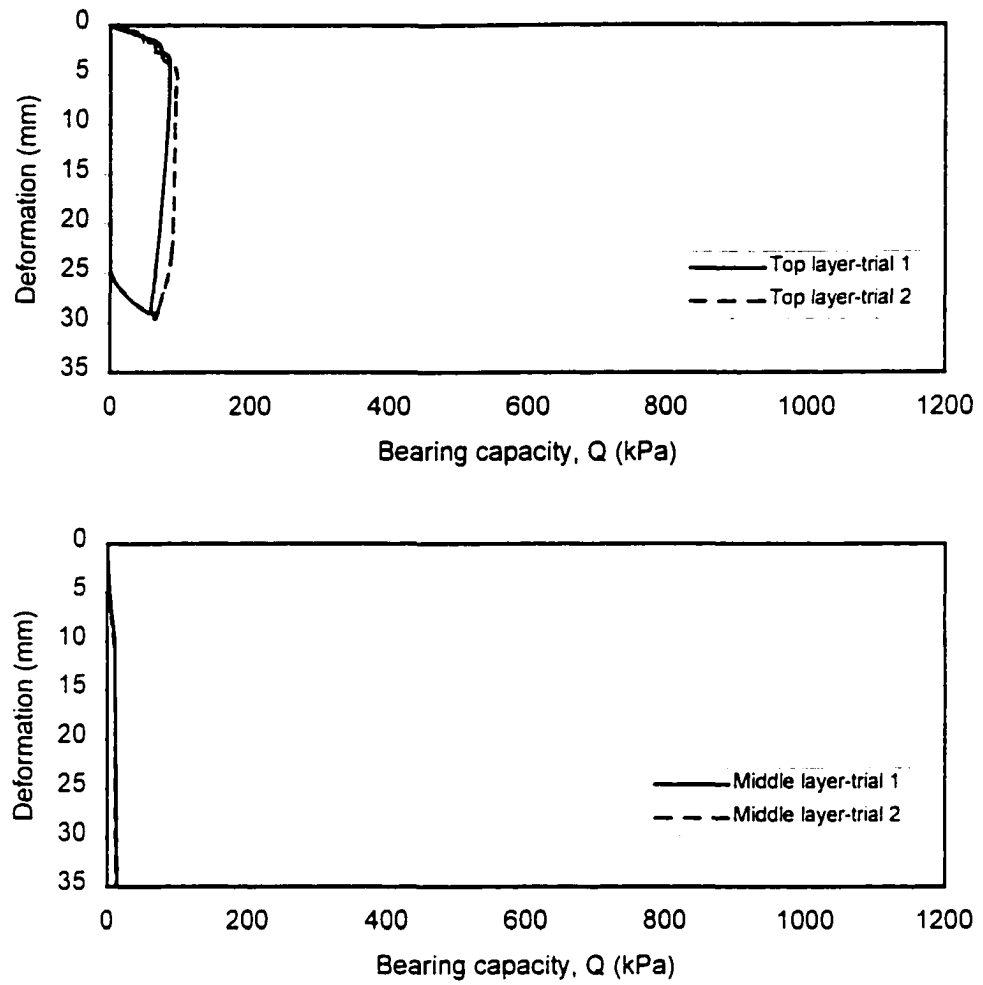


**Figure C.5** PLT results on two different layers of control 6

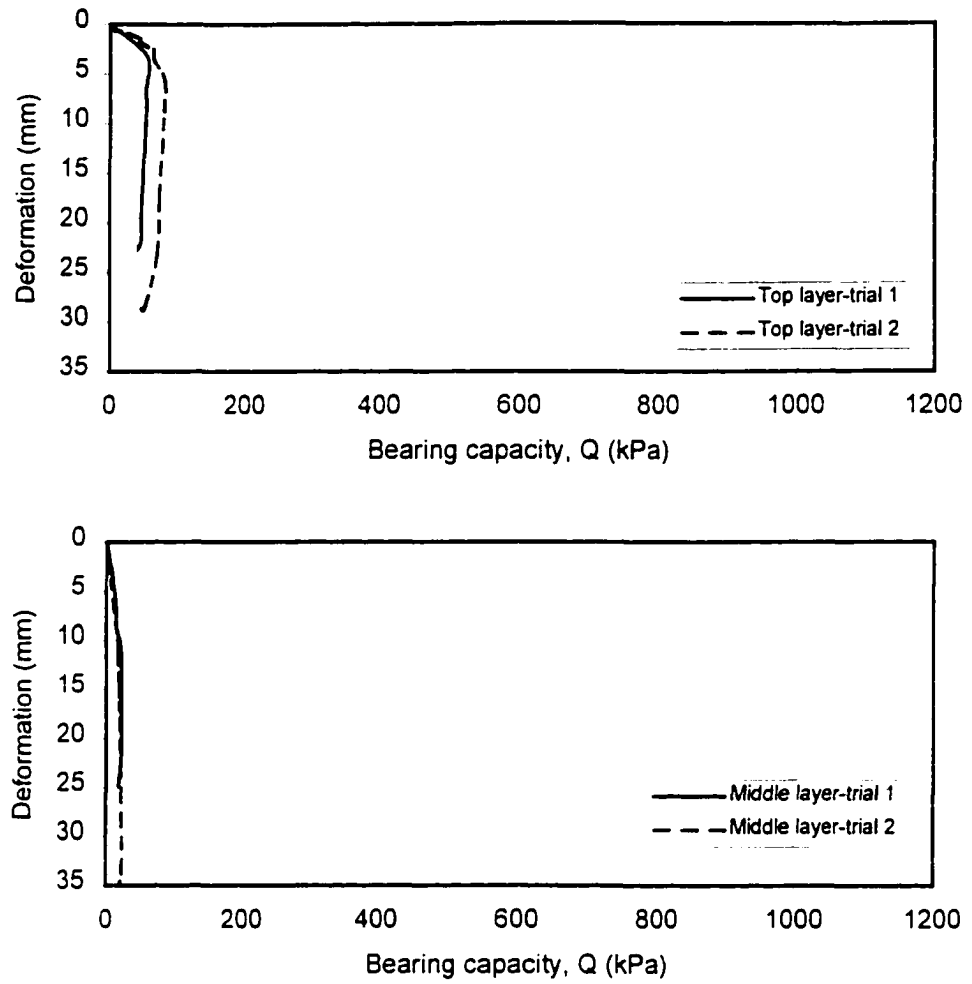


**Figure C.6 PLT results on two different layers of control 8**

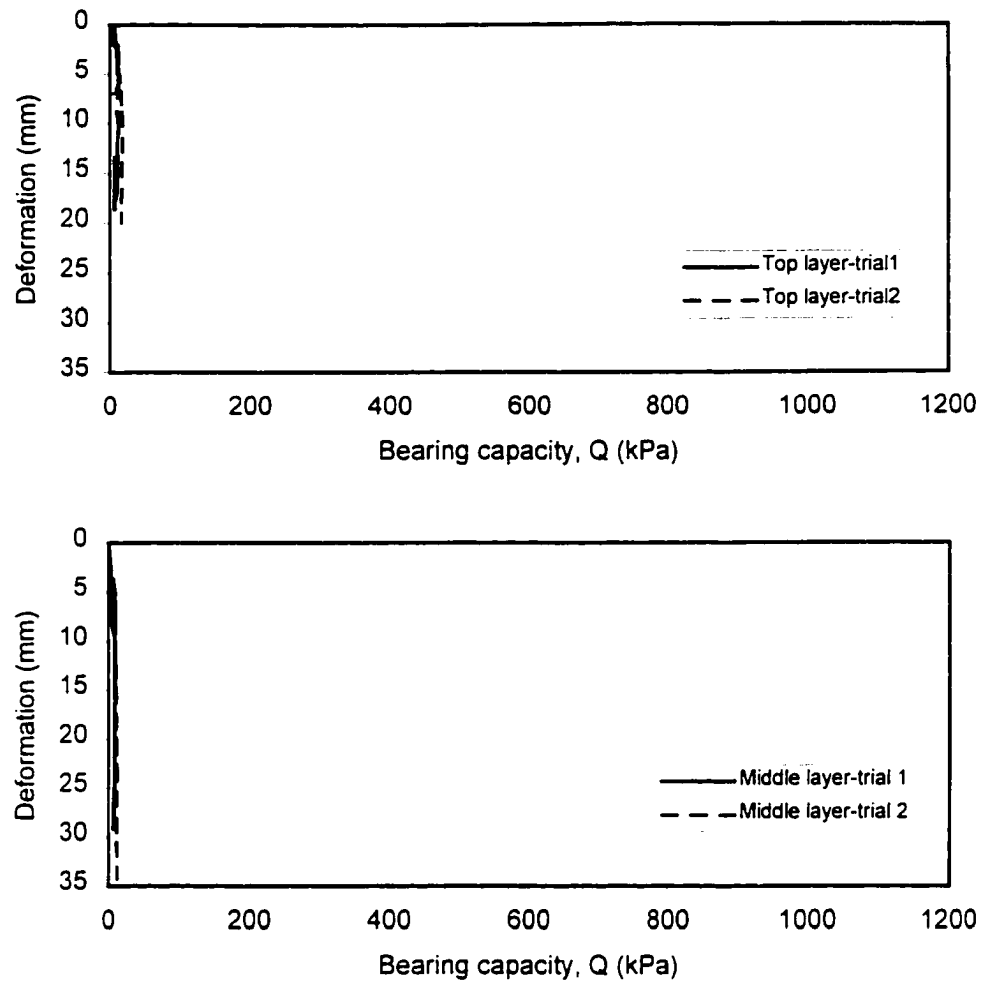


**Figure C.7** PLT results on two different layers of control 10

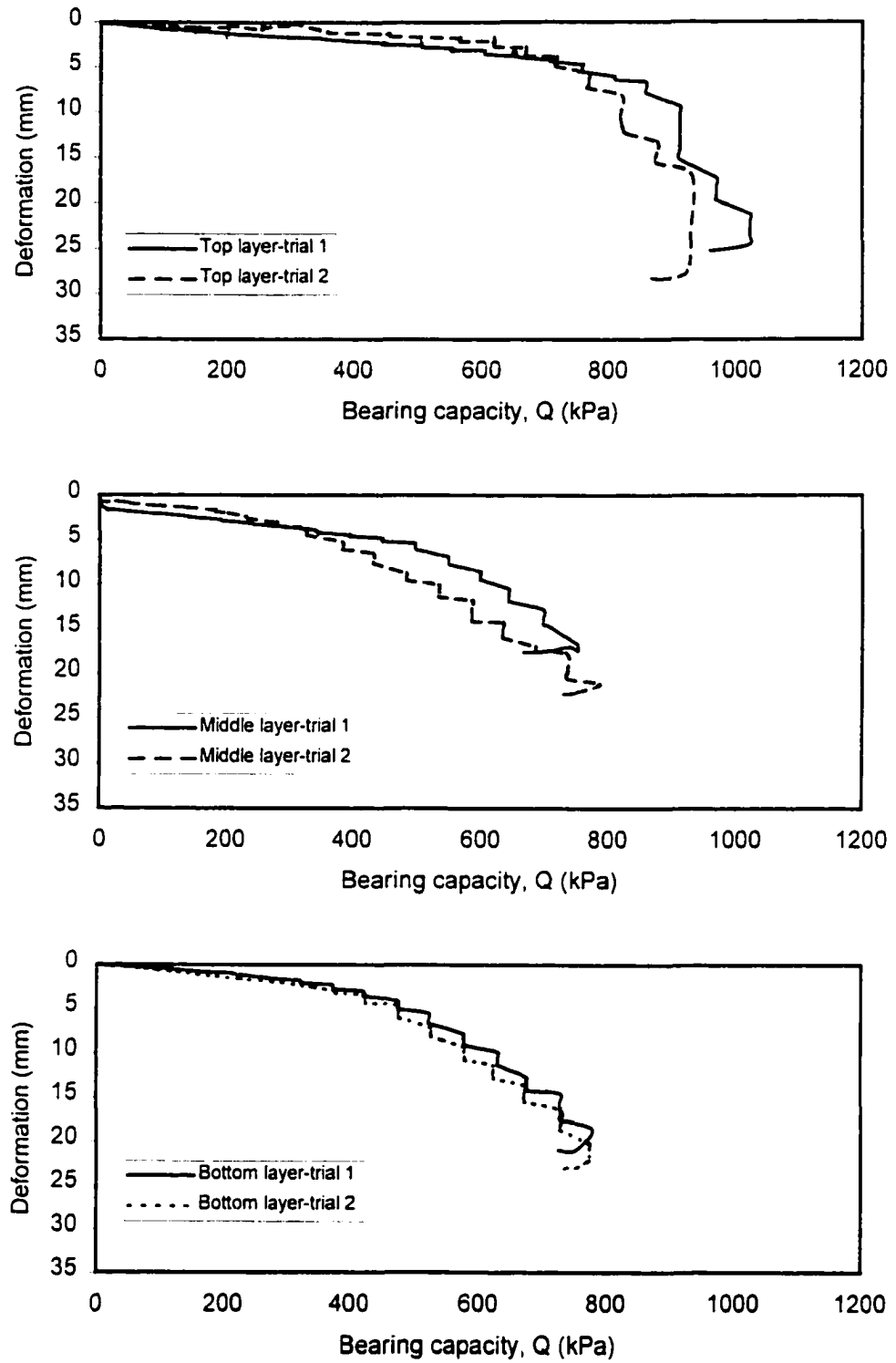


**Figure C.8 PLT results on three different layers of creeping foxtail 5**



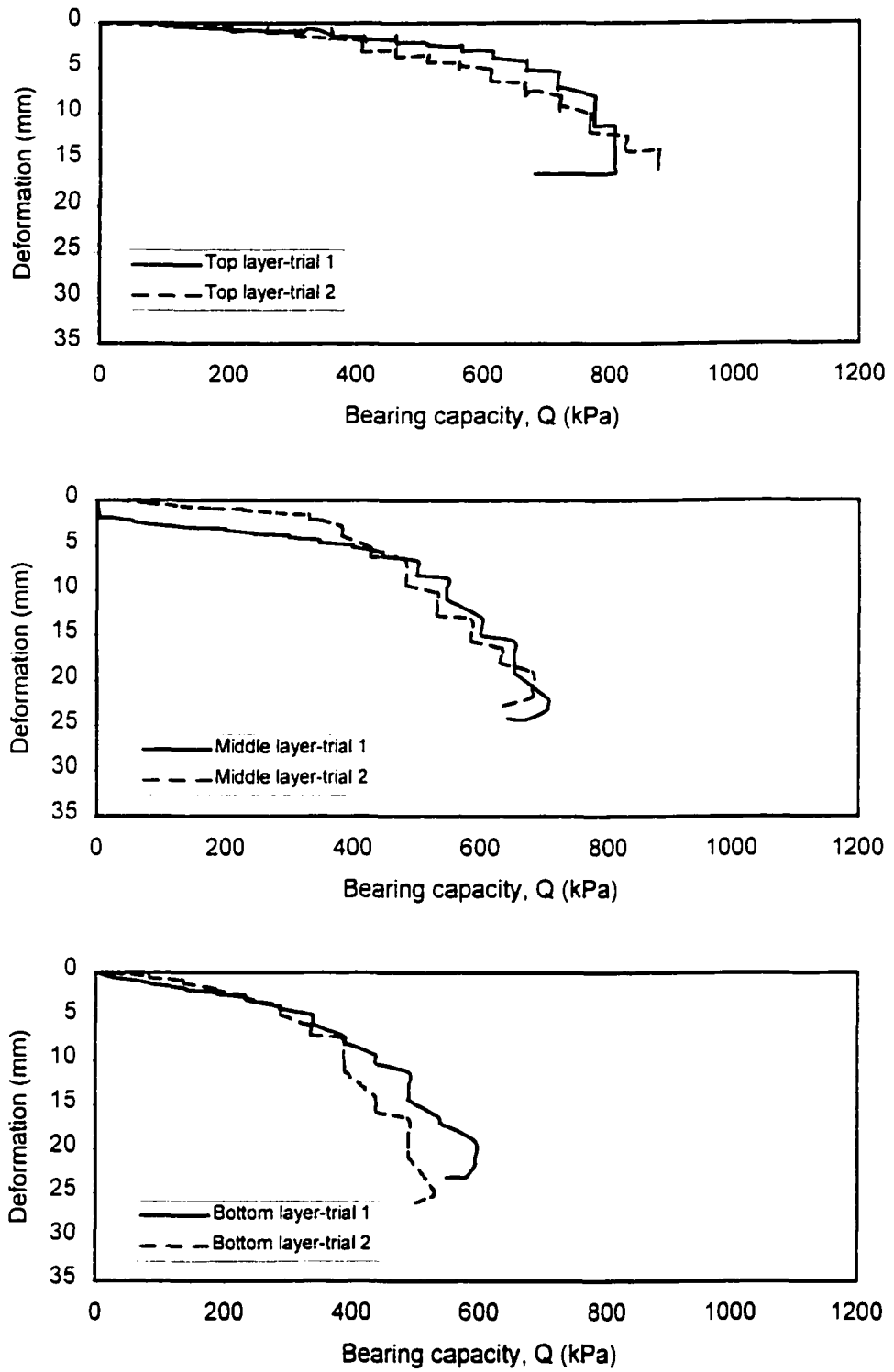


**Figure C.9 PLT results on three different layers of creeping foxtail 12**

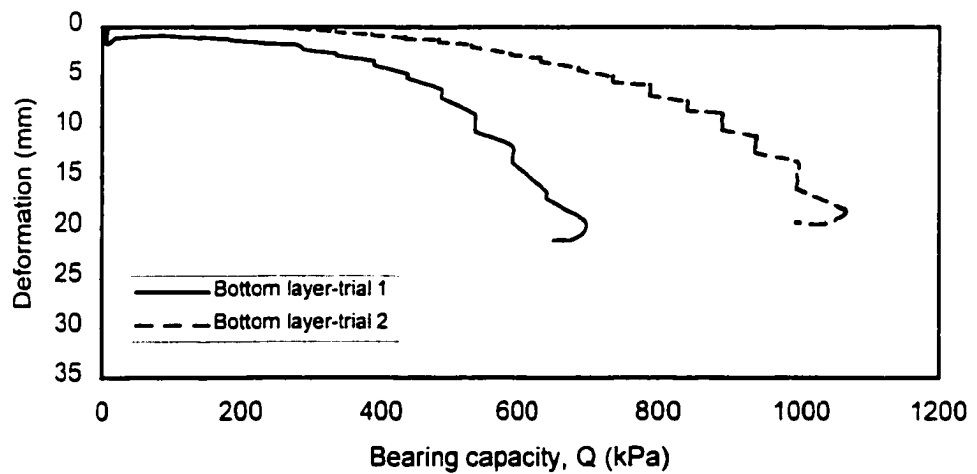
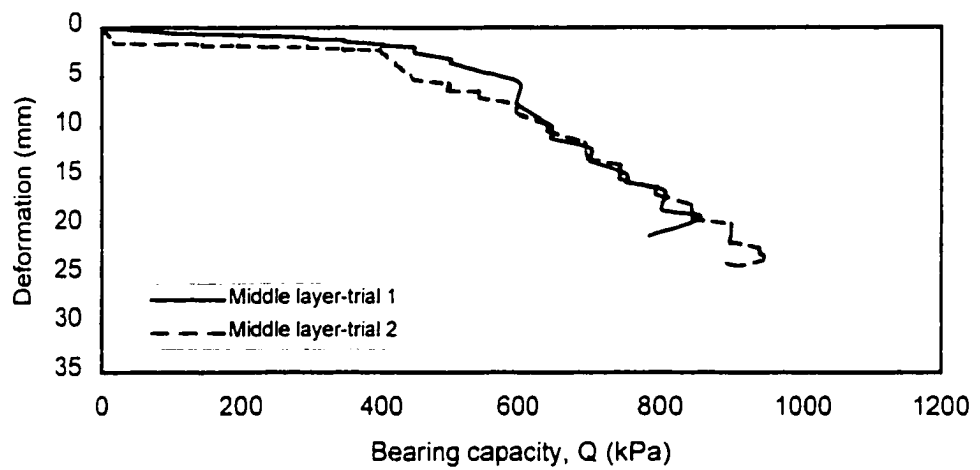
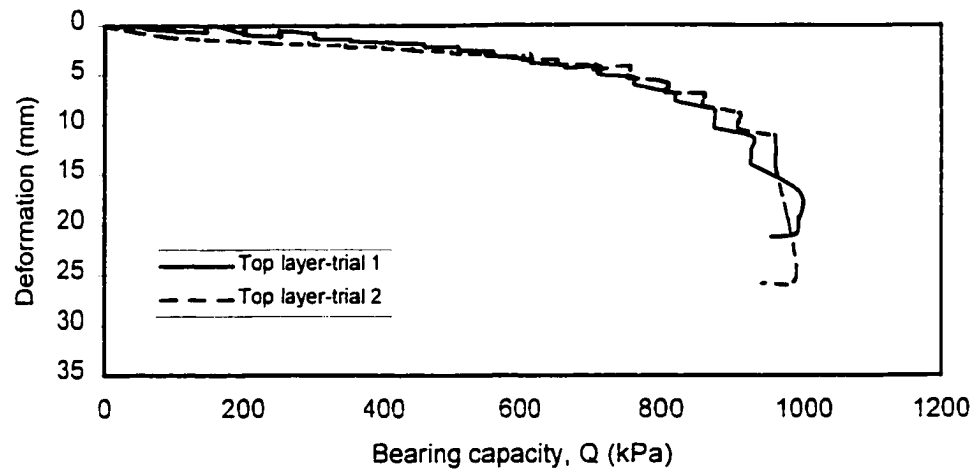


**Figure C.10** PLT results on three different layers of creeping foxtail 18

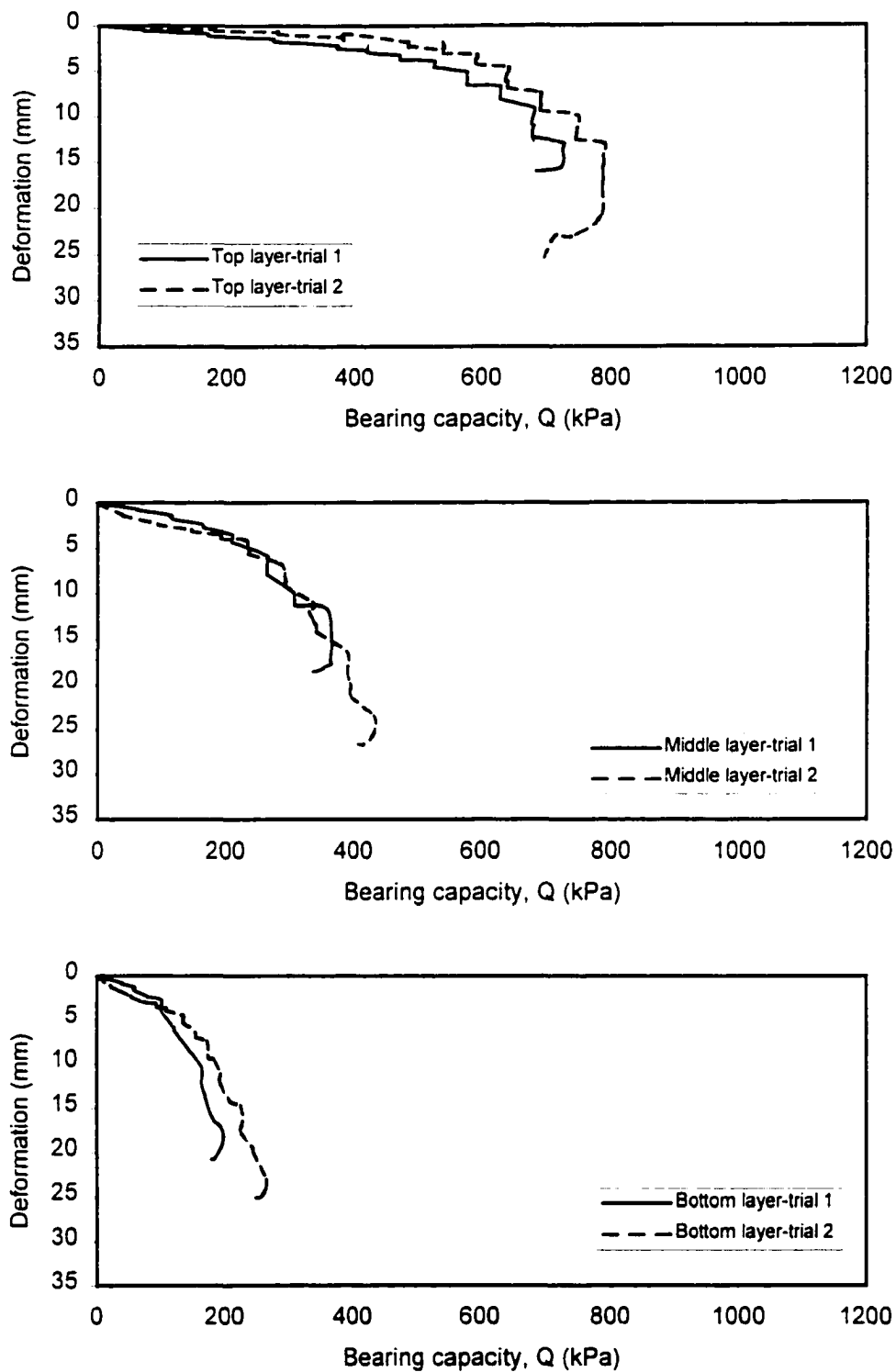


**Figure C.11** PLT results on three different layers of red top 3

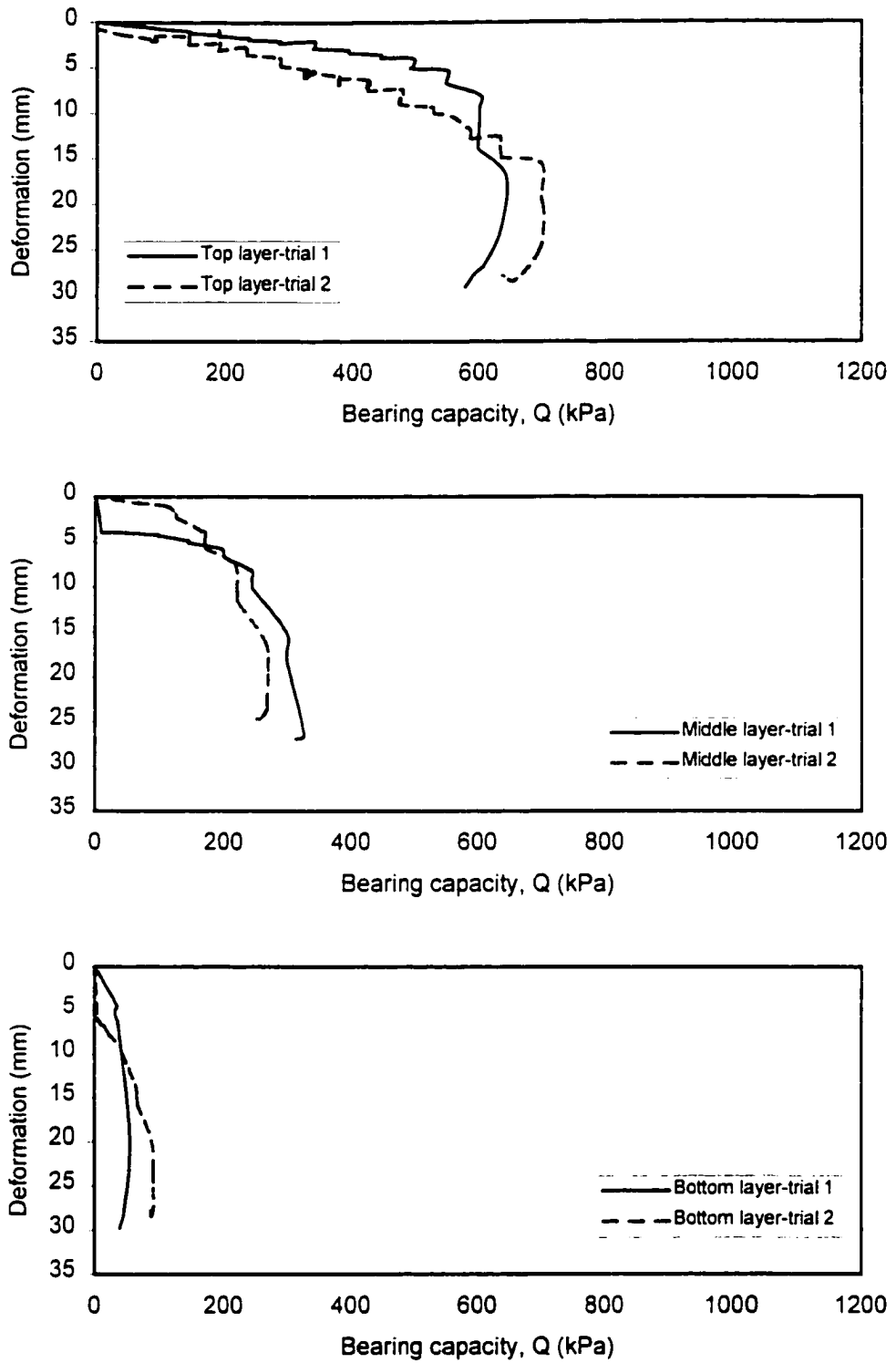


**Figure C.12 PLT results on three different layers of red top 11**

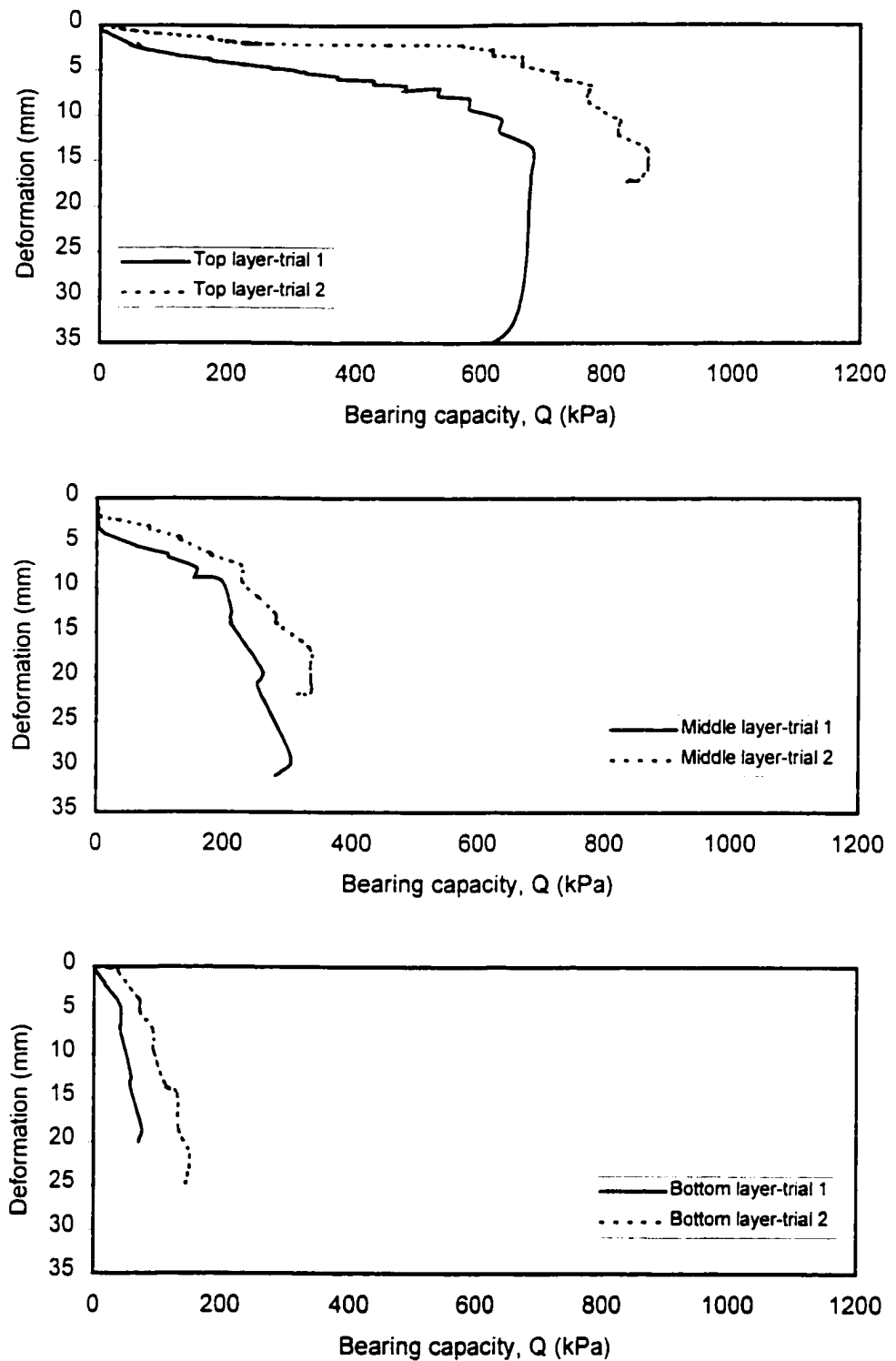


**Figure C.13 PLT results on three different layers of red top 16**

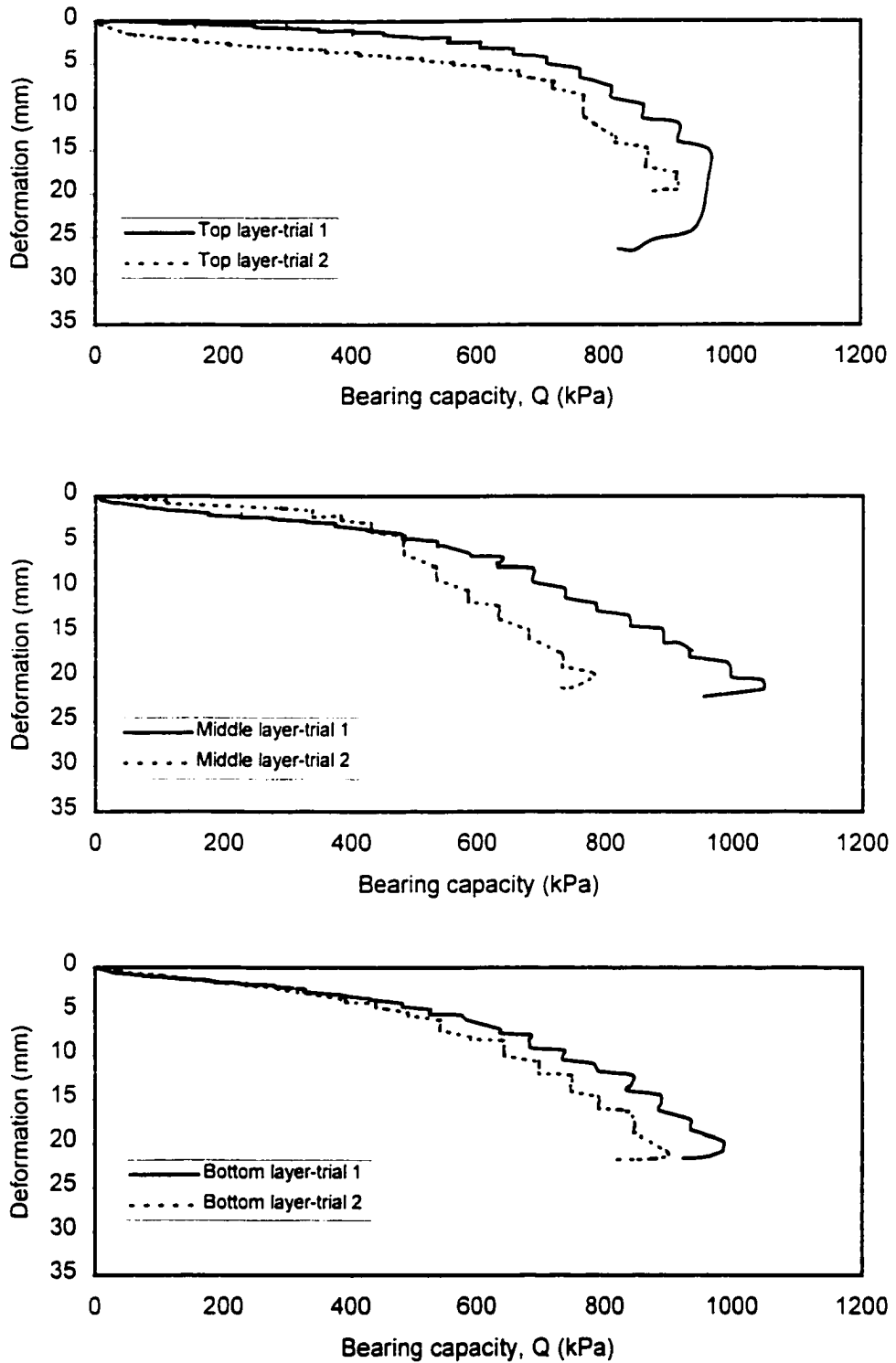


**Figure C.14** PLT results on three different layers of reed canarygrass 4

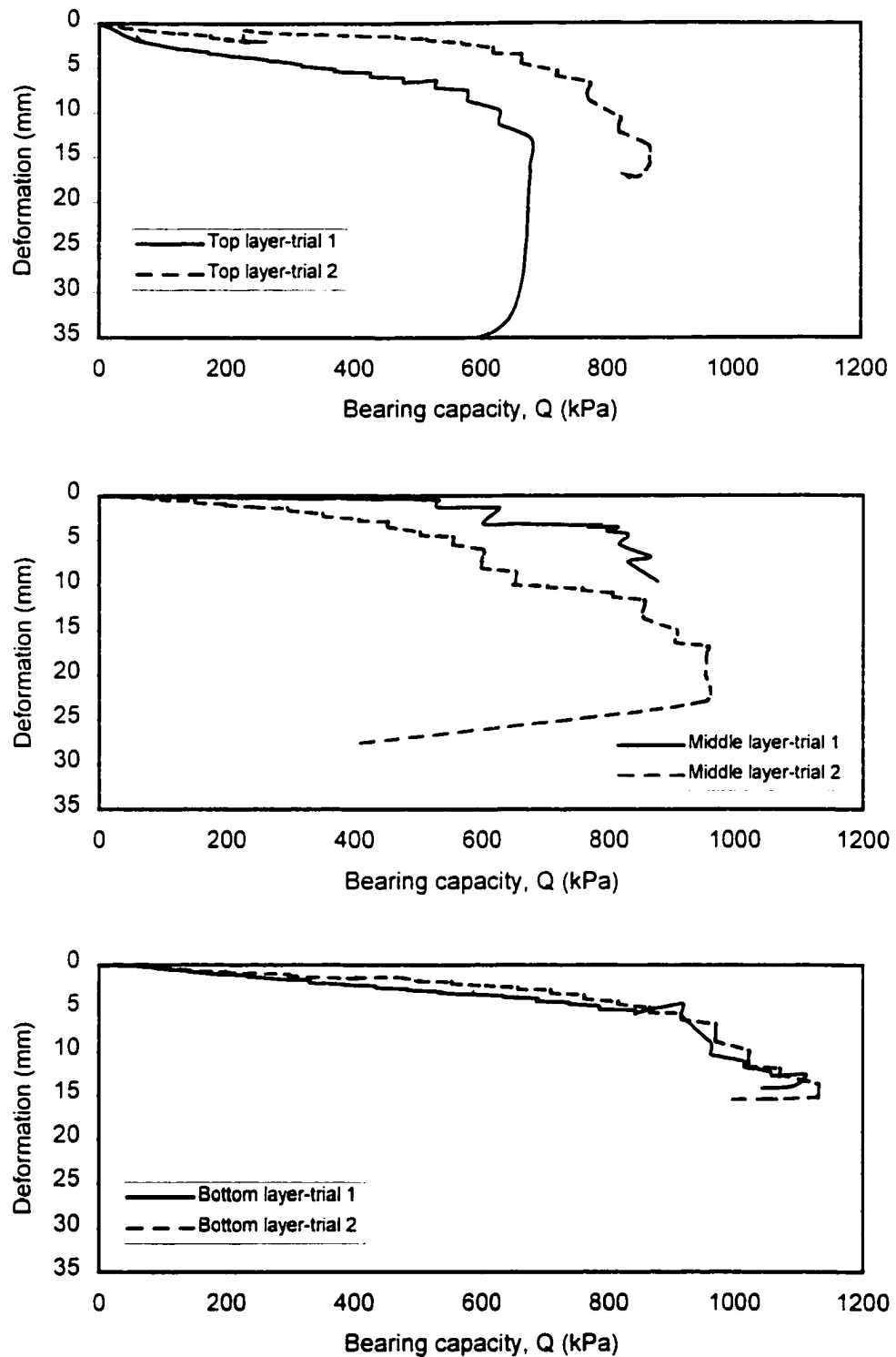


**Figure C.15** PLT results on three different layers of reed canarygrass 13

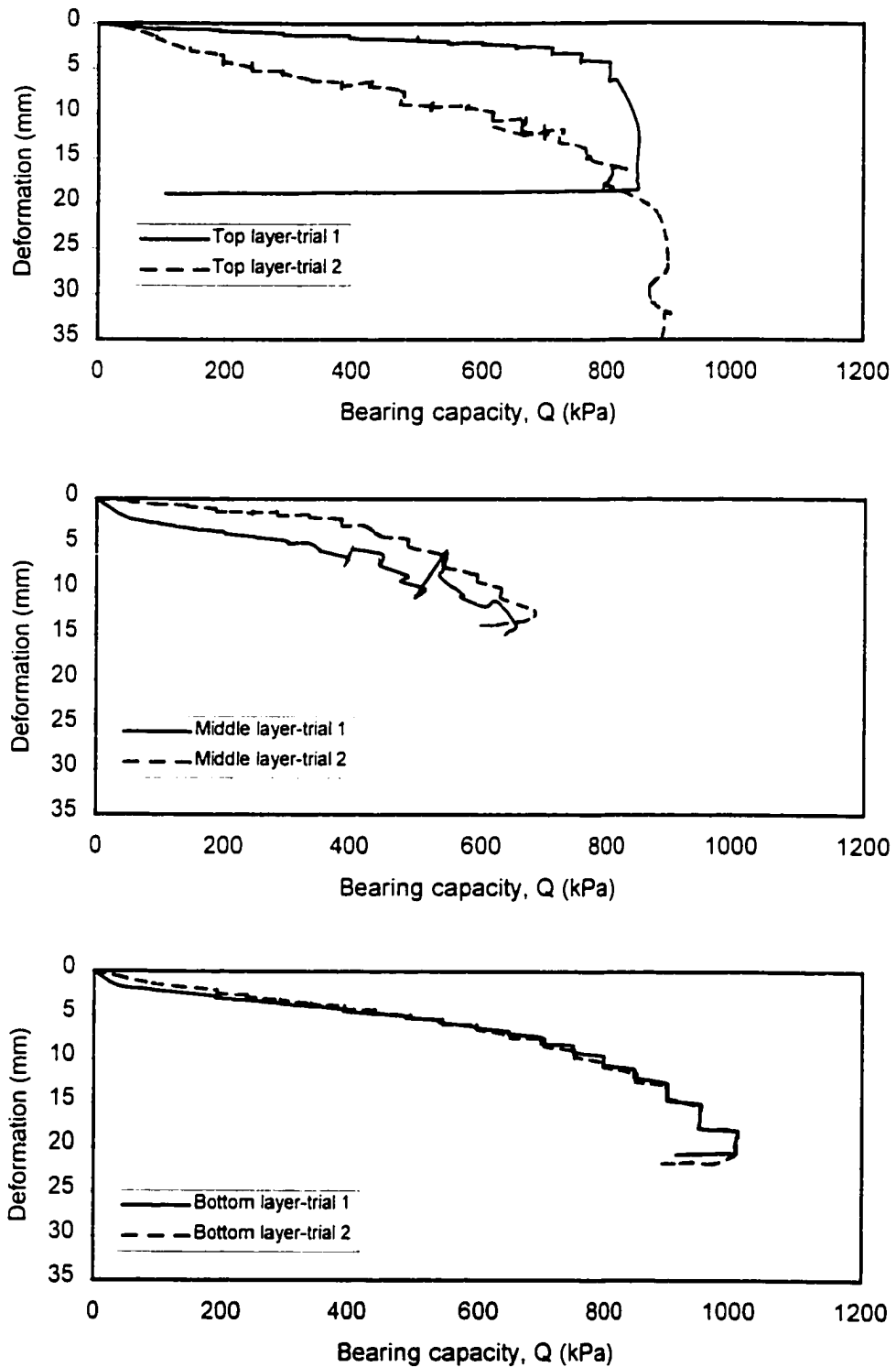


**Figure C.16 PLT results on three different layers of reed canarygrass 15**



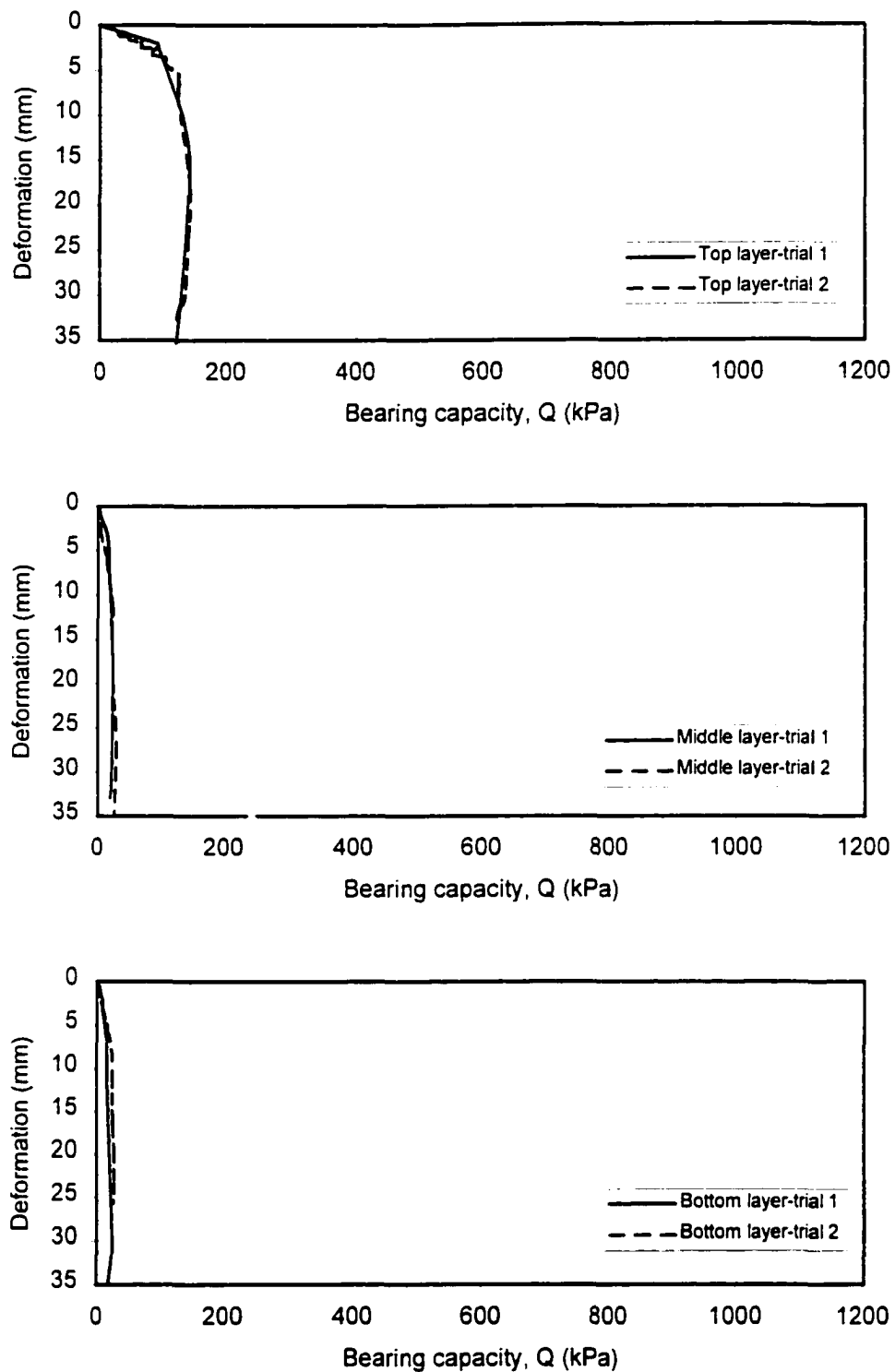


**Figure C.17** PLT results on three different layers of streambank wheatgrass 7

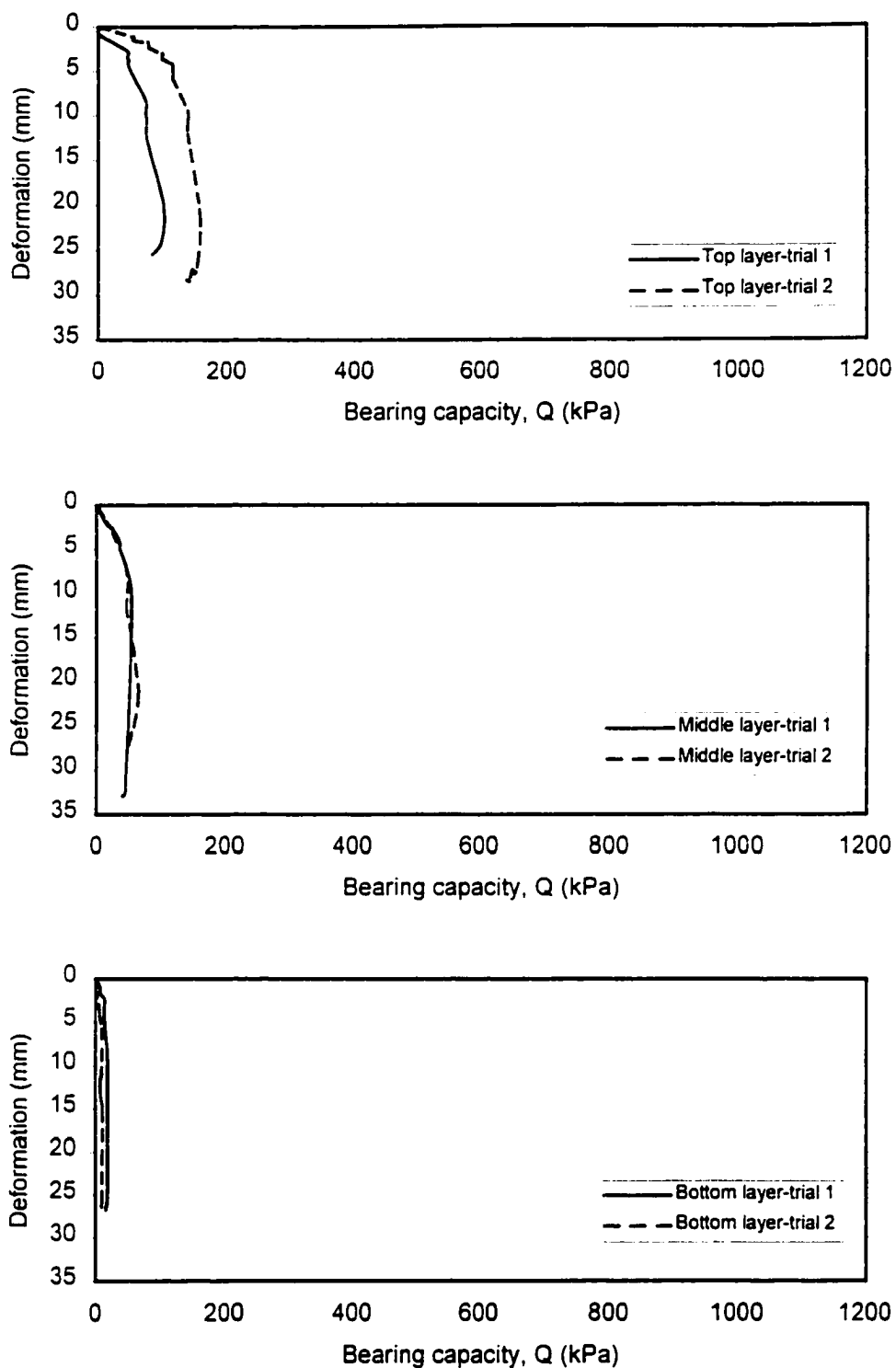


**Figure C.18 PLT results on three different layers of streambank wheatgrass 14**

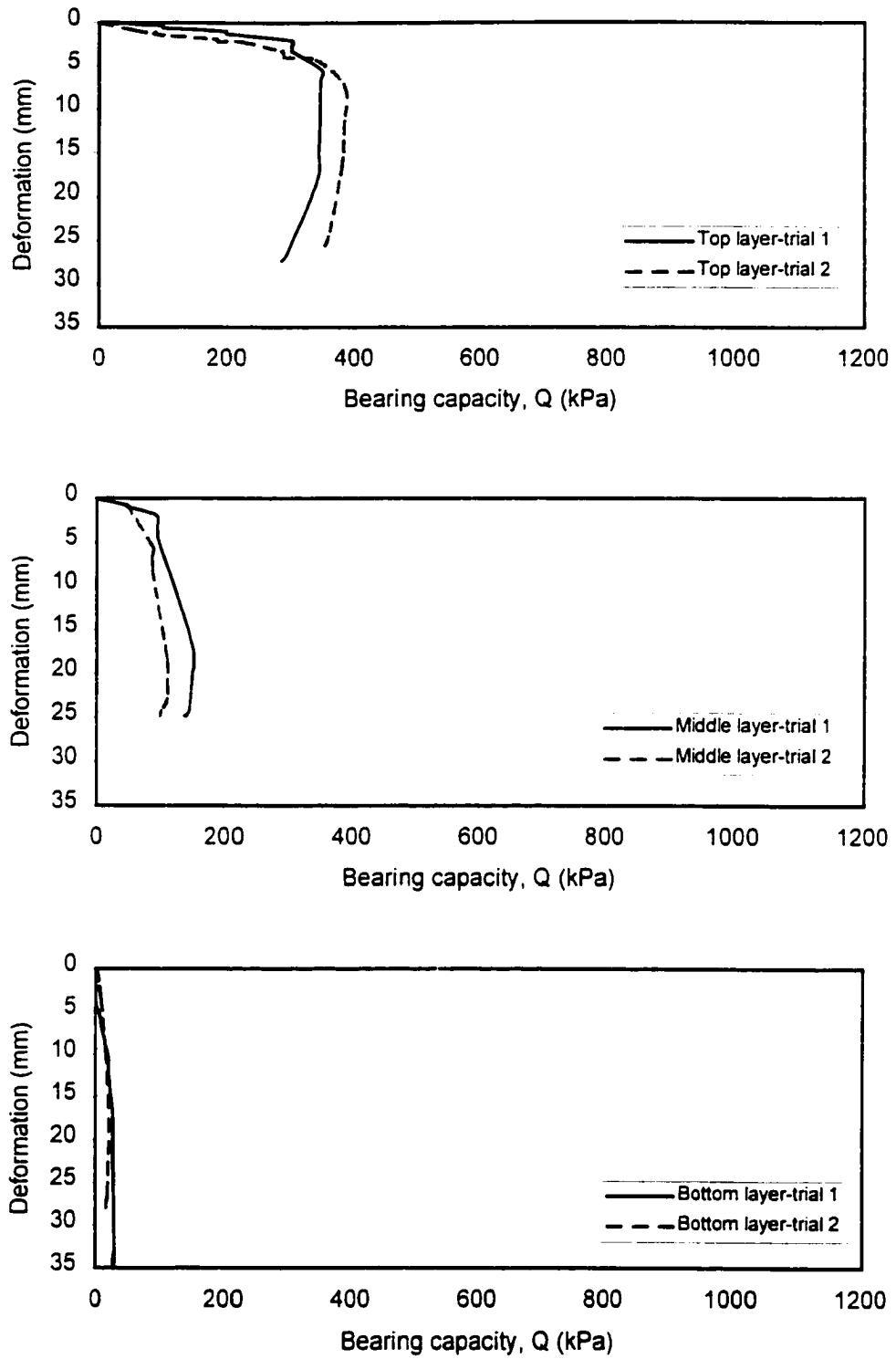


**Figure C.19 PLT results on three different layers of streambank wheatgrass 17**

## **Appendix D**

### ***Plant measurements***

---

This appendix presents the plant measurements taken during the greenhouse experiment conducted to calibrate and validate the plant dewatering model. These measurements include the plant heights, leaf areas and calculated LAI, fitting curves for LAI, parameters of the S-shape equation that describe the temporal variation of the LAI, root and shoot dry weights. The procedure to measure the leaf area is described in detail in Chapter 5 of the thesis.

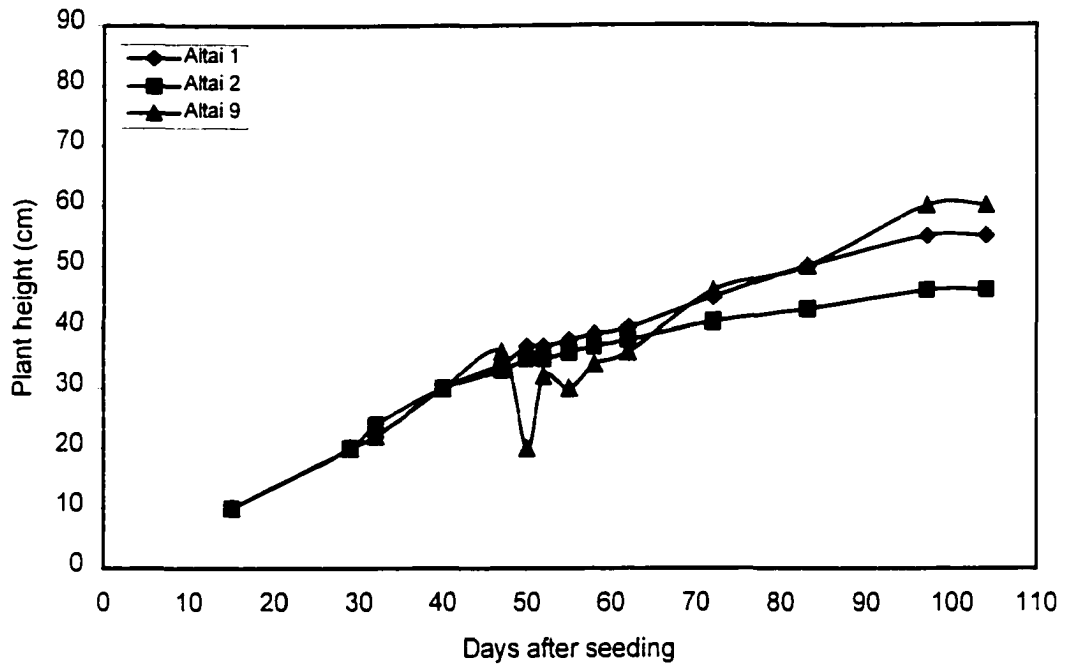


**Figure D.1** Temporal variations in plant height of Altai wildrye

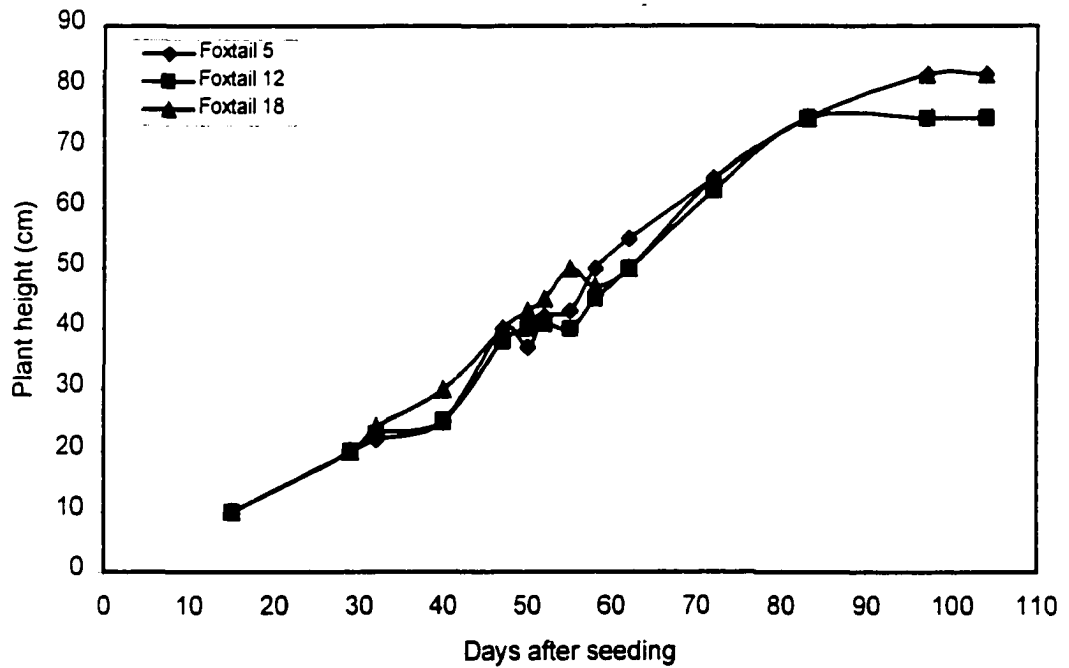


**Figure D.2** Temporal variations in plant height of creeping foxtail

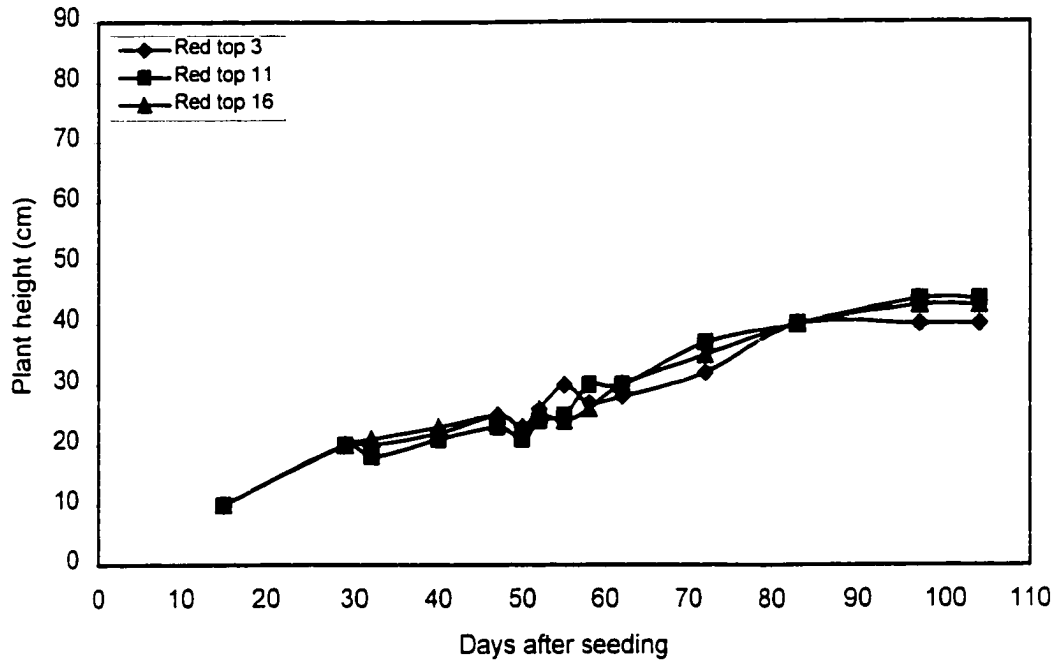


Figure D.3 Temporal variations in plant height of red top

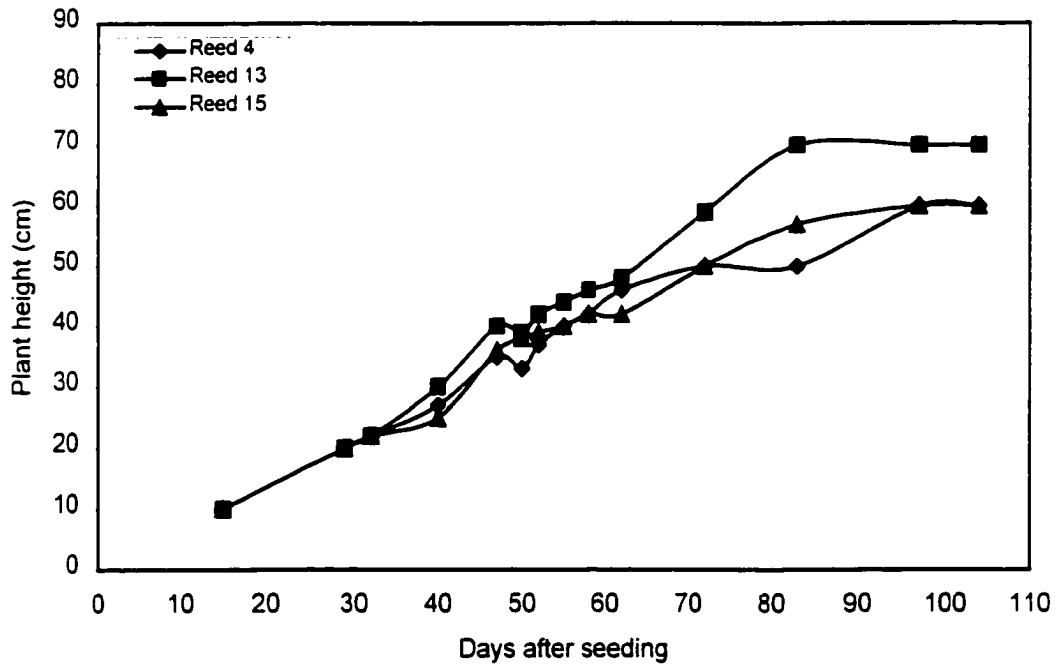
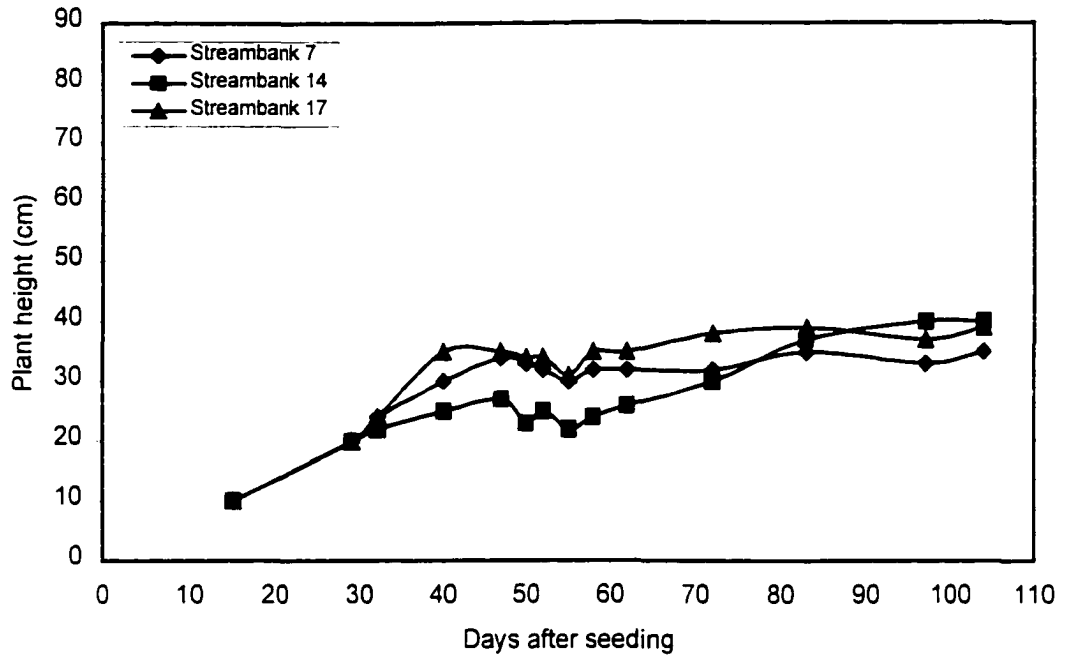


Figure D.4 Temporal variations in plant height of reed canarygrass



**Figure D.5** Temporal variations in plant height of streambank wheatgrass

Day	Plant species	#	Leaf area of 5 plants (cm <sup>2</sup> )	Number of plants	Total leaf area (cm <sup>2</sup> )	LAI	Mean LAI
25	Altai	1	111	44	977	0.38	0.33
		2	104	52	1079	0.42	
		9	64	38	488	0.19	
	Foxtail	5	152	44	1336	0.52	0.41
		12	116	42	977	0.38	
		18	85	50	848	0.33	
	Red top	3	49	45	437	0.17	0.18
		11	54	50	540	0.21	
		16	43	48	411	0.16	
	Reed	4	131	50	1311	0.51	0.45
		13	123	50	1234	0.48	
		15	103	45	925	0.36	
Stream	7	77	30	463	0.18	0.21	
	14	69	30	411	0.16		
	17	116	32	745	0.24		
33	Altai	1	155	45	1399	0.54	0.57
		2	173	54	1868	0.73	
		9	148	38	1128	0.44	
	Foxtail	5	207	50	2066	0.8	0.92
		12	252	48	2422	0.94	
		18	237	55	2607	1.01	
	Red top	3	167	50	1674	0.65	0.62
		11	148	52	1540	0.60	
		16	158	50	1578	0.61	
	Reed	4	342	55	3762	1.46	1.22
		13	262	56	2931	1.14	
		15	282	48	2705	1.05	
Stream	7	160	30	962	0.40	0.40	
	14	164	30	986	0.38		
	17	173	32	1104	0.43		
45	Altai	1	228	49	2235	0.87	0.92
		2	235	52	2441	0.95	
		9	318	38	2415	0.94	
	Foxtail	5	392	78	6117	2.38	2.12
		12	331	76	5037	1.96	
		18	360	72	5191	2.02	
	Red top	3	162	66	2133	0.83	0.88
		11	207	57	2364	0.92	
		16	168	68	2287	0.89	
	Reed	4	506	80	8096	3.15	2.91
		13	445	82	7299	2.84	
		15	489	72	7042	2.74	
Stream	7	154	46	1413	0.55	0.53	
	14	163	45	1464	0.57		
	17	126	48	1207	0.47		

**Table D.1 Summary of leaf areas and LAI**



Day	Plant species	#	Leaf area of 5 plants (cm <sup>2</sup> )	Number of plants	Total leaf area (cm <sup>2</sup> )	LAI	Mean LAI
55	Altai	1	292	49	2862	1.11	1.07
		2	285	52	2965	1.15	
		9	320	38	2432	0.95	
	Foxtail	5	587	80	9388	3.65	3.13
		12	511	80	8172	3.20	
		18	435	75	6521	2.54	
	Red top	3	201	70	2817	1.10	1.12
		11	230	60	2763	1.10	
		16	211	70	2953	1.15	
	Reed	4	582	85	9900	3.85	3.92
		13	542	85	9219	3.59	
		15	743	75	11139	4.33	
Stream	7	144	48	1384	0.54	0.57	
	14	120	48	1150	0.45		
	17	185	50	1848	0.72		
33	Altai	1	234	46	2157	0.84	1.20
		2	217	45	1955	1.25	
		9	285	68	3882	1.51	
	Foxtail	5	747	90	13442	5.23	5.30
		12	694	85	11806	4.59	
		18	864	90	15544	6.05	
	Red top	3	300	75	4497	1.75	2.10
		11	423	69	5833	2.27	
		16	420	74	6219	2.42	
	Reed	4	565	90	10177	3.96	4.30
		13	684	92	12590	4.90	
		15	660	81	10690	4.16	
Stream	7	238	55	2621	1.02	1.20	
	14	266	56	2981	1.16		
	17	288	62	3572	1.39		

**Table D.1 (Cont.) Summary of leaf areas and LAI**

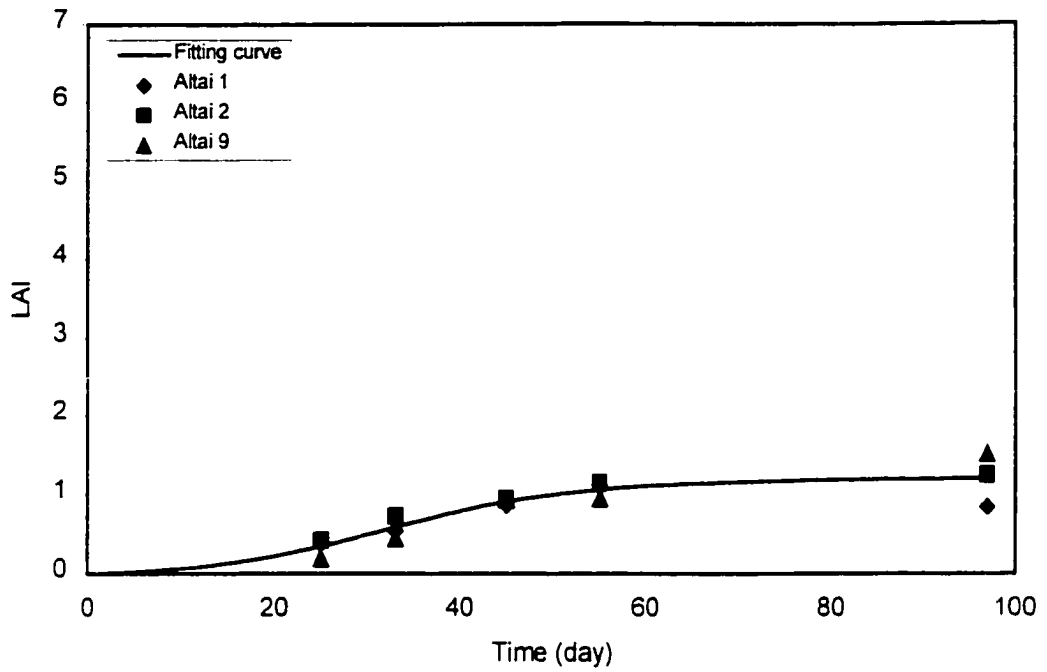


**Figure D.6 LAI and fitting curve of Altai wildrye**

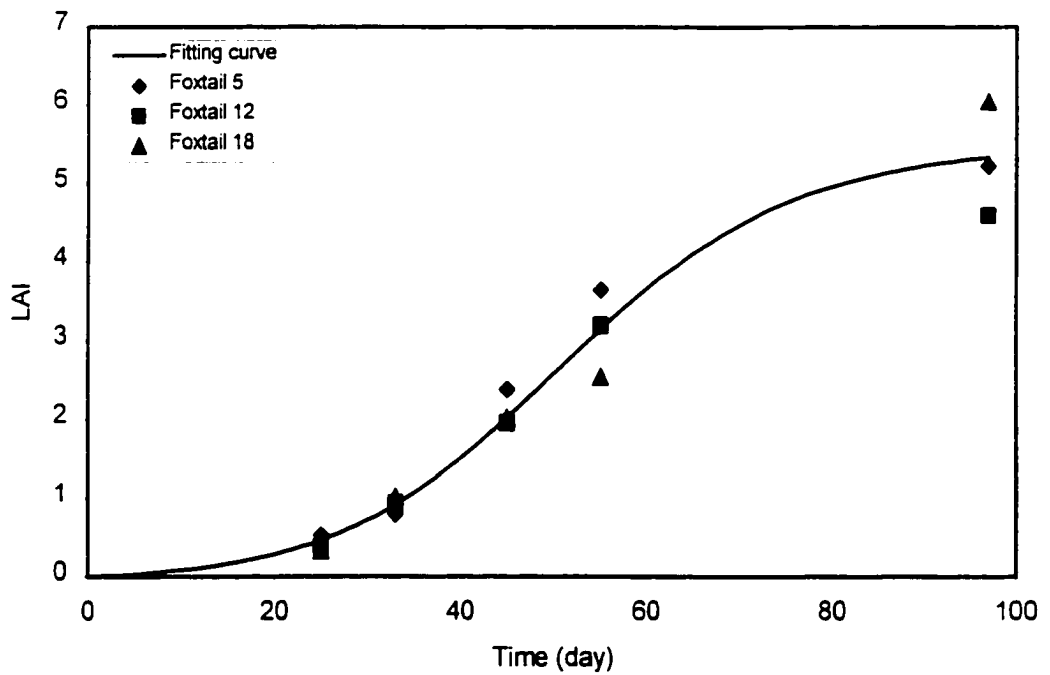


**Figure D.7 LAI and fitting curve of creeping foxtail**

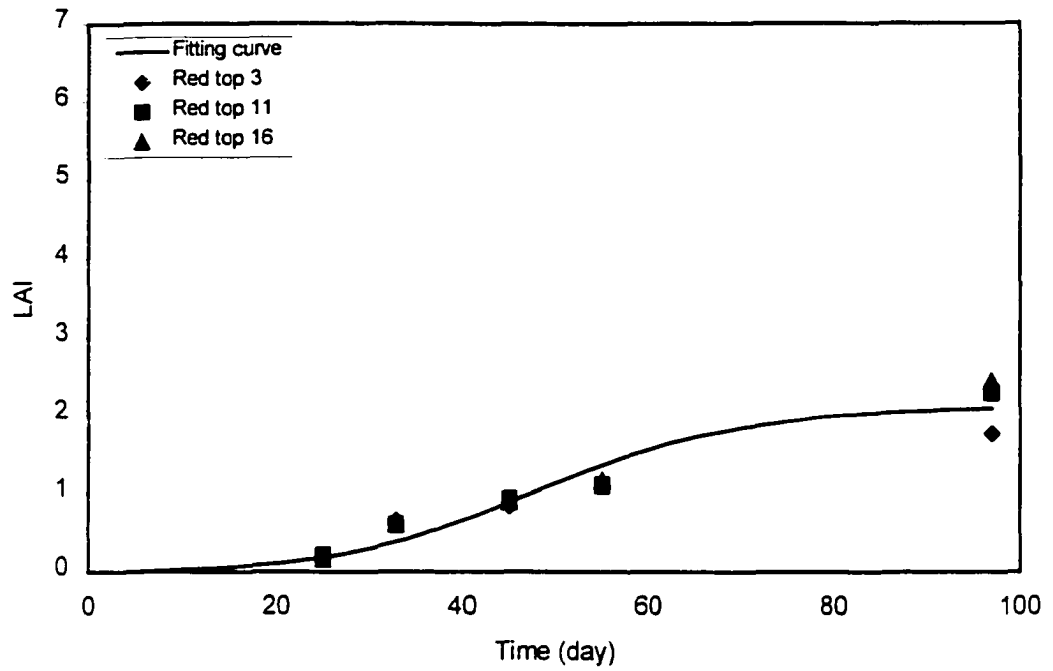


**Figure D.8 LAI and fitting curve of red top**

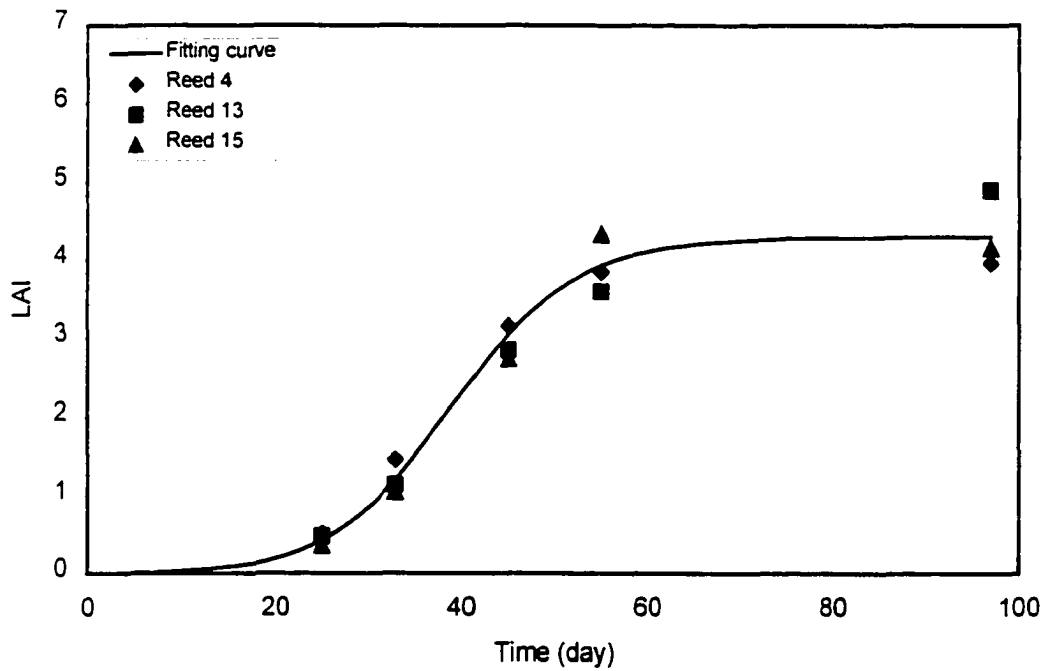


**Figure D.9 LAI and fitting curve of creeping foxtail**

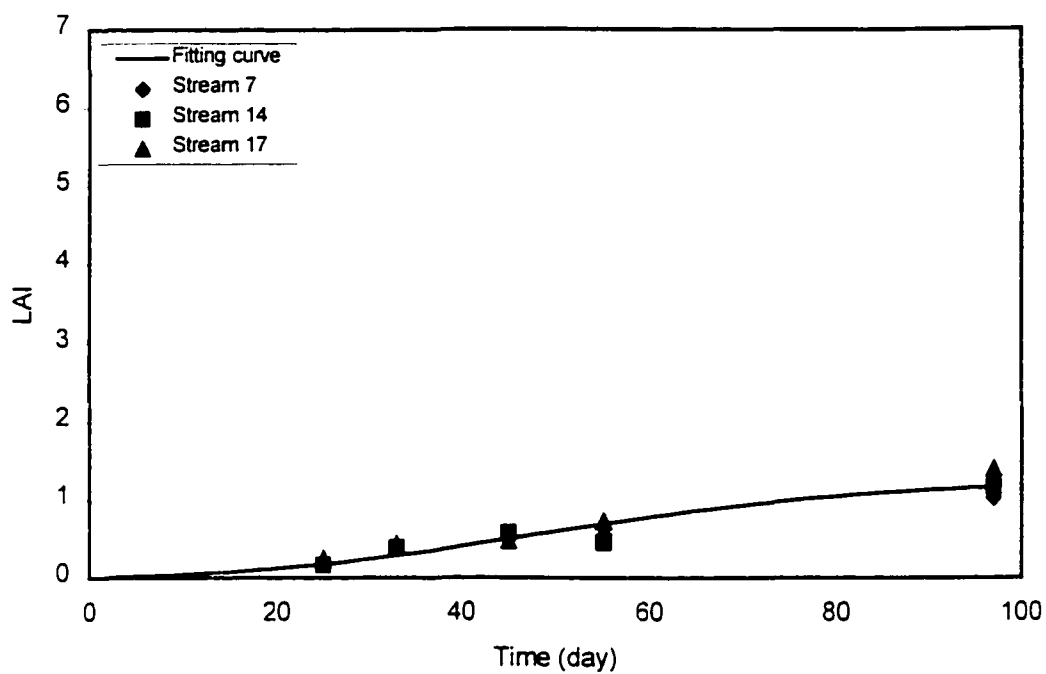


**Figure D.10 LAI and fitting curve of streambank wheatgrass**

<b>Plant species</b>	<b><math>c_1</math></b>	<b><math>c_2</math></b>
Altai wildrye	1.35	7.0
Creeping foxtail	2.6	6.1
Red top	2.8	7.0
Reed canarygrass	4.0	12.2
Streambank wheatgrass	1.5	4.0

**Table D.2 Fitting parameters of the S-shape curve, which describes LAI of plants**

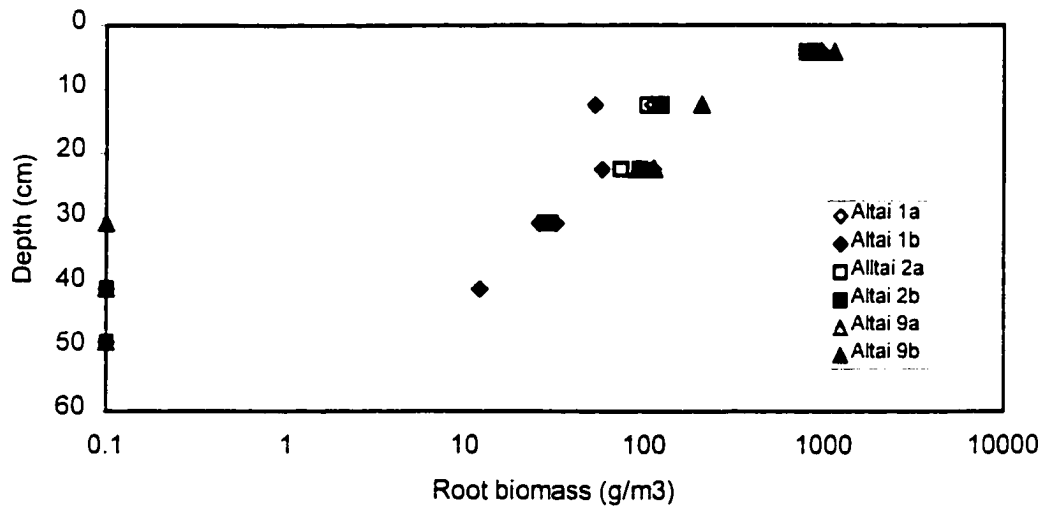


Figure D.11 Root biomass of Altai wildrye

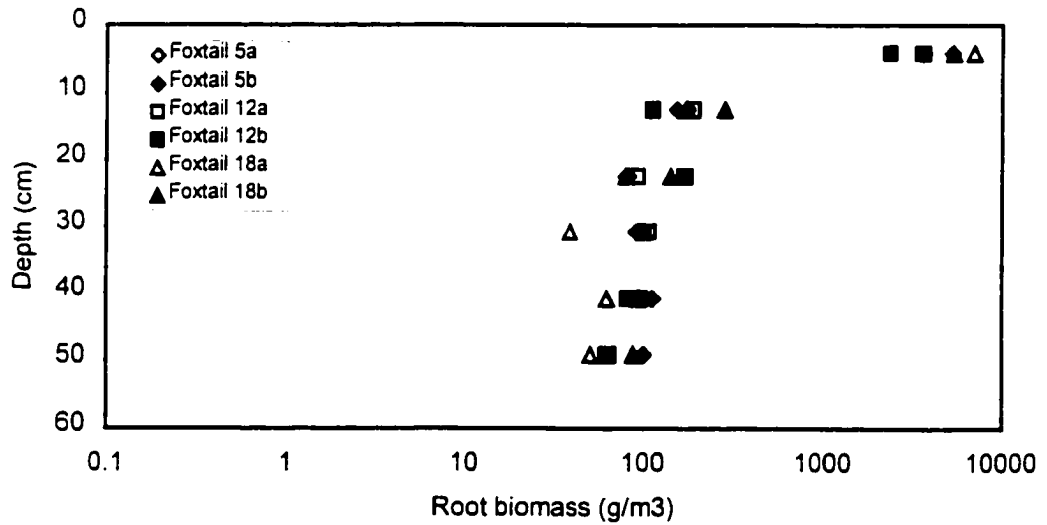


Figure D.12 Root biomass of creeping foxtail

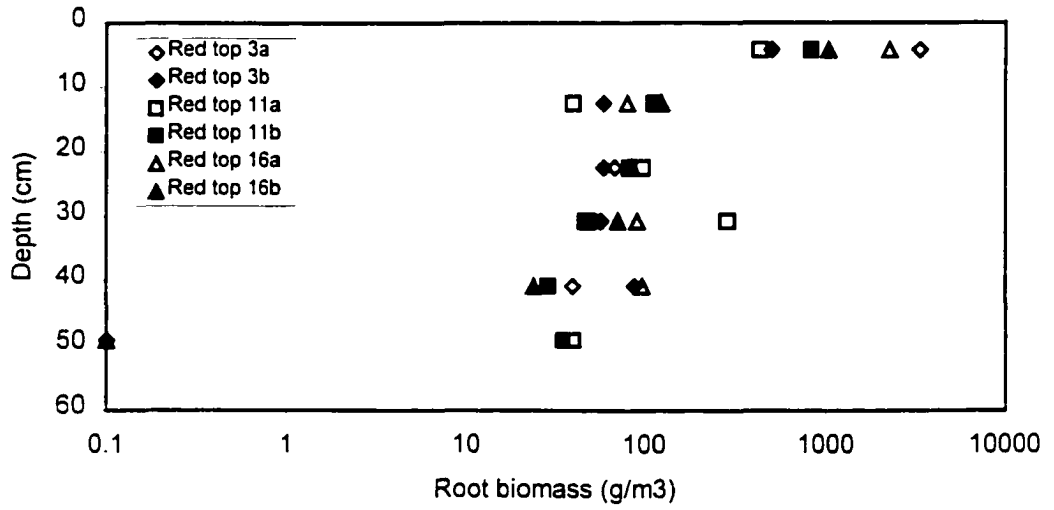


Figure D.13 Root biomass of red top

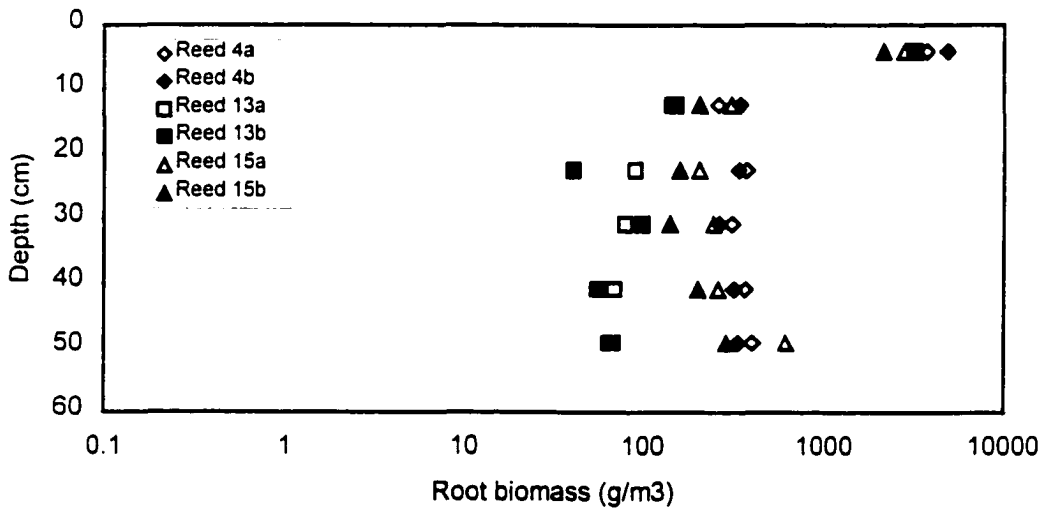
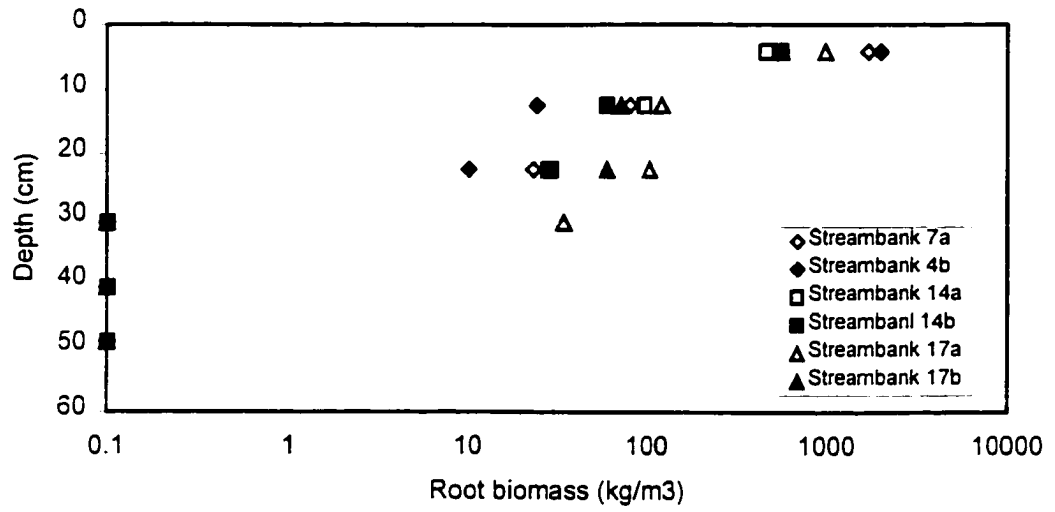


Figure D.14 Root biomass of reed canarygrass



**Figure D.15 Root biomass of streambank wheatgrass**

<b>Plant species</b>	<b>#</b>	<b>Dry shoot weight (g)</b>
Altai wildrye	1	32.73
	2	32.27
	9	48.22
Creeping foxtail	5	117.88
	12	114.70
	18	127.33
Red top	3	73.01
	11	92.98
	16	94.21
Reed canarygrass	4	126.62
	13	150.29
	15	126.04
Streambank wheatgrass	7	22.79
	14	25.40
	17	32.43

**Table D.3      Dry shoot weights of plants**



## Appendix E

### ***Surface settlement, model prediction, growth room ambient measurements and watering***

---

This appendix presents the measurements of the surface settlements occurred in each lysimeter, measurements of climatic parameters in the growth room, dates and amount of water added to each lysimeter.

The measured and fitted Soil Water Characteristic Curve of CT that was utilized in the model in presented in Figure E.1. This curve was used to determine the unsaturated hydraulic conductivity versus suction curve (Figure E.2). The procedure was described in Chapter 3 of the thesis.

Figures E.3 to E.8 present a comparison of the measured tailings settlements with those predicted with the plant dewatering model.

Figures E.9 to E.14 present a comparison of the measured solids contents with those predicted with the plant dewatering model. On Day 1 the black circles represent the initial solids contents, which were measured from samples taken with a mini-piston sampler built at the University of Alberta. On Days 20, 42, 61 and 77 the white circles represent measurements of solids content taken by either the TDR probes or the neutron probe. On Day 77 the black circles represent the solids content measured from samples taken at the end of the experiment. Finally, the solid line shown in all figures represent the solids content profile predicted with the plant dewatering model.

Figure E.15 present a comparison of measured and predicted bearing capacity for each treatment. These figures are described in detail in Chapter 4 of the thesis.

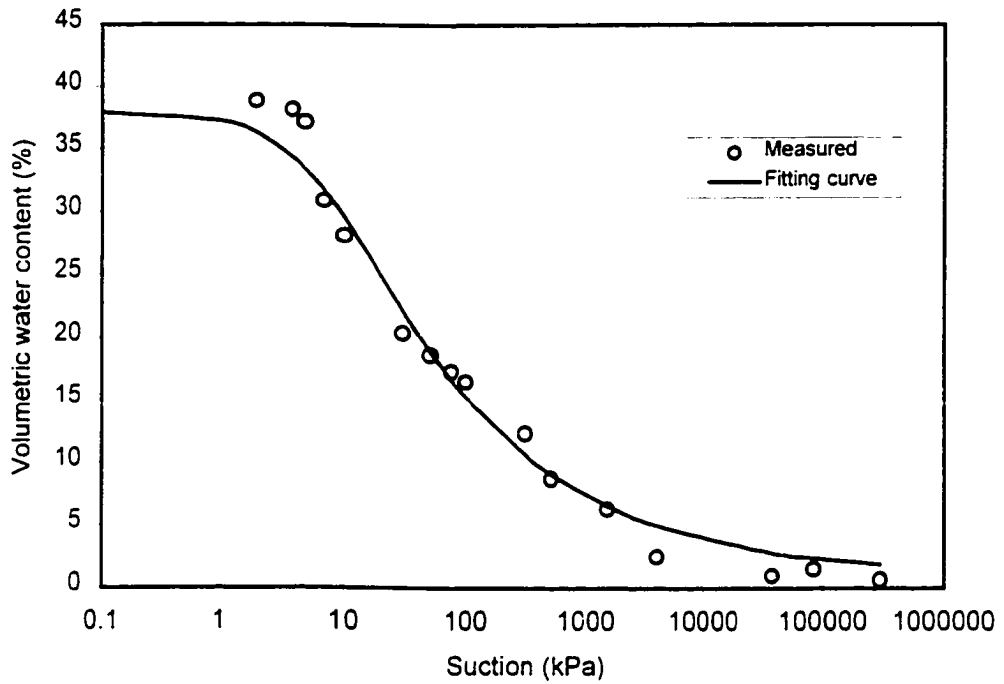


**Figure E.1 Measured and fitted Soil Water Characteristic Curve (SWCC) of CT**

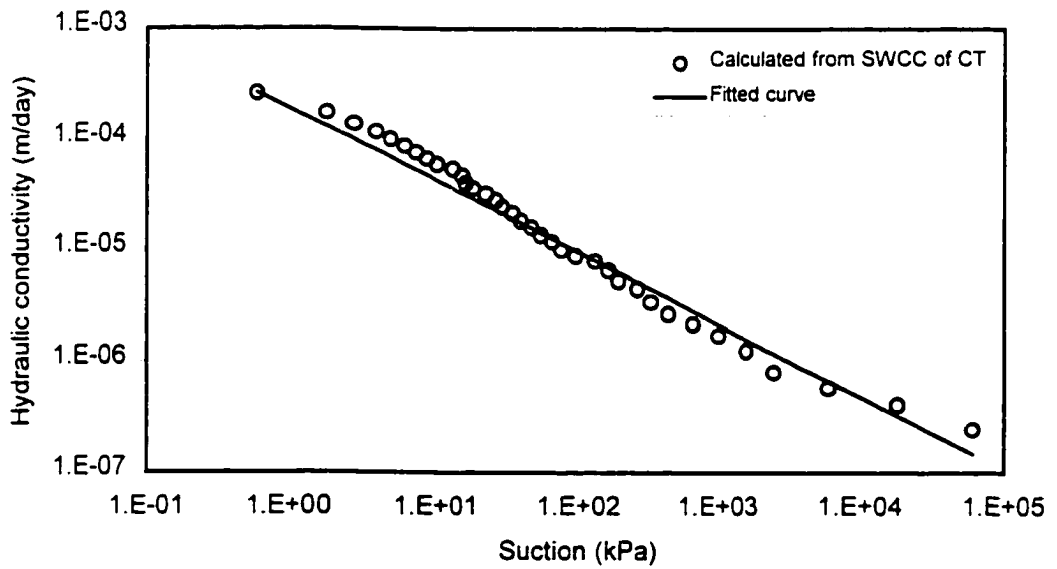


**Figure E.2 Unsaturated hydraulic conductivity of CT**

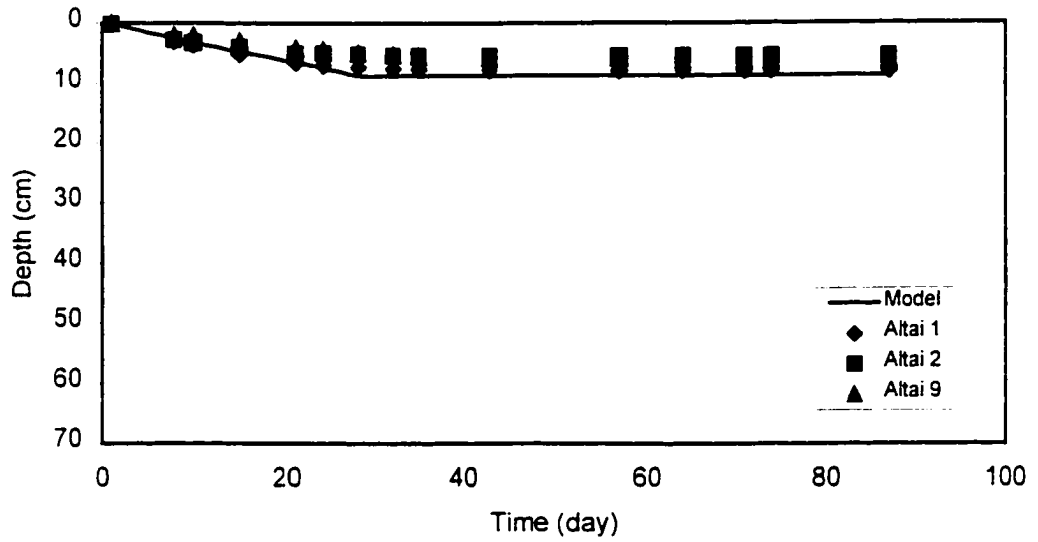


**Figure E.3 Tailings settlement on Altai wildrye**

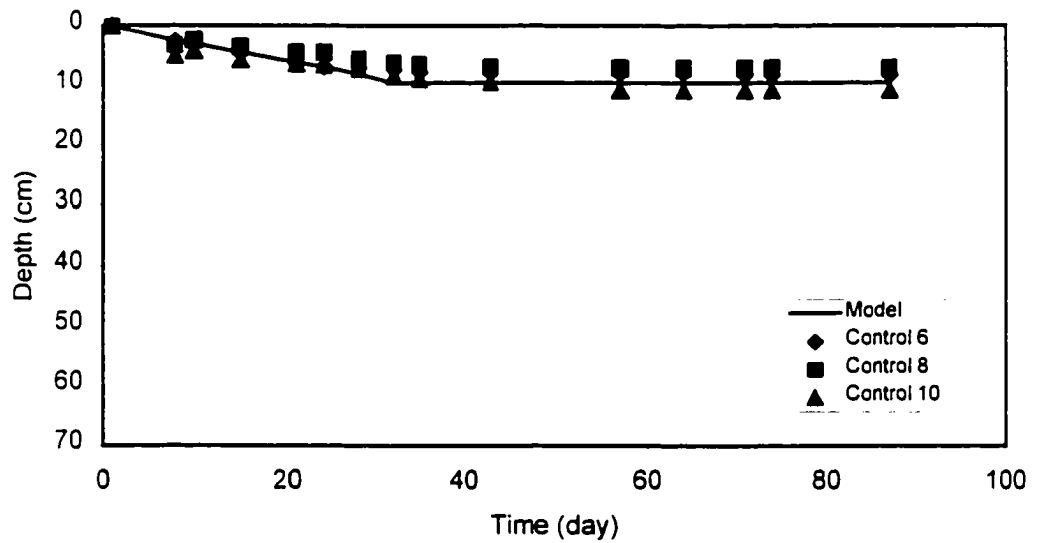


**Figure E.4 Tailings settlement on control**

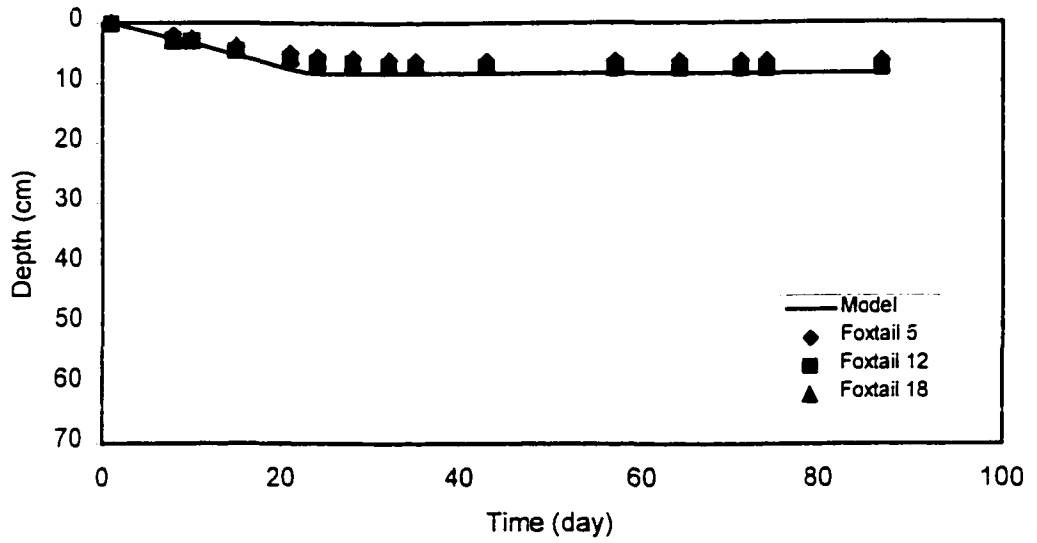


**Figure E.5 Tailings settlement on creeping foxtail**

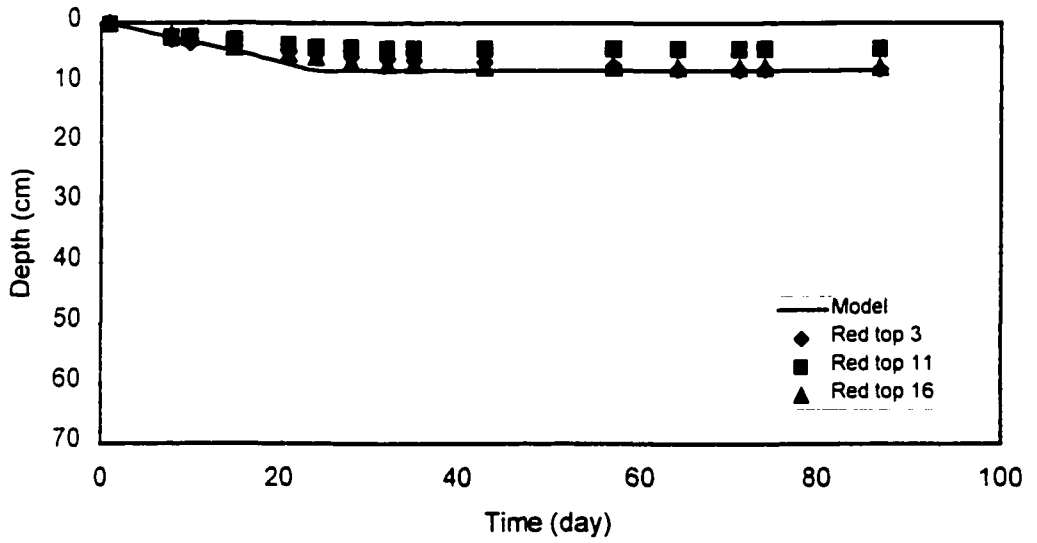


**Figure E.6 Tailings settlement on red top**

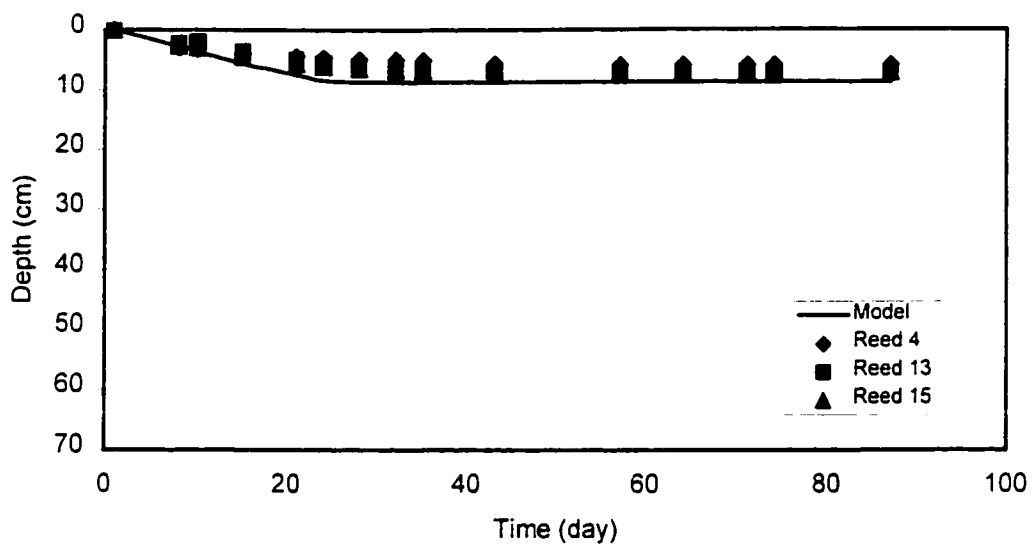


**Figure E.7 Tailings settlement on reed canarygrass**

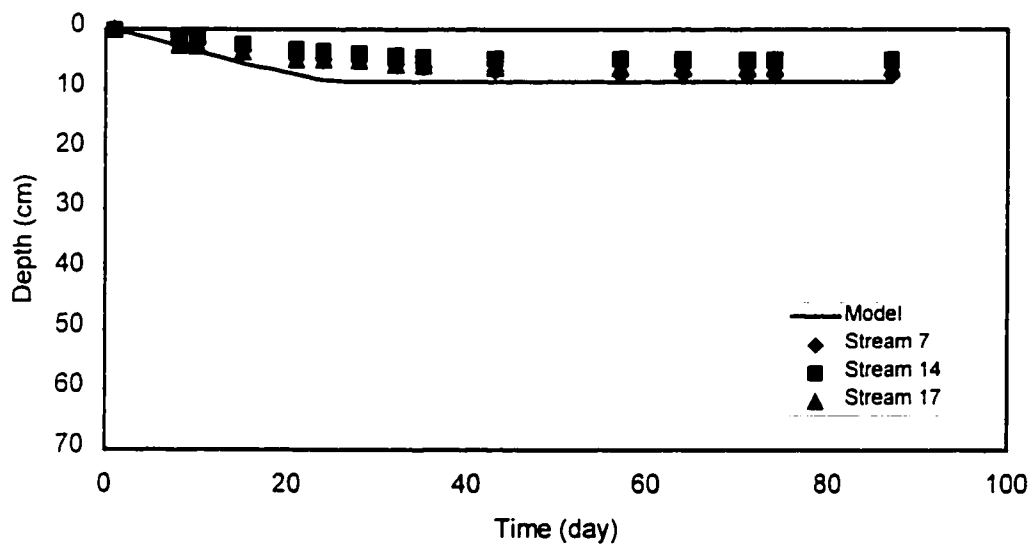


**Figure E.8 Tailings settlement on streambank wheatgrass**

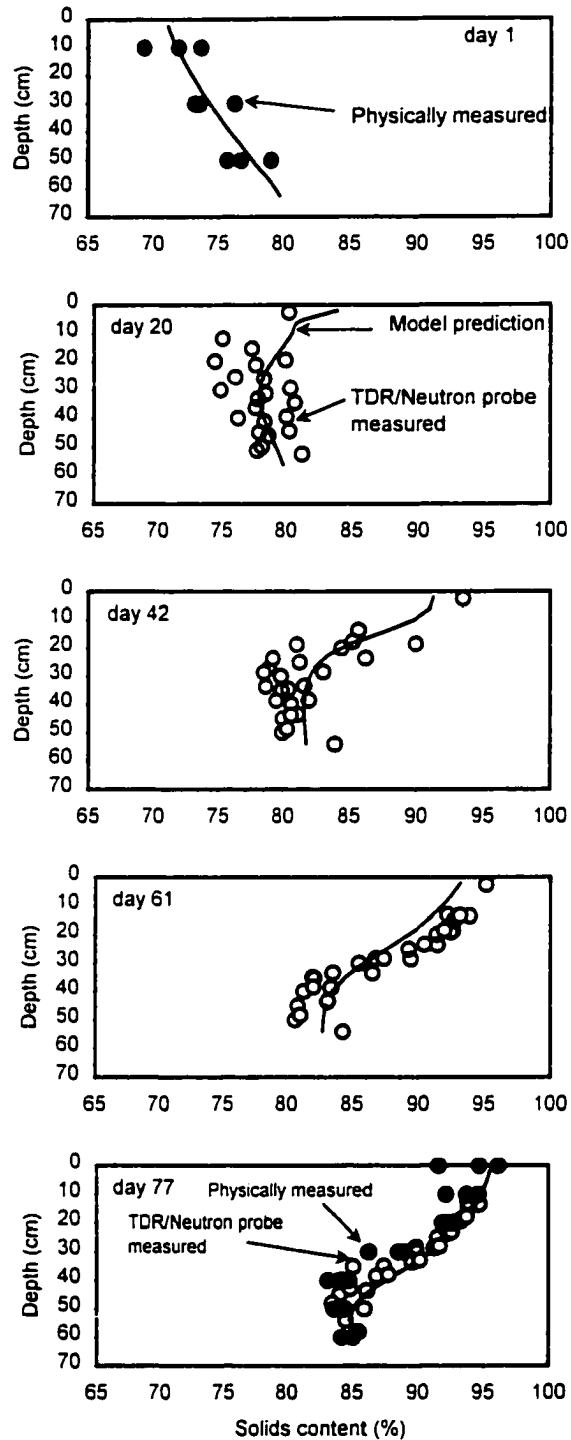


**Figure E.9 Measured and predicted solids content profile of Altai wildrye**

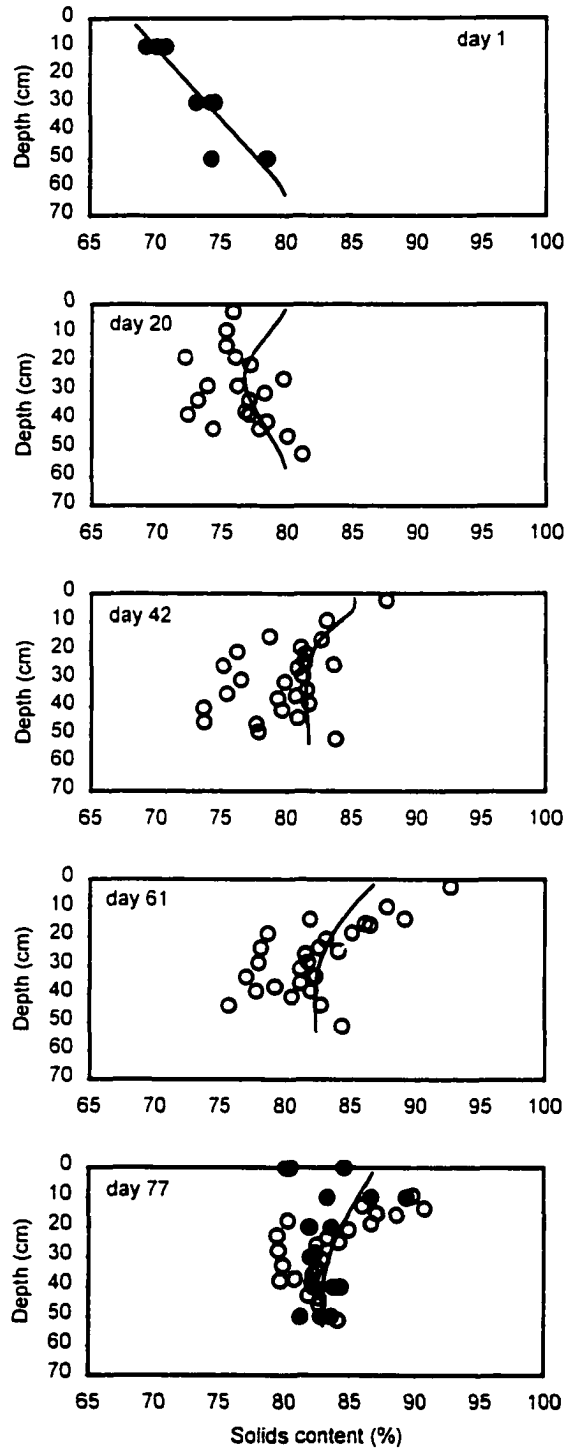


**Figure E.10 Measured and predicted solids content profile of control**

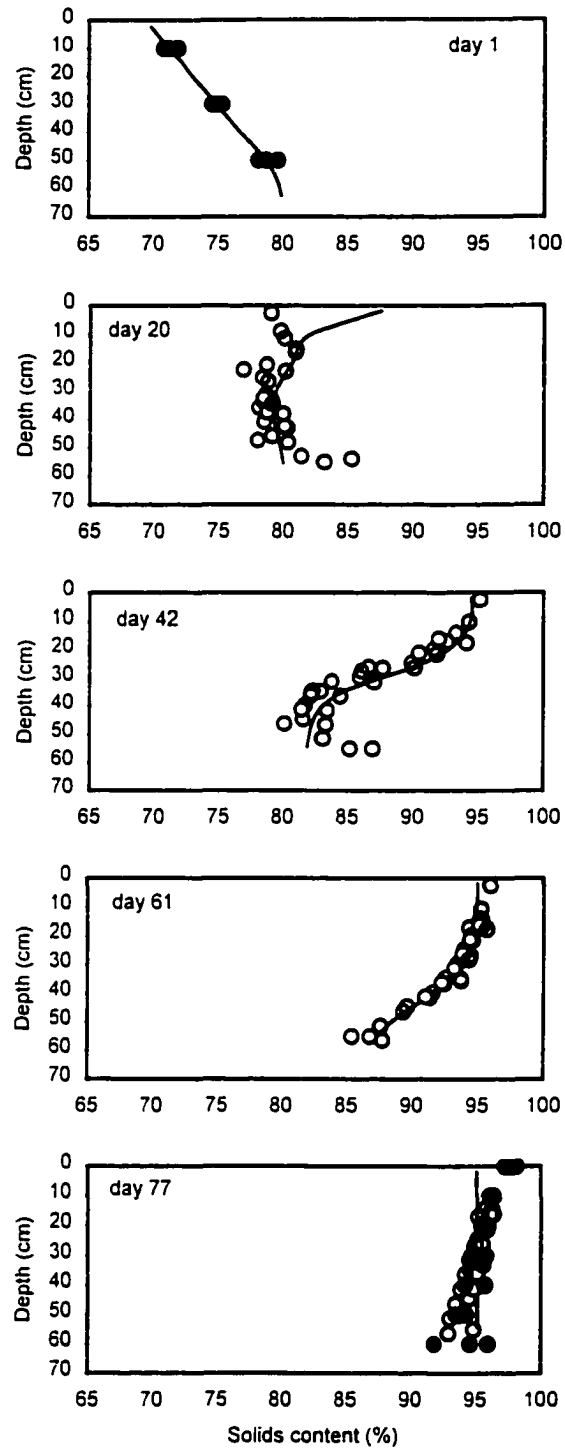


**Figure E.11 Measured and predicted solids content profile of creeping foxtail**



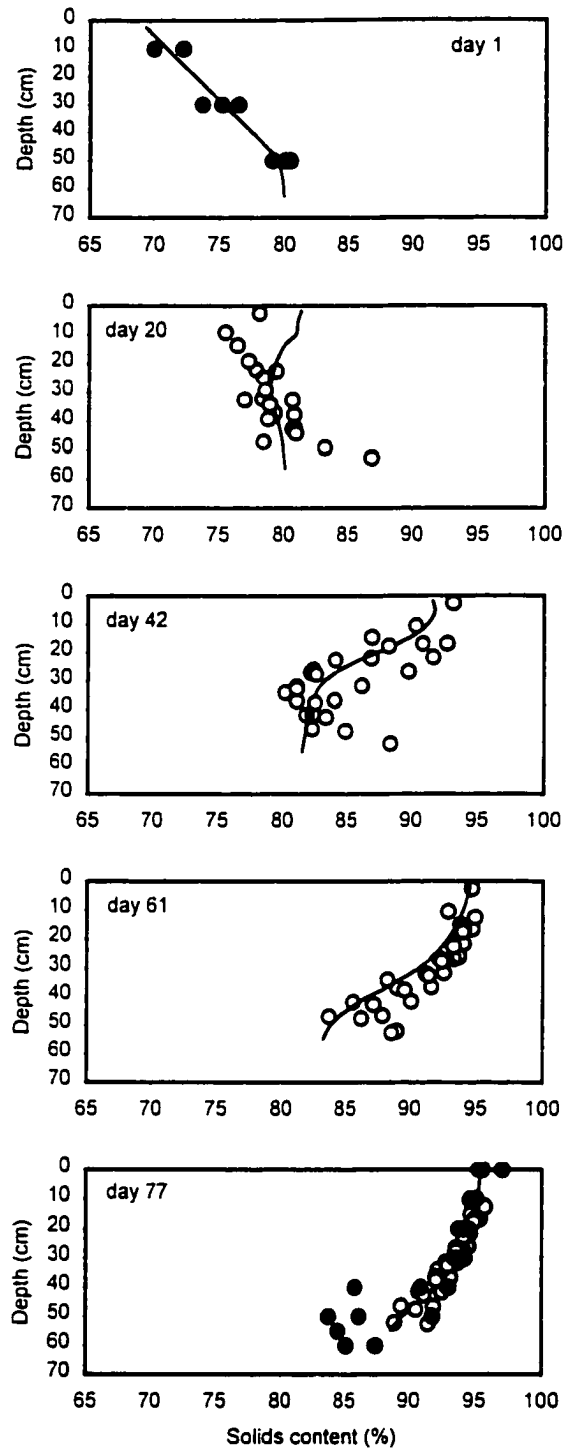


**Figure E.12 Measured and predicted solids content profile of red top**

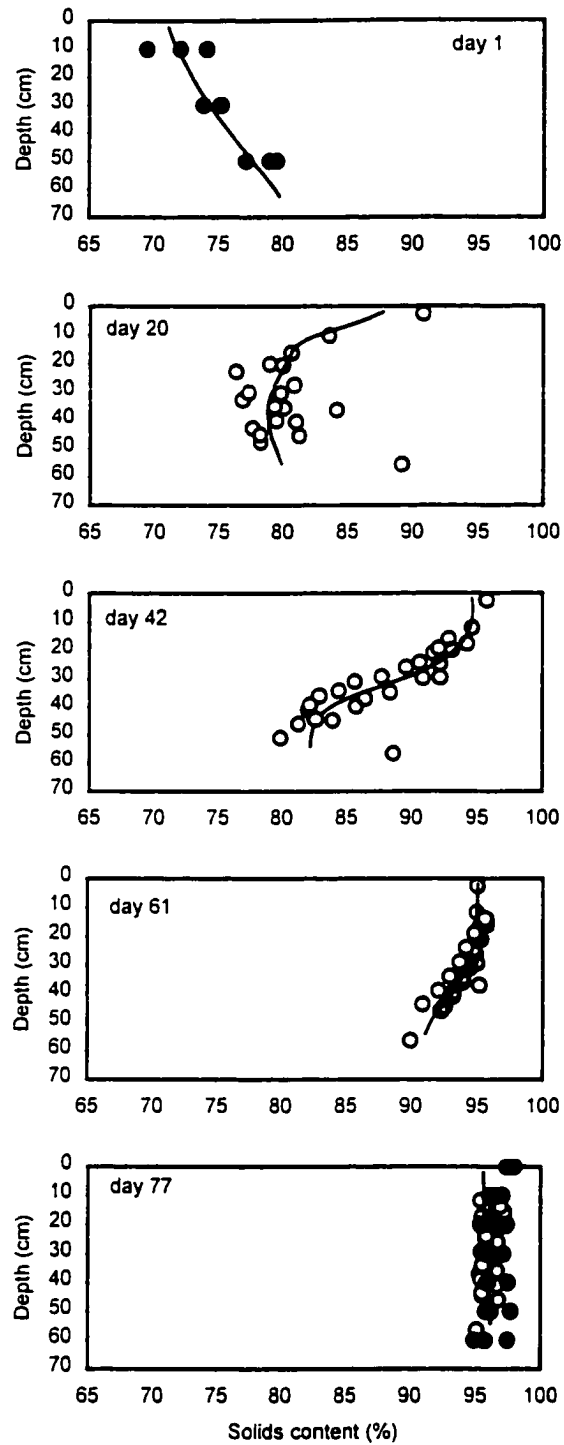


**Figure E.13 Measured and predicted solids content profile of reed canarygrass**

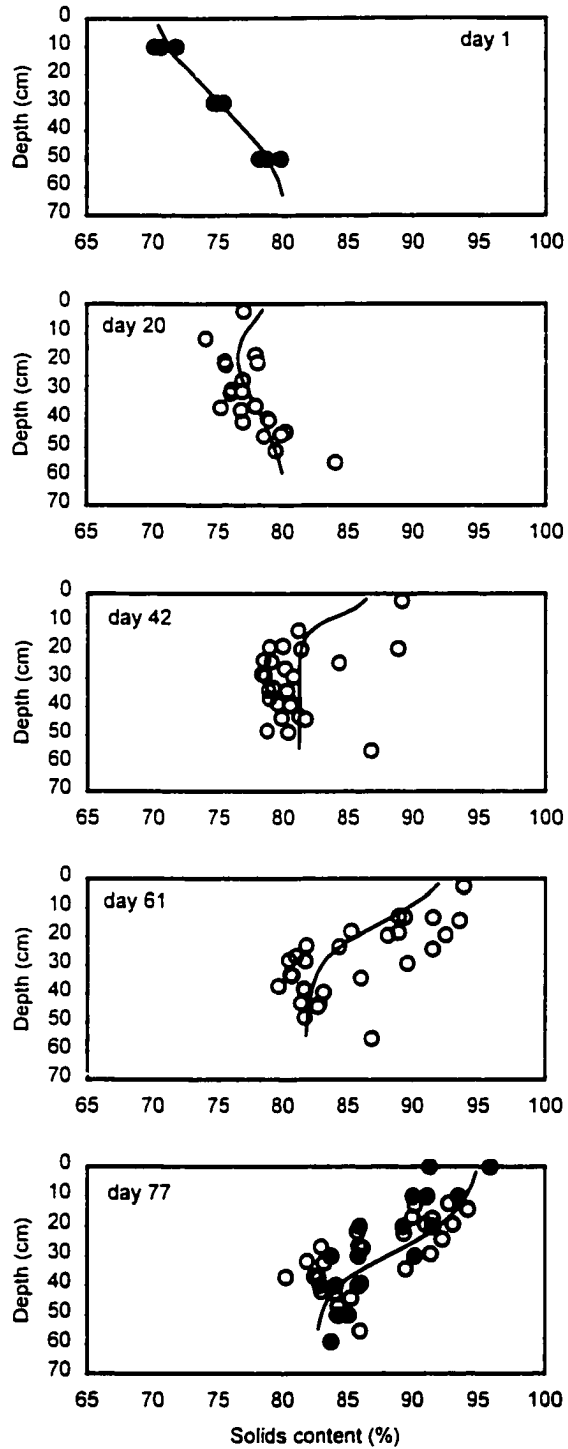


**Figure E.14 Measured and predicted solids content profile of streambank wheatgrass**

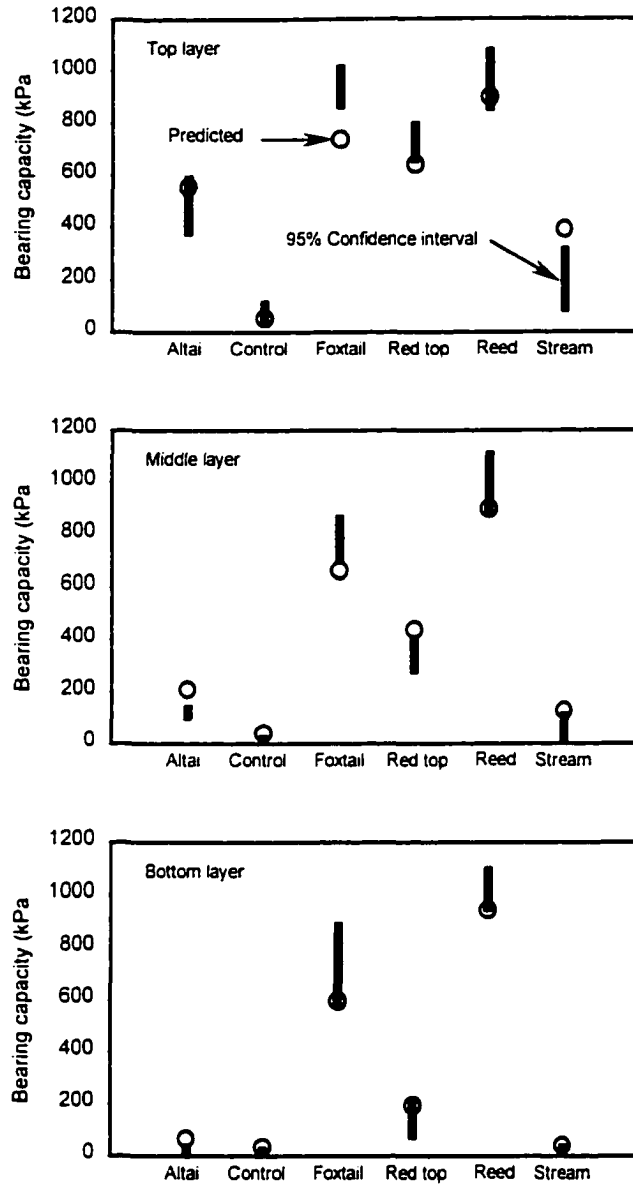


**Figure E.15 Measured and predicted bearing capacity**

Day	T <sub>max</sub>	T <sub>min</sub>	RH	T <sub>mean</sub>	e <sub>s</sub> (T <sub>mean</sub> ) kPa	E (mm)
26	24.5	21.5	0.6	23.0	2.8	3.9
27	24.0	21.5	0.6	22.8	2.8	3.8
32	24.5	20.5	0.6	22.5	2.7	4.0
33	24.0	20.5	0.5	22.3	2.7	4.4
34	24.0	20.5	0.5	22.3	2.7	4.6
35	24.5	20.5	0.6	22.5	2.7	3.8
36	25.0	21.0	0.5	23.0	2.8	4.4
39	25.0	20.5	0.5	22.8	2.8	4.5
40	24.5	20.5	0.5	22.5	2.7	4.4
41	25.0	20.5	0.5	22.8	2.8	4.8
42	24.0	20.5	0.6	22.3	2.7	4.0
43	24.5	21.0	0.5	22.8	2.8	4.7
46	25.0	20.5	0.5	22.8	2.8	4.6
47	25.0	20.5	0.5	22.8	2.8	4.6
48	25.0	20.5	0.5	22.8	2.8	4.8
49	25.0	20.5	0.5	22.8	2.8	5.0
53	25.0	20.5	0.5	22.8	2.8	4.3
55	25.0	20.5	0.5	22.8	2.8	4.6
70	25.0	20.5	0.5	22.8	2.8	4.4
75	25.0	20.5	0.5	22.8	2.8	4.7
82	25.0	20.5	0.5	22.8	2.8	4.7
85	25.0	20.5	0.5	22.8	2.8	4.3
Avg	24.7	20.6	0.5	22.7	Average	4.4

**Table E.1**      **Measurements of temperature, relative humidity and pan evaporation taken on the growth room (Day 26 corresponds to March 3, 1998)**

<b>Day</b>	<b>Altai 1</b>	<b>Altai 2</b>	<b>Altai 9</b>	<b>Control 6</b>	<b>Control 8</b>	<b>Control 10</b>
40	0.97	0.97	0.00	0.00	0.00	0.00
42	0.47	0.47	0.00	0.00	0.00	0.00
43	0.97	0.97	0.00	0.00	0.00	0.00
47	0.97	0.97	0.39	0.39	0.00	0.00
54	0.97	0.97	0.97	0.97	0.97	0.00
56	1.95	1.95	1.95	1.28	0.69	0.37
62	1.95	1.95	1.95	0.97	0.97	0.00
67	1.95	0.97	0.97	0.97	0.97	0.00
69	0.00	0.97	0.97	0.00	0.00	0.00
71	0.97	0.97	0.97	0.97	0.97	0.00
75	0.00	0.00	0.00	0.00	0.00	0.00
81	0.00	0.00	0.00	0.00	0.00	0.00

<b>Day</b>	<b>Foxtail 5</b>	<b>Foxtail 12</b>	<b>Foxtail 18</b>	<b>Reed 4</b>	<b>Reed 13</b>	<b>Reed 15</b>
40	0.97	1.95	0.78	1.95	0.78	0.97
42	0.47	0.47	0.47	0.47	0.47	0.47
43	0.00	0.97	0.00	0.97	0.00	0.97
47	0.97	0.97	0.97	0.97	0.97	0.97
54	0.97	0.97	0.97	0.97	0.97	0.97
56	2.09	1.95	1.95	1.95	1.95	1.95
62	1.95	1.95	1.95	3.89	1.95	2.92
67	2.92	2.92	2.92	3.89	3.89	3.89
69	0.00	0.00	0.00	0.00	0.00	0.00
71	0.97	0.97	0.97	3.89	1.95	1.95
75	1.95	1.95	1.95	3.89	1.95	1.95
81	0.00	0.00	0.00	2.92	2.92	2.92

<b>Day</b>	<b>Red 3</b>	<b>Red 11</b>	<b>Red 16</b>	<b>Stream 7</b>	<b>Stream 14</b>	<b>Stream 17</b>
40	1.17	0.97	0.00	0.00	0.00	0.97
42	0.47	0.47	0.47	0.00	0.00	0.47
43	0.97	0.00	0.00	0.00	0.00	0.97
47	0.97	0.97	0.97	0.00	0.39	0.97
54	0.97	0.97	0.97	0.00	0.97	0.97
56	1.95	1.95	1.95	0.97	1.95	1.95
62	1.95	1.95	1.95	0.97	1.95	1.95
67	0.97	0.97	0.97	0.97	0.97	1.95
69	0.97	0.97	0.97	0.00	0.97	0.00
71	0.97	0.97	0.97	0.00	0.97	0.97
75	0.00	0.00	0.00	0.00	0.00	0.00
81	0.00	0.00	0.00	0.00	0.00	0.00

**Table E.2      Amount of water added to each lysimeter (Day 40 corresponds to March 17, 1998)**

## Appendix F

### **Climatic data and calculated $ET_0$ for Fort McMurray for 1997 and 1998**

Hourly climatic data of the Fort McMurray region were provided by Gord McKenna from Syncrude Canada Ltd. These hourly data were reduced to daily values to be used in the plant dewatering model. The reduced data are presented in its entirety in this appendix. The calculated values of potential evapotranspiration using the Penman-Monteith equation are also included. These data were used to conduct a Class A prediction of bearing capacity on composite tailings as described in Chapter 6 of the thesis.

DATE	T <sub>max</sub> (C)	T <sub>min</sub> (C)	RH <sub>max</sub> (%)	RH <sub>min</sub> (%)	u <sub>z</sub> (m/s)	R <sub>s</sub> (MJ/m <sup>2</sup> /d)	P (mm)	ET <sub>0</sub> (mm/d)
1-May-97	13.14	-1.42	87.60	17.76	2.23	25.35	0	5.55
2-May-97	16.69	-2.14	98.00	18.35	1.59	24.27	0	4.51
3-May-97	19.36	0.15	94.10	17.23	1.76	23.03	0	5.07
4-May-97	14.59	2.78	65.23	26.80	3.48	20.65	0	8.02
5-May-97	17.53	0.77	101.30	24.15	2.10	22.45	0	4.95
6-May-97	16.82	5.15	103.30	49.74	3.76	12.82	2.2	4.37
7-May-97	13.33	2.14	96.40	34.06	2.87	19.97	0	5.03
8-May-97	18.58	4.15	91.00	31.55	2.59	18.21	0	5.38
9-May-97	22.14	5.40	95.80	18.24	3.96	15.47	0	7.85
10-May-97	15.31	5.75	101.10	37.84	3.68	18.66	0.4	5.77
11-May-97	18.19	3.79	101.30	24.62	2.48	20.56	0.2	5.42
12-May-97	18.81	5.74	85.60	33.51	6.36	10.34	0.8	9.83
13-May-97	10.16	2.44	75.10	38.84	4.13	22.96	0	7.41
14-May-97	14.72	-0.81	89.50	37.67	5.12	21.65	0	7.66
15-May-97	21.31	6.59	75.20	24.39	5.06	25.85	0	12.51
16-May-97	15.38	2.12	99.40	45.71	2.48	14.10	0	3.43
17-May-97	10.68	5.00	86.50	48.13	3.73	11.29	0	4.61
18-May-97	9.49	3.75	74.00	44.60	2.49	9.19	0	3.56
19-May-97	10.36	2.19	76.00	39.02	3.22	11.50	0	4.82
20-May-97	10.98	4.20	86.90	45.32	1.76	8.09	0	2.29
21-May-97	7.37	3.34	102.00	58.47	2.48	7.07	2.6	1.78
22-May-97	10.51	2.22	104.80	53.40	1.49	13.23	0	2.11
23-May-97	12.81	4.35	100.00	45.92	1.61	12.15	0	2.40
24-May-97	18.82	7.21	81.00	32.31	4.13	19.37	0	8.58
25-May-97	12.21	3.75	90.80	56.55	4.49	20.29	0	5.67
26-May-97	13.60	2.12	97.50	54.79	4.17	20.55	0	5.11
27-May-97	13.49	2.88	105.20	76.90	2.91	13.44	1.6	2.23
28-May-97	23.04	6.84	99.60	39.96	2.02	18.12	0.4	4.42
29-May-97	19.11	9.46	96.90	26.30	2.21	24.07	0	6.13
30-May-97	19.82	6.70	99.60	33.74	3.09	14.64	5.4	5.23
31-May-97	26.27	8.88	105.30	22.63	1.38	23.26	0.2	5.22

**Table F.1 Climatic data and calculated potential evapotranspiration for May, 1997**



DATE	T <sub>max</sub> (C)	T <sub>min</sub> (C)	RH <sub>max</sub> (%)	RH <sub>min</sub> (%)	u <sub>z</sub> (m/s)	R <sub>s</sub> (MJ/m <sup>2</sup> /d)	P (mm)	ET <sub>0</sub> (mm/d)
1-Jun-97	18.26	12.32	103.20	50.42	1.94	6.93	3.6	2.24
2-Jun-97	24.00	9.43	101.00	26.98	3.12	27.75	0	8.20
3-Jun-97	25.88	9.64	79.10	23.90	1.74	28.25	0	7.30
4-Jun-97	25.07	10.94	96.50	37.61	2.42	10.68	1.8	4.28
5-Jun-97	19.08	12.49	103.40	71.90	2.29	4.90	6.6	1.34
6-Jun-97	23.81	14.66	105.70	42.42	2.44	17.65	0	5.16
7-Jun-97	25.33	14.04	98.80	30.70	2.02	23.59	0	6.25
8-Jun-97	24.35	12.16	104.50	47.61	2.52	10.97	9.6	3.79
9-Jun-97	22.74	9.24	102.20	25.08	4.37	29.44	0.2	10.24
10-Jun-97	23.91	9.66	86.60	27.83	2.53	29.17	0	8.22
11-Jun-97	24.15	9.50	102.10	36.55	1.94	29.82	0	6.49
12-Jun-97	25.67	9.97	96.70	28.04	2.17	29.22	0	7.35
13-Jun-97	18.49	13.51	103.80	50.74	3.30	8.58	3	3.82
14-Jun-97	24.20	13.85	106.30	30.21	2.83	21.79	0.2	7.00
15-Jun-97	22.79	12.35	98.90	47.72	2.56	19.60	0	5.22
16-Jun-97	24.47	13.04	104.10	39.47	3.06	18.24	0.8	6.12
17-Jun-97	24.99	11.02	105.90	32.86	1.42	22.88	0.2	4.97
18-Jun-97	24.55	15.09	91.10	47.83	3.79	17.84	0.2	7.16
19-Jun-97	16.01	12.23	104.60	77.00	3.41	4.87	1.4	1.54
20-Jun-97	17.94	11.40	104.90	76.90	3.14	7.78	2.4	1.90
21-Jun-97	20.62	12.51	99.90	47.28	1.86	19.39	1.2	4.33
22-Jun-97	24.11	11.55	94.20	30.70	2.09	20.38	0	5.78
23-Jun-97	23.95	9.49	102.30	40.40	2.22	20.51	0	5.18
24-Jun-97	20.48	12.57	100.30	38.69	3.07	20.18	0	6.20
25-Jun-97	23.70	10.19	91.90	35.94	1.98	21.16	0	5.52
26-Jun-97	24.41	10.77	104.20	33.20	2.15	23.58	3	6.01
27-Jun-97	14.53	7.60	106.20	61.53	2.68	16.45	11	3.45
28-Jun-97	15.08	6.86	97.70	47.63	1.72	20.79	0.8	3.89
29-Jun-97	18.87	6.31	100.30	35.92	2.03	19.17	0	4.46
30-Jun-97	21.61	5.91	106.40	28.49	1.47	27.08	0	5.32

**Table F.2 Climatic data and calculated potential evapotranspiration for June, 1997**

DATE	T <sub>max</sub> (C)	T <sub>min</sub> (C)	RH <sub>max</sub> (%)	RH <sub>min</sub> (%)	u <sub>z</sub> (m/s)	R <sub>s</sub> (MJ/m <sup>2</sup> /d)	P (mm)	ET <sub>0</sub> (mm/d)
1-Jul-97	23.81	14.10	83.10	39.39	4.43	25.52	0	10.62
2-Jul-97	25.42	9.80	89.20	16.80	2.23	28.32	0	8.09
3-Jul-97	28.76	11.40	88.30	22.89	2.00	21.48	0	6.68
4-Jul-97	29.33	13.64	91.50	23.37	1.59	26.64	0	6.84
5-Jul-97	30.98	13.82	92.40	17.28	2.24	27.64	0	8.61
6-Jul-97	31.92	14.32	89.80	19.28	2.13	25.87	0	8.22
7-Jul-97	31.91	18.32	77.90	22.19	2.84	26.09	0.4	10.64
8-Jul-97	30.84	16.66	86.30	15.45	1.83	24.06	0	7.67
9-Jul-97	28.87	17.81	91.30	35.32	2.14	18.37	0	6.08
10-Jul-97	32.31	14.32	98.40	22.04	1.58	25.87	0	6.70
11-Jul-97	27.63	17.74	93.90	47.27	1.96	11.44	2.4	3.85
12-Jul-97	20.46	16.20	97.80	87.20	3.68	5.98	13.8	1.42
13-Jul-97	19.56	13.71	92.80	45.88	8.35	12.48	0.2	11.32
14-Jul-97	15.63	7.96	97.50	44.41	5.10	11.34	2.2	6.10
15-Jul-97	21.10	6.39	96.40	32.21	1.76	25.79	0	5.50
16-Jul-97	25.26	10.28	93.10	39.33	1.73	23.86	0	5.53
17-Jul-97	26.63	16.35	97.10	49.73	2.72	14.59	6.2	4.95
18-Jul-97	24.23	13.59	96.20	47.29	3.14	17.18	0.4	5.81
19-Jul-97	26.09	14.01	90.70	42.61	1.73	22.06	0	5.46
20-Jul-97	22.40	12.39	87.60	38.45	4.34	16.99	0	8.45
21-Jul-97	21.43	9.57	90.90	35.44	2.25	20.16	0	5.62
22-Jul-97	23.76	11.38	91.80	33.63	1.45	19.05	0	4.57
23-Jul-97	28.57	12.62	89.40	22.39	3.56	22.84	0	9.91
24-Jul-97	30.75	16.24	80.00	24.87	3.32	19.10	0	9.82
25-Jul-97	27.14	15.30	92.10	27.04	3.06	17.28	2	7.61
26-Jul-97	30.23	13.19	81.40	18.94	2.89	24.28	0	9.80
27-Jul-97	24.85	14.76	69.97	26.66	3.21	19.57	0	9.57
28-Jul-97	19.75	13.02	80.50	42.19	3.21	14.34	0	6.42
29-Jul-97	24.86	7.48	97.20	22.16	1.75	25.57	0.2	6.09
30-Jul-97	29.86	12.54	81.50	23.26	4.48	23.35	0	12.54
31-Jul-97	23.81	14.10	83.10	39.39	1.91	16.04	1.4	5.02

**Table F.3 Climatic data and calculated potential evapotranspiration for July, 1997**

DATE	T <sub>max</sub> (C)	T <sub>min</sub> (C)	RH <sub>max</sub> (%)	RH <sub>min</sub> (%)	u <sub>z</sub> (m/s)	R <sub>s</sub> (MJ/m <sup>2</sup> /d)	P (mm)	ET <sub>0</sub> (mm/d)
1-Aug-97	25.50	11.96	104.10	36.98	2.72	20.07	0	6.14
2-Aug-97	26.36	10.08	101.20	32.83	2.08	22.67	0	5.86
3-Aug-97	26.80	11.87	105.60	34.16	1.26	20.24	0	4.40
4-Aug-97	29.65	11.86	105.90	34.97	0.91	22.90	0	4.47
5-Aug-97	33.31	14.21	106.10	34.89	1.47	22.89	0	5.54
6-Aug-97	35.66	15.33	103.40	25.57	1.50	22.24	0	5.94
7-Aug-97	27.72	17.80	96.80	38.38	3.44	18.91	0.8	7.58
8-Aug-97	18.03	10.54	106.30	61.13	4.40	8.01	11.6	3.72
9-Aug-97	17.77	6.94	103.50	67.49	2.25	8.72	0.4	1.93
10-Aug-97	23.47	12.77	102.40	51.92	2.74	11.28	1.6	3.82
11-Aug-97	18.50	9.32	102.60	43.90	2.47	20.50	0	4.97
12-Aug-97	24.40	7.50	102.50	45.64	3.83	23.42	0	7.01
13-Aug-97	25.19	14.79	105.50	60.90	2.97	12.35	8.6	3.83
14-Aug-97	16.81	13.62	108.30	101.80	1.96	3.20	32.6	0.00
15-Aug-97	15.18	11.47	106.70	83.10	4.47	4.90	6.8	1.46
16-Aug-97	14.51	10.50	105.00	74.60	1.58	7.47	0	1.18
17-Aug-97	19.08	10.73	102.90	52.91	1.01	10.87	0	1.91
18-Aug-97	22.54	11.09	105.20	43.54	1.27	22.05	0	4.25
19-Aug-97	22.95	9.50	106.20	55.71	1.86	17.92	0	3.76
20-Aug-97	22.74	8.22	106.50	50.23	1.55	20.65	0	4.01
21-Aug-97	26.77	10.29	105.20	45.77	3.39	20.00	0	6.36
22-Aug-97	22.90	14.90	106.80	69.38	2.59	8.95	1.2	2.42
23-Aug-97	26.22	10.48	107.40	38.98	2.08	18.63	0.2	4.95
24-Aug-97	23.39	14.43	106.10	61.00	1.61	15.01	6.2	3.09
25-Aug-97	24.34	11.02	106.70	55.45	1.37	18.03	0.2	3.47
26-Aug-97	25.92	12.35	106.80	49.58	1.39	20.06	2.4	4.10
27-Aug-97	25.33	14.73	105.40	56.21	3.05	8.93	17.8	3.63
28-Aug-97	24.61	10.41	107.50	41.14	1.80	20.07	0.2	4.67
29-Aug-97	20.88	8.37	107.60	46.29	2.77	12.09	0.4	3.97
30-Aug-97	16.57	9.47	101.50	53.91	3.23	10.14	0.4	3.52
31-Aug-97	16.19	4.16	105.10	52.38	1.76	15.37	0	2.90

**Table F.4 Climatic data and calculated potential evapotranspiration for August, 1997**

DATE	T <sub>max</sub> (C)	T <sub>min</sub> (C)	RH <sub>max</sub> (%)	RH <sub>min</sub> (%)	u <sub>z</sub> (m/s)	R <sub>e</sub> (MJ/m <sup>2</sup> /d)	P (mm)	ET <sub>0</sub> (mm/d)
1-Sep-97	22.11	4.34	105.10	36.81	3.74	19.50	0	6.48
2-Sep-97	25.26	15.59	89.00	47.13	3.72	14.57	0	6.83
3-Sep-97	26.61	10.43	107.30	33.47	1.50	17.52	0	4.23
4-Sep-97	17.97	10.34	103.00	82.60	3.15	7.80	0	1.55
5-Sep-97	20.22	12.20	105.90	67.56	2.43	11.90	0	2.74
6-Sep-97	15.32	10.71	105.30	76.10	4.40	4.00	2	1.87
7-Sep-97	14.98	10.12	107.00	86.00	2.75	5.86	3.6	0.92
8-Sep-97	22.98	9.32	106.70	41.65	1.86	17.16	0	4.13
9-Sep-97	23.94	8.59	106.50	56.32	1.88	13.16	0	3.01
10-Sep-97	20.19	9.76	106.10	60.94	2.12	13.76	0.2	3.02
11-Sep-97	11.70	7.90	107.50	100.50	2.42	2.82	9.2	0.00
12-Sep-97	10.74	7.18	107.40	106.10	5.66	1.62	36.8	0.00
13-Sep-97	7.19	3.06	107.20	97.90	5.55	4.51	9.8	0.20
14-Sep-97	7.08	1.55	107.20	84.50	1.76	4.78	0	0.43
15-Sep-97	8.03	5.34	107.70	89.80	2.28	1.34	12.4	0.34
16-Sep-97	8.22	5.70	107.90	84.10	2.84	3.74	0.6	0.66
17-Sep-97	7.17	2.50	106.10	75.30	2.61	7.20	0.6	1.23
18-Sep-97	8.97	2.41	104.20	66.23	1.86	9.95	1	1.58
19-Sep-97	14.59	0.43	107.10	58.12	2.91	10.03	0	2.57
20-Sep-97	20.96	5.04	106.70	52.57	2.60	13.38	0.2	3.54
21-Sep-97	15.34	8.07	93.10	47.50	2.10	9.32	0	2.87
22-Sep-97	19.58	4.10	104.30	51.50	3.46	10.79	0	3.82
23-Sep-97	25.53	7.63	106.50	37.26	2.74	13.99	0	4.91
24-Sep-97	25.16	10.54	95.50	29.79	2.46	13.94	0	5.28
25-Sep-97	27.05	6.23	107.10	39.12	2.01	13.34	0	3.84
26-Sep-97	28.54	7.85	107.10	35.80	1.73	12.10	0	3.55
27-Sep-97	11.08	9.94	105.60	97.30	4.04	2.34	0	0.18
28-Sep-97	11.53	8.82	106.10	99.00	2.17	1.61	16.6	0.04
29-Sep-97	12.77	6.68	104.60	68.52	3.02	4.27	0.6	1.54
30-Sep-97	11.69	1.28	107.90	73.50	1.77	3.47	2.6	0.68

**Table F.5 Climatic data and calculated potential evapotranspiration for September, 1997**

DATE	T <sub>max</sub> (C)	T <sub>min</sub> (C)	RH <sub>max</sub> (%)	RH <sub>min</sub> (%)	u <sub>z</sub> (m/s)	R <sub>s</sub> (MJ/m <sup>2</sup> /d)	P (mm)	ET <sub>0</sub> (mm/d)
1-Oct-97	7.47	3.28	107.60	78.80	2.60	4.04	0	0.77
2-Oct-97	11.48	6.18	104.90	83.90	2.46	1.42	5.4	0.62
3-Oct-97	9.75	3.66	106.40	64.31	3.65	4.45	0.6	1.93
4-Oct-97	8.43	-0.12	100.80	41.52	2.90	11.88	0	3.13
5-Oct-97	8.52	-1.21	95.20	57.46	2.67	5.28	0	1.77
6-Oct-97	11.76	-0.43	106.40	51.59	2.94	10.35	0.2	2.74
7-Oct-97	0.38	-1.74	107.30	92.20	4.97	1.72	0.4	0.42
8-Oct-97	-1.05	-2.46	107.00	90.50	4.54	3.59	1.8	0.45
9-Oct-97	-0.40	-4.29	100.70	77.70	2.23	5.13	3.2	0.59
10-Oct-97	1.38	-2.27	107.80	99.60	2.31	3.86	6.2	0.01
11-Oct-97	2.25	0.08	108.10	102.10	2.70	3.14	1.2	0.00
12-Oct-97	1.13	-2.57	107.80	78.80	4.04	4.08	2.4	0.93
13-Oct-97	1.59	-3.26	98.70	74.80	3.37	4.55	0	1.00
14-Oct-97	2.52	0.29	95.10	82.70	1.95	1.79	0	0.52
15-Oct-97	4.46	0.79	96.90	76.60	1.32	2.31	0	0.44
16-Oct-97	6.62	2.47	92.70	71.90	3.32	2.13	0	1.58
17-Oct-97	7.76	3.80	95.80	70.50	4.31	2.61	0	2.05
18-Oct-97	10.74	1.14	90.80	28.03	3.24	8.54	0	4.25
19-Oct-97	13.49	0.79	82.20	39.45	2.64	5.68	0	3.25
20-Oct-97	15.39	1.79	93.60	41.36	2.55	6.28	0	2.85
21-Oct-97	18.51	5.95	73.30	27.91	2.67	6.17	0	4.87
22-Oct-97	1.92	-4.54	107.60	93.00	2.96	0.00	0.2	0.22
23-Oct-97	4.20	-0.85	99.40	65.42	2.09	4.58	0	0.93
24-Oct-97	4.57	-2.88	106.00	69.12	3.06	5.84	0	1.27
25-Oct-97	3.15	-3.35	106.50	81.60	3.93	3.09	0.8	0.81
26-Oct-97	11.87	0.84	105.50	67.85	2.60	4.51	0	1.24
27-Oct-97	4.77	-2.02	107.50	79.20	3.27	1.49	3	0.81
28-Oct-97	-2.04	-6.71	105.10	80.30	2.61	4.09	2.6	0.47
29-Oct-97	-2.28	-8.27	102.70	86.30	2.12	3.69	0	0.25
30-Oct-97	-1.10	-3.69	103.00	96.40	3.99	1.60	0	0.14
31-Oct-97	1.21	-2.00	106.50	97.40	1.24	1.64	0	0.04

**Table F.6 Climatic data and calculated potential evapotranspiration for October, 1997**

DATE	T <sub>max</sub> (C)	T <sub>min</sub> (C)	RH <sub>max</sub> (%)	RH <sub>min</sub> (%)	u <sub>z</sub> (m/s)	R <sub>s</sub> (MJ/m <sup>2</sup> /d)	P (mm)	ET <sub>0</sub> (mm/d)
1-Jun-98	13.56	5.65	102.70	37.39	3.73	25.10	0	6.56
2-Jun-98	15.84	2.15	90.00	27.40	2.09	30.18	0	6.16
3-Jun-98	17.28	1.88	96.20	31.56	2.92	28.08	0	6.59
4-Jun-98	17.64	4.63	96.80	38.22	1.65	22.79	0	4.41
5-Jun-98	20.47	5.58	94.60	32.87	2.18	21.62	0	5.37
6-Jun-98	21.76	10.04	93.70	34.01	2.02	17.59	0	4.90
7-Jun-98	24.64	6.69	105.70	21.93	2.18	28.71	0	7.06
8-Jun-98	26.77	11.72	81.40	21.49	4.03	23.45	0	11.33
9-Jun-98	21.72	13.07	99.80	39.04	2.16	9.70	2.4	3.52
10-Jun-98	27.12	10.80	106.00	28.00	1.87	30.40	0	7.12
11-Jun-98	29.33	13.10	81.80	22.75	3.91	26.67	0	11.96
12-Jun-98	21.05	10.35	77.70	33.73	3.86	25.43	0	9.83
13-Jun-98	15.68	7.72	98.20	49.21	2.93	15.92	0	4.31
14-Jun-98	15.74	8.21	103.50	79.00	2.17	12.77	5.4	2.01
15-Jun-98	19.39	9.89	105.50	51.90	2.78	19.29	0.4	4.78
16-Jun-98	17.92	9.70	106.90	70.30	2.43	12.21	4	2.51
17-Jun-98	20.56	8.95	107.90	56.08	1.68	18.83	0.2	3.61
18-Jun-98	24.27	8.57	107.40	35.63	2.16	29.82	0	6.74
19-Jun-98	24.19	10.83	97.00	39.85	3.09	28.08	0	7.75
20-Jun-98	25.36	11.14	99.20	27.67	2.99	30.75	0	8.79
21-Jun-98	29.94	8.67	102.00	17.22	1.95	29.92	0.2	7.65
22-Jun-98	31.68	12.88	103.10	24.90	2.07	24.92	0	7.08
23-Jun-98	30.60	14.63	90.40	28.67	2.70	27.44	0	8.98
24-Jun-98	30.61	14.77	94.60	29.95	2.31	22.17	0	7.07
25-Jun-98	26.18	14.62	105.00	59.36	1.98	14.94	6.8	3.55
26-Jun-98	25.14	14.57	106.60	67.20	3.04	15.26	10.8	3.96
27-Jun-98	17.36	16.31	95.80	90.20	4.63	5.46	17.6	1.48
28-Jun-98	20.37	16.09	96.80	78.00	4.18	9.11	0.2	2.95
29-Jun-98	25.61	16.81	90.50	49.28	3.08	22.50	0	7.18
30-Jun-98	28.02	16.09	92.00	29.07	2.44	21.40	0	7.25

**Table F.8 Climatic data and calculated potential evapotranspiration for June, 1998**

DATE	T <sub>max</sub> (C)	T <sub>min</sub> (C)	RH <sub>max</sub> (%)	RH <sub>min</sub> (%)	u <sub>z</sub> (m/s)	R <sub>s</sub> (MJ/m <sup>2</sup> /d)	P (mm)	ET <sub>0</sub> (mm/d)
1-May-98	25.61	3.58	101.30	18.99	2.53	23.10	0	6.68
2-May-98	29.65	5.39	96.80	16.92	1.96	23.56	0	6.50
3-May-98	20.68	10.09	82.20	31.18	4.10	17.02	0	8.71
4-May-98	17.52	4.42	98.80	31.00	3.42	24.11	0.8	6.80
5-May-98	12.46	4.48	101.50	44.69	3.80	6.81	1.2	3.59
6-May-98	18.23	0.84	105.80	30.16	5.24	22.03	0	8.25
7-May-98	22.03	9.21	85.80	30.95	3.45	16.02	0	7.31
8-May-98	23.61	5.99	100.80	21.01	1.65	23.67	0	5.41
9-May-98	16.70	7.20	101.70	49.58	3.08	6.25	1.2	2.98
10-May-98	19.02	3.05	95.80	23.86	2.76	25.76	0	6.74
11-May-98	16.04	2.66	98.80	40.41	3.46	25.69	0	6.22
12-May-98	18.85	0.92	105.70	38.18	2.66	25.13	0	5.51
13-May-98	16.88	3.80	76.90	31.80	3.01	26.04	0	7.51
14-May-98	20.05	3.17	88.60	35.91	2.99	26.18	0	6.97
15-May-98	18.54	3.97	96.40	41.13	3.04	25.79	0	6.24
16-May-98	18.37	3.38	102.00	38.47	2.33	26.50	0	5.49
17-May-98	23.61	3.70	104.30	25.53	1.28	27.00	0	5.12
18-May-98	25.17	6.86	103.80	20.39	1.44	24.61	0	5.41
19-May-98	24.10	9.44	88.60	32.22	2.97	19.71	0.2	7.07
20-May-98	26.19	9.19	101.50	29.01	2.25	22.23	0	6.12
21-May-98	28.22	9.97	100.70	22.34	1.61	26.43	0	6.29
22-May-98	28.47	12.00	97.70	29.93	2.17	15.03	2.4	5.18
23-May-98	26.78	14.43	103.30	42.75	2.20	14.94	0.4	4.53
24-May-98	29.13	11.68	97.90	34.35	3.45	24.82	0	8.49
25-May-98	28.65	12.29	104.00	32.95	2.15	19.29	2.6	5.64
26-May-98	24.36	12.28	107.90	38.80	2.69	24.09	0	6.61
27-May-98	22.24	9.41	90.40	25.88	3.36	24.15	0	8.50
28-May-98	15.45	3.47	94.50	27.66	2.76	27.91	0	6.62
29-May-98	20.34	1.74	103.50	23.82	2.40	26.64	0	6.21
30-May-98	15.34	3.27	77.80	29.83	3.10	29.55	0	7.94
31-May-98	9.04	5.16	106.10	45.54	2.93	4.13	7.2	2.36

**Table F.7 Climatic data and calculated potential evapotranspiration for May, 1998**

DATE	T <sub>max</sub> (C)	T <sub>min</sub> (C)	RH <sub>max</sub> (%)	RH <sub>min</sub> (%)	u <sub>z</sub> (m/s)	R <sub>s</sub> (MJ/m <sup>2</sup> /d)	P (mm)	ET <sub>0</sub> (mm/d)
1-Jul-98	23.81	14.10	83.10	39.39	4.43	25.52	0	10.62
2-Jul-98	25.42	9.80	89.20	16.80	2.23	28.32	0	8.09
3-Jul-98	28.76	11.40	88.30	22.89	2.00	21.48	0	6.68
4-Jul-98	29.33	13.64	91.50	23.37	1.59	26.64	0	6.84
5-Jul-98	30.98	13.82	92.40	17.28	2.24	27.64	0	8.61
6-Jul-98	31.92	14.32	89.80	19.28	2.13	25.87	0	8.22
7-Jul-98	31.91	18.32	77.90	22.19	2.84	26.09	0.4	10.64
8-Jul-98	30.84	16.66	86.30	15.45	1.83	24.06	0	7.67
9-Jul-98	28.87	17.81	91.30	35.32	2.14	18.37	0	6.08
10-Jul-98	32.31	14.32	98.40	22.04	1.58	25.87	0	6.70
11-Jul-98	27.63	17.74	93.90	47.27	1.96	11.44	2.4	3.85
12-Jul-98	20.46	16.20	97.80	87.20	3.68	5.98	13.8	1.42
13-Jul-98	19.56	13.71	92.80	45.88	8.35	12.48	0.2	11.32
14-Jul-98	15.63	7.96	97.50	44.41	5.10	11.34	2.2	6.10
15-Jul-98	21.10	6.39	96.40	32.21	1.76	25.79	0	5.50
16-Jul-98	25.26	10.28	93.10	39.33	1.73	23.86	0	5.53
17-Jul-98	26.63	16.35	97.10	49.73	2.72	14.59	6.2	4.95
18-Jul-98	24.23	13.59	96.20	47.29	3.14	17.18	0.4	5.81
19-Jul-98	26.09	14.01	90.70	42.61	1.73	22.06	0	5.46
20-Jul-98	22.40	12.39	87.60	38.45	4.34	16.99	0	8.45
21-Jul-98	21.43	9.57	90.90	35.44	2.25	20.16	0	5.62
22-Jul-98	23.76	11.38	91.80	33.63	1.45	19.05	0	4.57
23-Jul-98	28.57	12.62	89.40	22.39	3.56	22.84	0	9.91
24-Jul-98	30.75	16.24	80.00	24.87	3.32	19.10	0	9.82
25-Jul-98	27.14	15.30	92.10	27.04	3.06	17.28	2	7.61
26-Jul-98	30.23	13.19	81.40	18.94	2.89	24.28	0	9.80
27-Jul-98	24.85	14.76	69.97	26.66	3.21	19.57	0	9.57
28-Jul-98	19.75	13.02	80.50	42.19	3.21	14.34	0	6.42
29-Jul-98	24.86	7.48	97.20	22.16	1.75	25.57	0.2	6.09
30-Jul-98	29.86	12.54	81.50	23.26	4.48	23.35	0	12.54
31-Jul-98	23.81	14.10	83.10	39.39	1.91	16.04	1.4	5.02

**Table F.9 Climatic data and calculated potential evapotranspiration for July, 1998**



DATE	T <sub>max</sub> (C)	T <sub>min</sub> (C)	RH <sub>max</sub> (%)	RH <sub>min</sub> (%)	u <sub>z</sub> (m/s)	R <sub>s</sub> (MJ/m <sup>2</sup> /d)	P (mm)	ET <sub>0</sub> (mm/d)
1-Aug-98	28.45	14.81	92.30	24.47	2.51	21.15	0	7.52
2-Aug-98	30.71	14.82	89.00	24.22	1.69	20.40	0	6.14
3-Aug-98	33.13	15.57	93.90	22.00	2.18	22.73	0	7.57
4-Aug-98	36.17	18.51	90.00	22.23	3.22	22.37	3.8	10.29
5-Aug-98	35.83	17.87	96.30	21.73	2.86	20.93	3.4	8.79
6-Aug-98	27.22	16.09	86.90	27.32	5.35	21.27	2	12.99
7-Aug-98	26.22	14.95	63.15	21.05	5.43	23.29	0	16.71
8-Aug-98	28.22	10.20	92.80	18.14	1.86	19.39	0	5.97
9-Aug-98	33.53	11.90	91.50	16.38	2.84	21.75	0	8.94
10-Aug-98	28.26	16.86	68.04	21.75	2.71	15.29	0	8.61
11-Aug-98	27.26	11.69	55.37	15.93	3.77	22.00	0	13.11
12-Aug-98	27.08	14.19	93.10	29.25	2.70	13.08	3.4	6.00
13-Aug-98	21.63	11.32	92.50	35.20	2.93	15.35	0	5.89
14-Aug-98	25.70	8.60	97.60	24.84	2.17	18.71	0	5.65
15-Aug-98	21.12	10.59	97.00	34.69	3.76	21.92	0	7.69
16-Aug-98	24.21	6.83	97.80	26.90	1.87	21.29	0	5.33
17-Aug-98	26.73	10.77	91.10	28.10	3.39	21.15	0	8.42
18-Aug-98	25.15	13.58	82.70	28.45	2.91	21.05	0	8.19
19-Aug-98	20.12	11.48	84.10	38.07	3.78	16.00	0	7.48
20-Aug-98	20.99	9.58	88.60	48.61	2.74	19.13	0	5.55
21-Aug-98	26.44	11.96	93.90	38.95	2.64	12.07	0	4.98
22-Aug-98	27.19	11.20	98.40	25.99	1.46	17.92	0	4.59
23-Aug-98	24.78	13.15	87.10	24.43	1.68	16.89	0	5.18
24-Aug-98	22.32	11.66	85.10	27.86	2.90	13.90	0.2	6.53
25-Aug-98	24.49	6.43	98.80	30.10	2.22	11.69	0	4.16
26-Aug-98	21.51	11.48	94.70	51.40	2.36	9.26	1.4	3.28
27-Aug-98	22.83	9.96	95.50	24.26	3.76	14.05	0	7.42
28-Aug-98	23.87	9.51	76.00	18.09	3.81	18.96	0	10.23
29-Aug-98	31.81	7.48	93.60	17.09	2.42	18.41	0	6.91
30-Aug-98	23.41	11.98	60.52	13.57	3.86	15.09	0	11.50
31-Aug-98	20.06	8.17	84.70	21.24	3.19	16.67	0	7.37

**Table F.10 Climatic data and calculated potential evapotranspiration for August, 1998**

DATE	T <sub>max</sub> (C)	T <sub>min</sub> (C)	RH <sub>max</sub> (%)	RH <sub>min</sub> (%)	u <sub>z</sub> (m/s)	R <sub>s</sub> (MJ/m <sup>2</sup> /d)	P (mm)	ET <sub>0</sub> (mm/d)
1-Sep-98	22.15	3.76	97.70	24.97	3.12	11.15	0	5.30
2-Sep-98	27.35	9.25	83.60	11.74	3.00	8.42	0	7.09
3-Sep-98	23.08	9.54	70.00	15.46	3.39	16.80	0	9.52
4-Sep-98	20.03	10.23	72.20	24.07	2.74	10.91	0	6.38
5-Sep-98	20.49	6.75	82.10	22.32	2.53	12.54	0	5.61
6-Sep-98	20.30	3.05	98.30	28.54	1.80	13.57	0	3.58
7-Sep-98	24.06	12.55	87.20	26.91	3.49	13.15	0	7.56
8-Sep-98	18.62	9.64	93.20	44.60	1.73	6.55	0	2.33
9-Sep-98	18.50	6.73	96.20	41.38	2.26	5.02	0	2.60
10-Sep-98	19.27	7.82	88.80	33.27	3.06	9.41	0	5.08
11-Sep-98	24.23	5.22	96.50	21.73	3.95	10.49	0	6.96
12-Sep-98	22.52	7.99	83.60	20.30	3.23	13.20	0	7.25
13-Sep-98	14.45	9.02	92.40	48.38	4.40	5.95	3.2	4.71
14-Sep-98	14.58	4.93	92.10	44.48	1.83	11.07	0	2.81
15-Sep-98	16.25	6.73	96.90	52.01	1.80	9.36	6.2	2.30
16-Sep-98	8.78	3.83	99.00	86.70	1.29	2.68	1.4	0.26
17-Sep-98	13.43	1.65	97.20	28.38	2.02	15.31	0	3.67
18-Sep-98	15.60	7.74	69.90	24.58	1.41	14.26	0	3.98
19-Sep-98	17.57	0.66	97.20	19.10	0.90	14.46	0	2.55
20-Sep-98	20.87	1.78	94.40	31.46	2.05	12.81	0	3.79
21-Sep-98	24.66	6.07	95.30	18.25	2.33	13.35	0	5.22
22-Sep-98	19.32	7.59	95.00	33.20	1.77	13.19	0	3.62
23-Sep-98	17.21	3.16	98.00	43.46	2.18	8.20	0.2	2.64
24-Sep-98	12.47	5.81	97.60	43.77	2.35	10.07	0	2.96
25-Sep-98	7.21	2.63	97.70	72.40	1.88	2.11	1.6	0.77
26-Sep-98	13.55	1.70	97.20	54.13	2.57	5.33	0	2.03
27-Sep-98	10.44	3.82	97.10	60.83	2.00	6.38	0.6	1.52
28-Sep-98	11.46	4.58	98.90	61.06	1.97	5.51	0	1.37
29-Sep-98	9.67	1.15	91.50	38.19	3.38	9.17	0	3.90
30-Sep-98	9.64	-3.65	98.20	42.47	2.79	6.18	0.2	2.32

**Table F.11 Climatic data and calculated potential evapotranspiration for September, 1998**

DATE	T <sub>max</sub> (C)	T <sub>min</sub> (C)	RH <sub>max</sub> (%)	RH <sub>min</sub> (%)	u <sub>z</sub> (m/s)	R <sub>s</sub> (MJ/m <sup>2</sup> /d)	P (mm)	ET <sub>0</sub> (mm/d)
1-Oct-98	19.11	7.10	58.05	29.90	5.26	10.70	0	11.44
2-Oct-98	17.29	7.44	47.27	23.62	6.44	8.31	0	15.08
3-Oct-98	13.02	7.86	79.90	32.87	5.53	5.66	0	8.15
4-Oct-98	14.32	4.53	91.50	36.12	3.25	10.23	0.8	4.57
5-Oct-98	11.68	1.58	95.40	56.48	1.84	5.47	0	1.45
6-Oct-98	12.58	1.32	98.30	52.56	1.21	6.61	0	1.18
7-Oct-98	17.27	5.52	87.00	47.63	3.05	8.76	0	4.02
8-Oct-98	5.54	1.49	98.10	76.90	4.49	2.82	0.6	1.45
9-Oct-98	2.62	0.05	97.00	87.60	5.08	4.21	0.2	0.93
10-Oct-98	2.17	-1.21	91.40	76.30	3.00	3.63	0	1.11
11-Oct-98	3.54	-0.61	91.00	67.94	1.32	2.47	0.2	0.65
12-Oct-98	4.95	-5.24	98.30	52.34	3.90	7.11	0	2.43
13-Oct-98	2.41	-0.02	97.10	69.35	5.03	1.95	0	1.99
14-Oct-98	2.52	0.29	95.10	82.70	1.95	1.79	0	0.52
15-Oct-98	4.46	0.79	96.90	76.60	1.32	2.31	0	0.44
16-Oct-98	6.62	2.47	92.70	71.90	3.32	2.13	0	1.58
17-Oct-98	7.76	3.80	95.80	70.50	4.31	2.61	0.8	2.05
18-Oct-98	10.74	1.14	90.80	28.03	3.24	8.54	0	4.25
19-Oct-98	13.49	0.79	82.20	39.45	2.64	5.68	0	3.25
20-Oct-98	15.39	1.79	93.60	41.36	2.55	6.28	0	2.85
21-Oct-98	18.51	5.95	73.30	27.91	2.67	6.17	0	4.87
22-Oct-98	18.87	0.88	94.80	28.63	1.20	7.42	0.2	1.93
23-Oct-98	11.33	-0.47	97.90	54.89	1.87	7.03	0	1.57
24-Oct-98	7.77	-1.01	99.10	74.60	3.77	3.18	0	1.28
25-Oct-98	11.38	2.71	97.20	65.93	4.84	3.56	0	2.63
26-Oct-98	14.85	4.69	80.90	15.05	5.30	6.66	0	9.23
27-Oct-98	9.93	-0.05	57.06	22.52	3.26	4.35	0	5.39
28-Oct-98	9.93	3.64	75.60	28.24	4.21	1.11	0	5.91
29-Oct-98	7.91	-2.53	91.20	37.28	3.30	6.02	0	3.16
30-Oct-98	1.50	-6.22	89.80	45.68	2.35	5.76	0	1.67
31-Oct-98	3.65	-9.77	94.80	46.27	2.37	3.34	0	1.36

**Table F.12 Climatic data and calculated potential evapotranspiration for October, 1998**

## Appendix G

### Input and output data and source code of the plant dewatering model

#### G.1 INTRODUCTION

This appendix presents the computer code of the plant dewatering mechanism. The program was written in Macro Language using Visual Basic for Application (VBA). The input and output data are written in Excel Worksheets, which create automatically selected charts. A good knowledge of VBA is required to understand the information described in this appendix. The worksheets presented here are just samples of input and output data of the real model.

#### G.2 INPUT DATA SAMPLES

Compartment	Solids content	Thickness of each compartment ( m)
1	0.7220	0.05
2	0.7260	0.05
3	0.7300	0.05
4	0.7340	0.05
5	0.7380	0.05
6	0.7420	0.05
7	0.7460	0.05
8	0.7500	0.05
9	0.7540	0.05
10	0.7580	0.05
.	.	.
.	.	.
.	.	.

**Table G.1 Initial solids content input data**

Day	Precipitation (m)	DayLAI	LAI	Reference Evt (m)	Transpiration (m)	Soil Evaporation (m)	Root Depth (m)	Root Biomass (kg/m <sup>3</sup> )
1		0.22	0.257	0.00555	0.00080	0.00474	0.020	0.010
2		0.23	0.301	0.00451	0.00078	0.00372	0.025	0.012
3		0.24	0.351	0.00507	0.00104	0.00403	0.030	0.015
4		0.26	0.409	0.00802	0.00190	0.00612	0.035	0.018
5		0.27	0.473	0.00495	0.00134	0.00360	0.041	0.021
6	0.0022	0.28	0.546	0.00437	0.00134	0.00303	0.048	0.024
7		0.29	0.627	0.00503	0.00173	0.00330	0.055	0.027
8		0.30	0.718	0.00538	0.00206	0.00332	0.062	0.031
9		0.31	0.818	0.00785	0.00332	0.00453	0.070	0.035
10	0.0004	0.32	0.927	0.00577	0.00268	0.00309	0.078	0.039
11	0.0002	0.33	1.045	0.00542	0.00274	0.00268	0.086	0.043
12	0.0008	0.34	1.173	0.00983	0.00539	0.00444	0.095	0.047
13		0.35	1.309	0.00741	0.00438	0.00303	0.104	0.052
14		0.36	1.453	0.00766	0.00486	0.00281	0.114	0.057
15		0.37	1.603	0.01251	0.00846	0.00405	0.124	0.062
16		0.38	1.759	0.00343	0.00246	0.00097	0.134	0.067
17		0.39	1.918	0.00461	0.00350	0.00111	0.145	0.072
18		0.40	2.079	0.00356	0.00285	0.00071	0.156	0.078
19		0.41	2.240	0.00482	0.00404	0.00078	0.167	0.084
20		0.42	2.399	0.00229	0.00200	0.00029	0.179	0.090
21	0.0026	0.43	2.555	0.00178	0.00161	0.00016	0.191	0.096
22		0.44	2.706	0.00211	0.00201	0.00011	0.203	0.102
23		0.45	2.851	0.00240	0.00228	0.00012	0.216	0.108
24		0.46	2.989	0.00858	0.00815	0.00043	0.229	0.114
25		0.47	3.118	0.00567	0.00539	0.00028	0.242	0.121
26		0.48	3.239	0.00511	0.00486	0.00026	0.255	0.128
27	0.0016	0.49	3.351	0.00223	0.00212	0.00011	0.269	0.134
28	0.0004	0.50	3.454	0.00442	0.00420	0.00022	0.283	0.141
29		0.51	3.548	0.00613	0.00582	0.00031	0.297	0.148
30	0.00054	0.52	3.633	0.00523	0.00497	0.00026	0.311	0.155
.	.	.	.	.	.	.	.	.
.	.	.	.	.	.	.	.	.
.	.	.	.	.	.	.	.	.

**Table G.2 Rainfall, ET and root growth input data**

Number of Compartments	20
Wilting Point	0.065
Saturation Point	0.38
Time Step (day)	0.042
Evaporation Rate	0.6
Number of Days	368
A (1/kPa)	0.9952
B	-0.1811
C (m/d)	5.18E-04
D	1.3754
Specific Gravity (Gs)	2.6
Minimum Suction (kPa)	-20
Maximum Surface Storage (m)	0
Minimum Void Ratio	0.61
Cohesion (kPa)	3
Angle of Internal Friction	30
Residual Water Content	0.01
Alpha (1/m)	-0.15
m	0.259
n	1.35
P	0.65
Maximum Change of Volume (m)	0.00001
Maximum Time Step (day)	0.042
Limiting available water (LAW) (kPa)	-1000

**Table G.3 Main data input**

### G.3 SAMPLE OF MODEL RESULTS

Theta (%)	Thickness of Compartment (cm)	Pore Pressure (kPa)	Excess Pore Pressure (kPa)	Void Ratio	Flux mm/day	Solids Content (%)	Elevation (cm)
7.45	4.03	-980.34	0.00	0.61	-0.04	95.58	86.69
7.39	4.07	-1006.96	0.00	0.61	-0.04	95.62	82.64
7.33	4.11	-1034.08	0.00	0.61	-0.04	95.65	78.55
7.27	4.15	-1061.77	0.00	0.61	-0.05	95.68	74.42
7.21	4.19	-1090.10	0.00	0.61	-0.05	95.72	70.24
7.16	4.24	-1119.17	0.00	0.61	-0.05	95.75	66.03
7.10	4.28	-1149.09	0.00	0.61	-0.05	95.78	61.77
7.04	4.32	-1180.00	0.00	0.61	-0.04	95.81	57.47
6.99	4.36	-1212.02	0.00	0.61	-0.04	95.85	53.13
6.93	4.41	-1245.30	0.00	0.61	-0.04	95.88	48.75
6.87	4.45	-1279.98	0.00	0.61	-0.04	95.91	44.32
6.82	4.49	-1316.19	0.00	0.61	-0.04	95.94	39.85
6.76	4.54	-1354.11	0.00	0.61	-0.03	95.98	35.33
6.70	4.58	-1393.88	0.00	0.61	-0.03	96.01	30.77
6.64	4.63	-1435.68	0.00	0.61	-0.02	96.04	26.16
6.58	4.68	-1479.65	0.00	0.61	-0.02	96.08	21.51
6.52	4.72	-1525.98	0.00	0.61	-0.02	96.11	16.81
6.46	4.77	-1574.84	0.00	0.61	-0.01	96.14	12.06
6.40	4.82	-1626.41	0.00	0.61	-0.01	96.18	7.27
6.34	4.86	-1680.27	0.00	0.61	0.00	96.22	2.43
<b>Time =</b>	368 days	-1680.27	0.00		0.00		0.00
<b>Balance =</b>	-389.0021 mm						
<b>Runoff =</b>	313.3507 mm						

	<b>c suction</b>	<b>c roots</b>	<b>c sat</b>	<b>c global</b>	<b>Bearing capacity</b>
<b>Top</b>	19.7921	2.2	0.2	22.237	808.938
<b>Middle</b>	21.2905	1.8	0.2	23.316	847.780
<b>Bottom</b>	22.9411	1.4	0.2	24.530	891.494

**Table G.4 Model output data**

<b>Elevation</b>	<b>Elevation of Top of Compartment</b>	<b>Degree of Saturation</b>	<b>Depth</b>	<b>Depth of Top of Compartment</b>	<b>Root Biomass</b>	<b>Shear Strength</b>	<b>Bearing Capacity</b>
<b>(cm)</b>	<b>(cm)</b>		<b>(cm)</b>	<b>(cm)</b>	<b>(kg/m<sup>3</sup>)</b>	<b>(kPa)</b>	<b>(kPa)</b>
86.69	88.70	19.6	2.02	0.00	0.49	21.72	808.83
82.64	84.67	19.4	6.07	4.03	0.47	21.97	
78.55	80.60	19.3	10.16	8.10	0.45	22.23	
74.42	76.49	19.1	14.29	12.21	0.43	22.49	
70.24	72.34	19.0	18.46	16.36	0.41	22.76	
66.03	68.15	18.8	22.68	20.56	0.39	23.03	858.00
61.77	63.91	18.7	26.93	24.79	0.37	23.30	
57.47	59.63	18.5	31.23	29.07	0.34	23.59	
53.13	55.31	18.4	35.57	33.39	0.32	23.89	
48.75	50.95	18.2	39.96	37.75	0.30	24.19	
44.32	46.54	18.1	44.39	42.16	0.28	24.51	916.06
39.85	42.09	17.9	48.86	46.61	0.26	24.85	
35.33	37.60	17.8	53.38	51.11	0.23	25.20	
30.77	33.06	17.6	57.94	55.64	0.21	25.56	
26.16	28.48	17.5	62.54	60.23	0.19	25.95	
21.51	23.85	17.3	67.20	64.86	0.16	26.35	989.54
16.81	19.17	17.2	71.90	69.53	0.14	26.78	
12.06	14.45	17.0	76.64	74.26	0.12	27.23	
7.27	9.68	16.8	81.43	79.03	0.09	27.71	
2.43	4.86	16.7	86.27	83.84	0.07	28.20	
0.00	0.00						

**Table G.4 (Cont.) Model output data**



## G.4 COMPUTER CODE OF THE PLANT DEWATERING MODEL

### MAIN PROGRAM

#### Option Explicit

```

Public NL As Integer, NSTEPS As Integer, NDAY As Integer, NLL As Integer
Public I As Integer, J As Integer, K As Long, COUNTER As Integer, LL As Integer
Public FC As Single, WP As Single, SAT As Single, DT As Single, LAI(400) As Single
Public DEPOSIT As Single, PE(4000) As Single, ETR(4000) As Single, EVT(4000) As Single
Public ZR(4000) As Single, PEDT(100000) As Single, ETRDT(100000) As Single
Public ZRDT(100000) As Single, YCOM(200) As Single, ZCOM(200) As Single
Public THETANEW(200) As Double, ITHETA(200) As Double, THETA(200) As Double
Public ZBOUND(200) As Single, YBOUND(200) As Single, DIST(200) As Double
Public VOID(200) As Single, DSAT(200) As Single, RESIDUAL As Single, EVAPRATE As Single
Public XALPHA As Single, XM As Single, XN As Single, SATCOND As Single
Public AVTIMETHETA(200) As Double, THETACALC(200) As Double, COND(200) As Double
Public ETREM(200) As Single, AVCOND(200) As Double, VOIDNEW(200) As Single
Public POREPR(200) As Single, EXCESS(200) As Single, HYDROSTATIC(200) As Single
Public DELTAPORE(200) As Single, SOLIDS(200) As Single, SHEAR(200) As Single
Public A As Single, B As Single, C As Single, D As Single, DTMAX As Single
Public FLUX(200) As Double, X(200) As Single, Y(200) As Single, VOLWRES(200) As Single
Public TIEMPO As Single, MAXSTORAGE As Single, GS As Single, CUMRUNOFF As Single
Public INFILCAP As Single, WATEXCESS As Single, RUNOFF As Single, BOTROOT As Integer
Public EVAP As Single, POTEVAP(4000) As Single, INFILT As Single, VOLWNEW(200) As
Double
Public MPOT(200) As Double, MINPOT As Single, VOIDMIN As Single, YR(4000) As Single
Public AVTIMESLOPE(200) As Double, RATIO(200) As Single, FLAG As Boolean
Public BALANCE As Single, ELEVATION(200) As Single, P As Single, AVMPOT(200) As Double
Public AVTHETA(200) As Double, PHY As Single, DISSIPATION As Single, LAW As Single
Public IVOLW(200) As Single, VOLW(200) As Double
Public SATURATION As Boolean, ACCURACY As Boolean, COHESION As Single
Public XX(200) As Double, YY(200) As Double, AA(200) As Double, BB(200) As Double
Public CC(200) As Double, DD(200) As Double, ALPHA(200) As Double, BETA(200) As Double
Public NU As Integer, XF(200) As Double, YF(200) As Double, THETAOLD(200) As Double
Public AVTIMEVOLW(200) As Single, AVTIMEVOID(200) As Single, PHYF(200) As Double
Public VOLWCALC(200) As Double, VOIDCALC(200) As Single, AVOID(200) As Single
Public VOLWMIN(200) As Single, VOLWSAT(200) As Single, SATDEPTH As Single, SATPOINT
As Integer
Public DELTAVOLW(200) As Double, DELTAVOLWMAX As Double, CHANGEVOLWMAX As
Double
Public DAY As Integer, POTEVAPDT(100000) As Single, DTNEW As Single, EXCESSOLD(200)
As Single
Public TOPROOT As Single, SATPOINTOLD As Single, MOISTURERATIO(200) As Single
Public ROOTBIO(200) As Single, BIOMASS(400) As Single
Public Const GAMMAW = 9.81 '(kN/m3)
Public Static Sub PhytoDewater()

```

---

FLAG = False

Call Data

TIEMPO = DT

DAY = 1

K = 1

CUMRUNOFF = 0

Do While TIEMPO <= NDAY

```
PEDT(K) = PE(DAY)
ETRDT(K) = ETR(DAY)
ZRDT(K) = ZR(DAY)
POTEVAPDT(K) = POTEVAP(DAY)
Call RootUptake
Call Calculation
TIEMPO = TIEMPO + DT
If (TIEMPO - DAY) >= 0 Then DAY = DAY + 1
K = K + 1
Loop
If TIEMPO > NDAYS Then TIEMPO = TIEMPO - DT
Call Result
End Sub
```

**SUBROUTINE "DATA"****Option Explicit**

Public Static Sub Data()

Sheets("Main Data Input").Select

NL = Cells(1, 2) '10  
 FC = Cells(4, 2) '0.2  
 WP = Cells(5, 2) '0.07  
 SAT = Cells(6, 2) '0.39  
 DEPOSIT = Cells(17, 2) '1 (m)  
 DT = Cells(7, 2) '0.125 (day)  
 EVAPRATE = Cells(8, 2) '16  
 NDAYS = Cells(9, 2) '2 (days)  
 A = Cells(10, 2) '0.02871  
 B = Cells(11, 2) '-0.3097  
 C = Cells(12, 2) '0.00000000007425  
 D = Cells(13, 2) '3.847  
 GS = Cells(14, 2) '2.27  
 MINPOT = Cells(15, 2)  
 MAXSTORAGE = Cells(16, 2) '0  
 VOIDMIN = Cells(18, 2)  
 COHESION = Cells(19, 2)  
 PHY = Cells(20, 2)  
 RESIDUAL = Cells(21, 2)  
 XALPHA = Cells(22, 2)  
 XM = Cells(23, 2)  
 XN = Cells(24, 2)  
 P = Cells(25, 2)  
 DELTAVOLWMAX = Cells(26, 2)  
 DTMAX = Cells(27, 2)  
 LAW = Cells(28, 2)

NLL = NL + 1

Sheets("Rain, ET, Root").Select

For I = 1 To NDAYS  
     PE(I) = Cells(I + 1, 2)  
     LAI(I) = Cells(I + 1, 4)  
     EVT(I) = Cells(I + 1, 5)  
     ETR(I) = Cells(I + 1, 6)  
     POTEVAP(I) = Cells(I + 1, 7)  
     ZR(I) = Cells(I + 1, 8)  
     YR(I) = Cells(I + 1, 9)  
     BIOMASS(I) = Cells(I + 1, 10)

Next I

Sheets("Initial Solids Content").Select

For I = 1 To NL  
     SOLIDS(I) = Cells(I + 1, 3)  
     YCOM(I) = Cells(I + 1, 4)

Next I

For I = 1 To NL

DSAT(I) = GS \* (1 / SOLIDS(I) - 1) / VOIDMIN  
 If DSAT(I) > 1 Then DSAT(I) = 1  
 VOID(I) = GS \* (1 / SOLIDS(I) - 1) / DSAT(I)  
 ZCOM(I) = YCOM(I) / (1 + VOID(I))  
 MOISTURERATIO(I) = DSAT(I) \* VOID(I)  
 VOLW(I) = MOISTURERATIO(I) \* ZCOM(I)  
 IVOLW(I) = VOLW(I)

```
VOLWMIN(I) = WP * (1 + VOIDMIN) * ZCOM(I)
VOLWRES(I) = RESIDUAL * (1 + VOIDMIN) * ZCOM(I)
VOLWSAT(I) = SAT * (1 + VOIDMIN) * ZCOM(I)
Next I
SATCOND = C * VOIDMIN ^ D
If VOLW(1) >= VOLWSAT(1) Then SATURATION = True Else SATURATION = False
YBOUND(1) = 0
VOLWRES(NLL) = VOLWRES(NL)
VOLWSAT(NLL) = VOLWSAT(NL)
For I = 2 To NLL
    YBOUND(I) = YBOUND(I - 1) + YCOM(I)
Next I
End Sub
```

**SUBROUTINE "ROOTUPTAKE"****Option Explicit**

Public Static Sub RootUptake()

TOPROOT = YBOUND(1)

If K &gt; 1 Then

For I = 1 To NL

If VOLW(I) &lt;= VOLWMIN(I) Then

TOPROOT = YBOUND(I + 1)

Exit For

End If

Next I

End If

If ZRDT(K) &gt; YBOUND(NLL) Then ZRDT(K) = YBOUND(NLL)

If TOPROOT &gt;= YBOUND(NL) Then GoTo 30

If ETRDT(K) = 0 Then GoTo 10

For I = NLL To 1 Step -1

If ZRDT(K) - YBOUND(I) &gt;= 0 Then

BOTROOT = I

Exit For

End If

Next I

For I = 1 To BOTROOT - 1

Select Case YBOUND(I)

Case Is &lt; TOPROOT

ETREM(I) = 0

Case Is &gt;= TOPROOT

If ZRDT(K) &gt; 0 Then

ETREM(I) = ETRDT(K) / (YR(DAY) + 1) \* (YBOUND(I + 1) - YBOUND(I)) /

(ZRDT(K) - TOPROOT) ^ 2 \* ((YR(DAY) - 1) \* (YBOUND(I) + YBOUND(I + 1)) + 2 \* ZRDT(K) - 2

\* YR(DAY) \* TOPROOT)

Else

ETREM(I) = 0

End If

End Select

Next I

If ZRDT(K) &gt; 0 Then

ETREM(BOTROOT) = ETRDT(K) / (YR(DAY) + 1) \* (ZRDT(K) - YBOUND(BOTROOT)) /

(ZRDT(K) - TOPROOT) ^ 2 \* ((YR(DAY) - 1) \* (YBOUND(BOTROOT) + ZRDT(K)) + 2 \* ZRDT(K)

- 2 \* YR(DAY) \* TOPROOT)

Else

ETREM(BOTROOT) = 0

End If

For I = BOTROOT + 1 To NL

ETREM(I) = 0

Next I

GoTo 20

10 For I = 1 To NL

ETREM(I) = 0

Next I

GoTo 20

30 For I = 1 To NL

ETREM(I) = 0

Next I

ETREM(NL) = ETRDT(K)

20 End Sub

**SUBROUTINE "CALCULATION"****Option Explicit**

Public Static Sub Calculation()

If K = 1 Then

ZBOUND(1) = 0

For I = 2 To NLL

ZBOUND(I) = ZBOUND(I - 1) + ZCOM(I)

Next I

For I = 2 To NL

DIST(I) = 0.5 \* (ZCOM(I - 1) + ZCOM(I))

Next I

DIST(1) = ZCOM(1)

DIST(NLL) = ZCOM(NL)

FLUX(NLL) = 0

End If

For I = 1 To NL

VOLWNEW(I) = 0.999999 \* VOLW(I)

Next I

COUNTER = 0

Do

AVTIMEVOLW(1) = 0.5 \* (VOLW(1) + VOLWNEW(1))

AVTIMEVOLW(NLL) = 0.5 \* (VOLW(NL) + VOLWNEW(NL))

For I = 2 To NL

AVTIMEVOLW(I) = 0.25 \* (VOLW(I) + VOLW(I - 1) + VOLWNEW(I) + VOLWNEW(I -

1))

Next I

COUNTER = COUNTER + 1

ACCURACY = True

For I = 1 To NLL

DSAT(I) = AVTIMEVOLW(I) / VOIDMIN / DIST(I)

If DSAT(I) &gt; 1 Then DSAT(I) = 1

AVTIMEVOID(I) = AVTIMEVOLW(I) / DSAT(I) / DIST(I)

AVTIMETHETA(I) = AVTIMEVOLW(I) / (1 + AVTIMEVOID(I)) / DIST(I)

Next I

For I = 1 To NL

AVOID(I) = 0.5 \* (AVTIMEVOID(I) + AVTIMEVOID(I + 1))

AVTHETA(I) = 0.5 \* (AVTIMETHETA(I) + AVTIMETHETA(I + 1))

Next I

For J = NL To 1 Step -1

If AVTIMEVOLW(J) &lt; VOLWSAT(J) Then

SATPOINT = J + 1

Exit For

Else

SATPOINT = J

End If

Next J

For I = 1 To NLL

RATIO(I) = Abs((AVTIMEVOLW(I) - VOLWRES(I)) / (VOLWSAT(I) - VOLWRES(I)))

If RATIO(I) &gt;= 1 Then

AVCOND(I) = C \* AVTIMEVOID(I) ^ D

If SATPOINT = 1 Then AVCOND(1) = Sqr(C \* AVTIMEVOID(1) ^ D \* C \* AVOID(1) ^ D)

XF(I) = GS - 1

YF(I) = -(AVTIMEVOID(I) / A) ^ (1 / B - 1) / (A \* B \* GAMMAW \* DIST(I))

```

Else
  MPOT(I) = (RATIO(I) ^ (-1 / XM) - 1) ^ (1 / XN) / XALPHA
  If MPOT(I) >= -0.6 Then AVCOND(I) = SATCOND Else AVCOND(I) =
SATCOND * (0.6 / Abs(MPOT(I))) ^ P
  AVTIMESLOPE(I) = -GAMMAW * XM * XALPHA * (VOLWSAT(I) -
VOLWRES(I)) * RATIO(I) ^ (1 / XM) * (1 - RATIO(I) ^ (1 / XM)) ^ XM
  XF(I) = -1 - AVTIMEVOID(I)
  YF(I) = AVTIMESLOPE(I) ^ (-1)
  If MPOT(I) < LAW And MPOT(I) >= -2000 Then ETREM(I) = ETREM(I) *
(2000 + MPOT(I)) / (2000 + LAW)
  If MPOT(I) < -2000 Then ETREM(I) = 0
End If
Next I
For I = 1 To NL
  PHYF(I) = AVCOND(I) / (1 + AVTIMEVOID(I))
Next I
Call Infiltration
'FLUX(1) = -AVCOND(1) * (MPOT(1) / DIST(1) / (1 + AVTIMEVOID(1)) - 1)
Call MATRIX
Call THOMAS
For I = 1 To NL
  VOLWCALC(I) = XX(I)
  If RATIO(I) >= 1 Then
    Select Case VOLWCALC(I)
      Case Is >= VOLW(I)
        VOLWCALC(I) = VOLW(I)
    End Select
  Else
    Select Case VOLWCALC(I)
      Case Is >= VOLWSAT(I)
        VOLWCALC(I) = VOLWSAT(I) - 0.0001
    End Select
  End If
Next I
For I = 1 To NL
  If Abs(VOLWNEW(I) - VOLWCALC(I)) > Abs(0.0001 * VOLWCALC(I)) Then
ACCURACY = False
  VOLWNEW(I) = VOLWCALC(I)
Next I
If COUNTER = 1000 Then ACCURACY = True
Loop Until ACCURACY = True
CUMRUNOFF = CUMRUNOFF + RUNOFF * DT
For I = 2 To NL
  FLUX(I) = -PHYF(I) * (XF(I) + YF(I) / DIST(I) * (VOLWNEW(I) - VOLWNEW(I - 1)))
Next I
For I = 1 To NL
  DELTAVOLW(I) = Abs(VOLW(I) - VOLWNEW(I))
Next I
CHANGEVOLWMAX = DELTAVOLW(1)
For I = 2 To NL
  If DELTAVOLW(I) > CHANGEVOLWMAX Then CHANGEVOLWMAX = DELTAVOLW(I)
Next I
If CHANGEVOLWMAX = 0 Then DTNEW = DT Else DTNEW = DELTAVOLWMAX * DT /
CHANGEVOLWMAX
If DTNEW > DTMAX Then DTNEW = DTMAX
If DTNEW > 1.1 * DT Then DTNEW = 1.1 * DT

```

```

DT = DTNEW
For I = 1 To NL
  VOLW(I) = VOLWNEW(I)
  DSAT(I) = VOLW(I) / VOIDMIN / ZCOM(I)
  If DSAT(I) > 1 Then DSAT(I) = 1
  If VOLW(I) <= VOLWSAT(I) Then VOID(I) = VOIDMIN Else VOID(I) = VOLW(I) / ZCOM(I)
  If VOID(I) < VOIDMIN Then VOID(I) = VOIDMIN
  THETA(I) = VOLW(I) / (1 + VOID(I)) / ZCOM(I)
  YCOM(I) = ZCOM(I) * (1 + VOID(I))
Next I
VOLW(NLL) = VOLW(NL)
For I = 2 To NLL
  YBOUND(I) = YBOUND(I - 1) + YCOM(I - 1)
Next I
PHYF(NLL) = PHYF(NL)
For J = NL To 1 Step -1
  If VOLW(J) < VOLWSAT(J) Then
    SATPOINT = J + 1
    Exit For
  Else
    SATPOINT = J
    SATDEPTH = YBOUND(J)
    EXCESS(J) = 0
    POREPR(J) = 0
  End If
Next J
For I = 1 To NLL
  RATIO(I) = Abs((VOLW(I) - VOLWRES(I)) / (VOLWSAT(I) - VOLWRES(I)))
  If RATIO(I) >= 1 Then
    DELTAPORE(I) = (FLUX(I) / PHYF(I)) * DIST(I) * GAMMAW
    EXCESS(I) = EXCESS(I - 1) - DELTAPORE(I)
    If K > 1 And EXCESS(I) > EXCESSOLD(I) Then EXCESS(I) = EXCESSOLD(I)
    If EXCESS(I) < 0 Then EXCESS(I) = 0
    POREPR(I) = (YBOUND(I) - SATDEPTH) * GAMMAW + EXCESS(I)
    EXCESSOLD(I) = EXCESS(I)
  Else
    EXCESS(I) = 0
    POREPR(I) = (RATIO(I) ^ (-1 / XM) - 1) ^ (1 / XN) / XALPHA
  End If
Next I
If VOLW(1) >= VOLWSAT(1) Then SATURATION = True Else SATURATION = False
End Sub

```



**SUBROUTINE "MATRIX"****Option Explicit**

Public Static Sub MATRIX()

AA(1) = 0

CC(1) = -DT \* PHYF(2) \* YF(2) / 2 / DIST(2)

BB(1) = 1 - CC(1)

DD(1) = VOLW(1) \* (1 + CC(1)) - CC(1) \* VOLW(2) + DT \* FLUX(1) + DT \* PHYF(2) \* XF(2) - DT \* ETREM(1)

AA(NL) = -DT \* PHYF(NL) \* YF(NL) / 2 / DIST(NL)

CC(NL) = 0

BB(NL) = 1 - AA(NL)

DD(NL) = VOLW(NL) \* (1 + AA(NL)) - AA(NL) \* VOLW(NL - 1) - DT \* FLUX(NL) - DT \*

PHYF(NL) \* XF(NL) - DT \* ETREM(NL)

For I = 2 To NL - 1

AA(I) = -DT \* PHYF(I) \* YF(I) / 2 / DIST(I)

CC(I) = -DT \* PHYF(I + 1) \* YF(I + 1) / 2 / DIST(I + 1)

BB(I) = 1 - AA(I) - CC(I)

DD(I) = VOLW(I) \* (1 + AA(I) + CC(I)) - AA(I) \* VOLW(I - 1) - CC(I) \* VOLW(I + 1) - DT \*

PHYF(I) \* XF(I) + DT \* PHYF(I + 1) \* XF(I + 1) - DT \* ETREM(I)

Next I

End Sub

**SUBROUTINE "THOMAS"****Option Explicit**

```
Public Static Sub THOMAS()  
ALPHA(1) = BB(1)  
BETA(1) = CC(1) / ALPHA(1)  
YY(1) = DD(1) / ALPHA(1)  
For I = 2 To NL  
    ALPHA(I) = BB(I) - AA(I) * BETA(I - 1)  
    BETA(I) = CC(I) / ALPHA(I)  
    YY(I) = (DD(I) - AA(I) * YY(I - 1)) / ALPHA(I)  
Next I  
XX(NL) = YY(NL)  
NU = NL - 1  
For I = 1 To NU  
    J = NL - I  
    XX(J) = YY(J) - BETA(J) * XX(J + 1)  
Next I  
End Sub
```

**SUBROUTINE "RESULT"****Option Explicit**

Public Static Sub Result()

For I = 1 To NL

SOLIDS(I) = 1 / (1 + VOID(I) \* DSAT(I) / GS)

Next I

For I = 1 To NL

ELEVATION(I) = YBOUND(NLL) - YBOUND(I) - 0.5 \* YCOM(I)

Next I

BALANCE = 0

For I = 1 To NL

BALANCE = BALANCE + (VOLW(I) - IVOLW(I))

If RATIO(I) &gt;= 1 Then

SHEAR(I) = COHESION + A \* (THETA(I) / (1 - THETA(I))) ^ B \* Tan(3.14159 / 180 \*

PHY)

If SHEAR(I) &lt; 0 Then SHEAR(I) = 0

Else

SHEAR(I) = COHESION + 17 \* (YBOUND(I) - YBOUND(1)) \* Tan(3.14159 / 180 \*

PHY) + 0.285 \* (Abs(POREPR(I)) ^ 0.69 \* Tan(3.14159 / 180 \* PHY))

If SHEAR(I) &lt; 0 Then SHEAR(I) = 0

End If

Next I

Sheets("Unsaturated Results").Select

Cells(4 + NL, 1) = "Time ="

Cells(4 + NL, 2) = DAY - 1 &amp; " days"

Cells(5 + NL, 1) = "Balance ="

Cells(5 + NL, 2) = BALANCE \* 1000 &amp; " mm"

Cells(6 + NL, 1) = "Runoff ="

Cells(6 + NL, 2) = CUMRUNOFF \* 1000 &amp; " mm"

For I = 1 To NL

Cells(3 + I, 1) = THETA(I) \* 100

Cells(3 + I, 2) = YCOM(I) \* 100

Cells(3 + I, 3) = POREPR(I) \* MPOT(I)

Cells(3 + I, 4) = VOID(I)

Cells(3 + I, 5) = FLUX(I) \* 1000

Cells(3 + I, 6) = ELEVATION(I) \* 100

Cells(3 + I, 7) = (YBOUND(NLL) - YBOUND(I)) \* 100

Cells(3 + I, 8) = SHEAR(I)

Cells(3 + I, 9) = DSAT(I) \* 100

Next I

Sheets("Saturated Results").Select

Cells(4 + NL, 1) = "Time ="

Cells(4 + NL, 2) = DAY - 1 &amp; " days"

Cells(5 + NL, 1) = "Balance ="

Cells(5 + NL, 2) = BALANCE \* 1000 &amp; " mm"

Cells(6 + NL, 1) = "Runoff ="

Cells(6 + NL, 2) = CUMRUNOFF \* 1000 &amp; " mm"

For I = 1 To NL

Cells(3 + I, 1) = THETA(I) \* 100

Cells(3 + I, 2) = YCOM(I) \* 100

Cells(3 + I, 3) = POREPR(I)

Cells(3 + I, 4) = EXCESS(I)

Cells(3 + I, 5) = VOID(I)

Cells(3 + I, 6) = FLUX(I) \* 1000

Cells(3 + I, 7) = SOLIDS(I) \* 100

```

Cells(3 + I, 8) = ELEVATION(I) * 100
Cells(3 + I, 9) = (YBOUND(NLL) - YBOUND(I)) * 100
Cells(3 + I, 11) = DSAT(I) * 100
Cells(3 + I, 12) = (YBOUND(NLL) - YBOUND(1) - ELEVATION(I)) * 100
Cells(3 + I, 13) = (YBOUND(I) - YBOUND(1)) * 100
If ZR(DAY - 1) > 0 Then
    ROOTBIO(I) = BIOMASS(DAY - 1) * (ZR(DAY - 1) - Cells(3 + I, 12) / 100) /
ZR(DAY - 1)
    If ROOTBIO(I) >= 0 Then Cells(3 + I, 14) = ROOTBIO(I) Else Cells(3 + I, 14) = 0
    Else
        Cells(3 + I, 14) = 0
    End If
    Cells(3 + I, 10) = SHEAR(I) + 5 * Cells(3 + I, 14)
Next I
Cells(4 + NL, 3) = POREPR(NLL)
Cells(4 + NL, 4) = EXCESS(NLL)
Cells(4 + NL, 6) = FLUX(NLL)
Cells(4 + NL, 8) = 0
Cells(4 + NL, 9) = 0
Sheets("Root Extraction").Select
Cells(1, 1) = "ETREM"
Cells(2, 1) = "TIME = " & TIEMPO
For I = 1 To NL
    Cells(3 + I, 1) = ETREM(I) * 1000
Next I
Sheets("Saturated Results").Select
End Sub

```

**SUBROUTINE "INFILTRATION"**

```

Option Explicit
Public Static Sub Infiltration()
Select Case SATURATION
  Case True
    DISSIPATION = -PHYF(1) * (XF(1) + YF(1) / DIST(1) * (AVTIMEVOLW(2) -
AVTIMEVOLW(1)))
    If DISSIPATION >= -EVAPRATE * POTEVAPDT(K) And POTEVAPDT(K) > 0 Then
DISSIPATION = -EVAPRATE * POTEVAPDT(K)
    If DISSIPATION >= 0 Then DISSIPATION = 0
  Case False
    DISSIPATION = 0
    INFILCAP = Abs(-PHYF(1) * (XF(1) + YF(1) / 2 / DIST(1) * (VOLW(1) + VOLWNEW(1) -
2 * VOLWSAT(1))))
    FLUX(2) = -PHYF(2) * (XF(2) + YF(2) / 2 / DIST(2) * (VOLW(2) + VOLWNEW(2) -
VOLW(1) - VOLWNEW(1)))
  End Select
  If VOLWNEW(1) >= VOLWSAT(1) Then INFILCAP = 0
  WATEXCESS = PEDT(K) - INFILCAP
  If PEDT(K) > 0 Then GoTo 350
  RUNOFF = 0
  If WATEXCESS <= 0 Then GoTo 330
  EVAP = POTEVAPDT(K)
  INFILT = INFILCAP
  FLUX(1) = INFILT
  GoTo 390
330 INFILT = 0
Select Case SATURATION
  Case True
    EVAP = EVAPRATE * POTEVAPDT(K)
    If EVAP < -DISSIPATION Then EVAP = -DISSIPATION
  Case False
    Select Case MPOT(1)
      Case Is > MINPOT
        EVAP = EVAPRATE * POTEVAPDT(K)
      Case Is <= MINPOT
        EVAP = EVAPRATE * POTEVAPDT(K)
        If EVAP > -FLUX(2) Then EVAP = -FLUX(2)
    End Select
  End Select
  FLUX(1) = -EVAP
  GoTo 390
350 EVAP = 0
  INFILT = INFILCAP
  If PEDT(K) < INFILCAP And WATEXCESS <= 0 Then INFILT = PEDT(K)
  If DISSIPATION >= 0 Then FLUX(1) = INFILT Else FLUX(1) = DISSIPATION
  If WATEXCESS < MAXSTORAGE Then GoTo 390
  WATEXCESS = MAXSTORAGE
  RUNOFF = 0
  If PEDT(K) > INFILCAP Then RUNOFF = PEDT(K) - INFILCAP
390
End Sub

```